International
Progress Report

IPR-02-01

Äspö Hard Rock Laboratory

Rock stress measurements in Oskarshamn

Hydraulic fracturing and core testing in borehole KOV01

Fritz Rummel
Gerd Klee
Ulrich Weber

MeSy

January 2002

Svensk Kärnbränslehantering AB
Swedish Nuclear Fuel
and Waste Management Co
Box 5864
SE-102 40 Stockholm Sweden
Tel +46 8 459 84 00
Fax +46 8 661 57 19

Äspö Hard Rock
Laboratory

Report no.	No.
IPR-02-01	F73K
Author	Date
Rummel, Klee, Weber	02-01-04
Checked by	Date
Christer Andersson, Rolf Christiansson, Thomas Wallroth	02-01-10
Approved	Date
Christer Svemar	02-02-21

Äspö Hard Rock Laboratory

Rock stress measurements in Oskarshamn

Hydraulic fracturing and core testing in borehole KOV01

Fritz Rummel
Gerd Klee
Ulrich Weber

MeSy

January 2002

Keywords: Rock stress measurement, hydraulic fracturing, density, ultrasonic velocity, fracture toughness, hydrofrac test on minicores, numerical simulation

Summary

During 1. - 8.10.01 a total of 19 hydraulic fracturing tests / hydraulic stimulation tests on pre-existing fractures were carried out in borehole KOV01 using the MeSy wireline technique where both the double straddle -packer sonde and the impression packer unit for fracture orientation determination were moved within the borehole via a 7-conductor logging cable winch. The 19 tests covered the borehole interval from a depth of 280 m to app. 700 m.

For the generation of new fractures injection pressures up to app. 25 MPa were required for breakdown, while induced or pre-existing fractures could more easily be opened. Comparison of breakdown and refrac pressures yield a (hydraulic) tensile strength of the granitic rock of app. 5 to 6 MPa. Most tests showed rather distinct shut-in pressure values which generally increased with depth. From induced fractures only a small fraction of the injected water was recovered, while stimulated pre-existing fractures showed a significant water recovery rate. Most of the induced or stimulated fractures were axial or steeply inclined with a mean strike direction of NW - SE (145° ± 18°). This consistent fracture orientation did not allow to derive a reliable stress profile by an inversion calculation. Therefore, the principal horizontal stresses had to be calculated for each test at each of the 19 test sections. The derived stresses increase with depth but are significantly scattered and do not suggest a linear stress profile. In particular, rather high horizontal stresses can be observed at a depth of app. 600 to 700 m (S_h = 14 to 18 MPa, S_H = 30 to 45 MPa). The observed hydrofrac records could be simulated using a fracture mechanics approach and relevant physical rock property data derived from laboratory tests on the core material (fracture toughness tests, laboratory hydrofrac tests). This analysis also indicated the existence of microfractures of a characteristic dimension of app. 30 mm in the intact granitic rock.

The derived stress data in borehole KOV01 are in good agreement with the stress data obtained in the Laxemar borehole KLX02. If one adds the stress information from the two boreholes an almost gapless data profile exists which could be representative for the stress regime in the Oskarshamn - Laxemar - Äspö region.

Each hydrofrac test cycle in borehole KOV01 was preceeded by a pressure pulse test where the pressure decay was observed. This test was mainly conducted to probe the suitability of a test section for hydrofracturing, but it also allowed to derive information on the hydraulic rock properties at each section. This was mainly possible due to the stiff hydrofrac test system. The tests yield a hydraulic rock mass conductivity of (0.3 to 46) $\cdot 10^{-11}$ m/s depending whether the test section penetrated solid rock or contained pre-existing fractures.

Sammanfattning

Den 1 till 8 oktober 2001 genomfördes totalt 19 stycken hydrauliska spräckningar och injektionsförsök i borrhål KOV01. För testerna användes MeSy:s wireline system där både dubbelmanschetten och avtrycksmanschetten transporterades i borrhålet med en kabelvinsch där kabeln innehåller 7 ledare för avläsning av instrument i manschetterna. De 19 testerna genomfördes i ett djupintervall från 280 m till 700 m.

I de fall hydrauliska spräckningar genomfördes krävdes spräcktryck på cirka 25 MPa medan befintliga sprickor kunde öppnas vid lägre tryck. En jämförelse av spräcktrycken och sprickornas återöppningstryck visar att den hydrauliska draghållfastheten i berget är cirka 5 till 6 MPa. Huvuddelen av testerna hade relativt distinkta återförslutningstryck vilka generellt ökade med djupet. Från de sprickor som skapades genom spräckning försvann huvuddelen av det injekterade vattnet i berget medan stimulerade befintliga sprickor gav tillbaka det mesta av det injekterade vattnet. Huvuddelen av både de skapade och stimulerade sprickorna var parallella med borrhålet eller brantstående med en medelstrykning på NV – SO (145° ± 18°). Eftersom de uppmätta sprickorienteringarna var så likartade blev det nödvändigt att beräkna den största horisontella huvudspänningen vid vart och ett av de 19 försöks sektionerna. De beräknade bergspänningarna ökar med djupet men har en så stor spridning att det inte är troligt att spänningsfördelningen är linjär mot djupet. Särskilt höga horisontalspänningar observerades från 600 till 700 m djup (S_h = 14 till 18 MPa och S_H = 30 till 45 MPa). Responserna från de hydrauliska testerna kan simuleras genom att använda en sprick mekanisk ansats tillsammans med data om bergets fysiska egenskaper erhållna från laboratorietester av borrkärnor. Analyserna som bland annat bestod av ”fracture thoughness” test och hydrauliska tester på borrkärnorna påvisar en förekomst av mikrosprickor till ett avstånd på ca. 30 mm från borrhålsväggen.

De erhållna bergspänningarna i borrhålet KOV01 stämmer väl överens med resultat från tidigare bergspänningsmätningar genomförda i borrhålet KLX02 i Laxemar. Om resultaten från de två borrhålen superponeras erhålles en spänningsprofil med god överensstämmelse som troligen är representativ för spänningsfältet i Oskarshamn – Laxemar – Äspöregionen.

Varje hydralisk spräckning genomförd i KOV01 föregicks av ett tryckpuls test där trycksänkningen övervakades. Testet genomförs i huvudsak för att se om vald sektion är lämplig att genomföra ett hydrauliskt spräckförsök i. Testet ger också viss information om bergets hydrauliska egenskaper i sektionen eftersom ett styvt hydrauliskt system används. Den hydrauliska konduktiviteten i de olika sektionerna ligger enligt denna metod mellan 0,3 till $46 \cdot 10^{-11}$ m/s beroende på om testsektionen var belägen i homogent berg eller om den innehöll befintliga sprickor.

Content

SUMMARY 1

SAMMANFATTNING 3

1 INTRODUCTION 7

2 BOREHOLE DATA 9

3 TESTING PROCEDURES 13

3.1 Hydraulic Fracturing Principle 13
3.2 In - Situ Test Equipment 15
3.3 Test Section Selection, In - Situ Test Conduction 18
3.4 Laboratory Testing 23

4 RESULTS OF IN - SITU TESTS 27

4.1 Description of In - Situ Test Results 27
4.2 Characteristic Pressure Data 34
4.3 Fracture Orientation Data 38
4.4 Observation of Water Recovery 41
4.5 Analysis of the Pressure Pulse Test 42

5 DATA ANALYSIS 45

5.1 In - situ Stress Computation 45
5.2 Quality Control by Laboratory Test Results 48
5.2.1 Core Characterization 48
5.2.2 Fracture Toughness 50
5.2.3 Hydrofrac Tests on Minicores 51
5.2.4 Application of Laboratory Test Results 52

6 DISCUSSION 57

6.1 Rock Stress at Oskarshamn 57
6.2 Hydraulic Rock Mass Behaviour 57

REFERENCES 61

APPENDIX

A: Records from in-situ hydrofrac - tests together with evaluation of characteristic pressure data
B: Fracture traces on the impression packer sleeve
C: Core piece data sheets
D: Rock density test data
E: Ultrasonic velocity data sheets
F: Elasticity data sheets
G: Fracture toughness data sheets
H: Laboratory hydrofrac data sheets
I: Pressure pulse test records and permeability analysis

1 Introduction

For the design and construction of underground repositories for nuclear waste the knowledge of the in-situ stress regime is of outmost importance. At the potential Swedish first nuclear waste storage site at Äspö, therefore, numerous in-situ stress measurements have been conducted since 1989, both in the Äspö Hard Rock Laboratory (HRL) and in deep boreholes drilled in the Oskarshamn - Laxemar - Äspö granite complex. The existing stress data were presented e.g. by Lundholm (1999) and Ekman et al. (1999), and were summarized e.g. by Ljundgreen and Klasson (1997), Ask et al. (2001), or by Ekman (2001). The existing stress data mainly originate from both, overcoring tests with Doorstopper and Triaxial cells and hydraulic fracturing tests.

The 76 mm diameter borehole KOV01 located in the harbour of Oskarshamn was drilled in 2000 (completed in February 2001) to app. 1000 m depth to generally evaluate methods for testing of crystalline rock and, in particular, to complement the existing stress data base in the area by additional hydraulic fracturing / hydraulic stimulation tests on pre-existing fracture / weakness planes, and to compare stress data derived by different methods and by different research teams. It was originally planned to conduct the tests in the depth interval between 280 m and 700 m concentrating especially on the intervals between 300 and 400 m, 500 and 550 m, and 600 and 700 m depth. However, since MeSy proposed to carry out the test program with its wireline testing technique where both, the fracturing straddle packer tool and the impression packer unit for fracture orientation can quickly be moved within the borehole via a wireline winch on a 7-conducctor logging cable, it seemed appropriate to randomly select sutiable test sections at variable depths in order to derive a representative stress - depth profile.

In addition MeSy proposed to carry out a laboratory test program on core samples from the borehole to determine hydrofrac relevant fracture mechanics rock properties. Using these parameters in a MeSy fracture simulation program allows the interpretation of in-situ pressure records and thus yields a quality control for derived in-situ stress data.

2 Borehole Data

Borehole KOV01 is located in the harbour of Oskarshamn inside an instrument store building belonging to SKB. Drilling was completed in February 2001. After some initial logging tests the hole was available for testing from 17.9.01 onwards. The core material was displaced for inspection in the instrument store building. The borehole location is shown in Figures 2.1 and 2.2, the available information on the borehole is summarized in Table 2.1.

Table 2-1. Technical data of borehole KOV01.

location	Oskarshamn, Smaland, Sweden
borehole	KOV01
geogr. coordinates	N 57°15'39", E 16°28'01" (MeSy GPS)
nat coordinates (RT 38 2.5 W system)	N 6348516 m, E 1539942 m
altitude (RH 70 system)	3.05 m
borehole length / depth	1000.97 m / 969.0 m
inclination / bearing	app. 70° / 205° at 290 m app. 82° / 206° at 750 m
borehole diameters	3 inches / 76 mm
casing depth	to app. 100 m
casing diameter	200 mm ID
borehole fluid	water
fluid level	at surface
cored section	101.07 to 1000.97 m
core diameter	47 mm
drilling contractor	Drillcon AB
completed logs	camera log

Figure 2-1. *Borehole location Oskarshamn.*

Figure 2-2. *Borehole location at Oskarshamn.*

3 Testing Procedures

3.1 Hydraulic Fracturing Principle

The term hydraulic fracturing is used for fluid injection operations in sealed-off borehole intervals to induce and propagate tensile fractures in the borehole wall-rock. It was first applied in oil industry to stimulate productivity from low permeable oil-bearing formations (Clark 1949). It was first proposed by Scheidegger (1962) to derive the state of stress from such hydrofrac operations. The classical concept for the interpretation of hydrofrac pressure records was developed by Hubbert & Willis (1957). The concept is based on the Kirsch (1898) equation for the tangential stress σ_θ around a pressurized borehole oriented perpendicular to the far-field principal stresses S_1 and S_3. For compressive far-field stresses the maximum tensile stress at the borehole wall is given by

$$\sigma_{\theta,max} = -S_1 + 3S_3 - P \qquad (1)$$

when the borehole is pressurized by a fluid pressure P in the borehole.

If the pressure P reaches a critical value, P_c, a radial tensile fracture will initiate:

$$P_c = 3\,S_3 - S_1 + P_{co} \qquad (2)$$

where P_{co} is the (hydraulic) tensile strength of the rock. P_c generally is called breakdown pressure.

After fracture initiation the pressure fluid will penetrate into the fracture and will force the fracture to propagate. During this phase the pumping pressure P_p during constant rate injection generally decreases (if the supply rate is less than the propagating fracture can consume). For isotropic rock we may also assume that the fracture will propagate the easiest path, i.e. perpendicular to the direction of the least principal far-field stress S_3.

In case the injection suddenly is interrupted (pumping system shut-in) the dynamic fracture propagation comes to a halt and the injection pressure in the pressurized borehole interval rapidly decreases. During this stage we may assume that a static equilibrium is reached, where the pressure in the pressurized borehole interval is equal to the fluid pressure within the fracture, which is determined by the minimum principal stress S_3 :

$$P_{si} = S_3 \qquad (3)$$

where P_{si} is generally called shut-in pressure.

After venting the test interval the fracture is drained and therefore will close. By subsequent injection the pressure must exceed the tangential stress at the borehole wall to reopen the induced fracture :

$$P_r = 3S_3 - S_1 \qquad (4)$$

Therefore, we denote this pressure as reopening (or refrac) pressure P_r, and the comparison of eq. (2) and (4) provides a simple relation for the rock tensile strength P_{co}:

$$P_{co} = P_c - P_r. \quad (5)$$

Equations (2) to (4) commonly are known as Hubbert & Willis equations of hydraulic fracturing which are being used to derive the principal stresses S_1 and S_3 from the characteristic pressure values P_r and P_{si}.

As one can imagine from the above formulations, the H & W concept is based on several severe assumptions, such as rock isotropy and intact (unfractured) rock. In particular, hydrofrac experiments in a rock mass have to take into account the existence of pre-existing fractures which are not aligned with respect to the orientation of the three principal stresses S_1, S_2 and S_3. Several approaches to attack this problem have been suggested in the past which mostly are focussed to pressurize and statically open pre-existing fractures intersecting the test interval at some angle by low-rate injection, and thus measure the normal stress acting across the fracture. If a sufficient number of pre-existing fractures with different orientations can be opened in different test sections, then this approach also allows an exact determination of the three principal stresses using some kind of inversion calculations.

Detailed information on the H & W stress analysis and the stress evaluation from pressurizing pre-existing fractures (PSI - method, HTPF - method) can be found in Amadei & Stephansson (1997), Cornet (1993), Rummel (1987) or Rummel (2001).

Finally, some remarks on the fracture mechanics approach to hydraulic fracturing for stress determination. Rocks per se contain fractures of different scales, i.e. microfractures which must not be initiated but propagate whenever the stress intensity at the crack tip reaches the fracture toughness of the rock. For tensile crack propagation the intensity of the stress field around the crack tip can easily be formulated in spite of the rather complex loading situation during hydraulic fracturing, using the principle of superposition :

$$K_I = K_I(S_1) + K_I(S_3) + K_I(P) + K_I(P_a) \quad (6)$$

where K_I denotes the stress intensity factors for S_1, S_3, P is the fluid pressure in the borehole, and P_a is the fluid pressure within the fracture of length a. The instability condition is given by

$$K_I \geq K_{IC} \quad (7)$$

where K_{IC} is the fracture toughness, a material property. The theory results in the following hydrofracturing relation :

$$P_c = \frac{K_{IC}}{(h_o + h_a)\sqrt{R}} + k_1 S_1 + k_2 S_3 \quad (8)$$

where h_o, h_a, k_1 and k_2 are normalized (known) stress intensity functions. For $S_1 = S_3 = 0$ eq. (8) yields a physical relation for the (hydraulic) tensile strength P_{co} (see eq. 5) :

$$P_{co} = \frac{K_{IC}}{(h_o + h_a)\sqrt{R}}.$$

For further information see Rummel (1987) or Rummel (2001).

3.2 In - Situ Test Equipment

The hydraulic / hydrofrac tests in the 76 mm diameter borehole KOV01 were carried out using the wireline technique where the packer sondes are moved within the borehole on a 7-conductor logging cable with the MeSy cable winch MKW 1500 - 20 kN. The set-up of the cable winch on top of the borehole within the SKB store building is shown in Figure 3.1. The following downhole and uphole equipment components were used (Figure 3.2) :

Downhole :

- double straddle packer sonde PERFRAC II (Figure 3.3) equipped with nylon-reinforced packer elements of S&K-type TK 48-V (length 1300 mm, sealing length app. 1000 mm, OD 70 mm) and with an injection interval between the packers of app. 700 mm,
- impression packer sonde PERFRAC II equipped with one S&K-type TK 48-V packer element wrapped with a soft rubber skin, and an adapter to a magnetic single-shot orientation device,
- single-shot unit EW type RG with a magnetic compass of range 0 - 20° / 0 - 90° and a clock range up to 990 minutes,
- 7-conductor logging cable of Rochester type 7-H - 314 A with GO cable head OD 8.2 mm,
- pressure transducer Keller type PA-23 (0-40 MPa) within the cable-head connector on top of the hydrofrac sonde,
- stainless steel coil tubing (OD 10 mm, ID 8 mm) as hydraulic line from surface to the packer sondes.

Uphole :

- electric -driven high pressure pump type Speck HP 400 / 2 - 12 lpm for fluid injection,
- cable winch MKW 1500 - 20 kN
- pressure control unit with 2 pressure transducers type Keller PA-23, 0 - 60 MPa and a flow meter UNIMESS OPT04, 0 - 10 lpm,
- digital data acquisition unit SILVI, 8 channels, 16 bit, 5 Hz,
- analog paper strip chart recorder BBC SE - 400, 4 channels

Figure 3-1. *Set-up of the MeSy winch MKW 1500 - 20 kN on the top of borehole KOV01 in the SKB store building at Oskarshamn*

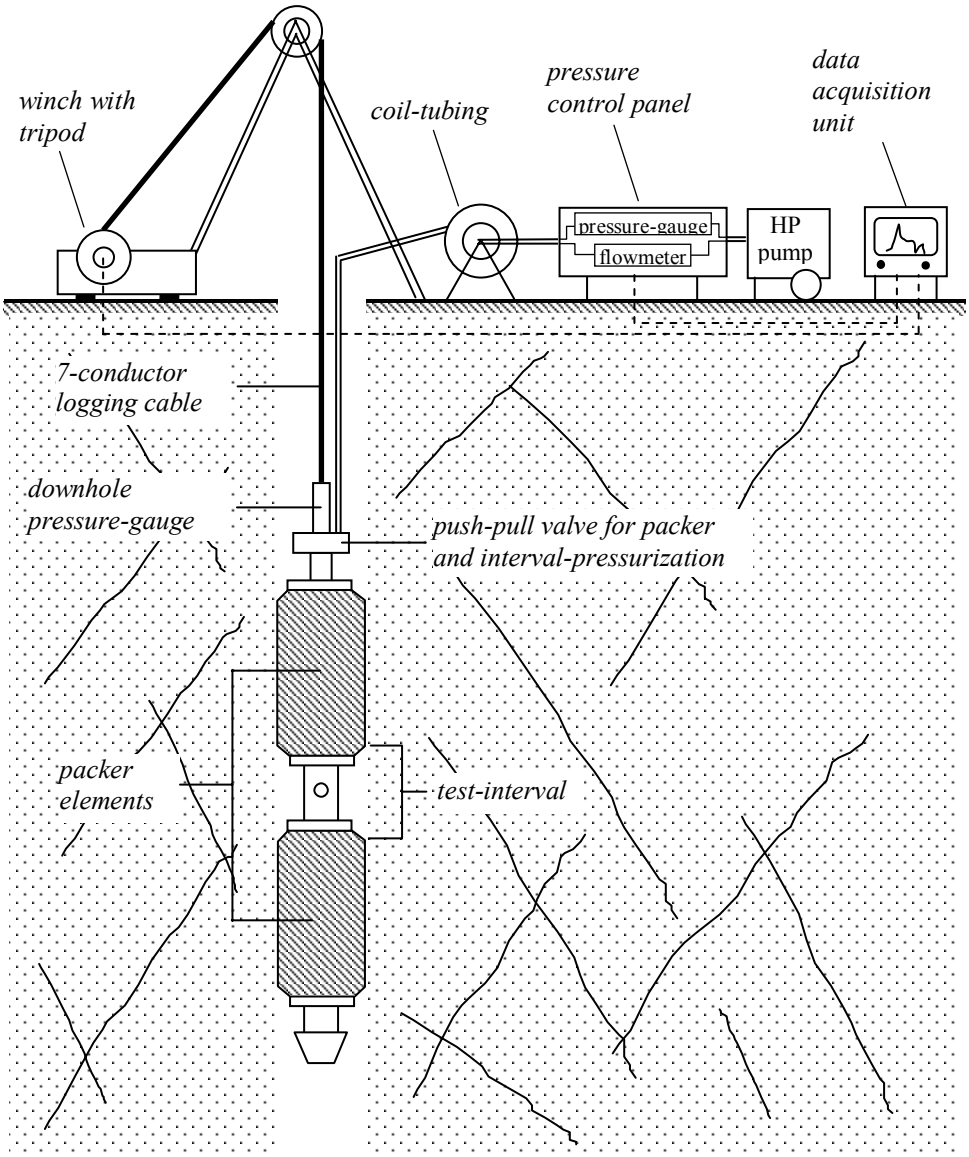

Figure 3-2. *Schematic view of the wireline hydrofrac system.*

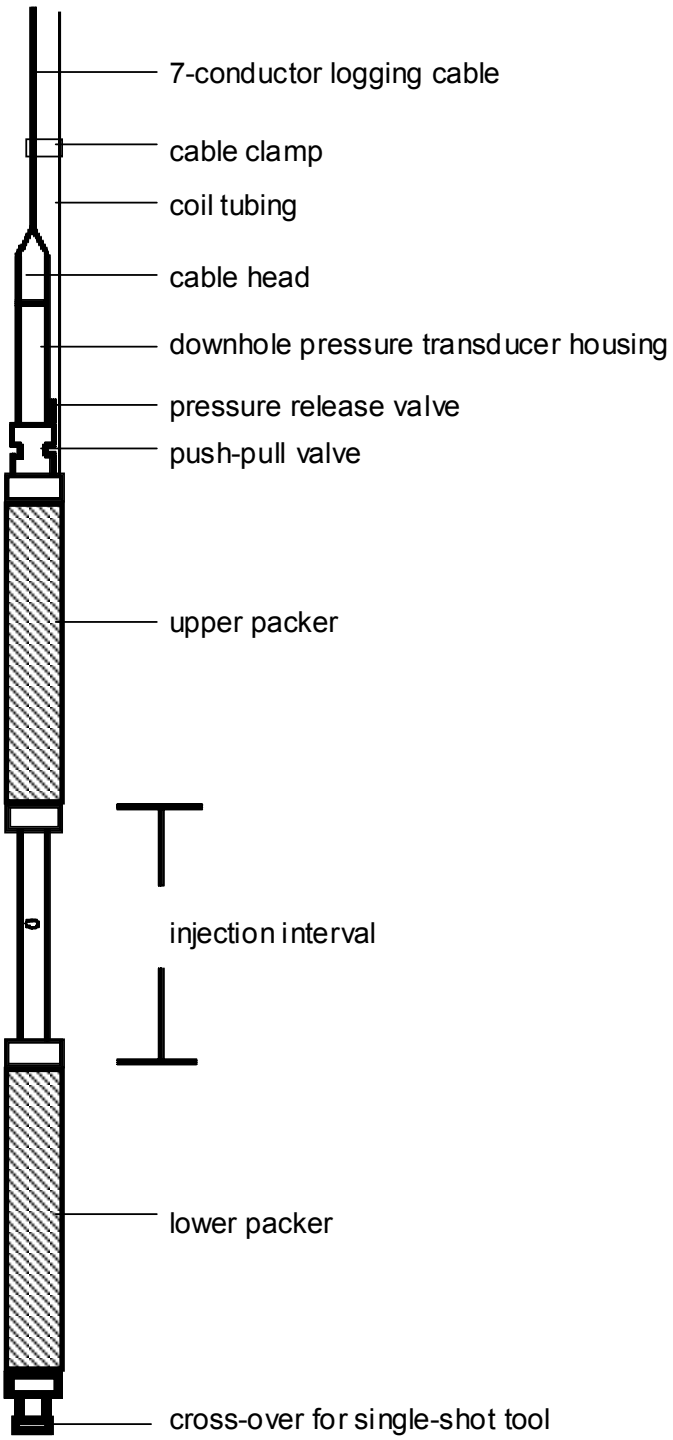

Figure 3-3. *Downhole system components.*

3.3 Test Section Selection, In - Situ Test Conduction

Prior to hydrofrac testing suitable test sections where selected on the basis of an overview core inspection. Initially, 15 test sections were selected for the borehole intervals between 300 - 400 m, 500 - 550 m, and 600 - 700 m, where the cores did not show any visible fractures. As it turned out during testing that in some of the selected

test sections no typical breakdown event was observed (an indication that weakness planes in the rock were stimulated), it was decided to randomly select further test sections at such depths to equally distribute tests over the total borehole interval of interest (280 to 710 m). Of course, the core sections of each additionally selected test section were inspected prior to each test, but it was recognized that the depth correlation between core depth and wireline depth may be erroneous by 1 to 2 m (an exact depth calibration of the wireline system within the borehole was not possible). By this strategy it was possible to meet the intended scope of the work to both, test intact borehole sections and stimulate borehole sections with pre-existing weakness planes / fractures / joints.

Prior to testing we also determined the hydraulic system stiffness by pressurizing the straddle packer sonde in a test pipe of 76 mm ID. Injection into the test interval (via the hydraulic stainless steel coil tubing used for downhole testing) yielded a system stiffness of 40 - 42 MPa / liter. Then, in order to check the borehole caliper condition a steel dummy with 70 mm OD and app. 100 kg weight (equivalent to the weight of the packer tool) was run to a depth of 715 m (MD).

During 3.10. to 8.10.01 a total of 20 injection tests were conducted at depth sections from 296 m to 713 m MD (measured depth), 19 of them showed typical breakdown or stimulation events, one test at 417.7 m MD / 395.5 m TVD was abandoned for stress testing but used for rock mass permeability determination. At each of the 19 test sections an impression packer test was carried out after the completion of all hydraulic injection tests, in order to determine the spatial orientation of induced or stimulated fractures.

The following test sections in borehole KOV01 were selected (MD measured or driller depth, TVD true vertical depth) :

No.	MD (m)	TVD (m)
1	296.0	280.9
2	303.5	288.0
3	319.3	302.8
4	325.4	308.5
5	331.5	314.2
6	383.5	363.0
7	416.0	393.8
8	417.7	395.5
9	471.0	446.9
10	490.5	465.8
11	499.5	474.8
12	510.8	485.6
13	517.0	491.6
14	579.0	552.2
15	604.2	577.0
16	681.0	652.9
17	689.5	661.3
18	702.5	674.2
19	708.0	679.6
20	712.8	684.4

Two typical hydrofrac / hydraulic injection test records illustrating the test procedure are shown in Figure 3.4. The two examples were chosen to illustrate a test with a typical breakdown event (test at 303.5 m MD / 288.0 m TVD) and a test where obviously a pre-existing fracture was stimulated (test at 702.5 m MD / 674.2 m TVD). Each test consisted of the following injection cycles after packer inflation to a differential pressure of 15 - 20 MPa :

- rapid pressurization of the test interval to a differential pressure of app. 10 MPa and subsequent monitoring the pressure decay for several minutes (P-test),
- release of the interval pressure,
- pressurization of the test interval with an injection rate of 1 to 2 lpm and monitoring the peak pressure (Frac-test) or a rather flat injection pressure level for the case of the presence of a pre-existing fracture, then shut-in of the system by injection stop and closure of the pressure line valve on surface,
- release of the interval pressure and monitoring the recovered fluid volume,
- conduction of several repressurization cycles with injection rates of 1 to 5 lpm until constant injection pressure is observed (Refrac cycles), the system shut-in for determination of shut-in pressure values, and interval venting with fluid recovery monitoring after each Refrac cycle,
- conduction of a Step-Rate injection with stepwise increasing the injection rate and monitoring the corresponding pressure increase,
- finally shut-in and venting the test interval, then packer deflation and lifting the packer unit to the next interval (generally, testing during one trip is conducted starting from the deepest test section).

The impression packer tests were carried out by pressurizing the impression packer element to a pressure app. 20% above the fracture re-opening pressure for app. 30 minutes. After recovery of the packer tool to the surface, the fracture trace is marked on the packer sleeve and transferred to a transparent plastic cover sheet wrapped around the packer. The film disc of the single-shot unit was developed documenting the orientation of the reference mark with respect to magnetic North in Oskarshamn. A typical example of fracture traces marked on the plastic cover sheets is shown in Figure 3.5 for the test section at 510.8 m MD / 485.6 m TVD.

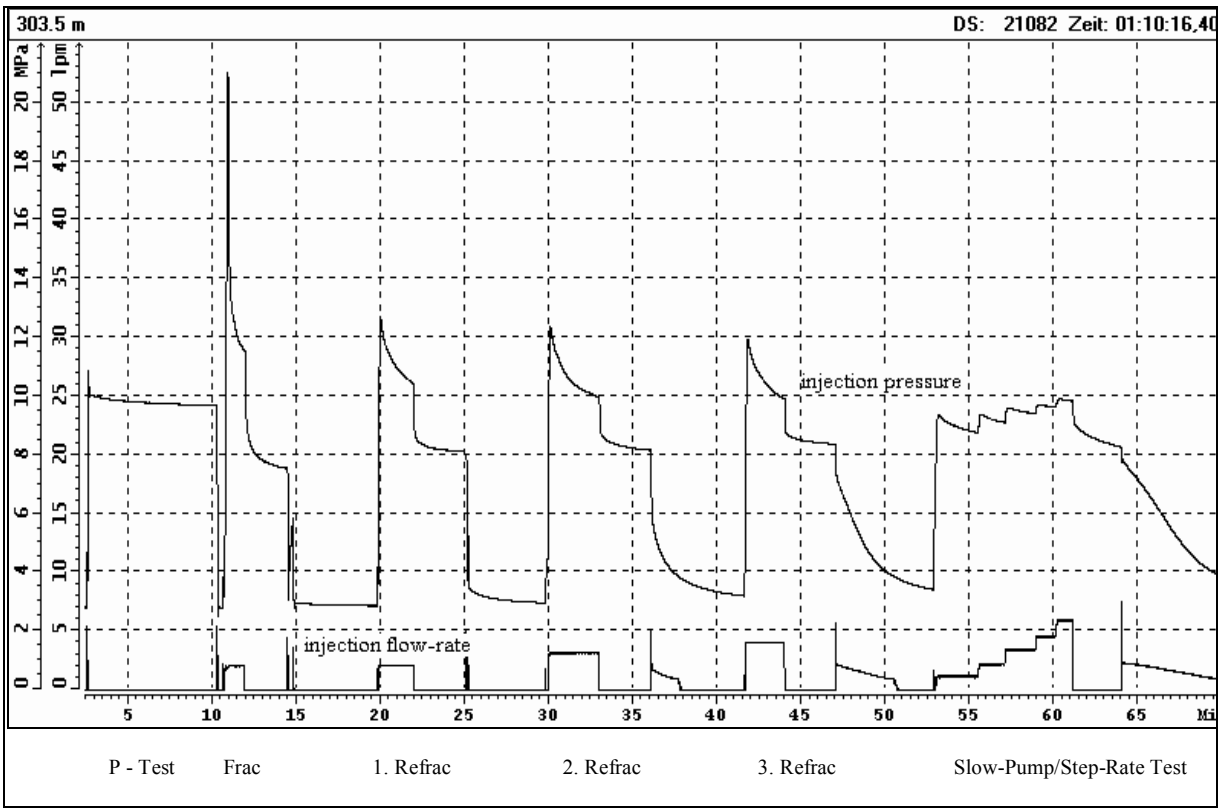

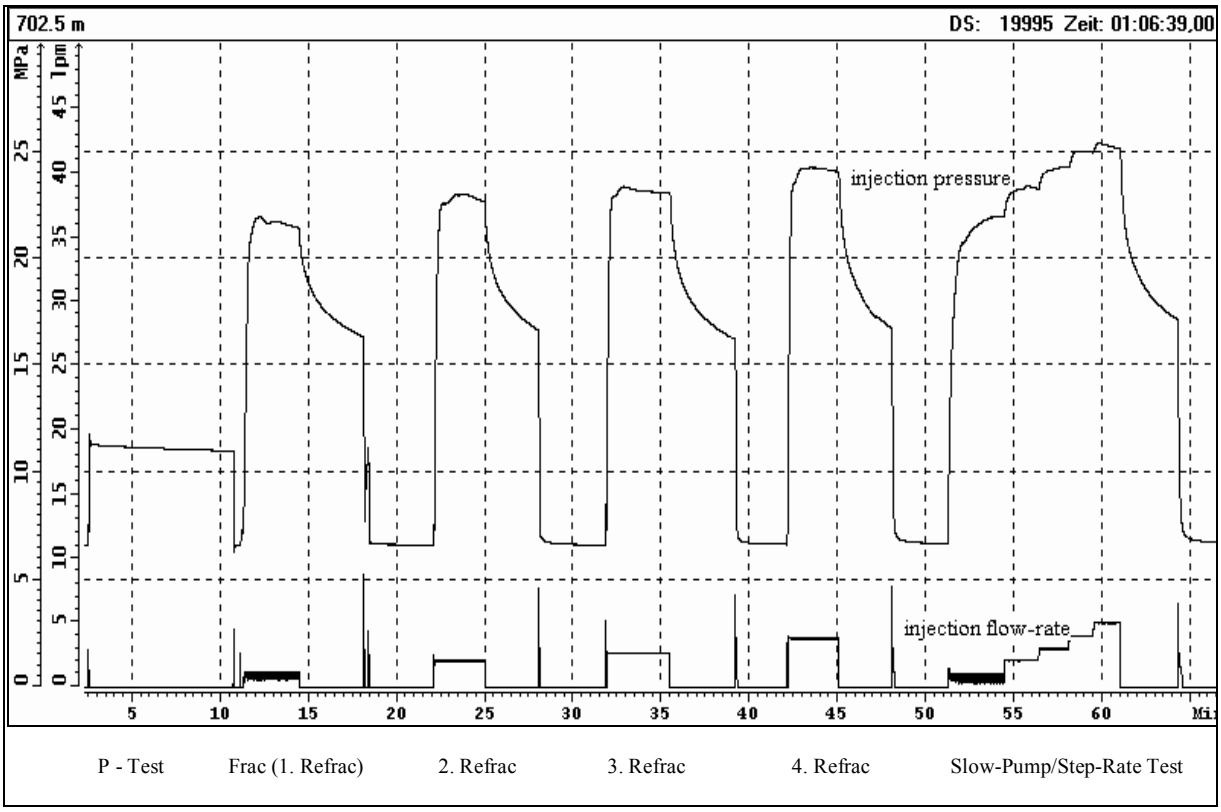

Figure 3-4. *Test records from test sections at (a) 303.5 m (MD) / 288.0 m (TVD) and (b) at 702.5 m (MD) / 674.2 m (TVD).*

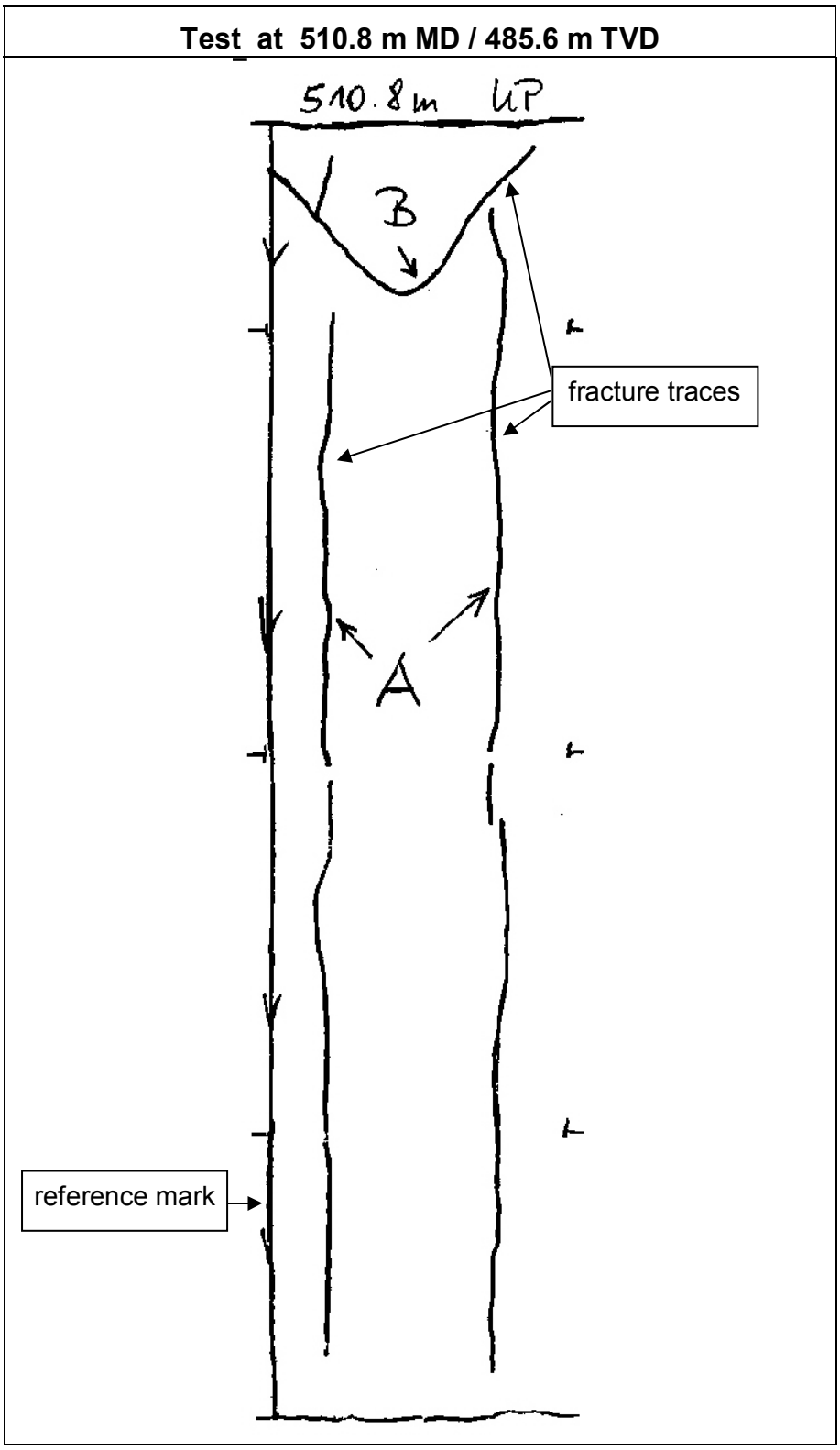

Figure 3-5. *A typical example of fracture traces on the packer sleeve of the impression packer test at 485.6 m (TVD) depth. The circumference of the packer is app. 230 mm, the length is app. 1000 mm.*

3.4 Laboratory Testing

The core material selected for material testing was first documented on a Core Piece Data Sheet (APPENDIX C). The core material is listed in Table 3.1. For core characterization density and ultrasonic velocities were measured on each core piece. Density measurements were done by the buoyancy method in water. Ultrasonic velocities were measured by pulse transmission across the core diameter according to the ISRM standard (1978). The experimental set-up is shown in Figure 3.6.

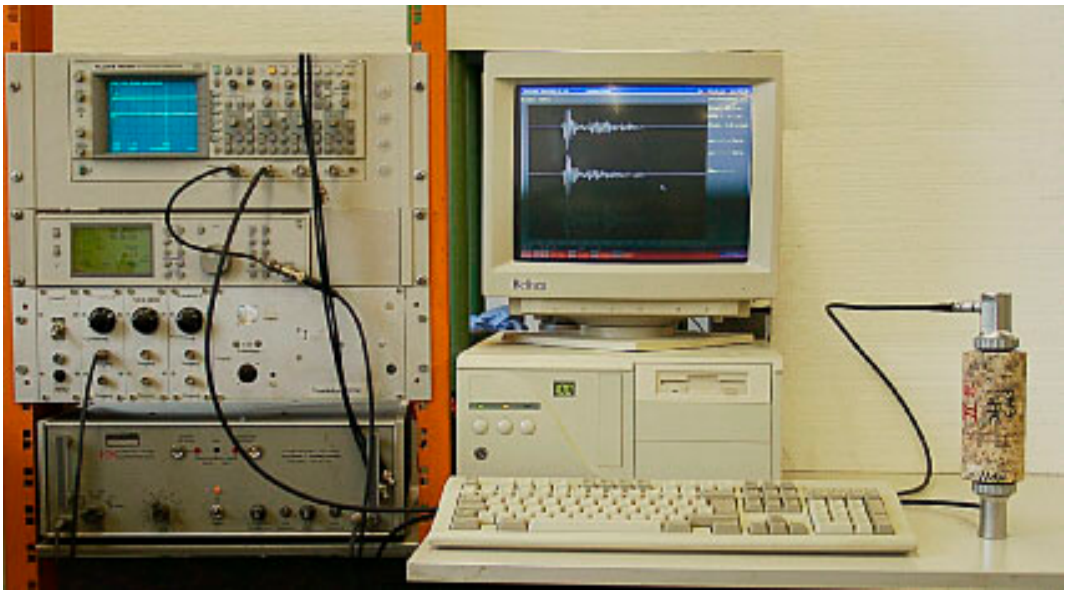

Figure 3-6. *Ultrasonic apparatus.*

Then, the original core pieces were used for fracture toughness tests after diamond-sawing of Chevron notches into the core pieces. Tests were done according to the ISRM standard (1988) by three-point loading with piston rate control. The piston displacement rate was app. 1 µm/s. The experimental set-up is shown in Figure 3.7.

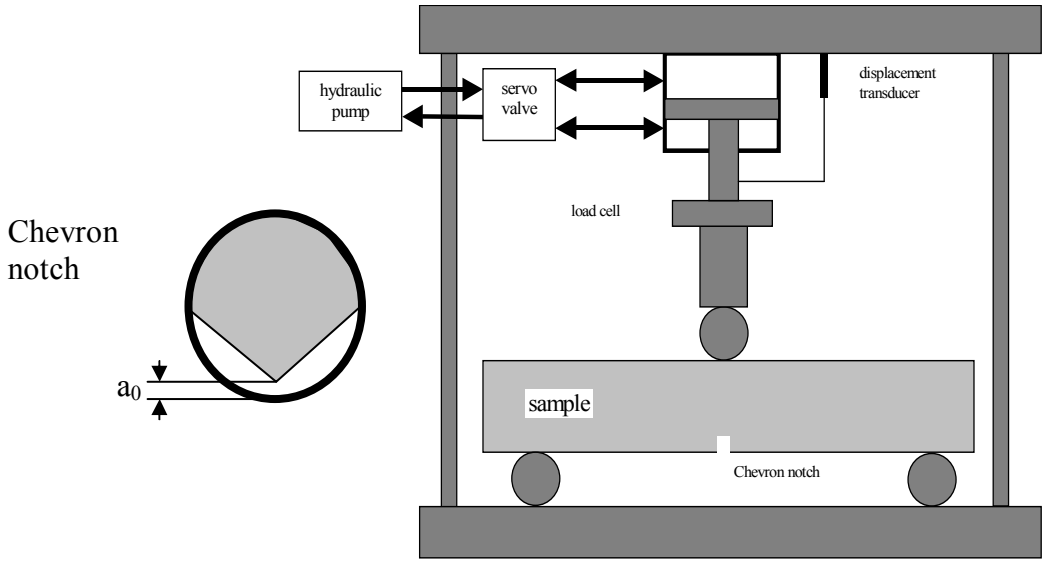

Figure 3-7. *Schematic view of the fracture toughness test apparatus.*

Laboratory hydrofrac tests were conducted on 50 mm long and 30 mm diameter core samples with a 3 mm diameter axial borehole for fluid injection. Sample preparation was carried out by diamond sawing, diamond drilling and diamond grinding using water as cooling fluid. Prior to hydrofracturing the samples were ultrasonic tested by axial pulse transmission for velocity determination. For hydrofrac tests the samples were jacketed with a rubber sleeve and subjected to axial stress and confining pressure. The experimental set-up is shown in Figure 3.8. The axial stress was slightly above the confining pressure. Internal pressurization was achieved by injection of oil (Shell Tellus 32, viscosity 25 cP) into the 3-mm diameter holes at a rate of 1 ml/s. Fracture initiation and dynamic fracture growth is characterized by a hydraulic short circuit between axial stress, confining pressure and injection pressure, which yields the breakdown pressure p_c. The dependence of p_c on the confining pressure p_m generally is given by a linear relation

$$p_c = p_{co} + k \cdot p_m$$

where p_{co} is the (hydraulic) tensile strength and k is the frac-coefficient. The confining pressure ranged from 0 to app. 40 MPa. Some hydrofrac tests with zero confining pressure were conducted on the original core pieces with axial holes of up to 8 mm diameter.

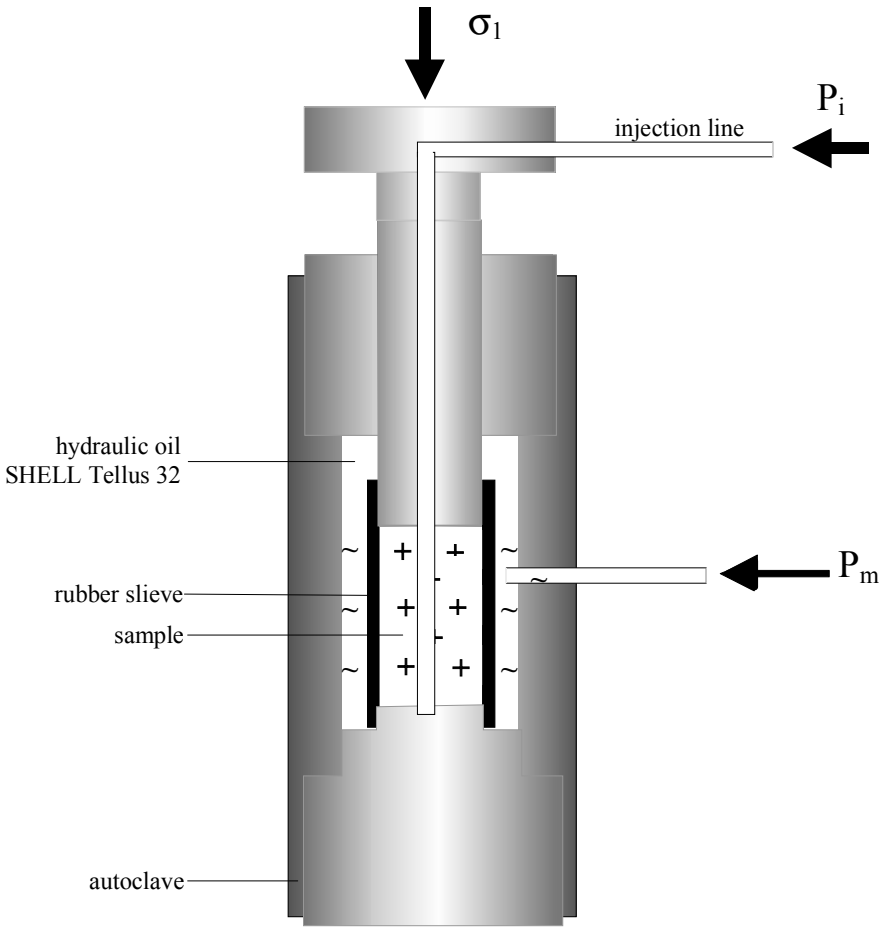

Figure 3-8. *Test chamber for mini-frac testing.*

Table 3-1. Core material from borehole KOV01 for laboratory testing.

core - piece no.	depth-range MD (m)	core-piece length min / max (mm)	diameter (mm)	remarks
1A	333.55 - 334.03	300 / 328	47.6	
1B		168 / 190	47.6	
2	382.96 - 383.35	390 / 402	47.4	
3A	438.12 - 438.53	140 / 150	47.4	
3B		145 / 165	47.4	
3C		105 / 120	47.4	
4A	463.60 - 464.10	160 / 175	47.4	
4B		175 / 202	47.4	
4C		140 / 180	47.4	
5	500.20 - 500.60	390 / 425	51.7	
6	559.70 - 560.10	400 / 420	47.2	
7	559.46 - 596.85	390 / 395	47.2	
8A	648.68 - 649.10	75 / 98	47.2	
8B		305 / 350	47.3	
9A	692.58 - 692.98	255 / 380	51.9	
9B		55 / 120	51.9	
10A	709.33 - 709.77	204 / 308	51.9	
10B		105 / 240	51.9	
G1 - G3[1)]	app. 500	app. 500	47	3 pieces

[1)] *This core from app. 500 m depth and app. 500 mm length consisted of 3 pieces. The core was provided to MeSy prior to in-situ testing for preliminary physical property evaluation. No core piece data sheet was made*.

4 Results of In - Situ Tests

4.1 Description of In - Situ Test Results

The test records are presented in APPENDIX A. For each test an overview plot is given which contains the pressure and injection rate graphs for each test cycle plus information on the injected and recovered fluid volumes, zoomed graphs for the identification of breakdown and refrac pressure values, 3 different plots for the determination of the characteristic shut-in pressure value from different test cycles, and a detailed plot of the step-rate test together with a pressure vs. injection rate graph. The impressions on the impression packer sleeve are shown in APPENDIX B.

The MeSy Routine Analysis used in Appendix A to identify reliable characteristic hydrofrac pressure data, breakdown pressure P_c, refrac or reopening pressure P_r, and shut-in pressure P_{si} consists of the following procedures :

(i) The breakdown pressure defined as the peak pressure during the first pressurization cycle (frac cycle) is obtained from a zoomed pressure P vs. time t plot.

(ii) The refrac pressure is taken from the zoomed pressure P vs. injected fluid volume V plots, generally from the first refrac cycle, as the pressure level when the plot significantly deviates from the linear pressure increase determined by the system stiffness dP / dV.

(iii) The shut-in pressure P_{si} is determined by the following three-step procedure :

- the upper limit of P_{si} is derived from zoomed plots of pressure P vs. injection flow rate Q for different refrac cycles. $P_{si,max}$ then correlates to the pressure level when Q = 0.

- The lower limit of P_{si} is derived from a Muskat - type plot of the difference between pressure P and an asymtotic pressure level P_a vs. time t, assuming that the linear portion of the plot is due to radial flow, i.e. the stimulated fracture is nearly closed.

- Then, the most reliable value of P_{si} is between the two limits and characterized by the transition of the initial rapid linear pressure drop to the beginning of a diffusion dominated slow pressure decay. This transition can be determined from the tangent to the linear pressure drop in the zoomed P vs. t plots for the shut-in stages of the various refrac cycles.

The P_{si} - value derived by this three-step analysis can be checked by the low step-rate injection test which is analysed similar as a classical Lugeon test using steady-state P-Q data pairs from the P vs. t plot.

It should be mentioned that various techniques to derive P_{si} -values are used by different researchers. A good summary of the different methods is given by Guo et al. (1993).

(iv) The monitoring of the recovery fluid volume from a fracture after test completion may be used to speculate whether the induced fractures has connected to the natural fracture network in the rock mass during its propagation. Low recovery rates may indicate that the fracture has connection to a natural joint system which easily consumed fluid. High recovery rates are generally observed from tests on pre-existing fractures

which are connected to a large fluid reservoir. However, this field is still open to further research in geohydrology.

In order to evaluate the quality of the tests, first a short description of each test is presented:

Test at 296.0 m MD / 280.9 m TVD

During the P-test the interval pressure rapidly decays from 8 to 5 MPa during 7 min., indicating a pre-existing fracture.

During the 4 subsequent injection cycles the fracture is repeatedly re-opened at a pressure level of 10 MPa (the detailed analysis yields a value of $P_r \approx 9.5$ MPa).

After system shut-in the pressure rapidly drops to app. 8 MPa (the detailed routine analysis yields a value of $P_{si} = 8.2$ MPa). The step-rate tests indicates that the fracture accepts 1 lpm at already 7.8 MPa.

It is interesting to note that app. 50% of the injected volume of 64 l is recovered.

The impression shows an inclined (46°) fracture trace with a strike direction of 161 degrees.

Test at 303.5 m MD / 288.0 m TVD

The P-test shows a completely tight test interval.

Consequently, we observe a typical Frac-cycle with $P_c = 21$ MPa, and almost identical Refrac-cycles with peak pressures of app. 12 MPa (the detailed analysis yields $P_r = 11.7$ MPa), and we can derive a P_{co} value of app. 9 MPa.

After shut-in the pressure rapidly drops to app. 8.5 MPa (the detailed routine analysis yields $P_{si} = 8.8$ MPa). During the Step-Rate test the induced fracture is already open at 9.3 MPa for a injection rate of 1.1 lpm.

A large quantity of the injected water was recovered (36%).

The impression test shows one inclined (26°) fracture with 137 degrees strike direction.

Test at 319.3 m MD / 302.8 m TVD

The P-test yields a pressure drop of only 0.1 MPa during app. 6 min, indicating a tight test interval.

The frac cycle is characterized by a distinct breakdown event (frac initiation at 17 MPa). All 3 Refrac cycles yield rather distinct refrac pressure peaks of app. 14.5 MPa (the detailed analysis shows $P_r = 13.5$ MPa which indicated a value of $P_{co} = 3.5$ MPa).

After the injection is stopped the pressure rapidly decreases to app. 11 MPa (the detailed analysis shows $P_{si} = 11.5$ MPa). During the step-rate test the induced fracture clearly is open at 13.4 MPa for an injection rate of 1.4 lpm.

The impression shows 2 more or less axial fracture traces with almost identical strike direction of 144 and 148 degrees.

Test at 325.4 m MD / 308.5 m TVD

The P-test shows a rather tight test interval with a pressure decline of 0.5 MPa within 7.5 min.

The Frac-cycle does not show a distinct breakdown (P_c = 15.5 MPa) when compared to the peaks of the 2 last Refrac-cycles (14.1 MPa), which indicates a low tensile strength of only app. 1.5 to 2 MPa (the detailed analysis yields a value of P_r = 13.5 MPa).

After system shut-in the pressure rapidly drops to app. 12 MPa. The routine analysis derives a shut-in pressure value of P_{si} = 12.4 MPa. The Step-Rate test shows that the fracture is already fully open at 12.6 MPa.

Only 9% of the injected water is recovered.

The impression shows 2 axial fracture traces with a strike direction of 141 degrees.

Test at 331.5 m MD / 314.2 m TVD

The P-test indicates some hydraulic leakage with a pressure decay of 0.9 MPa within 7.5 min.

In spite of the leakage the first injection cycle shows a distinct breakdown event with P_c = 13.8 MPa. Subsequent cycles are to some extent anomalous (sudden pressure decrease after an initial peak, then again a pumping pressure peak). The detailed analysis shows P_r = 10 MPa.

After injection stop the pressure declines rather gradual. The routine analysis yields a shut-in pressure of 9.5 MPa, however the Step-Rate test shows that the fracture is quite open at 9.5 MPa.

Only a small quantity of the injected water is recovered (4%).

The impression shows an inclined fracture with 176° strike direction.

Test at 383.5 m MD / 363.0 m TVD

The P-test indicates a tight test interval with a linear pressure decline of only 0.5 MPa during 8 min..

Consequently we observe a typical Frac-cycle with a breakdown at P_c = 17.7 MPa. Subsequent injection cycles demonstrate distinct peaks at app. 14 MPa (the detailed analysis results in a re-opening pressure value of P_r = 12.4 MPa).

After shut-in the pressure rapidly drops to app. 10 MPa in each of the cycles (the routine analysis determines a shut-in pressure of 10.1 MPa). The Step-Rate test indicates that the induced fracture is fully open at 11.2 MPa.

The impression shows an axial fracture with 132° strike direction.

Test at 416 m MD / 393.8 m TVD

During the P-test the pressure significantly decreases from app. 10 MPa to app. 6 MPa within 7 min. indicating the presence of a pre-existing fracture.

The peak pressure during the first cycle (P_c = 12.1 MPa) is only slightly above the peak pressures of the subsequent cycles (P ≈ 10.5 MPa). The routine analysis of the first cycle yields the value P_r = 11 MPa.

After shut-in the pressure drops rapidly to app. 8 MPa. The routine Psi - analysis derives a shut-in pressure value of P_{si} = 8.2 MPa.

A very small quantity of the injected volume was recovered.

The impression shows one axial fracture trace with 144° strike direction.

Test at 471 m MD / 446.9 m TVD

P-test : rapid pressure decline from app. 10 MPa to app. 7 MPa within 6.5 min..

Distinct peaks during the first 2 injection cycles (app. P_c = 13 MPa), anomalous pumping pressure during the last 2 cycles, with a pumping pressure P_p of app. 9.5 MPa. The routine analysis of the first cycle yields a value of P_r = 12.0 MPa.

After shut-in we only observe a small instantaneous pressure drop ($P_{si} \approx P_p$). The routine analysis yields a shut-in pressure of 9.4 MPa, the Step-Rate tests demonstrates that the fracture is fully open at 9.5 MPa.

25% of the injected fluid is recovered.

The impression shows a complex set of fracture traces, two app. axial traces with 158° and 107° strike direction, and one almost horizontal fracture .

Test at 490.5 m MD / 465.8 m TVD

P-test with almost zero pressure decay during 7 min. indicating an unfractured test section.

Consequently a prominent Frac-cycle with P_c = 22.4 MPa. Subsequent injection cycles, however, are more difficult to understand. From the last 2 injection cycles a refrac pressure of $P_r \approx 17$ MPa may present a valid value, which then results in $P_{co} \approx 5$ MPa.

In each of the cycles we observe an instantaneous pressure drop to app. 10 MPa (the detailed routine analysis yields a value of $P_{si} \approx 10.3$ MPa). The induced fracture is clearly open at 12 MPa (Step-Rate test).

Only a small fraction of water is recovered.

On the impression we observe an axial fracture trace with 102° strike direction.

Test at 499.8 m MD / 474.8 m TVD

The P-test suggests the presence of an open pre-existing fracture which permits migration of water at 8 MPa.

The 3 injection cycles show pumping pressures P_p of app. 11 MPa independent on injection rates. The identification of a re-opening pressure in this case is difficult. The routine analysis would give a value of P_r = 6.6 MPa. On the overview plot a major change in pressure increase in the last 2 Refrac-cycles can be observed at app. 10 MPa.

After shut-in we only observe a slight pressure drop ($P_p \approx P_{si}$). The routine analysis for shut-in pressure determination confirms this result.

It is difficult to understand the large quantity of recovered water (31%).

On the impression we observe a set of 3 steeply inclined fracture traces with a mean strike direction of 157 ± 16 degrees.

Test at 510.8 m MD / 485.6 m TVD

P-test : a perfectly tight interval.

Consequently, a characteristic Frac-test with P_c = 24.1 MPa. Independent of injection rate the fracture can be extended by a pumping pressure of app. $P_p \approx$ 12.5 MPa. The tensile strength can be estimated as $P_{co} \approx$ 12 MPa.

After shut-in the instantaneous pressure drop is small, the routine analysis yields P_{si} = 11.5 MPa. The fracture is open at 11.4 MPa (Step-Rate test).

11% of the injected water is recovered.

The impression shows 2 steeply inclined (axial) fractures with a mean strike direction of 172 ± 4 degrees.

Test at 517 m MD / 491.6 m TVD

The P-test indicates the presence of a pre-existing fracture.

For a small injection rate during the first injection cycle no pressure peak is observed. During subsequent pressure cycles the mean pumping pressure is $P_p \approx$ 13 MPa. The fracture opens at about P_r = 9.6 MPa (routine analysis).

After shut-in we can identify a rather clear shut-in pressure of 11.5 MPa. At 11.7 MPa the fracture is clearly open (Step-Rate test).

12% of the injected water is recovered.

The impression shows an axial fracture with 161° strike.

Test at 579 m MD / 552.2 m TVD

The P-test suggests a tight test section.

The Frac-test yields a breakdown of P_c = 17.6 MPa, subsequent injection cycles show distinct re-opening pressures of app. 14.5 MPa and a pumping pressure of app. 15 MPa (the routine analysis yields P_r = 13.4 MPa). P_{co} can be estimated as app. 4 MPa.

No distinct pressure drop can be observed after system shut-in ($P_{si} \approx P_p$). The detailed routine analysis yields P_{si} = 14.7 MPa, which is confirmed by the Step-Rate test (14.4 MPa).

Only a small fraction of water is recovered (6%).

The impression shows an axial fracture trace with 179° strike direction.

Test at 604.2 m MD / 577 m TVD

The P-test shows a gradual pressure decline indicating the presence of a permeable fracture.

During the injection cycles the peak pressure drops from P = 14.2 MPa for the first cycle to app. P_p = 12.5 MPa during the last two cycles, where the peak pressure corresponds to the pumping pressure. The fracture opens significantly at app. 12 MPa (the detailed routine analysis suggest a value of $P_r \approx 9.8$ MPa).

After shut-in we only observe a small instantaneous pressure drop to app. 12 MPa (the routine analysis yields a value of P_{si} = 12.1 MPa). The Step-Rate test, however, indicates an open fracture at 11.4 MPa for an injection rate of app. 1 lpm.

The recovered water volume is 23%.

The impression shows 4 traces of axial and steeply inclined fractures with a mean strike of 107 ± 27 degrees.

Test at 681 m MD / 652.9 m TVD

P-test : a perfectly tight test section.

Consequently, a typical Frac-cycle with a high breakdown pressure of P_c = 19.6 MPa. Subsequent injection cycles show distinct pressure peaks at app. 14.5 MPa (the detailed routine analysis yields P_r = 14.3 MPa for the first refrac cycle). As also observe in some other ideal frac experiments the pumping pressure increased during each cycle.

After shut-in we only observe a small instantaneous drop from the pumping pressure at app. 14.4 MPa. The routine analysis yields P_{si} = 13.7 MPa. At 13.9 MPa the fracture is open (Step-Rate test).

About 20% of water is recovered after the test.

The impression shown an induced axial fracture of 147° strike.

Test at 689.5 m MD / 661.3 m TVD

Although the P-test shows a significant pressure decay, the subsequent injection results in a rather high breakdown pressure of P_c = 18.1 MPa. During subsequent injection cycles the pumping pressure increases with time. The fracture opens at app. 14.2 MPa (the detailed analysis yields P_r = 14.5 MPa for the first refrac cycle).

After all injection cycles we observe small but clear instant pressure drops however, to different pressure levels (13.7, 14.3, 15.0 MPa); the routine analysis yields P_{si} = 13.7 MPa for the first cycle). The Step-Rate test shows that the fracture is clearly conductive at 14 MPa.

The recovery is 11%.

The impression shows axial to steeply inclined fracture traces with a mean strike direction of 135 ± 9 degrees.

Test at 702.5 m MD / 674.2 m TVD

The P-test yields a pressure drop of only 0.3 MPa in 8 min, indicating a tight test interval.

None of the injection cycles demonstrates a pressure peak. Fluid can be injected at constant pressure levels depending on injection rate. Thus, a clear indication for a pre-existing fracture which is opened at app. 17 MPa and is hydraulically fully active at pressures above 20 MPa (see Step-Rate test).

After injection stop in the first cycle the pressure rapidly decreases to app. 20.7 MPa (the detailed analysis yields a value of P_{si} = 20.7 MPa).

The impression shows 3 more or less axial fracture traces with a mean strike direction of 132 degrees.

Test at 708 m MD / 679.6 m TVD

No pressure drop during the P-test.

A breakdown at P_c = 24.9 MPa, followed by refrac cycles with distinct peaks at app. 22 MPa.

Clear shut-in pressures of app. 16 MPa (the routine analysis shows 16.7 MPa). From the Step-Rate test we observe that the fracture is open at 17.7 MPa.

Almost no recovery.

The impression shows an axial pressure of 127 degrees strike.

Test at 712.8 m MD / 684.4 m TVD

The P-test shows an almost linear pressure drop of 0.8 MPa during 8.5 min.

None of the injection cycles demonstrates a distinct pressure peak. Fluid can be injected at a constant pressure level of app. 22 MPa almost independent of injection rate. Thus, a clear indication for a pre-existing fracture, which is opened at app. 18 to 19.5 MPa. The Step-Rate test shows that the fracture is hydraulically fully active above 19.9 MPa.

After injection stop the pressure only slightly decreases rapidly, followed by a more continuous pressure decay which makes it difficult to identify a valid shut-in pressure (the detailed analysis procedure gives the value P_{si} = 19.7 MPa, with a minimum value of $P_{si,\,min}$ = 15 MPa.

The impression shows 1 axial fracture trace with a strike direction of 133 degrees and 2 inclined fracture traces with similar strike direction, dip, and dip direction.

4.2 Characteristic Pressure Data

The characteristic pressure data are listed in Table 4.1. Due to the uncertainty of the experimental data of the refrac- and shut-in pressures both, the exact values derived from the detailed routine analysis and the range of uncertainty determined from a more qualitative evaluation are given. The P_r- and P_{si} data from the routine analysis are presented in Figure 4.1 and Figure 4.2.

The value P_{max} generally is the breakdown pressure P_c at the moment of fracture initiation, but we note that the peak pressure during the first injection cycle can also be determined by the stimulation of a pre-existing fracture. Thus, we must differentiate two categories of tests:

- tests where unequivocally new fractures were induced at test sections with low pressure decay during the P-test and characterized by unique Frac-events with a high breakdown pressure; we observe 10 of such tests;

- tests on sections with obviously pre-existing fractures, generally characterized by a significant pressure decay during the P-test and by the absence of a typical breakdown event; we also observe 10 of such tests.

The fracture re-opening pressure P_r in some cases was difficult to identify since even "closed" fractures in crystalline rock accept significant amounts of fluid during low-rate injection during Step-Rate tests.

From the P_c- and P_r - data of tests on intact rock sections we can derive the (hydraulic) tensile rock strength P_{co}. The P_{co}-data range between 1.5 to 12 MPa with a mean of P_{co} = (5.2 ± 3) MPa.

Similar, the shut-in pressure data P_{si} in most cases were difficult to determine, because either there was no instantaneous rapid pressure drop at system shut-in, or the shut-in pressure varied for the different test cycles. Nevertheless, the routine detailed analysis provides rather objective values which in most cases can be confirmed or at least supported from the results of the Step-Rate tests.

We realize rather high P_r- and P_{si} - values in the depth range from 290 to 310 m and in the range from 675 to 685 m, while the pressure values between almost linearly increase with depth.

Table 4-1. Characteristic pressure data (P_{max}: maximum pressure, e.g. breakdown pressure, P_r: refrac pressure, P_{si}: shut-in pressure, MD: measured depth, TVD: true vertical depth).

MD (m)	TVD (m)	P_{max} (MPa)	P_r routine analysis (MPa)	P_r range[1)] (MPa)	P_{si} routine analysis (MPa)	P_{si} range[1)] (MPa)
296.0	280.9	10.5	9.5	8.2 - 10	8.2	8.1 - 8.2
303.5	288.0	20.9	11.7	9.3 - 12	8.8	8.4 - 8.8
319.3	302.8	17.0	13.5	13.4 - 14.5	11.5	9.2 - 11.5
325.4	308.5	15.5	13.5	12.6 - 14.1	12.4	10.9 - 12.4
331.5	314.2	13.8	10.0	9.5 - 10.5	9.5	7.8 - 9.5
383.5	363.0	17.7	12.4	12.5 - 14	10.1	8.8 - 10.1
416.0	393.8	12	11.0	9.5 - 11.0	8.2	7.2 - 8.2
417.7	395.5	-	-	> 7.5[2)]	-	> 7.5[2)]
471.0	446.9	13.5	12.0	8.9 - 12	9.4	9.0 - 9.4
490.5	465.8	22.4	18.3	12.5 - 18.3	10.3	9.4 - 10.3
499.5	474.8	11.5	6.6	10 - 11	11.1	10.2 - 11.1
510.8	485.6	24.1	10.7	10.7 - 12.5	11.5	10.3 - 11.5
517.0	491.6	14	9.6	9.6 - 13	11.6	10.8 - 11.6
579.0	552.2	17.6	13.4	13.4 - 15	14.7	13.8 - 14.7
604.2	577.0	14.2	9.8	9.8 - 12	12.1	11.2 - 12.1
681.0	652.9	19.6	14.3	13.9 - 14.3	13.7	12.9 - 13.7
689.5	661.3	18.1	14.5	14 - 14.5	13.7	12.6 - 14.0
702.5	674.2	24	17.2	17.2 - 20	20.7	18 - 20.7
708.0	679.6	24.9	21.2	17.7 - 21.2	16.7	15 - 16.7
712.8	684.4	22	19.4	19.4 - 20	19.7	15 - 19.7

[1)] *The routine analysis values were derived as described in Section 4.1. The range values indicate a subjective uncertainty when values are directly determined from the overview plots (see test description in Section 4.1).*

[2)] *no stimulation conducted, but used for permeability estimation*

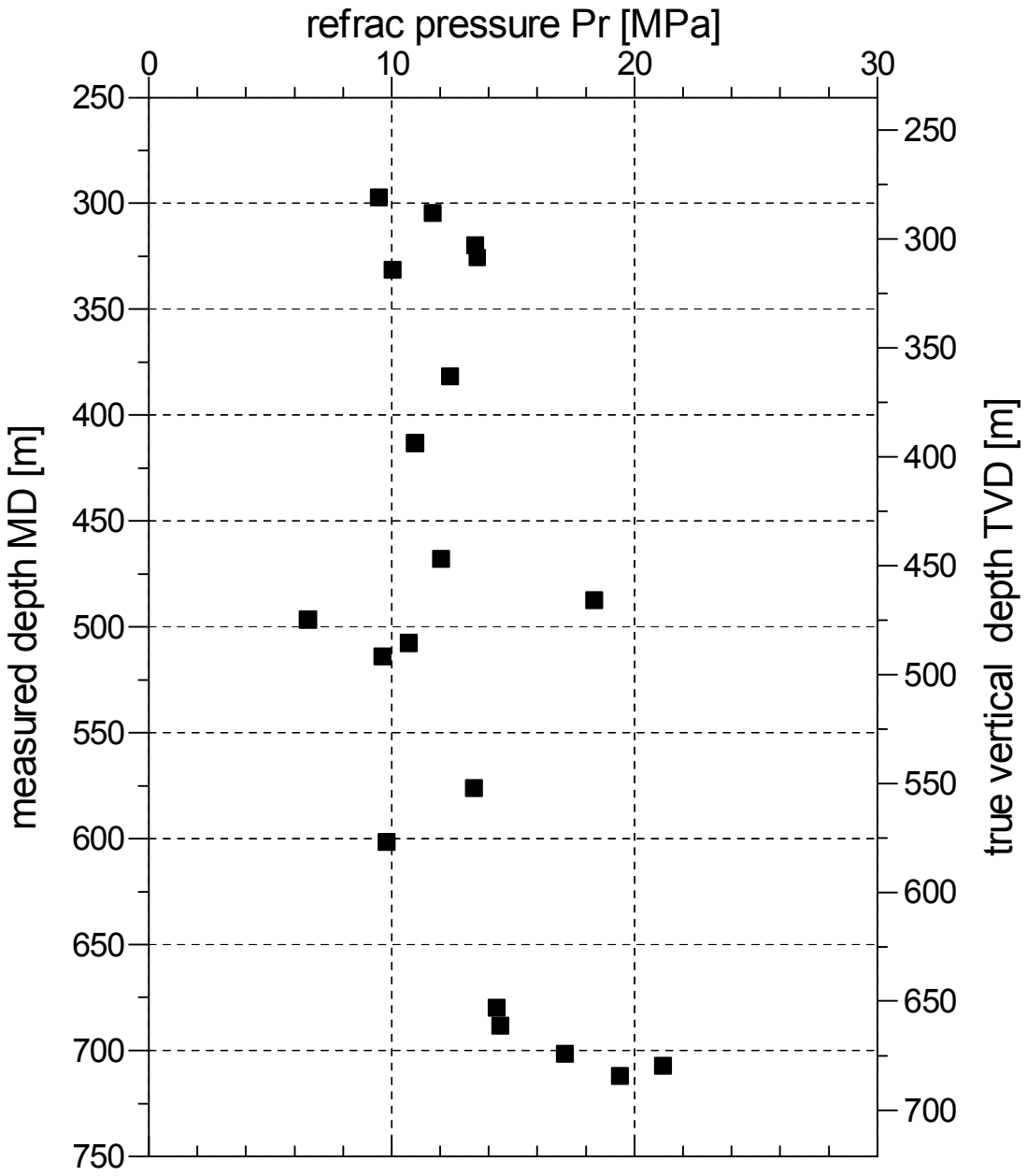

Figure 4-1. *Refrac pressure P_r.*

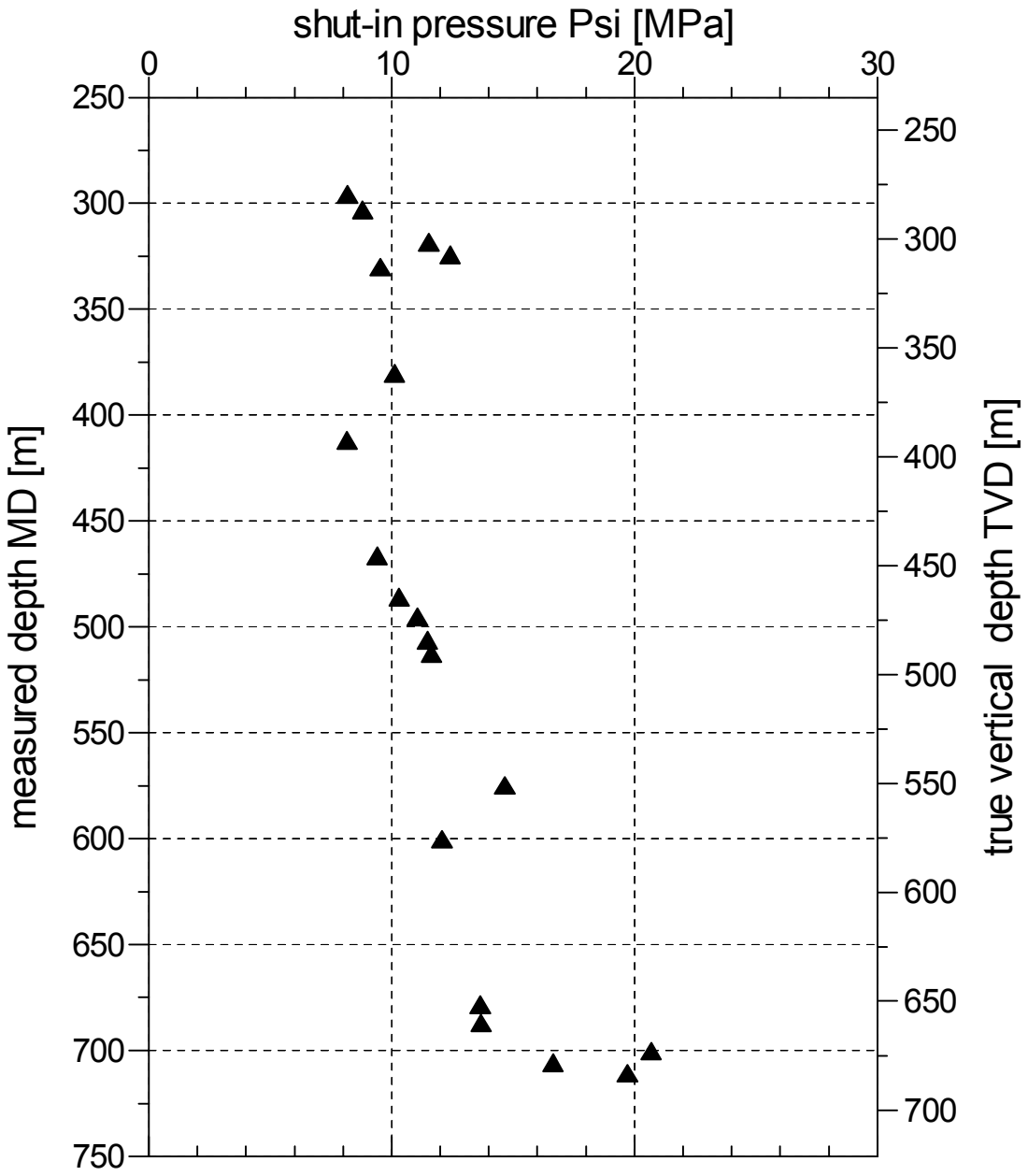

Figure 4-2. *Shut-in pressure Psi.*

4.3 Fracture Orientation Data

The information from the impression packer tests is summarized in Table 4.2, giving the strike, dip and dip directions of fractures identified from the fracture traces. Strike directions and dip are shown graphically in Figure 4.3 and in the lower hemisphere polar plot of Figure 4.4. It should be noted that the uncertainty of the orientation is app. ± 15 degrees, mainly due to the small borehole diameter. The angular values in Table 4.2 and Figures 4.3 and 4.4 are corrected with respect to the borehole inclination and with respect to the magnetic declination at Oskarshamn. To compensate the local magnetic declination 3 degrees have been added to the compass readings.

In most cases axial fractures (axial with respect to the borehole axis) were induced. Some of the stimulated inclined fractures (inclined with respect to the borehole axis) were nearly vertical fractures except the inclined fractures in the test sections at 280.9, 288 or 314.2 m (TVD). Surprisingly, all of the induced or stimulated fractures show azimuths between app. 102 and 175 degrees with a mean value of 145 ± 18 degrees (induced axial fractures : 148 ± 16 degrees, stimulated axial fractures : 135 ± 15 degrees). No conjugated natural joints / fractures with NE - SW strike was observed which one generally expects in crystalline rock masses. This fact creates a major difficulty to apply the PSI- or HTPF - inversion method to derive stresses from shut-in pressure data.

Table 4-2. Orientation of induced or stimulated fractures derived from impression packer testing in borehole no. KOV01. θ: strike direction (counted North over East), β: dip direction (counted North over East), α: dip (with respect to horizontal).

measured depth MD (m)	true vertical depth TVD (m)	fracture trace	θ (deg)	β (deg)	α (deg)	remarks
296.0	280.9	A	161	251	46	inclined fracture
303.5	288.0	A	137	227	26	inclined fracture
319.3	302.8	A	144	234	71	axial fracture
		B	148	58	81	inclined fracture
325.4	308.5	A	141	231	71	axial fracture
		B	141	51	83	inclined fracture
331.5	314.2	A	176	86	42	inclined fracture
383.5	363.0	A	132	222	70	axial fracture
416.0	393.8	A	144	234	74	axial fracture
471.0	446.9	A	158	248	78	axial fracture
		B	107	17	69	inclined fracture at upper end of impression tool
		C	92	2	13	horizontal fracture at lower end of impression tool
490.5	465.8	A	102	192	77	axial fracture
499.8	474.8	A	175	265	58	inclined fracture / joint
		B	158	248	79	axial fracture
		C	137	227	58	inclined fracture
510.8	485.6	A	168	258	80	axial fracture
		B	176	86	64	inclined fracture at upper end of impression tool
517.0	491.6	A	161	251	79	axial fracture
579.0	552.2	A	179	269	83	axial fracture
		B	21	110	83	inclined fracture at lower end of impression tool
604.2	577.0	A	119	209	90	steeply inclined fracture
		B	68	158	83	short axial single trace
		C	98	8	62	inclined fracture
		D	141	51	64	inclined fracture at lower end of impression tool
681.0	652.9	A	147	237	84	axial fracture
689.5	661.3	A	124	214	82	axial fracture
		B	135	45	79	inclined fracture at upper end of impression tool
		C	147	57	62	inclined fracture at lower end of impression tool
702.5	674.2	A	133	223	83	axial fracture
		B	135	45	76	inclined fracture
		C	128	38	76	inclined fracture at lower end of impression tool
708.0	679.6	A	127	217	82	axial single trace
712.8	684.4	A	133	223	82	axial fracture
		B	60	330	64	inclined fracture
		C	82	352	51	inclined fracture at lower end of impression tool

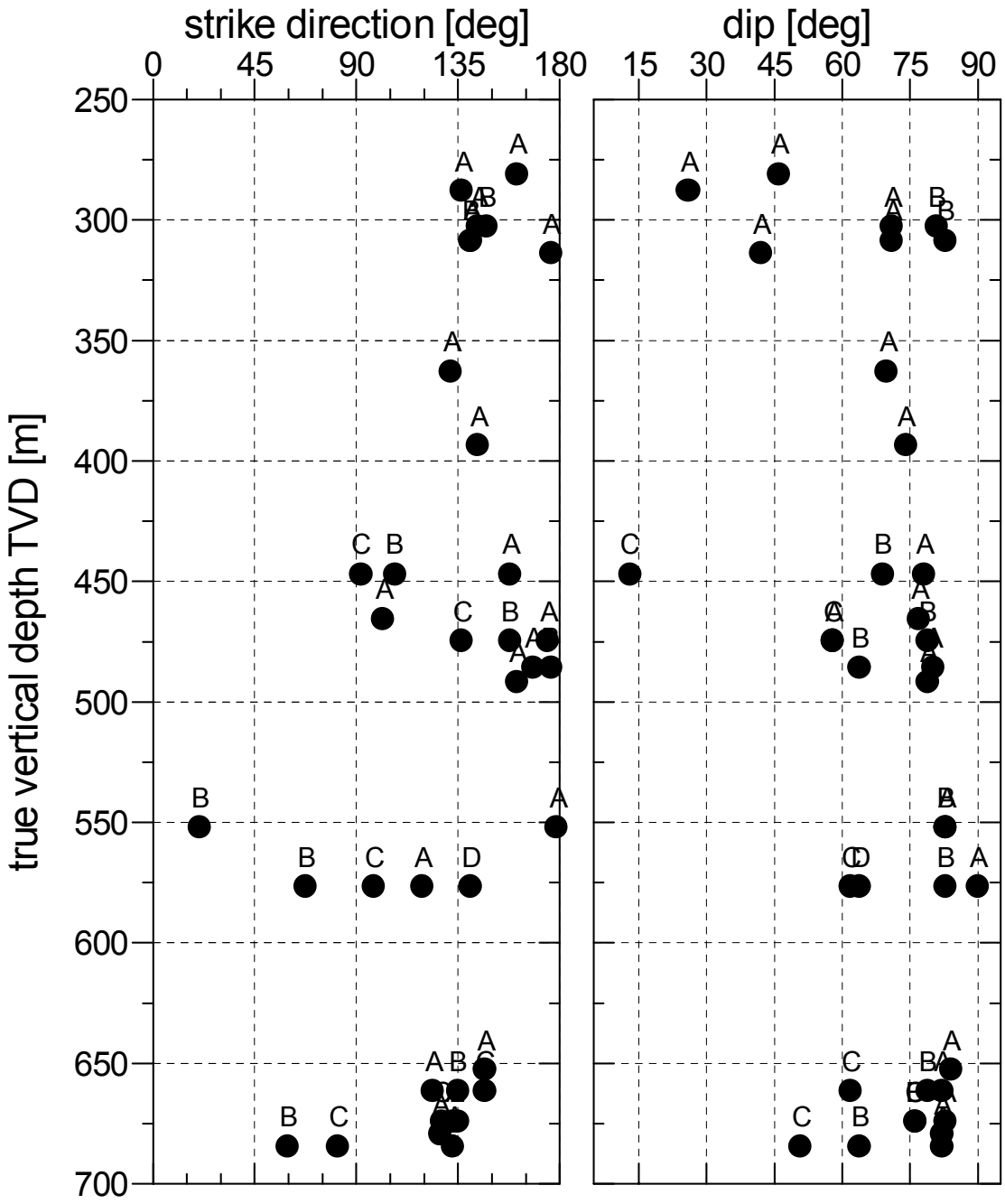

Figure 4-3. *Orientation of induced or stimulated fractures derived from impression packer testing in borehole no. KOV01.*

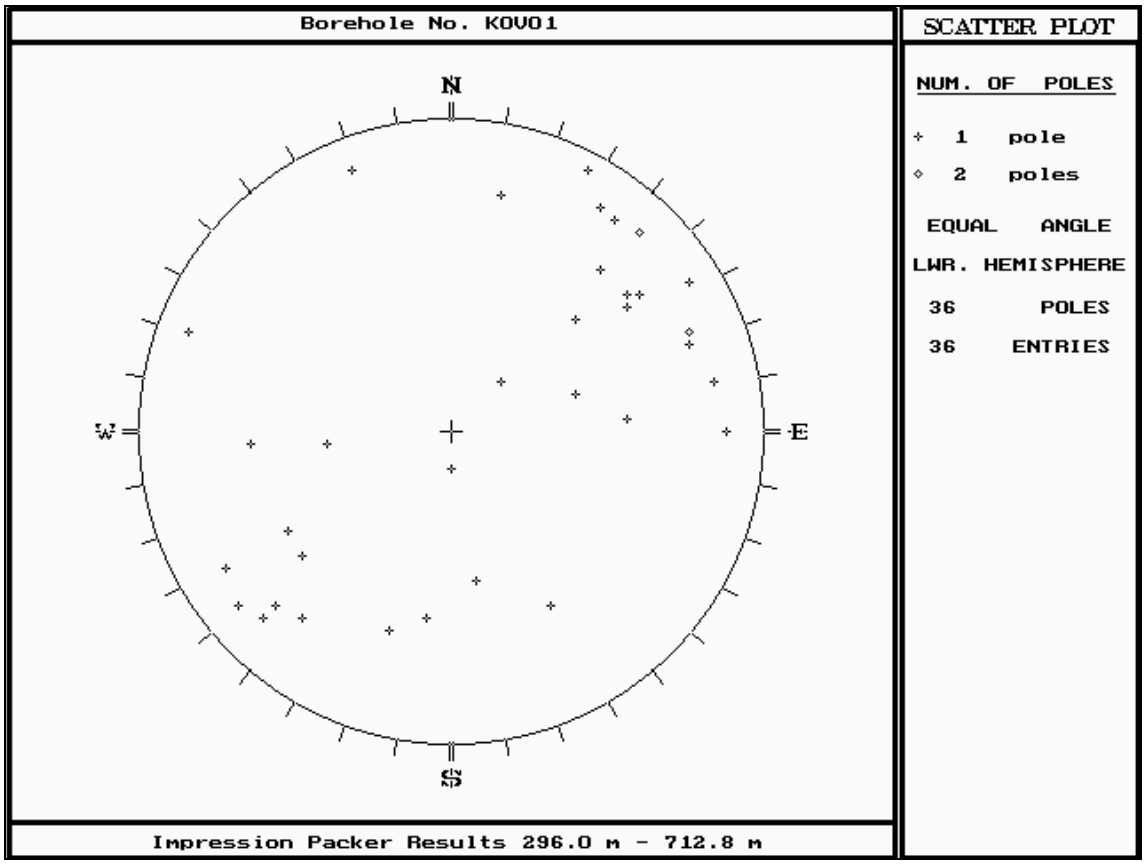

Figure 4-4. *Orientation of induced or stimulated fractures derived from impression packer testing in borehole no. KOV01 (lower hemisphere polar - plot).*

4.4 Observation of Water Recovery

In the test summary on the overview plots for each test (APPENDIX A) the total volume of injected water and the recovered water after the test is given. The information is summarized in Table 4.3.

It is interesting to note that the water recovery from stimulated pre-existing fractures is significant (say 25%) compared to the poor recovery from new induced fractures (some % only). However, there are some exceptions:

- the induced fractures at 288 m and 652.9 m show high recovery of 36 and 20%, respectively,
- the stimulated fractures at 393.8, 674.2 and 684.6 show poor recovery (1 - 3.5%).

Table 4-3. Injected and recovered water volumes.

[1] *induced fracture*
[2] *stimulated fracture*
[3] *no stimulation test, but used for permeability analysis*

MD (m)	TVD (m)	P_{max} (MPa)	V_{inj} (l)	V_{rec} (l)	V_{rec} (%)
296.0	280.9	10.5[2]	64	30	47
303.5	288.0	20.9[1]	49	18	36
319.3	302.8	17.0[1]	52	0.6	1
325.4	308.5	15.5[1]	56	5	9
331.5	314.2	13.8[1]	47	2	4
383.5	363.0	17.7[1]	66	1	1
416.0	393.8	12[2]	59	0.4	1
417.7	395.5[3]	-	-	-	-
471.0	446.9	13.5[2]	57	14	25
490.5	465.8	22.4[1]	66	1	2
499.8	474.8	11.5[2]	95	30	31
510.8	485.6	24.1[1]	45	5	11
517.0	491.6	14[2]	52	6	12
579.0	552.2	17.6[1]	55	3.5	6
604.2	577.0	14.3[2]	68	16	23
681.0	652.9	19.6[1]	44	9	20
689.5	661.3	18.1[2]	53	6	11
702.5	674.2	24[2]	54	2	4
708.0	679.6	24.9[1]	50	2	4
712.8	684.4	22[2]	50	1	2

4.5 Analysis of the Pressure Pulse Test

Before each hydraulic fracturing test cycle a short pressure pulse test (P-test) was conducted to test the suitability of the test interval for the subsequent fracturing test, but also to determine the rock permeability of the test section. The permeability estimate is based on the classical method suggested by Cooper et al. (1967) for the analysis of conventional slug tests. For the high stiffness wireline packer system MeSy has developed the software code PERM where theoretical and measured pressure decays are compared (master curve matching method). The theoretical pressure decay curves are calculated with a variety of input parameters such as storage coefficient and rock permeability.

The analysis of the pressure pulse tests is given in APPENDIX I. The derived permeability and conductivity data for each test interval are given in Table 4.4 and are graphically shown in Figure 4.5. Tight test intervals without pre-existing fractures are characterized by a rock permeability of app. 1 µDarcy while test intervals with obvious pre-existing fractures show apparent permeability values of some tens of µDarcy.

Table 4-4. Test section permeability / conductivity[1)].

measured depth MD (m)	true vertical depth TVD (m)	permeability k (μDarcy = 10^{-18} m^2)	conductivity K m/s
296.0	280.9	26.4	$26 \cdot 10^{-11}$
303.5	288.0	1.5	$0.1 \cdot 10^{-11}$
319.3	302.8	0.6	$0.6 \cdot 10^{-11}$
325.4	308.5	1.3	$1.3 \cdot 10^{-11}$
331.5	314.2	2.1	$2.0 \cdot 10^{-11}$
383.5	363.0	1.3	$1.3 \cdot 10^{-11}$
416.0	393.8	19.5	$19 \cdot 10^{-11}$
417.7	395.5	47.3	$46 \cdot 10^{-11}$
471.0	446.9	17.0	$17 \cdot 10^{-11}$
490.5	465.8	0.8	$0.8 \cdot 10^{-11}$
499.8	474.8	13.1	$13 \cdot 10^{-11}$
510.8	485.6	0.9	$0.9 \cdot 10^{-11}$
517.0	491.6	15.9	$15 \cdot 10^{-11}$
579.0	552.2	1.3	$1.3 \cdot 10^{-11}$
604.2	577.0	4.7	$4.6 \cdot 10^{-11}$
681.0	652.9	0.3	$0.3 \cdot 10^{-11}$
689.5	661.3	12.5	$12 \cdot 10^{-11}$
702.5	674.2	2.0	$2 \cdot 10^{-11}$
708.0	679.6	0.4	$0.4 \cdot 10^{-11}$
712.8	684.4	2.5	$2.5 \cdot 10^{-11}$

1) $K = \frac{k \cdot \rho_{water} \cdot g}{\eta}$

ρ_{water} : *density of water (10^3 kg / m^3)*
g : *gravity acceleration (9.81 m/s^2)*
η : *viscosity of water (1cP = 10^{-3} Pa·s)*

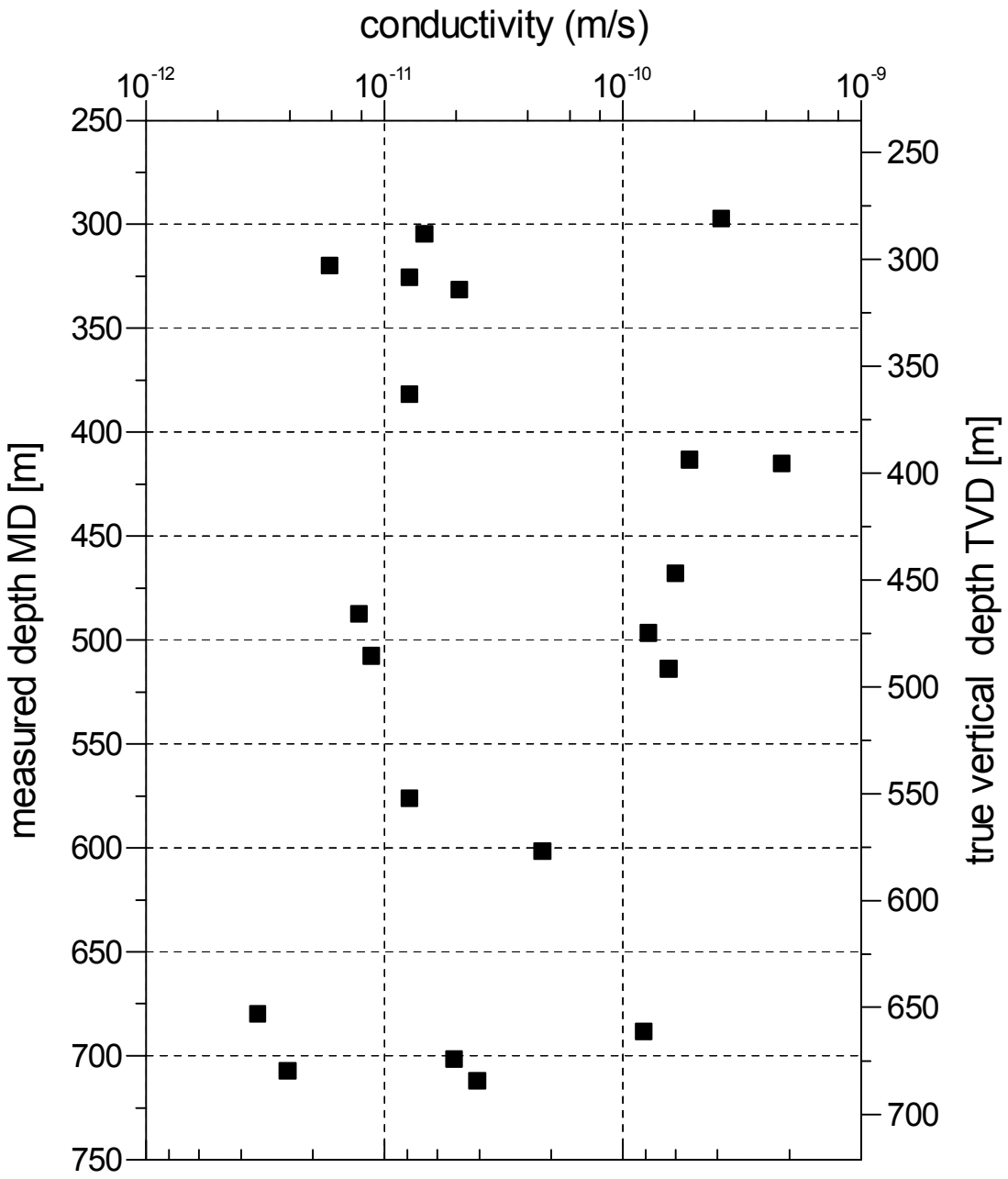

Figure 4-5. *Test section conductivity.*

5 Data Analysis

5.1 In - situ Stress Computation

As shown in chapter 4.1.3 in the majority of tests axial or vertical / sub-vertical fractures with a consistent NW - SE strike direction (145° ± 18°) were initiated or stimulated. Therefore, in-situ stresses can be calculated with the "classical" Hubbert & Willis (1957) concept (see Section 3.1):

- $S_v = \rho \cdot g \cdot z$
- $S_h = P_{si}$
- $S_H = 3\ S_h - P_r$

The vertical stress S_v is calculated assuming a constant density for the overburden rock of $\rho = 2.7$ g/cm^3. The relation $S_h = P_{si}$ is based on the assumption that the induced fractures propagated in a direction perpendicular to the least principal stress S_h or the most favourable oriented pre-existing fractures were stimulated and reopened. In the estimate of the major horizontal stress S_H the pore pressure is neglected with respect to the low porosity / permeability of crystalline rocks.

The calculation is carried out using the Refrac- and Shut-in pressure data P_r and P_{si} derived by the routine analysis shown in APPENDIX A and given in Table 4.1. The stress data are listed in Table 5.1 together with the azimuths of the axial fractures as given in Table 4.2. Note, that we assumed the axial fracture was the "active" fracture in the cases where more than one fracture trace was observed, and that the minimum horizontal stress S_h for the inclined fractures in the test interval at 280.9, 288.0 and 314.2 m TVD where derived by consideration of the dip angle α of the fractures. The stress data are shown graphically in Figure 5.1.

Due to the large variations in P_{si} - data and the narrow range for the fracture azimuths the stress calculation by an inversion method does not lead to any meaningful result. Thus, at present, the significant scatter in stress must be accepted, although a more homogeneous stress profile is expected for the homogeneous rock mass in the Oskarshamn - Laxemar - Äspö region.

Table 5-1. Magnitudes of vertical Stress S_v, the minor horizontal stress S_h, the major horizontal stress S_H, and the direction of S_H, θ_{SH}.

TVD (m)	S_v (MPa)	S_h (MPa)	S_H (MPa)	θ_{SH}, N over E (deg)
280.9	7.4	9.0[2)]	---	161
288.0	7.6	13.9[2)]	---	137
302.8	8.0	11.5	21.0	144
308.5	8.2	12.4	23.7	141
314.2	8.3	10.9[2)]	---	176
363.0	9.6	10.1	17.9	132
393.8	10.4	8.2	13.6	144
446.9	11.8	9.4	16.2	158
465.8	12.3	10.3	19.0[1)]	102
474.8	12.6	11.1	26.7	158
485.6	12.9	11.5	23.8	168
491.6	13.0	11.6	25.2	161
552.2	14.6	14.7	30.7	179
577.0	15.3	12.1	26.5	119
652.9	17.3	13.7	26.8	147
661.3	17.5	13.7	26.6	124
674.2	17.9	20.7	44.9	133
679.6	18.0	16.7	28.9	127
684.4	18.1	19.7	39.4	133

1) *the P_r - value is derived from the Step-Rate test, 12.5 MPa is used*

2) *S_h is calculated with the P_{si}-value and the value of S_v for an inclined fracture plane with dip α and a strike direction of θ_{SH} by*

$$S_h = \frac{P_{si} - \frac{1}{2} S_v (1 + cos\, 2\alpha)}{\frac{1}{2}(1 - cos\, 2\alpha)}$$

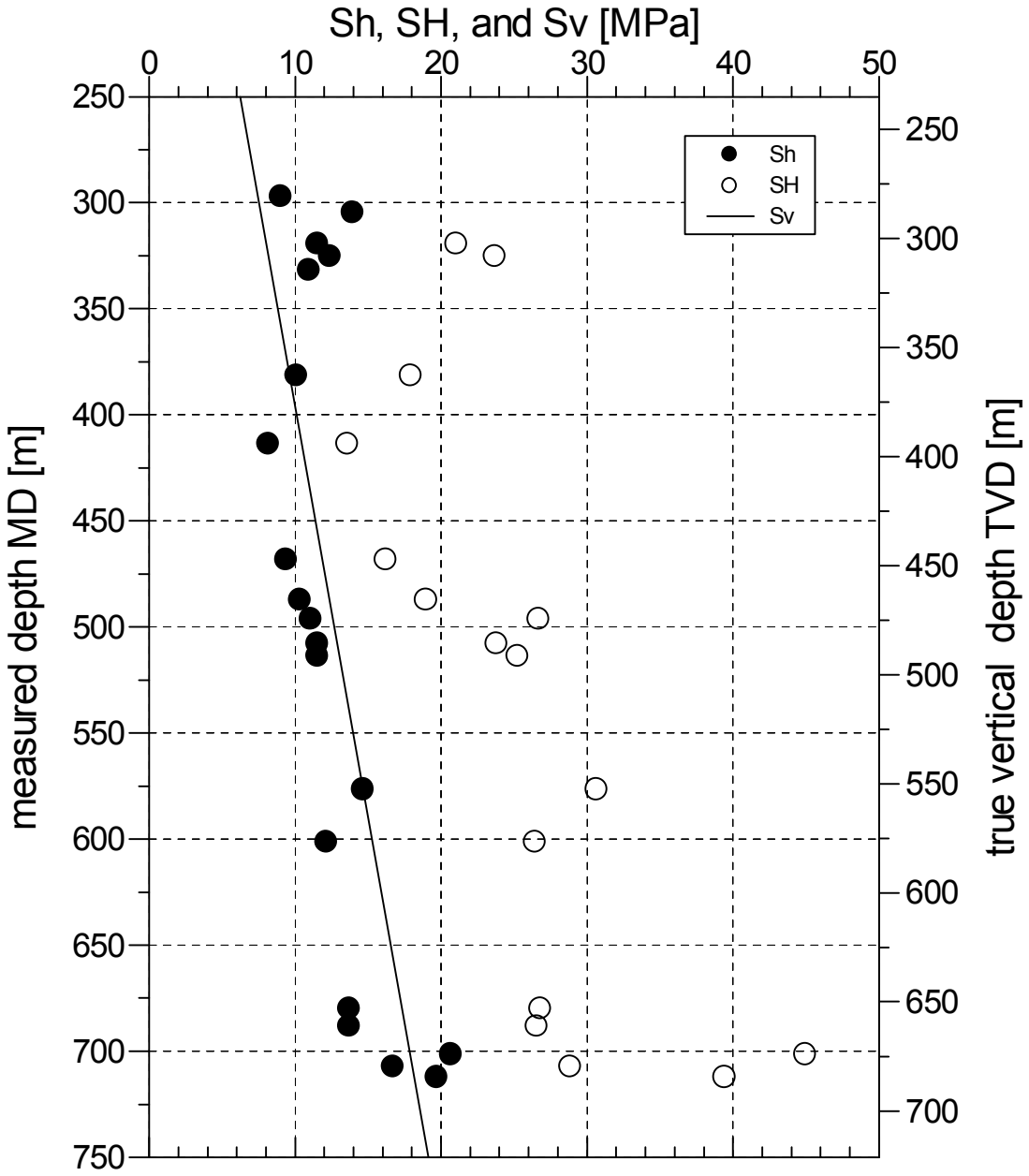

Figure 5-1. *Stress Magnitudes S_v, S_h and S_H in MPa for borehole KOV01.*

5.2 Quality Control by Laboratory Test Results

5.2.1 Core Characterization

The core material was first characterized by density and ultrasonic velocity testing. The rock density values are given in Table 5.2. The rock can be characterized by a mean density value of (2.69 ± 0.023) g/cm^3. The density test data are given in APPENDIX D.

Table 5-2. Rock density of the core material.

core piece - no.	mean depth (m)	density (g/cm^3)
1	333.79	2.705 ± .018
2	383.16	2.690 ± .031
3	438.33	2.680 ± .015
4	463.85	2.700 ± .008
5	500.40	2.694 ± .010
G1 - G3	app. 500	2.66 ± .04
6	559.90	2.722 ± .027
7	596.65	2.709 ± .012
8	648.89	2.701 ± .010
9	692.78	2.691 ± .014
10	709.55	2.637 ± .017
mean		**2.690 ± .023**

The ultrasonic test results are given in Table 5.3. The mean data are:

P - wave velocity v_p : 5.43 km/s (± 0.18)
S - wave velocity v_s : 3.05 km/s (± 0.12)
Young's modulus E : 64 GPa (± 4)
Poisson's ratio ν : 0.27 (± 0.01)

Concerning elasticity the rock can be described as isotropic. It may be of interest that the core from app. 700 m depth shows low velocities and consequently a low Young's modulus (E = 55 GPa). Otherwise the rock can be described also as homogenous with respect to elasticity. For details see also the Ultrasonic Velocity Data and Elasticity Data Sheets in APPENDIX E and APPENDIX F.

Table 5-3. Ultrasonic velocities v_p and v_s and dynamic elastic parameters Young's modulus E and Poisson's ratio ν.

ultrasonic velocities		radial		axial	
MeSy core-no./ sample-no	depth (m)	v_p (km/s)	v_s (km/s)	v_p (km/s)	v_s (km/s)
1	333.79	5.47±.08	3.14±.07	5.47±.12	2.72±.48
2	383.16	5.41	3.07	5.58±.02	3.15±.08
3	438.33	5.41±.09	3.08±.02	5.44±.08	3.07±.02
4	463.85	5.47±.10	3.11±.01	5.55±.01	3.17±.08
5	500.40	5.31	3.01	5.50±.05	3.12±.06
6	559.90	5.36	2.99	5.42±.11	3.12±.09
7	596.65	5.83	3.05	5.64±.06	3.20±.07
8	648.89	5.26±.09	3.01±.03	5.52±.02	3.16±.02
9	692.78	5.38±.11	3.01±.04	5.44±.12	3.07±.10
10	709.55	5.05±.21	2.86±.16	5.05±.04	2.92±.04
mean		**5.40±.19**	**3.03±.07**	**5.46±.15**	**3.07±.14**

elastic parameters		radial		axial	
MeSy core-no./ sample-no	depth (m)	E_{dyn} (GPa)	ν_{dyn}	E_{dyn} (GPa)	ν_{dyn}
1	333.79	67±3	0.26±.01	62±4	0.29±.01
2	383.16	64	0.26	68±3	0.27±.02
3	438.33	65±1	0.26±.01	64±1	0.27±.01
4	463.85	66±1	0.26±.01	68±3	0.26±.01
5	500.40	62	0.26	67±2	0.26±.01
6	559.90	62	0.28	66±4	0.26±.01
7	596.65	64	0.26	70±3	0.27±.01
8	648.89	62±1	0.26±.01	68±1	0.26
9	692.78	63±2	0.28±.01	65±3	0.26
10	709.55	55±6	0.27	56±1	0.25
mean		**63±3**	**0.265**	**65±4**	**0.265**

5.2.2 Fracture Toughness

The results of the fracture toughness tests on 20 core samples are given in Table 5.4. The K_{IC} Test Data Sheets are given in APPENDIX G. The tests yield a mean fracture toughness $K_{IC} = (2.54 \pm 0.27)$ MN/m$^{3/2}$.

Table 5-4. Fracture toughness K_{IC} of the core material.

sample no.	mean depth (m)	diameter D (mm)	Chevron notch length a_o (mm)	F_{max} (N)	K_{IC} (MN/m$^{3/2}$)
1A1-2	333.79	47.6	7.0	2927	2.90
1A2-3	333.79	47.6	7.0	2547	2.53
1B1-2	333.79	47.6	7.0	2617	2.60
2A1-2	383.16	47.4	6.9	2736	2.73
2A2-3	383.16	47.4	6.0	3023	2.83
4A1-2	463.85	47.4	6.8	2700	2.67
4B1-2	463.85	47.4	7.2	2665	2.71
5A1-2	500.40	51.7	7.3	2672	2.30
5A2-3	500.40	51.7	7.1	2698	2.30
G1[1)]	app. 500				2.18
G2[1)]	app. 500				2.37
G3[1)]	app. 500				2.41
6A1-2	596.65	47.2	7.0	2228	2.25
6A2-3	596.65	47.2	7.0	2900	2.93
7A1-2	578.16	47.2	7.1	1866	1.90
7A2-3	578.16	47.2	7.3	2585	2.67
8B1-2	648.89	47.3	7.2	2500	2.55
8B2-3	648.89	47.3	6.6	2416	2.37
9A1-2	692.78	51.9	7.0	2789	2.34
10A1-2	709.55	51.9	5.2	3385	2.53
mean					**2.54±.27**

[1)] no Test Data Sheet exists in App. G (preliminary test sample)

5.2.3 Hydrofrac Tests on Minicores

The results of the hydrofrac tests on core pieces of 47 mm diameter or on mini-plugs of 30 mm diameter are given in Table 5.5 and are shown graphically in Figure 5.2. The corresponding Hydrofrac Data sheets are given in APPENDIX H.

The breakdown pressure p_c as a function of confining pressure p_m can be described by a linear relation

$$p_c = p_{co} + k \cdot p_m$$

with $p_{co} = (29.4 \pm 2)$ MPa
$k = 1.33 \pm 0.08$.

The hydraulic tensile strength $p_{co} = 29.4$ MPa derived from samples subjected to confining pressure is confirmed by the unconfined test on sample G2B ($p_{co} = 34.7$ MPa, 3 mm ID, 1 ml/s). Unconfined tests on samples with a larger injection hole diameter (8 mm ID) and conducted at lower injection rates (0.5 / 0.1 ml/s) yield a significantly lower hydraulic tensile strength value. This indicates the size and injection rate dependence of hydraulic strength.

Table 5-5. Hydrofrac tests on mini-cores (σ_1: axial stress, p_m: confining pressure, p_c: breakdown pressure)

sample - no.	σ_1 (MPa)	p_m (MPa)	p_c (MPa)	remark
1A2a	22.5	18.6	55.3	3 mm ID / 1 ml/s
1A2b	66.6	39.4	81.1	dto.
2A3a	32.4	30.2	65.8	dto.
2A3b	21.8	10.8	48.9	dto.
3Ca	32.6	11.0	44.4	dto.
3Cb	61.4	34.6	72.7	dto.
4B1a	53.3	24.8	61.8	3 mm ID / 1 ml/s
4B1b	20.1	14.7	47.0	dto.
5A1a	11.0	5.3	38.4	dto.
5A1b	67.6	38.6	79.8	dto.
6A1a	32.5	25.2	68.2	dto.
6A1b	36.2	22.4	62.2	dto.
7A1a	30.1	26.8	69.7	dto.
7A1b	67.6	37.1	80.6	dto.
8B2a	12.7	7.9	41.6	dto.
9A1a	17.9	13.0	46.4	dto.
9A1b	10.6	7.8	32.8	dto.
10A1a	38.4	17.0	45.0	dto.
G1A[1)]	8.6	0	19.3	8 mm ID / 0.1 ml/s
G1B[1)]	7.9	0	20.4	dto.
G2A[1)]	8.0	0	27.2	8 mm ID / 0.5 ml/s
G2B[1)]	9.0	0	34.7	3 mm ID / 1 ml/s
G3A[1)]	4.6	0	24.6	3 mm ID / 0.1 ml/s
G3B[1)]	5.3	0	24.4	3 mm ID / 0.1 ml/s

[1)] *no Hydrofrac Data Sheet exists in App. H (preliminary test sample)*

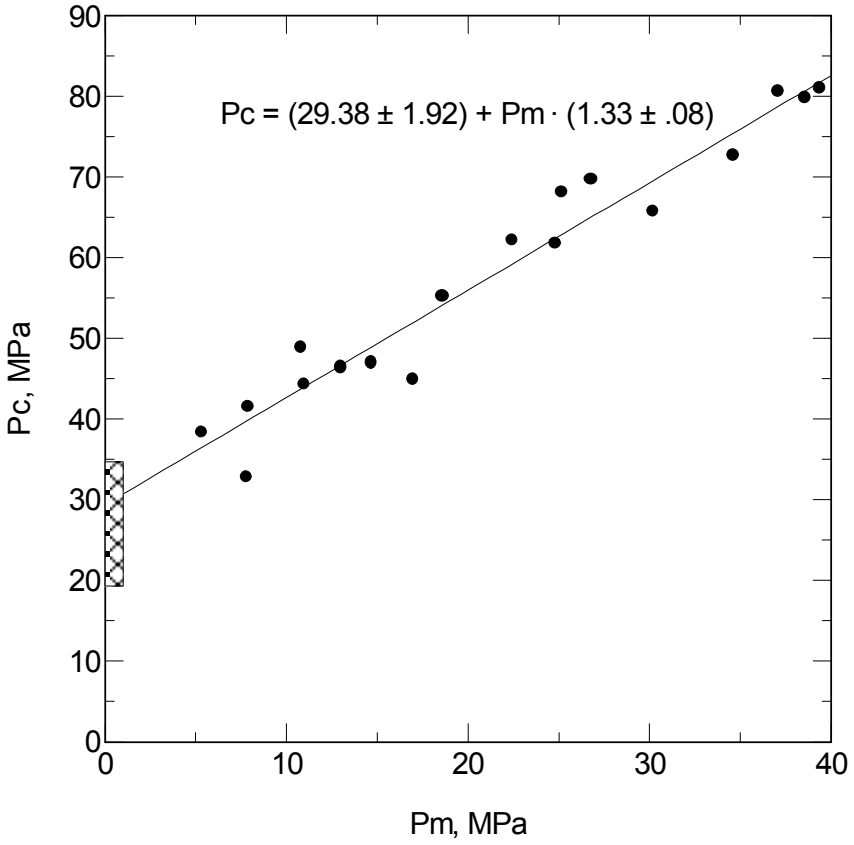

Figure 5-2. *Breakdown pressure p_c as a function of confining pressure p_m for hydrofrac tests on mini-cores.*

5.2.4 Application of Laboratory Test Results

The results of the laboratory tests on the core material from borehole KOV01 can be summarized as follows :

– rock density ρ, g/cm^3 : 2.69 ± 0.023

  The mean rock density of 2.7 g/cm^3 was used to estimate the overburden stress which is considered as a principal stress.

– Ultrasonic velocities v_p and v_s :

v_p, radial, km/s :	5.40 ± 0.19
v_p, axial, km/s :	5.46 ± 0.15
mean :	5.43 ± 0.18
v_s, radial, km/s :	3.03 ± 0.07
v_s, axial, km/s :	3.07 ± 0.14
mean :	3.05 ± 0.12

The ultrasonic velocity measurements served both, to characterize the rock with respect to homogeneity and isotropy, and to determine rock elasticity parameters. Considering the small scatter, the rock can be characterized as extremely homogeneous and isotropic with respect to elasticity.

– elasticity parameters Young's modulus E and Poisson's ratio ν:

The dynamic elasticity parameters E_{dyn} and ν_{dyn} were calculated by using the ultrasonic velocity data and the rock density data by the following relations :

$$E_{dyn} = 2\, v_s^2 \cdot \rho\, (1 + \nu_{dyn})$$

$$\nu_{dyn} = \frac{1}{2} \cdot \frac{2 - (v_p / v_s)^2}{1 - (v_p / v_s)^2}$$

The following mean values were obtained and were subsequently used in the hydrofrac simulation calculations in Section 5.2.4.3:

E_{dyn}, GPa : 64 ± 4

ν_{dyn} : 0.27 ± 0.01

– fracture toughness K_{IC}, $MN/m^{3/2}$:

The fracture toughness K_{IC} ranges between 1.9 and 2.9 $MN/m^{3/2}$ with a mean value of (2.54 ± 0.27) $MN/m^{3/2}$, which is used in the fracture mechanics hydrofrac simulation calculation of Section 5.2.4.3. The values are rather high when compared to other granite rocks (Atkinson & Meredith, 1987).

– tensile strength p_{co} and hydrofrac coefficient k :

p_{co}, MPa : 29.4 ± 2

k : 1.33 ± 0.08

The mean hydrofrac tensile strength of the rock is high when compared to other granites (e.g. Rummel 1987). Similarly, the value of k = 1.33 is high when compared to other granites (e.g. k = 1.04 for the coarse grained Falkenberg granite, Rummel 1987), but is much smaller then k = 2 for a flawless material. Thus, the k value observed which only depends on the crack size is an expression for the importance of a fracture mechanics analysis of hydraulic fracturing tests in crystalline rock as already indicated at the end of Section 3.1 and therefore such an approach can be considered as a necessary quality control particularly for hydrofrac tests in so-called "intact" rock sections - (again we refer to Rummel 1987 or Rummel 2001).

5.2.4.1 Comparison of In - Situ and Laboratory Tensile Rock Strength

Following a fracture mechanics approach to hydraulic fracturing (Rummel, 1987) a simple scaling relation between the in-situ and laboratory rock strength P_{co} and p_{co} exists :

$$P_{co} = p_{co} \sqrt{r / R}$$

where R and r are the radii of the injection boreholes for the in-situ and laboratory tests, respectively. Using the laboratory results of tests in 3 mm and 8 mm diameter boreholes, the in-situ tensile strength for tests in 76 mm diameter boreholes can thus easily be estimated:

r or R (mm)	1.5	4	38
p_{co} or P_{co} (MPa)	29.4	≈ 20	5.8

The in-situ measured hydraulic tensile strength was (5.2 ± 3) MPa and thus is in good agreement with the estimated strength value of 5.8 MPa. The result will not vary dramatically if we also consider that the laboratory tests were conducted with oil (viscosity: 25 cPoise) while the in-situ tests were conducted with water (1cPoise) as injection fluid. The injection rates of 1 ml/s (laboratory) and some l/min (in-situ) were appropriate with respect of the system stiffness.

5.2.4.2 Estimation of Crack Size

Again following Rummel (1987) the characteristic size for the in-situ rock at "intact" test intervals and for laboratory test specimens, the crack length A_o and a_o, may be estimated using the fracture mechanics definition of hydraulic tensile strength:

laboratory : $$p_{co} = \frac{K_{IC}}{(h_o + h_a) \cdot \sqrt{r}}$$

in-situ : $$P_{co} = \frac{K_{IC}}{(H_o + H_A) \cdot \sqrt{R}}$$

The functions h_o, h_a, H_o and H_A are known dimensionless stress intensity factors which only depend on the crack size (crack length a and A, respectively) and on the fluid pressure distribution within the cracks (h_a, H_A) (for reference see Rummel, 1987).

Using above relations and the measured values of K_{IC}, p_{co}, P_{co}, r and R, the values of (h_o + h_a) and (H_o + H_A) are obtained which then yield a_o and A_o. The calculation shows the following intrinsic microcrack sizes for fluid filled cracks:

laboratory rock sample : $a_o \approx 1$ mm
in-situ rock : $A_o \approx 30$ mm.

Considering the granitic rock type and the experimental procedure (low injection rates) this result can be accepted particularly for the TBM boring damaged zone around the borehole. This means that during the in-situ hydrofrac tests such microcracks were first saturated and pressurized before they became unstable and rapidly propagated during the initial frac-cycle.

5.2.4.3 Hydrofrac Simulation Calculation

Various analytical hydrofrac simulation models on the basis of the fracture mechanics and fluid dynamics were developed by MeSy (e.g. Rummel & Hansen 1989, te Kamp 1991). The models are used for sensitivity analysis of input parameters and to match simulated hydrofrac records with in-situ measured hydrofrac test records. The present analysis is conducted with the MeSy code HSIMU which contains the following input variables:

- borehole and test interval dimensions
- hydraulic system stiffness
- fluid viscosity and fluid injection rate
- rock elasticity and fracture toughness
- initial micro-crack size (length)
- principle stresses
- pressure loss at the fracture inlet.

Here only one simulation calculation was carried out as an example to simulate the hydrofrac test record obtained for the test section at 485.6 m (TVD). The input parameters are given in Table 5.6. The comparison is shown in Figure 5.3 and shows that the calculated pressure record for the frac cycle matches quite well with the frac cycle record observed during the in-situ test.

Table 5-6. Input parameter for the hydrofrac simulation at test interval at 485.6 m (TVD).

Number of simulation model: 3		
borehole:	radius	3.8 cm
	length of injection interval	0.7 m
rock:	permeability	1 μDarcy
	porosity	0 %
	Youngs's modulus	60 GPa
	Poisson's ratio	0.26
	fracture toughness	2.54 $MN/m^{3/2}$
stresses:	Sigma 1	23.8 MPa
	Sigma 3	11.5 / 12.0 MPa
frac-fluid:	density	1 g/cm^3
	viscosity	1 cPoise
	injection rate	1.1 lpm
	pressure loss (inlet)	0 %
	pressure loss (fracture)	0.3
crack characteristics:	microcrack length	30 mm
	final crack length	30 m
	number of add. cracks	0
	effectivness of cracks	0

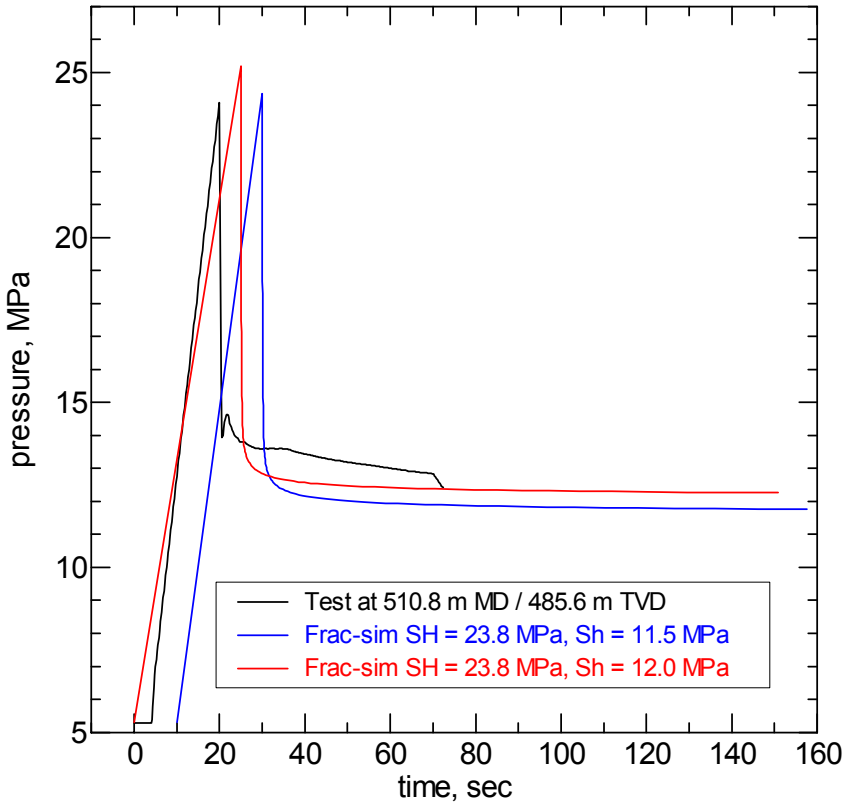

Figure 5-3. *Comparison of the simulated and measured hydrofrac record at the test section at 485.6 m (TVD).*

6 Discussion

6.1 Rock Stress at Oskarshamn

In the Oskarshamn region hydrofrac stress testing was conducted in the Äspö island boreholes KAS02 (to 737 m) and KAS03 (to 963 m), and in the Laxemar borehole KLX02 to a depth of 1340 m in the mid-nineties (Ljunggren & Klasson 1997). The data are summarized by Ekman (2001) and were recently reinterpreted by Ask et al. (2001).

Unfortunately, MeSy has not access to the original hydrofrac records and the exact stress data from the tests in the Äspö island boreholes. Therefore, it is only possible to compare the stress data derived from the MeSy tests in borehole KOV01 with the stress data in the Laxemar borehole KLX02 given by Ekman (2001, page 88). The result is shown for the depth range up to 1000 m in Figure 6.1. Both test series show a significant scatter in the profile and, in particular, a steep stress gradient in the depth range between 650 and 700 m.

If we compare (Figure 6.2) the azimuths of the major horizontal stress data (strike of induced or stimulated fractures) we observe a similar scatter but a general agreement that the fracture strike varies around 147 ± 19 degrees (if we neglect some odd data) :

θ_{SH} = 145° ± 18° for KOV01
θ_{SH} = 148° ± 20° for KLX02
with a mean of θ_{SH} = 147° ± 19°.

Thus, in summary: If we accept the reasonable agreement, the added information from both boreholes provides an almost gapless stress profile which may be representative for the Oskarshamn - Laxemar - Äspö region. The data from Äspö may further support this assumption.

6.2 Hydraulic Rock Mass Behaviour

From the pressure pulse tests we have derived permeability values k of app. 1µD (10^{-18} m^2) for intact test sections, and app. 25 µD ($25 \cdot 10^{-18}$ m^2) for test sections with pre-existing fractures. Considering water as the injection fluid we obtain hydraulic conductivity values of $K \approx (1 - 25) \cdot 10^{-11}$ m/s. Such values are acceptable for un-fractured granites but are three orders of magnitude smaller than the values derived from the pumping tests in 300 m long test sections carried out in borehole KLX02 (Ekman 2001, page 129 ff). The discrepancy can easily be explained by assuming one or a few highly conductive fractures or fracture zones in the granite.

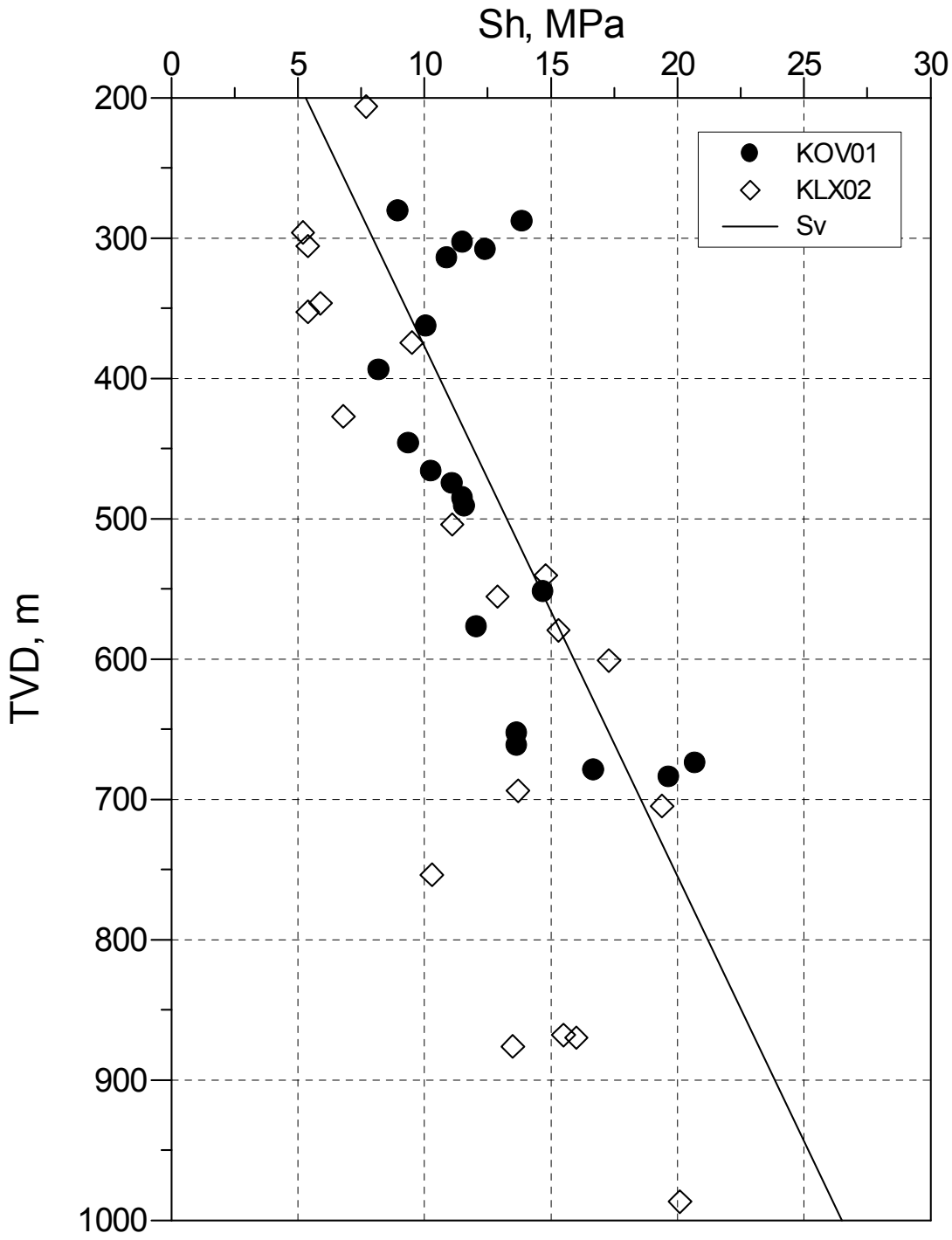

Figure 6-1a. *Minimum horizontal stress S_h in borehole KOV01 and borehole KLX02 (Ekman, 2001).*

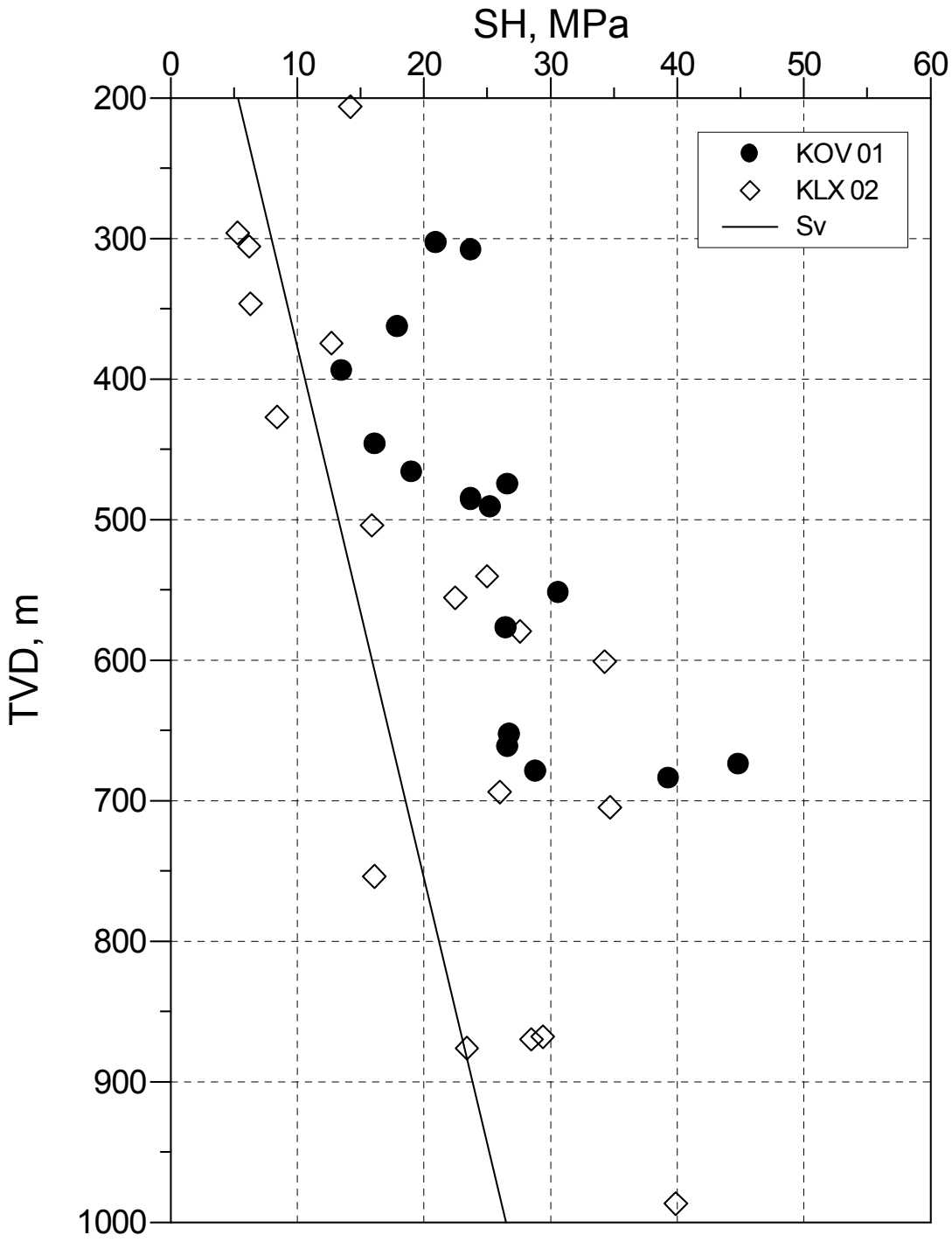

Figure 6-1b. *Major horizontal stress S_H in borehole KOV01 and borehole KLX02 (Ekman, 2001).*

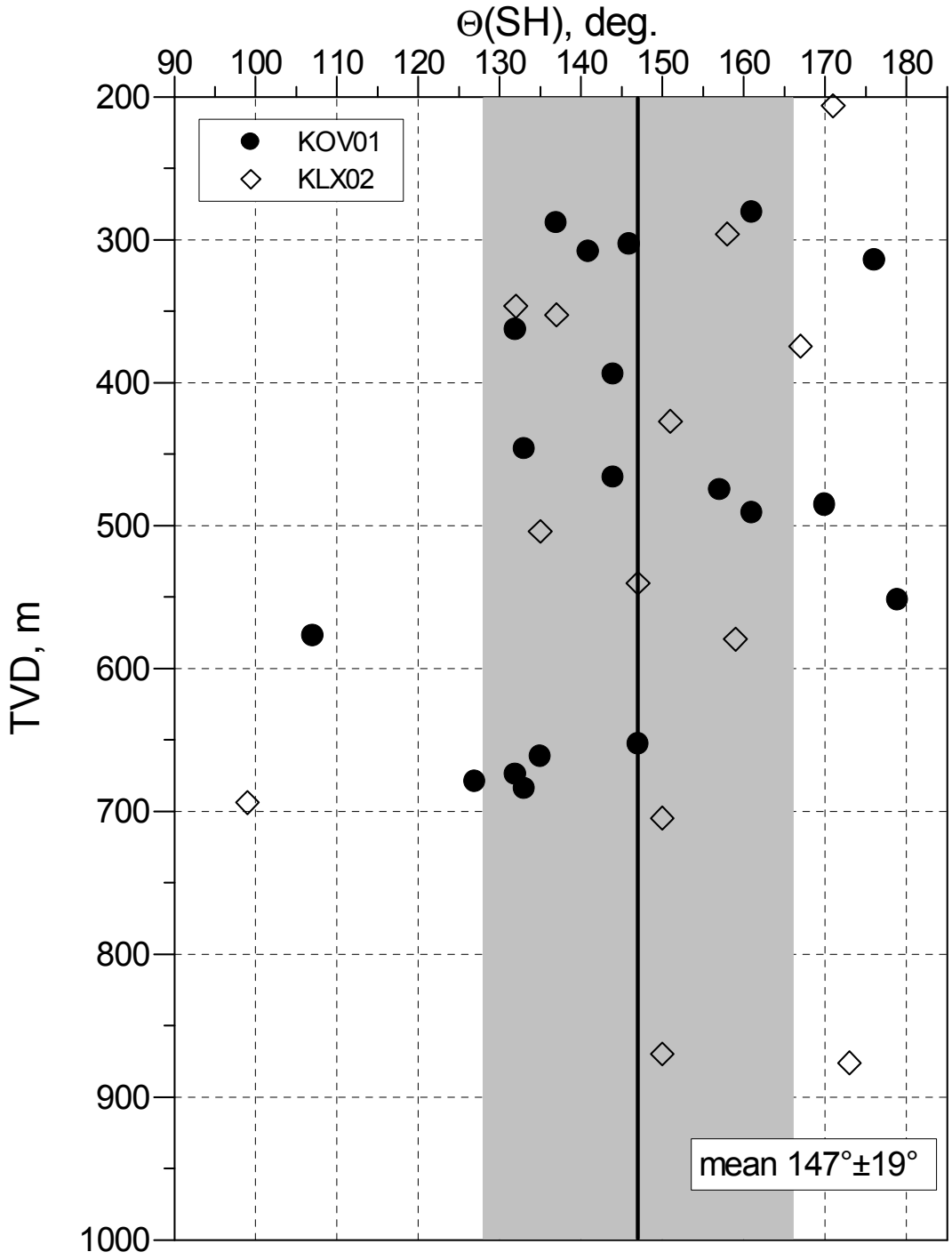

Figure 6-2. *Strike direction θ or azimuths θ for S_H, in boreholes KOV01 and KLX02.*

References

Amadei B, Stephansson O, 1997. Rock stresses and its measurement. Chapman & Hall.

Ask D, Stephansson O, Cornet F H, 2001. Integrated stress analysis of hydraulic stress data in the Äspö region. SKB - Rep., in print.

Atkinson B K, Meredith P G, 1987. Experimental fracture mechanics data for rocks and minerals. In : Fracture Mechanics of Rock (Atkinson ed.), 11, 477 - 527, Akad. Press Geol. Ser., London.

Baumgärtner J, 1987. Anwendung des Hydraulik - Fracturing Verfahrens für Spannungsmessungen im klüftigen Gebirge. Ber. Inst. Geophys. RU Bochum, A 21.

Clark J B, 1949. A hydraulic process for increasing the productivity of oil wells. Trans AIME, 186, 1-3.

Cooper H H, Bredehoeft J D, Papadopolus I S, 1967. Response of a finite diameter well to an instantaneous charge of water. Water Resource Res., 3, 263 - 269.

Cornet F H, 1993. Stresses in rock masses. In : Comprehensive Rock Engineering (J. Hudson ed.), 297 - 327, Pergamon.

Ekman D, Stephansson O, Cornet F H, 1999. Integrated stress analysis in the Äspö region. 2nd Euroconference on WSM, Äspö HRL Abstract Volume, p. 11.

Ekman L, 2001. Project deep drilling KLX02 - phase 2. SKB Tech. Rep. TR - 01 - 11, 73 - 89.

Guo F, Morgenstern N R, Scott J D, 1993. Interpretation of hydraulic fracturing pressure : a comparison of eight methods used to identify shut-in pressure. Int. J. Rock Mech., 30/6, 627 - 631.

Hubbert M K, Willis D K, 1957. Mechanics of hydraulic fracturing. Trans AIME, 210, 153 - 163.

ISRM Standard (Rummel & van Heerden), 1978. Suggested methods for determining sound velocity. Int. JRMMS, 15, 53 - 58.

ISRM Standard (Ouchterlony), 1988. Suggested methods for determining the fracture toughness of rock. Int. JRMMS, 25, 71 - 96.

teKamp L, 1991. Simulation of hydraulic fracturing experiments under the aspect of fracture mechanics and fluid dynamics. Shigen (Japan), 3/6, 26 - 40.

Kirsch G, 1898. Die Theorie der Elastizität und Bedürfnisse der Festigkeitslehre. Zeitschr. VDI, 42 / 29, 7797 - 807.

Lundholm B, 1999. State of stress at Äspö, Sweden. 2nd Euroconference on WSM, Äspö HRL Abstract Volume, p. 24.

Ljunggren C, Klasson H, 1997. Deep hydraulic fracturing rock stress measurements in borehole KLX01, Laxemar. SKB-Rep. U-97-27.

Rummel F, 1987. Fracture mechanics approach to hydraulic fracturing stress measurements. In : Fracture Mechanics of Rock (ed. B. Atkinson), 6, 217 - 239.

Rummel F, Hansen J, 1989. Interpretation of hydrofrac pressure recordings using a simple fracture mechanics simulation model. Int. JRMMS, 26/6, 483 - 488.

Rummel F, 2001. Crustal stress derived from fluid injection tests in boreholes. In: In-Situ Characterization of Rock (eds. Sharma and Saxena), Oxford & IBH Publ. Co., New Delhi, Chapt. 6, 205 - 244.

Scheidegger A E, 1962. Stresses in the Earth's crust as determined from hydraulic fracturing data. Geol. & Bauwesen, 27, 45 - 53.

APPENDIX A

Records from in-situ hydrofrac tests together with evaluation of characteristic pressure data

TEST AT 296.0 m MD / 280.9 m TVD

Test at 296.0 m MD : Overview - Plot

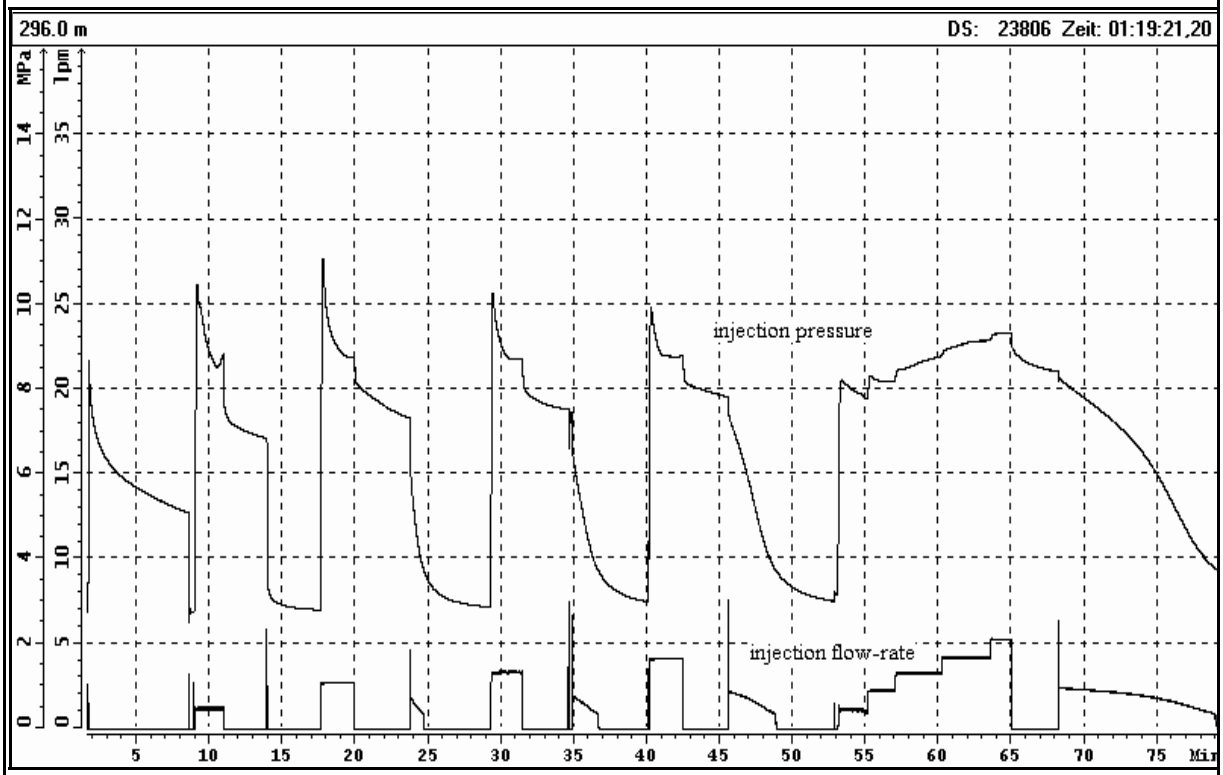

TEST SUMMARY

P - Test :	pressure decrease: 2.8 MPa in 6 min. 45 sec.
Frac (1. Refrac) - Cycle :	injection-rate Q_i= 1.2 lpm, injected volume V_i = 2.4 l, back-flow volume V_r = 0.1 l stimulation of an existing fracture (no breakdown event)
2. Refrac - Cycle :	Q_i = 2.7 lpm, V_i = 6.3 l, V_r = 1.3 l
3. Refrac - Cycle :	Q_i = 3.3 lpm, V_i = 7.2 l, V_r = 2.8 l
4. Refrac - Cycle :	Q_i = 4.1 lpm, V_i = 9.5 l, V_r = 5.3 l
Step-Rate Test :	Q_i = 1.1-5.3 lpm, V_i = 38.4 l, V_r = 20.3 l

total injected volume = 63.8 l, recovered volume = 29.8 l (46.7 %)

Test at 296.0 m MD: Estimation of P_r (Frac (1. Refrac) - Cycle)

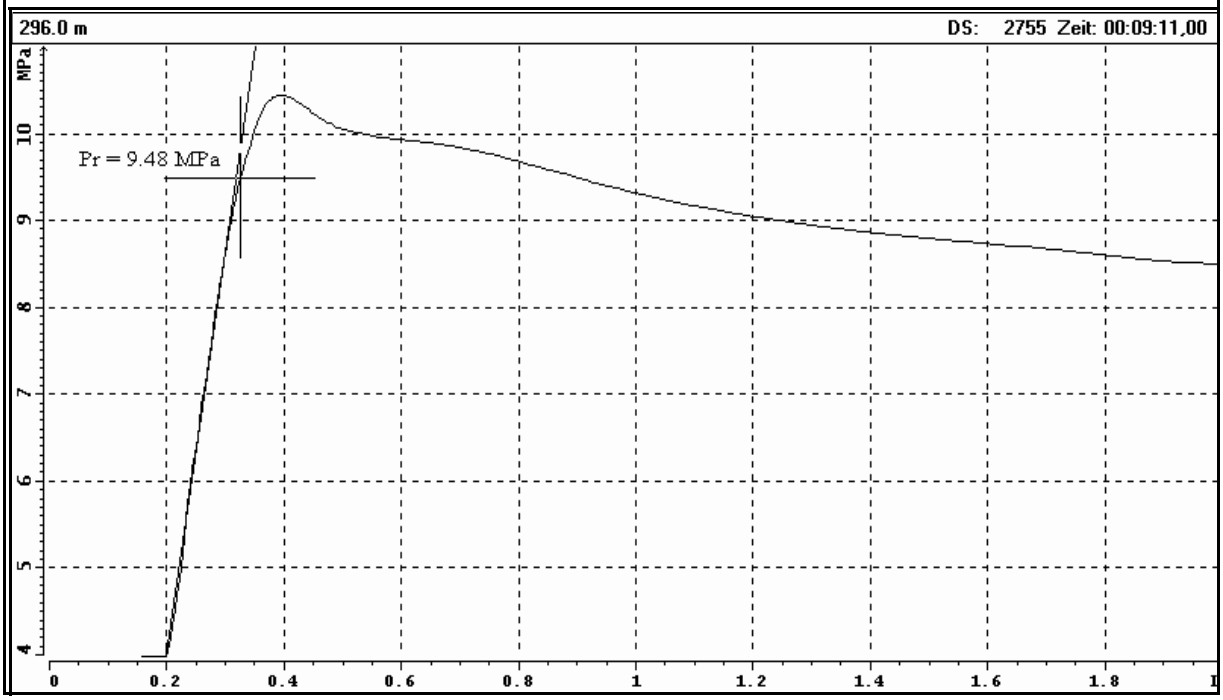

Test at 296.0 m MD: Estimation of P_r (2. Refrac - Cycle, for comparison)

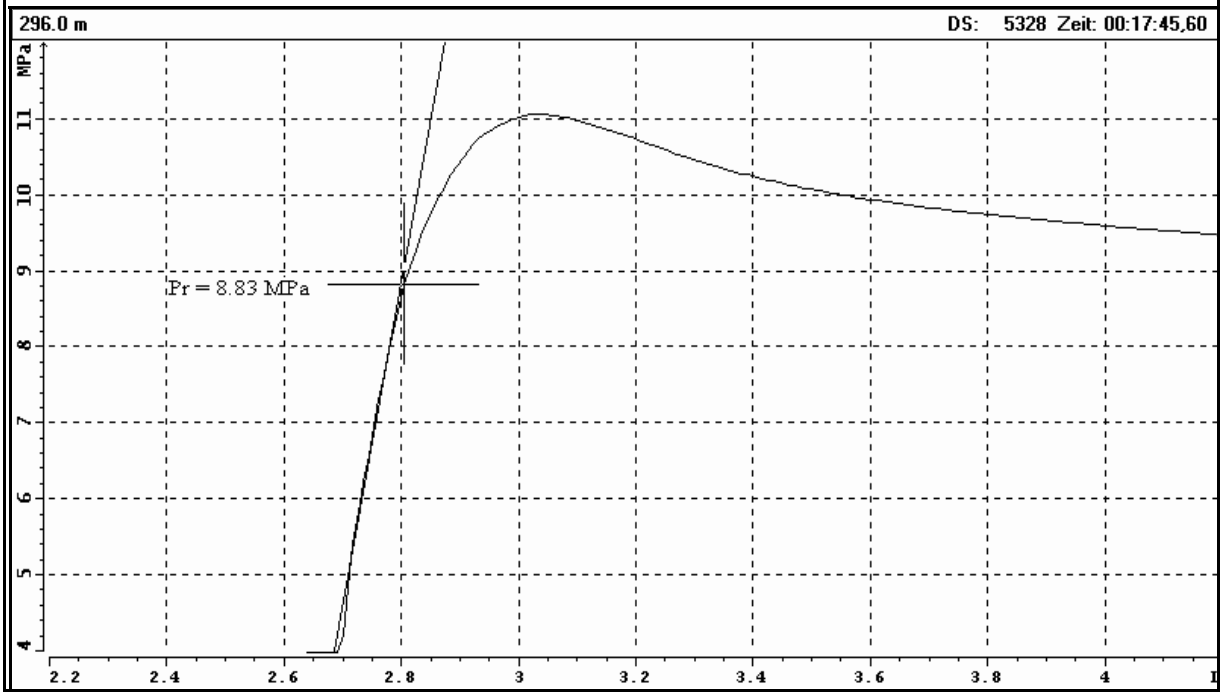

Test at 296.0 m MD: Estimation of $P_{si, max}$ (4. Refrac - Cycle)

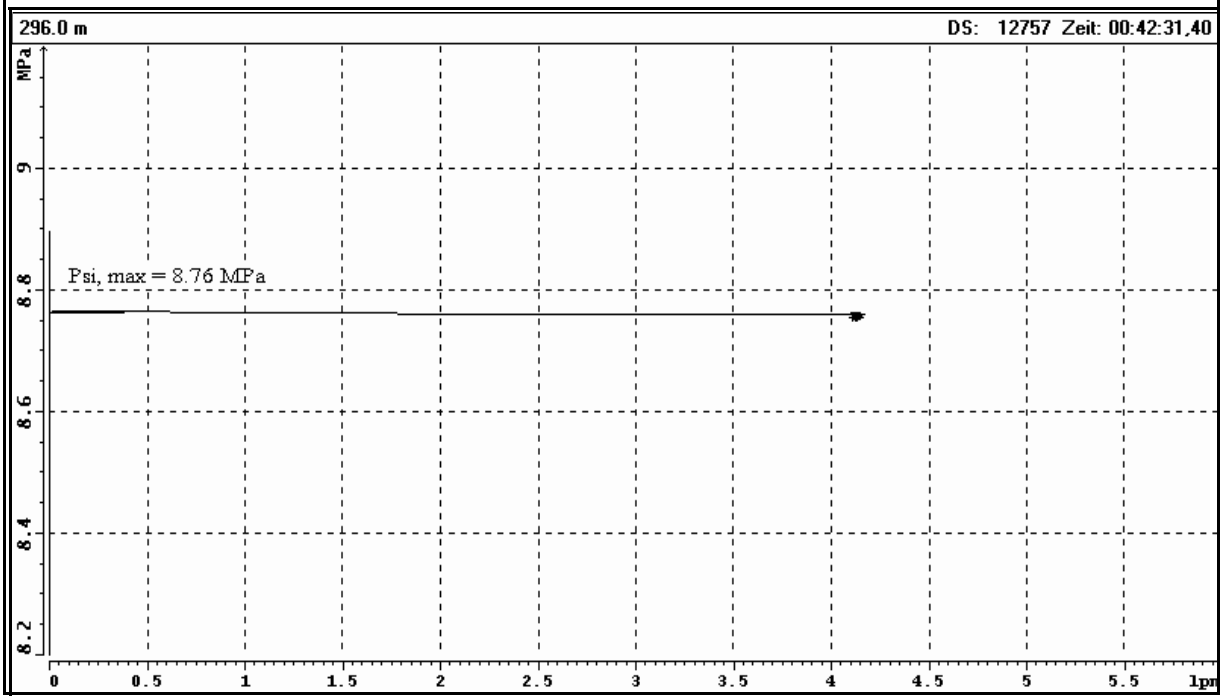

Test at 296.0 m MD: Estimation of $P_{si, min}$ (4. Refrac - Cycle)

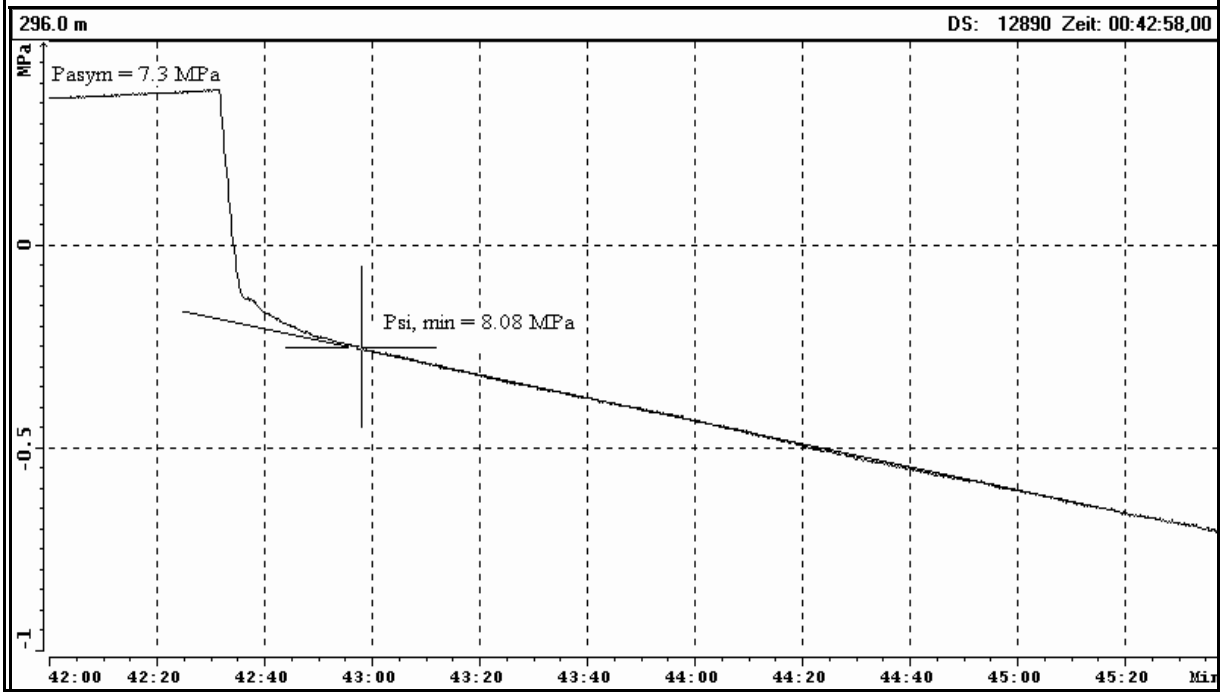

Test at 296.0 m MD: Estimation of P_{si} (4. Refrac - Cycle)

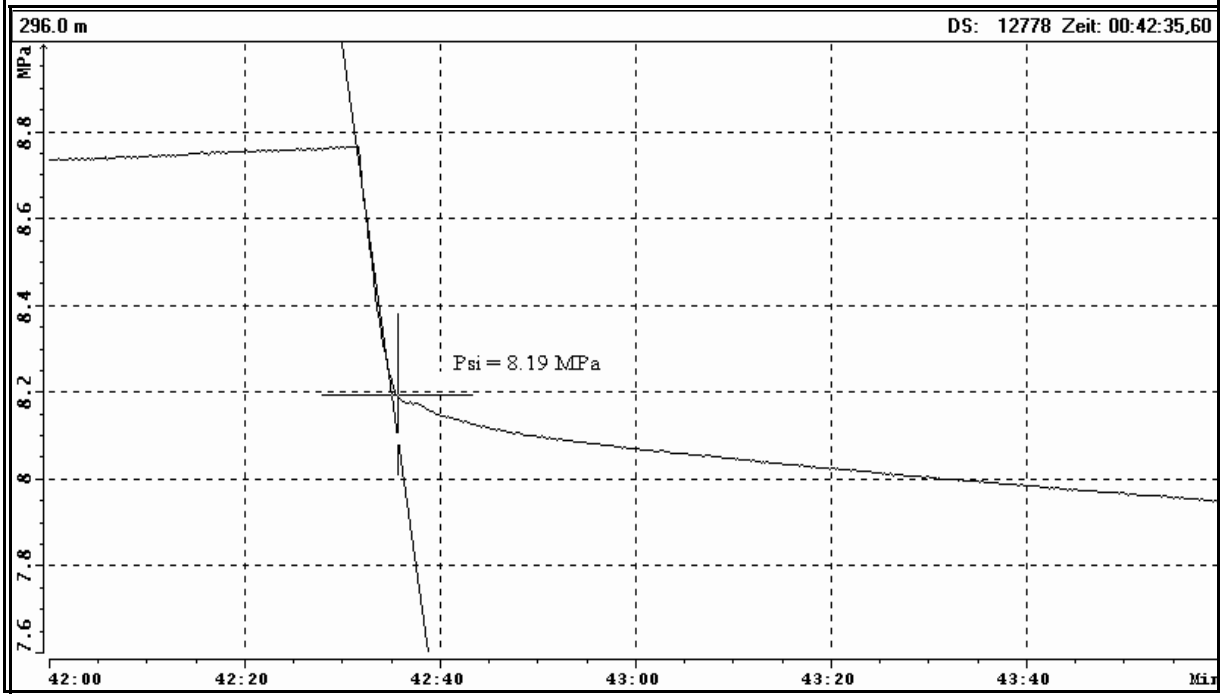

Test at 296.0 m MD: Analysis of Slow - Pump / Step - Rate - Test

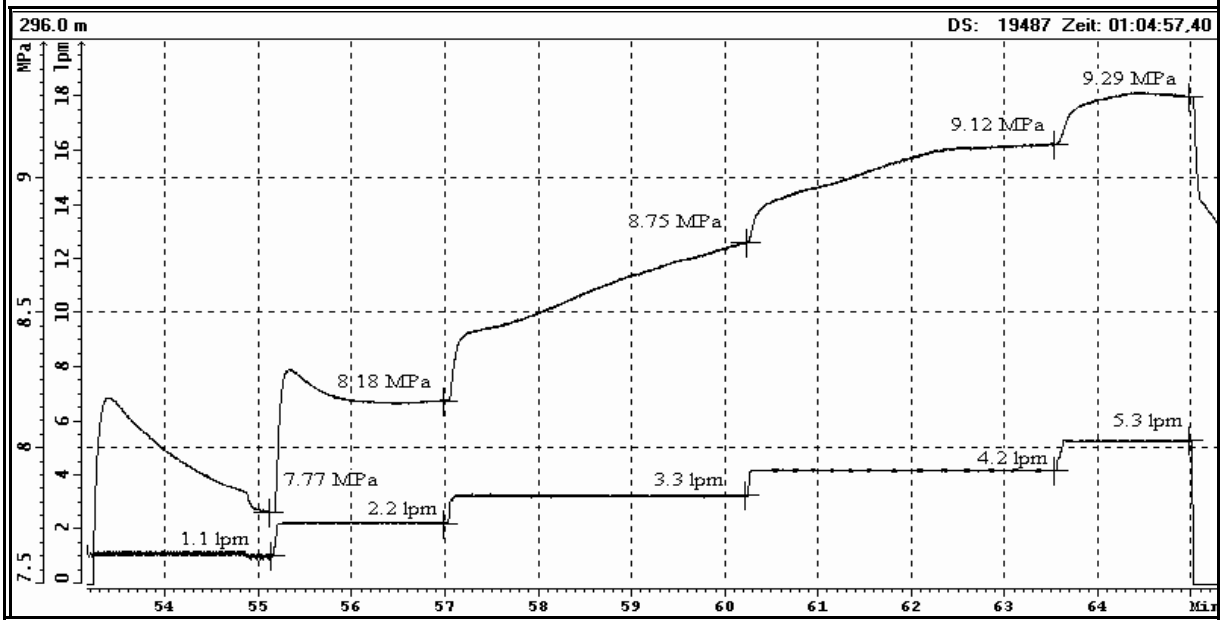

Test at 296.0 m MD: Examination of P_{si} (Step - Rate - Test)

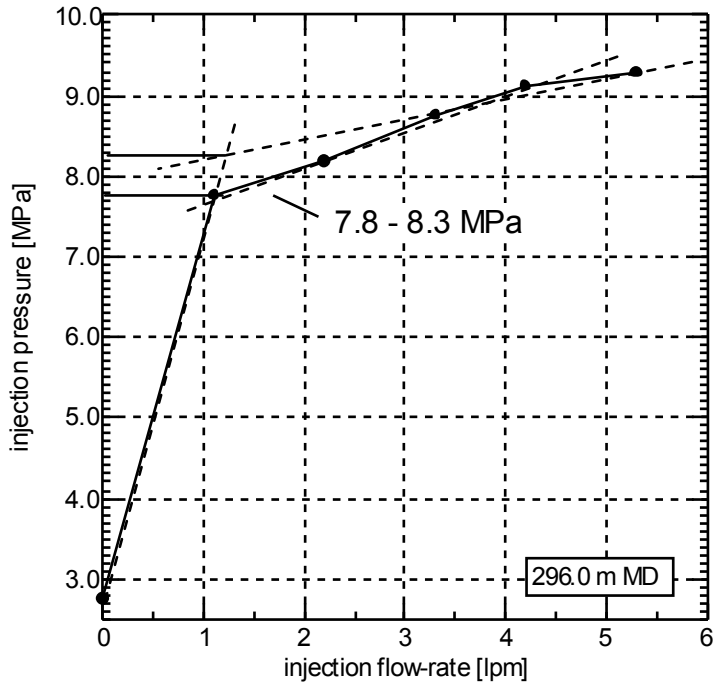

TEST AT 303.5 m MD / 288.0 m TVD

Test at 303.5 m MD: Overview - Plot

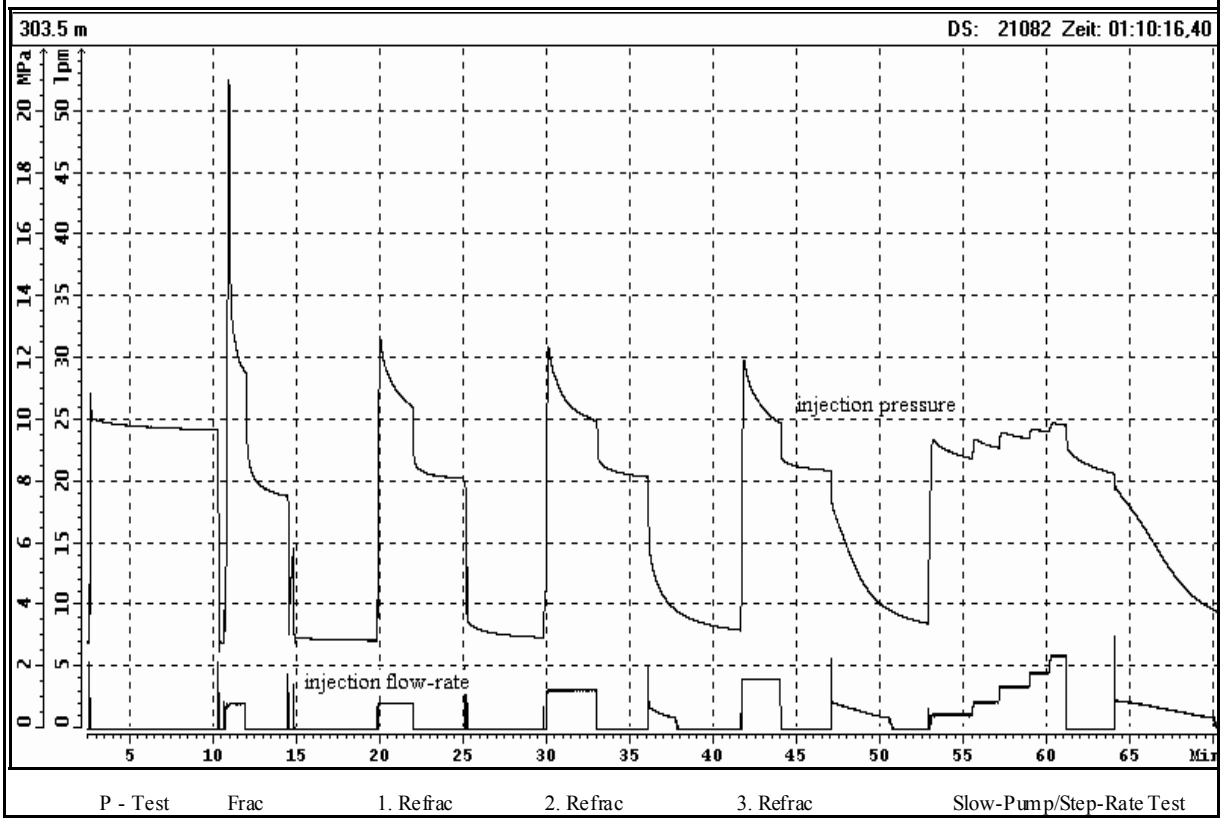

TEST SUMMARY

P - Test :	pressure decrease: 0.4 MPa in 7 min. 30 sec.
Frac - Cycle :	injection-rate Q_i= 1.9 lpm, injected volume V_i = 2.4 l, back-flow volume V_r = 0.2 l clear fracture initiation (breakdown event)
1. Refrac - Cycle :	Q_i = 2.1 lpm, V_i = 4.3 l, V_r = 0.2 l
2. Refrac - Cycle :	Q_i = 3.2 lpm, V_i = 9.6 l, V_r = 2.2 l
3. Refrac - Cycle :	Q_i = 4.0 lpm, V_i = 9.3 l, V_r = 5.3 l
Step-Rate Test :	Q_i = 1.1-5.9 lpm, V_i = 23.7 l, V_r = 9.8 l

total injected volume = 49.3 l, recovered volume = 17.7 l (35.9 %)

Test at 303.5 m MD: Estimation of P_c (Frac - Cycle)

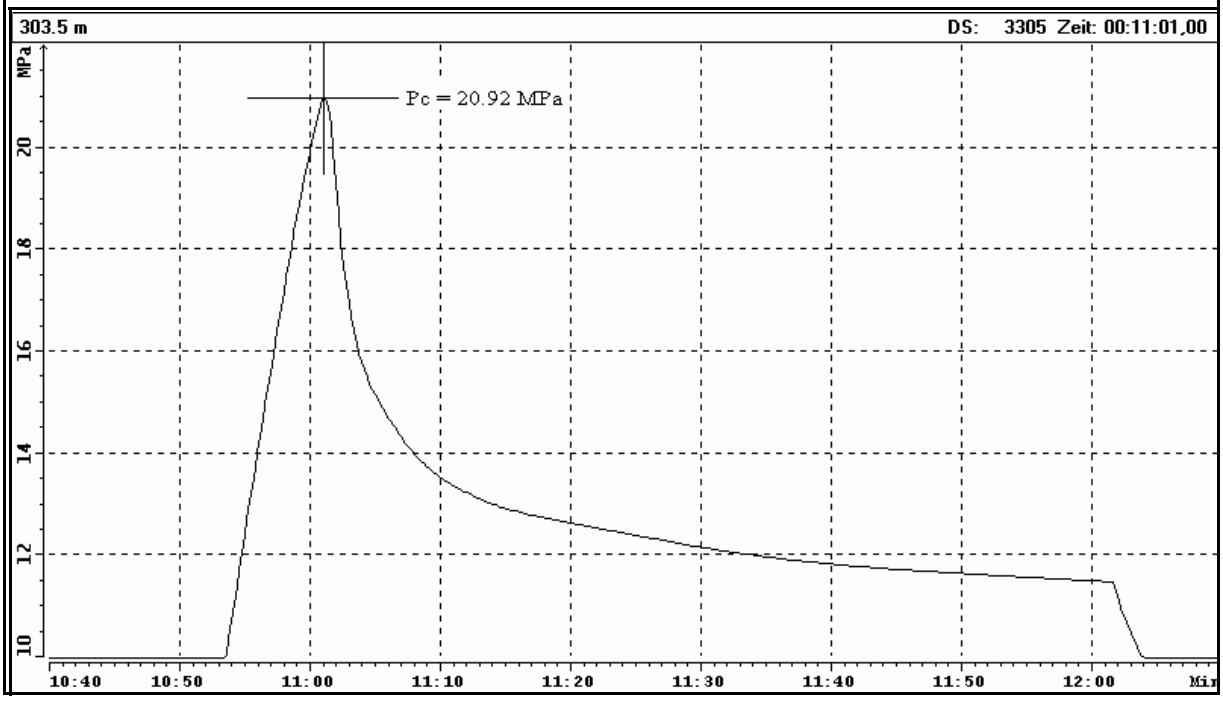

Test at 303.5 m MD: Estimation of P_r (1. Refrac - Cycle)

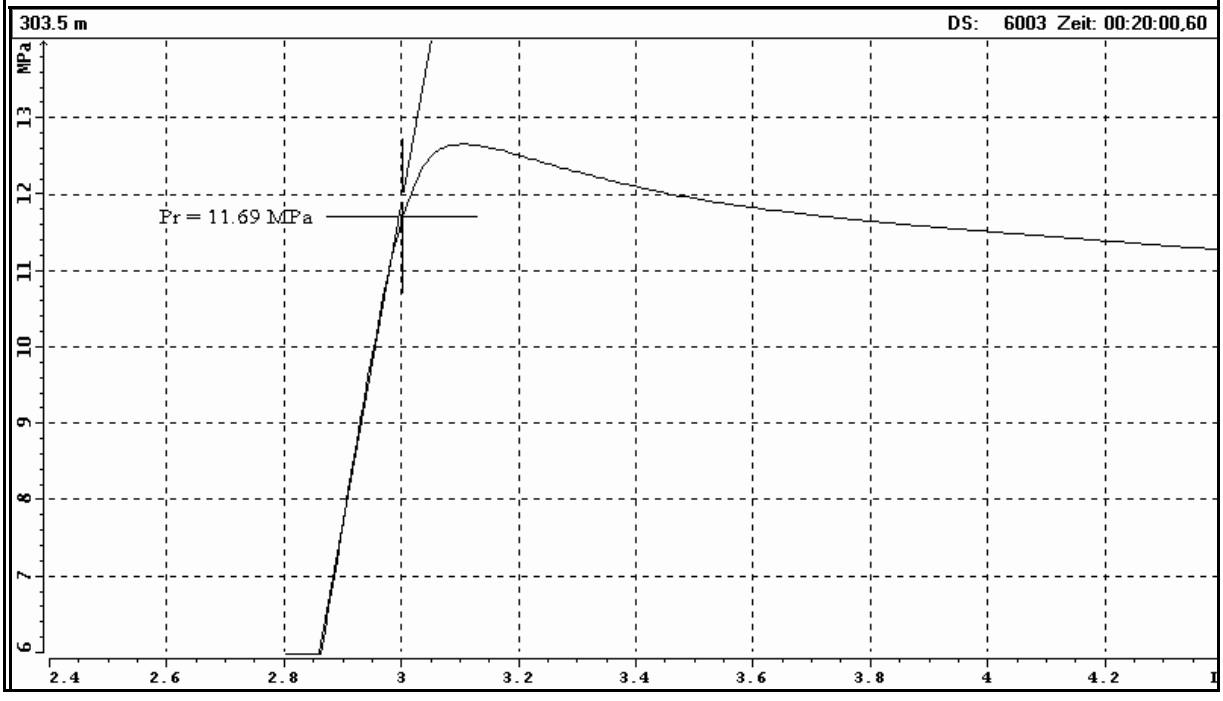

Test at 303.5 m MD: Estimation of $P_{si,\,max}$ (3. Refrac - Cycle)

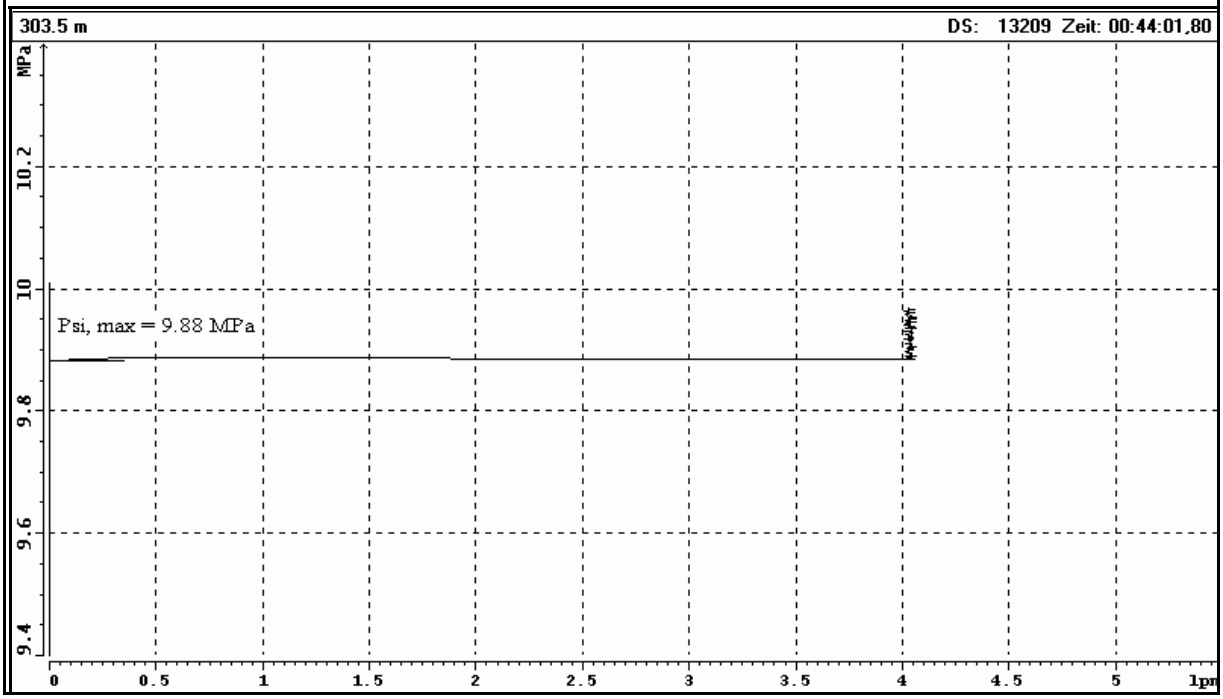

Test at 303.5 m MD: Estimation of $P_{si,\,min}$ (3. Refrac - Cycle)

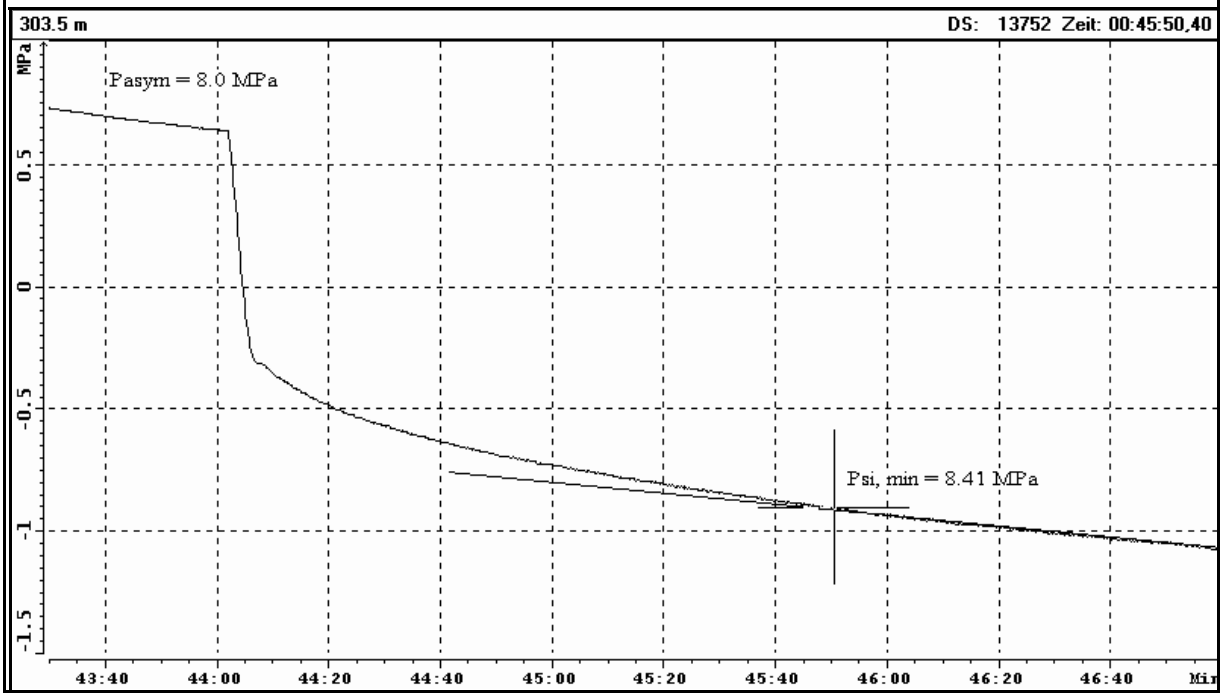

Test at 303.5 m MD: Estimation of P_{si} (3. Refrac - Cycle)

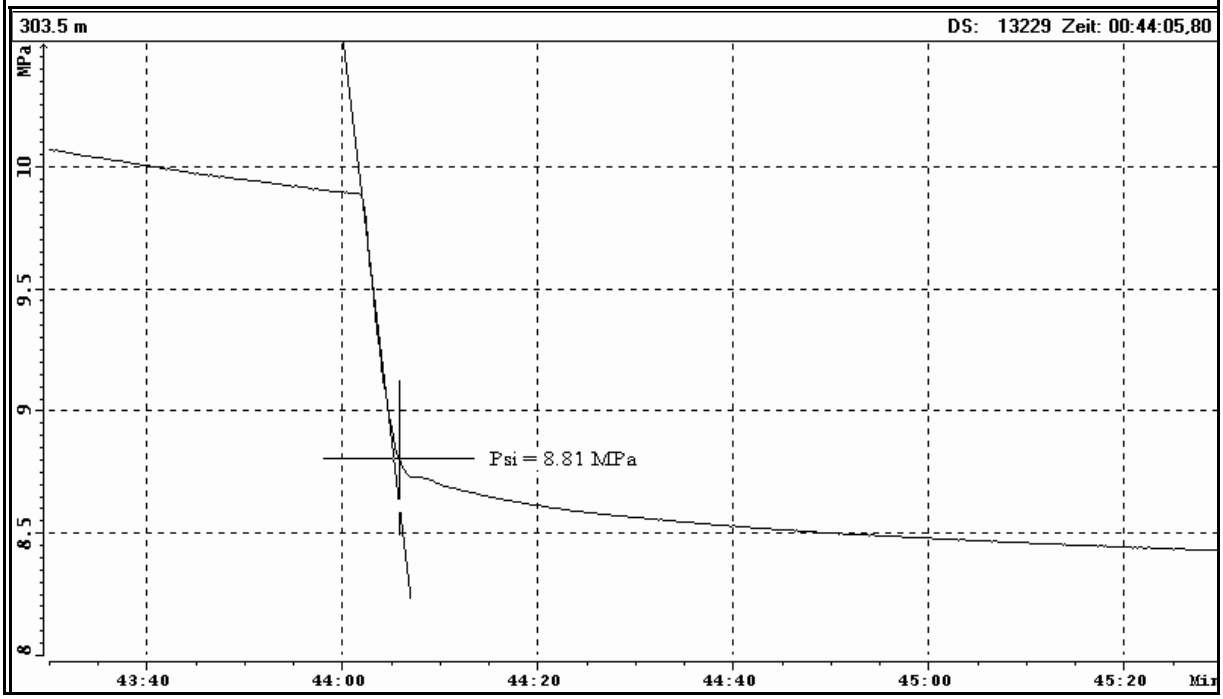

Test at 303.5 m MD: Analysis of Slow - Pump / Step - Rate - Test

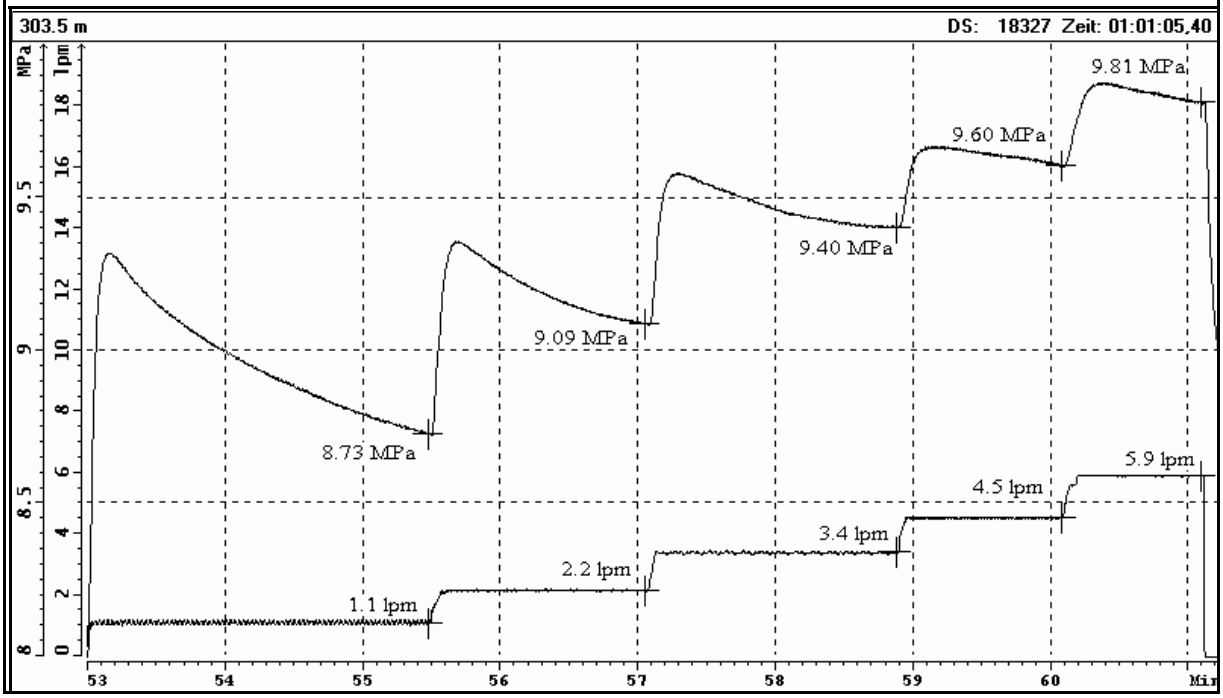

Test at 303.5 m MD: Examination of P_{si} (Step - Rate - Test)

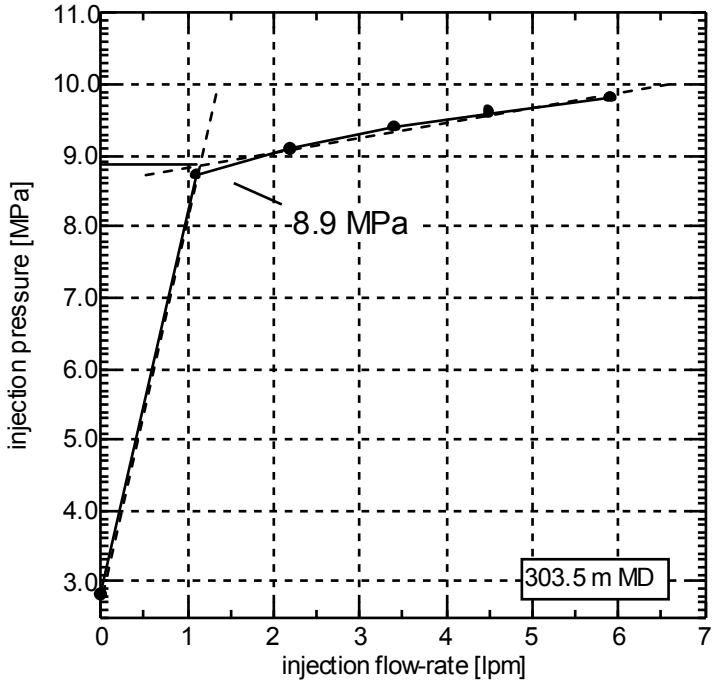

TEST AT 319.3 m MD / 302.8 m TVD

Test at 319.3 m MD: Overview - Plot

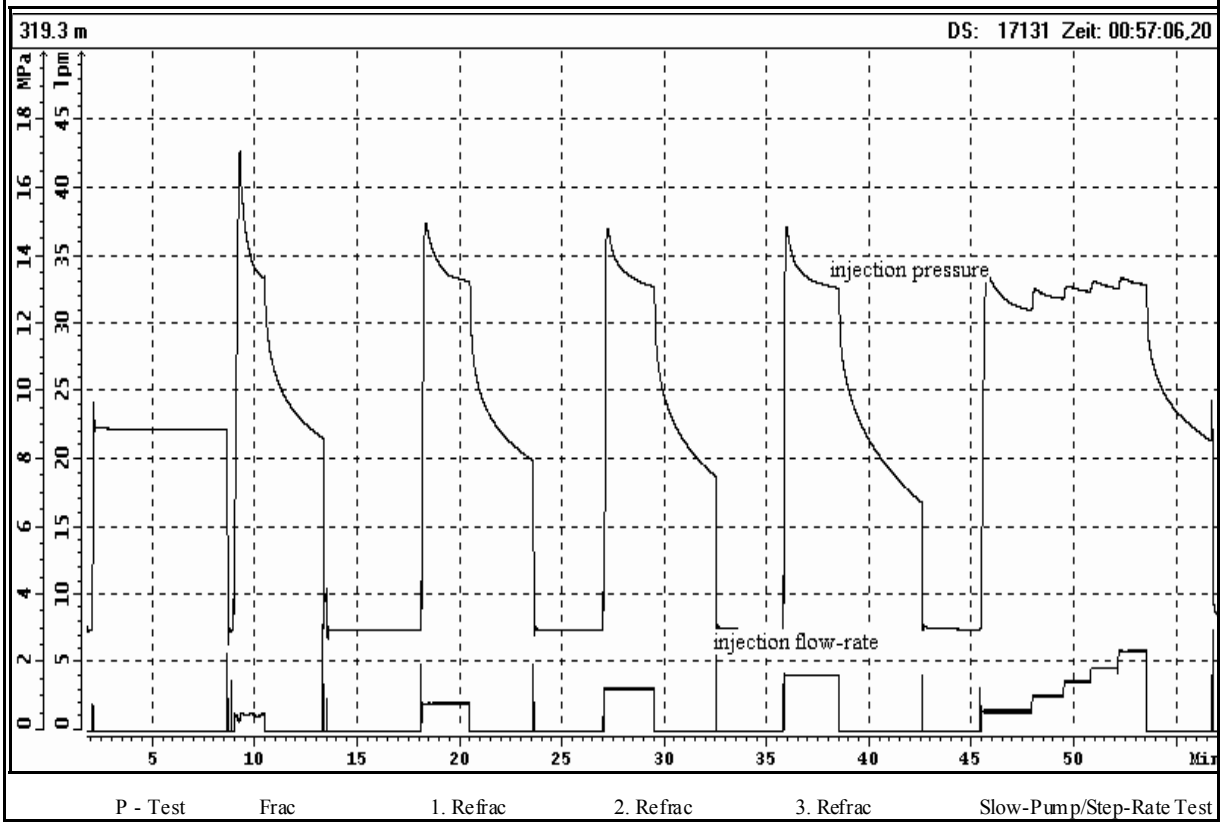

TEST SUMMARY

P - Test :	pressure decrease: 0.1 MPa in 6 min. 20 sec.
Frac - Cycle :	injection-rate Q_i= 1.1 lpm, injected volume V_i = 1.8 l, back-flow volume V_r = 0.1 l clear fracture initiation (breakdown event)
1. Refrac - Cycle :	Q_i = 2.0 lpm, V_i = 4.8 l, V_r = 0.1 l
2. Refrac - Cycle :	Q_i = 3.1 lpm, V_i = 7.6 l, V_r = 0.1 l
3. Refrac - Cycle :	Q_i = 4.1 lpm, V_i = 11.0 l, V_r = 0.1 l
Step-Rate Test :	Q_i = 1.4-5.9 lpm, V_i = 26.7 l, V_r = 0.2 l

total injected volume = 51.9 l, recovered volume = 0.6 l (1.1 %)

Test at 319.3 m MD: Estimation of P_c (Frac - Cycle)

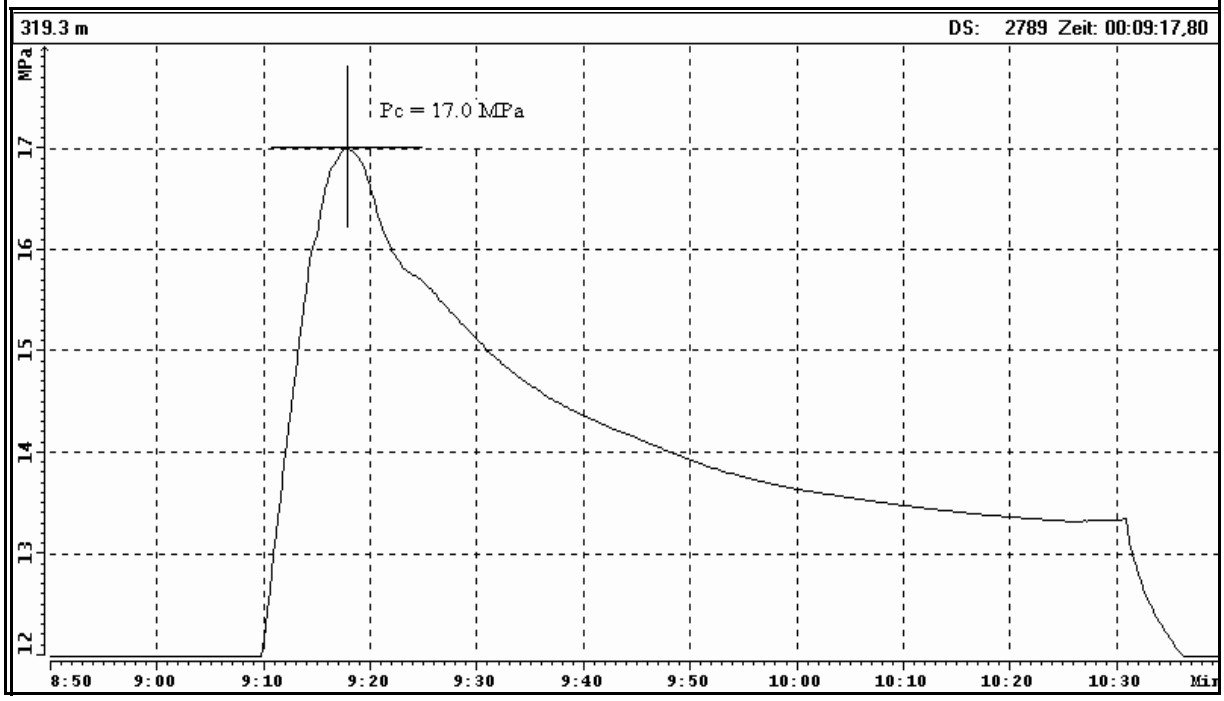

Test at 319.3 m MD: Estimation of P_r (1. Refrac - Cycle)

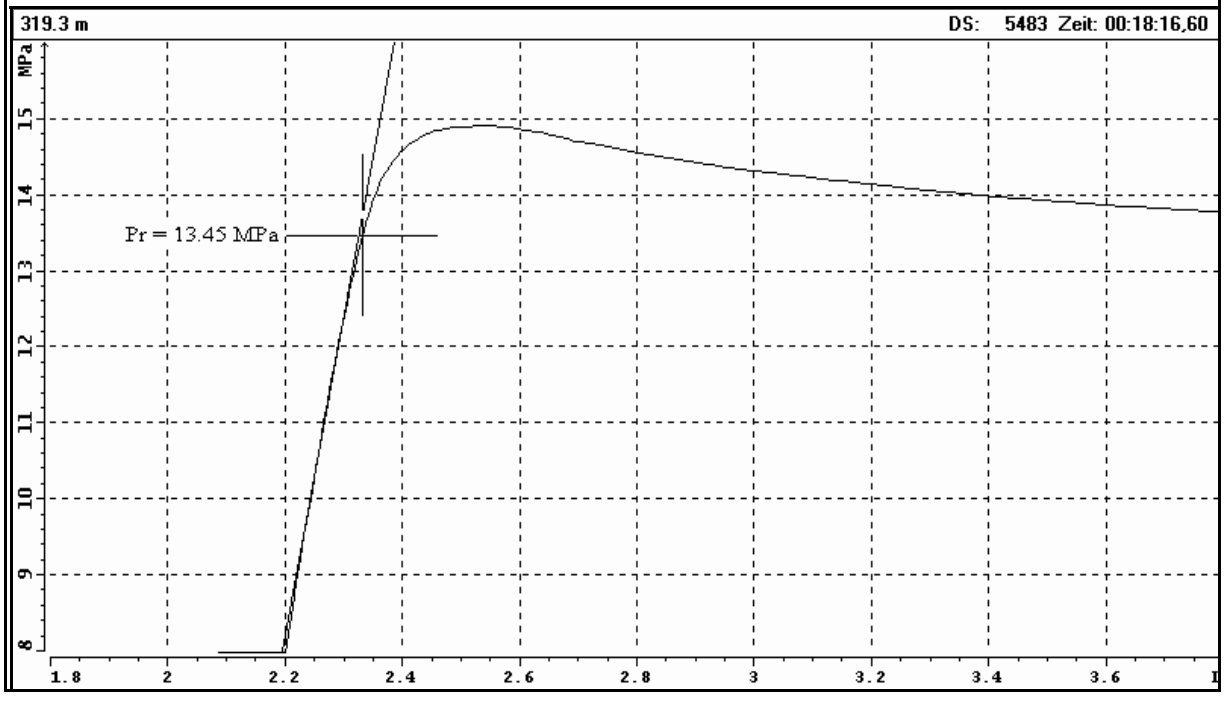

Test at 319.3 m MD: Estimation of $P_{si,\,max}$ (3. Refrac - Cycle)

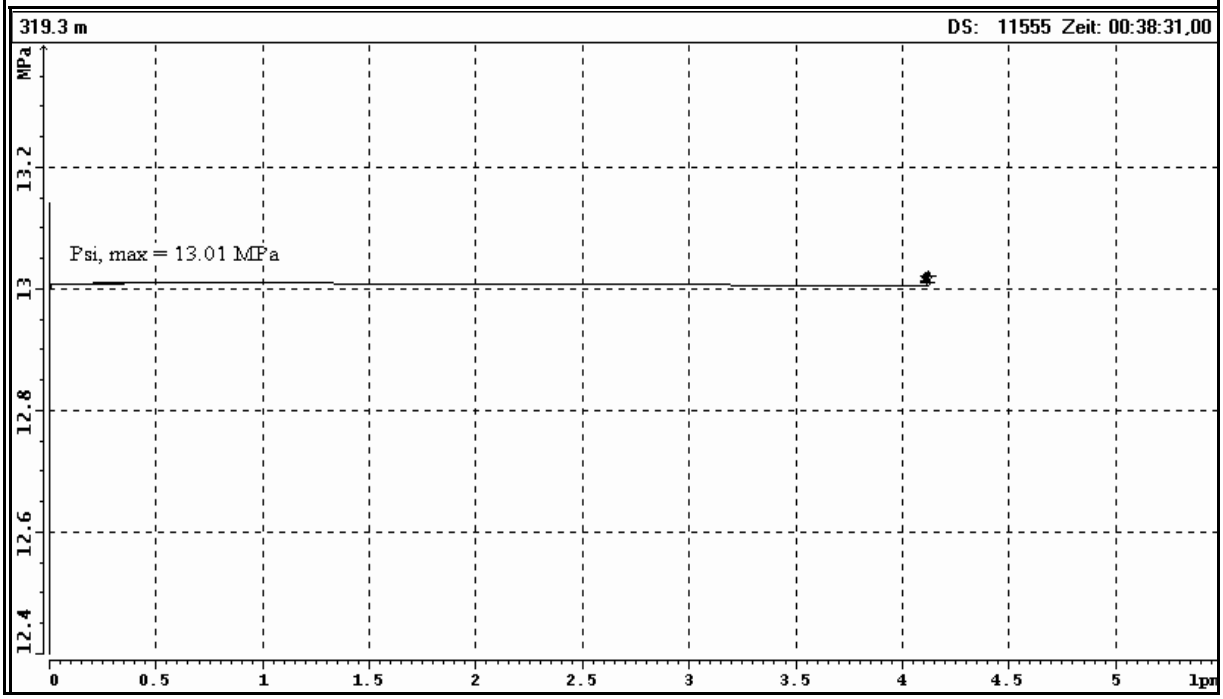

Test at 319.3 m MD: Estimation of $P_{si,\,min}$ (3. Refrac - Cycle)

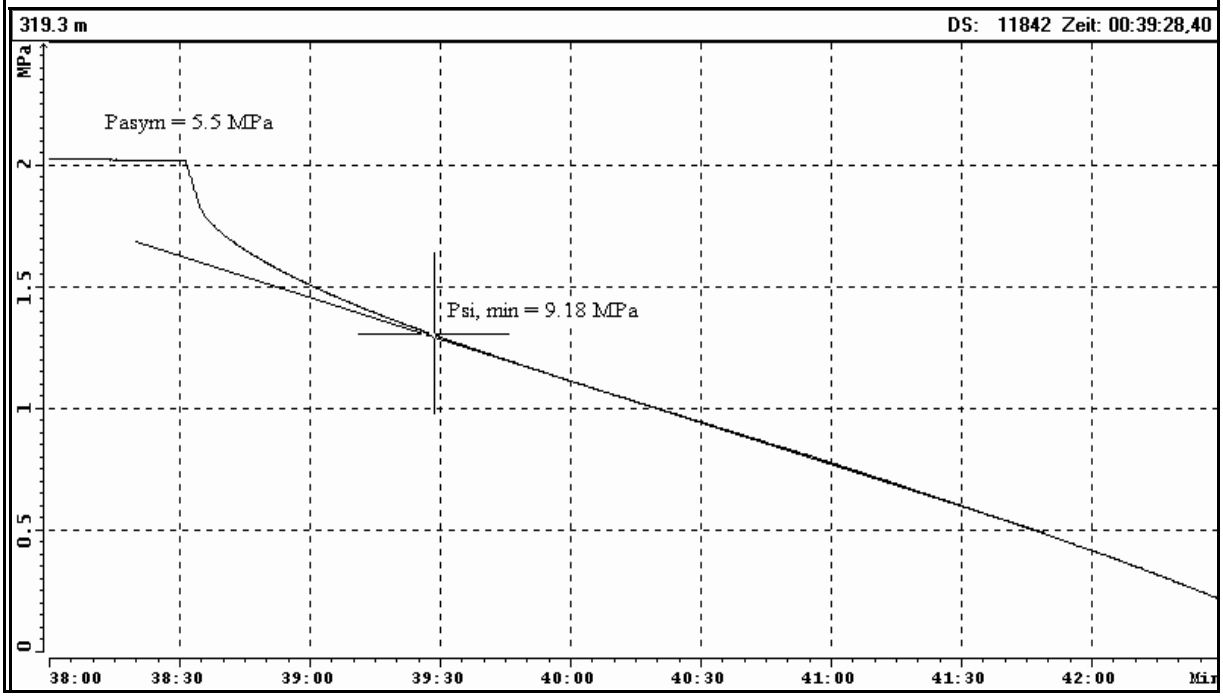

Test at 319.3 m MD: Estimation of P_{si} (3. Refrac - Cycle)

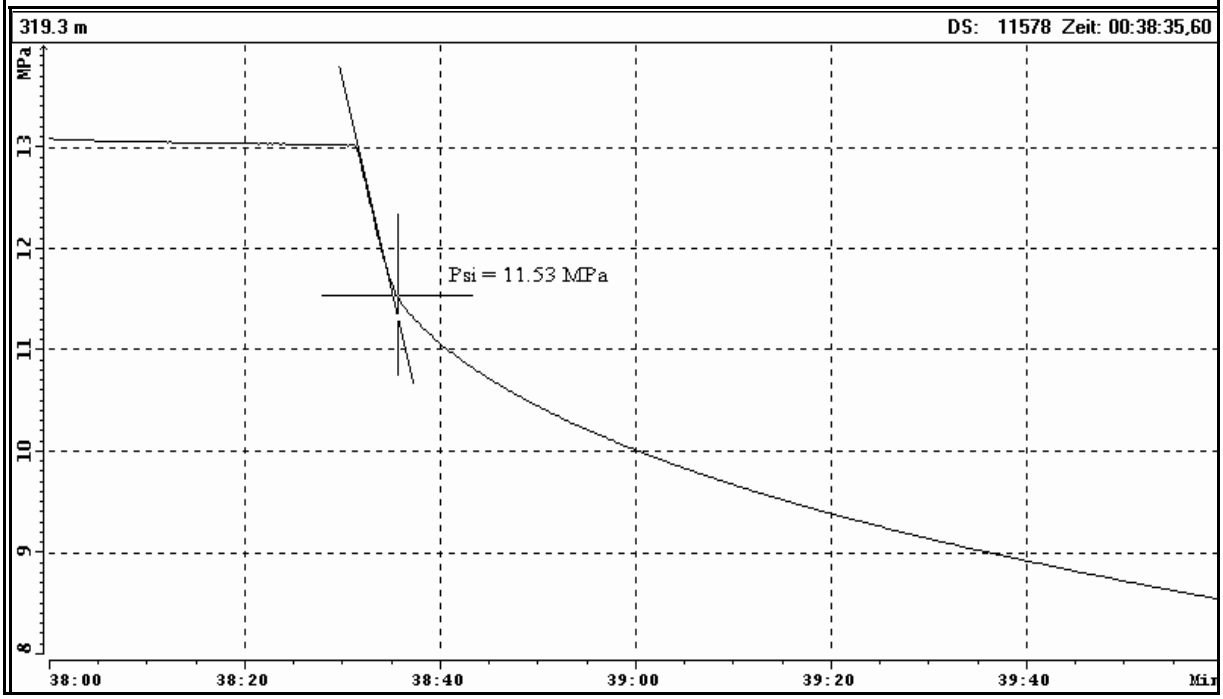

Test at 319.3 m MD: Analysis of Slow - Pump / Step - Rate - Test

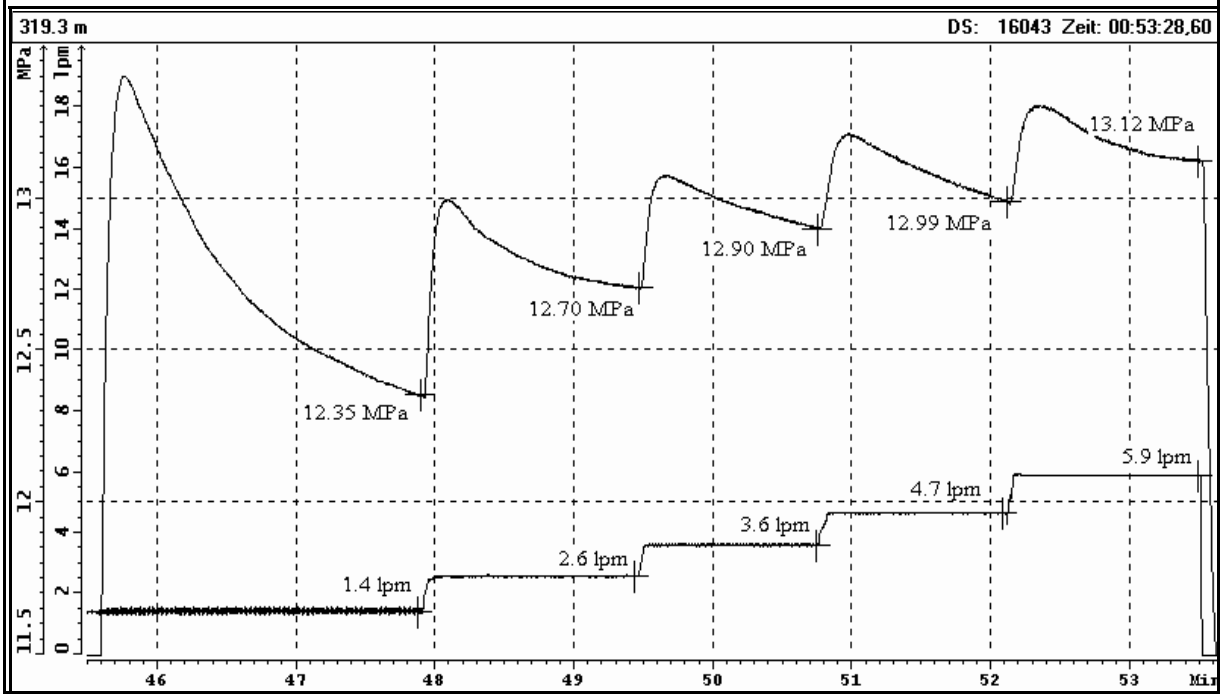

Test at 319.3 m MD: Examination of P_{si} (Step - Rate - Test)

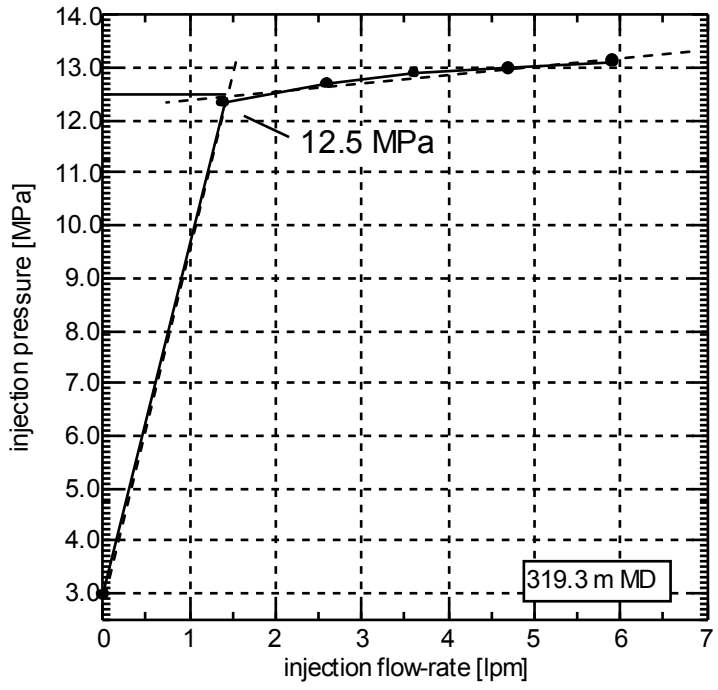

TEST AT 325.4 m MD / 308.5 m TVD

Test at 325.4 m MD : Overview - Plot

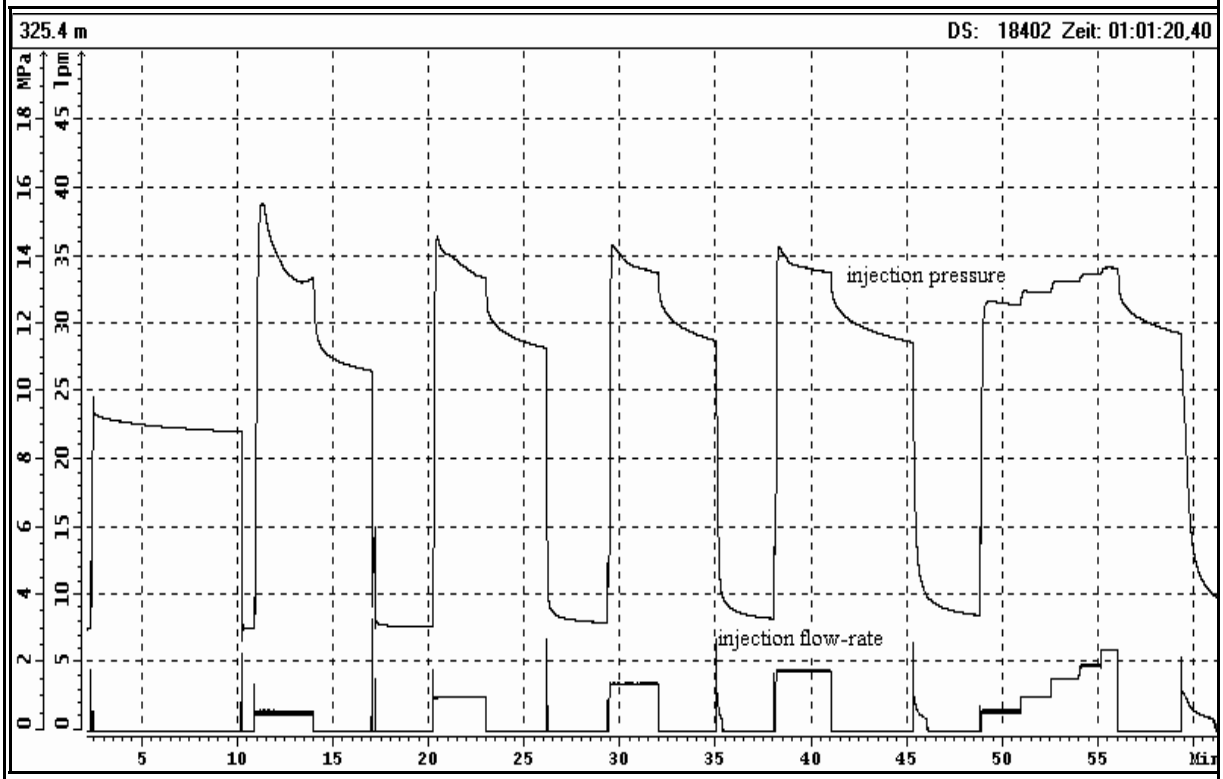

TEST SUMMARY

P - Test :	pressure decrease: 0.5 MPa in 7 min. 38 sec.
Frac (1. Refrac) - Cycle :	injection - rate Q_i= 1.3 lpm, injected volume V_i = 4.2 l, back-flow volume V_r = 0.2 l stimulation of an existing fracture (no breakdown event)
2. Refrac - Cycle :	Q_i = 2.5 lpm, V_i = 6.9 l, V_r = 0.3 l
3. Refrac - Cycle :	Q_i = 3.5 lpm, V_i = 8.9 l, V_r = 0.6 l
4. Refrac - Cycle :	Q_i = 4.5 lpm, V_i = 12.8 l, V_r = 1.1 l
Step-Rate Test :	Q_i = 1.1-6.0 lpm, V_i = 23.4 l, V_r = 2.8 l

total injected volume = 56.2 l, recovered volume = 5.0 l (8.9 %)

Remark: During the injection - cycles, an increase of the shut-in pressure was observed. The P_{si} - value was therefore determined from the 1. refrac - cycle.

Test at 325.4 m MD: Estimation of P_r (Frac (1. Refrac) - Cycle)

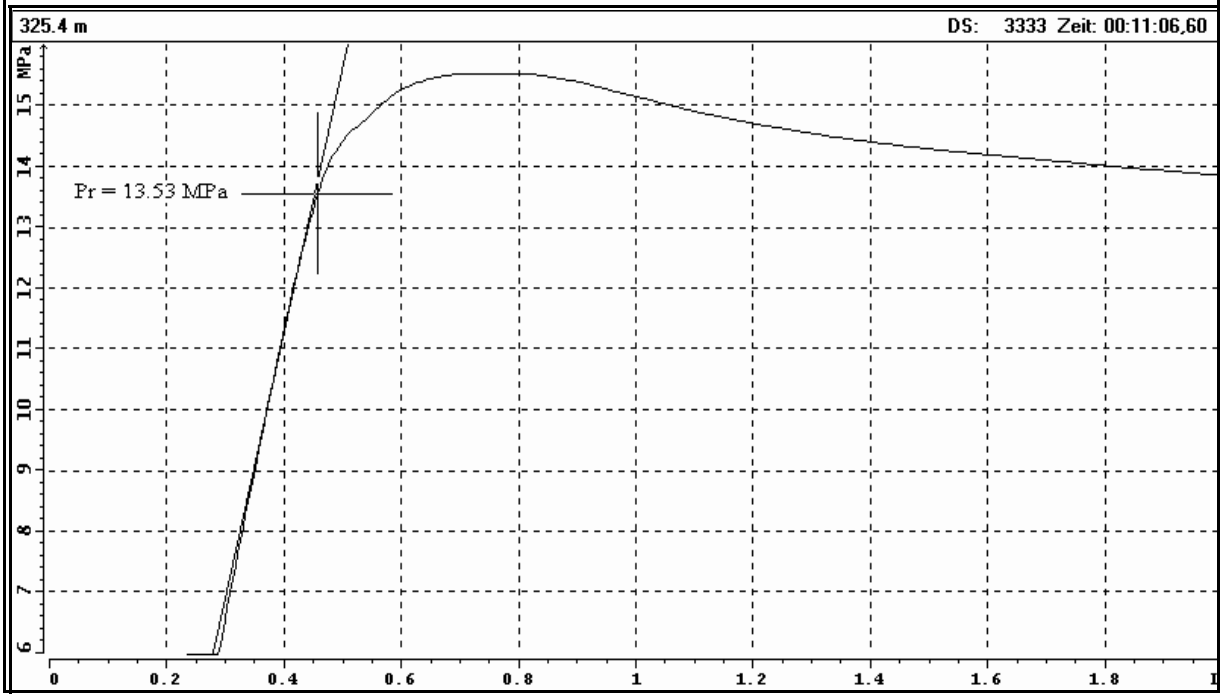

Test at 325.4 m MD: Estimation of $P_{si, max}$ (1. Refrac - Cycle)

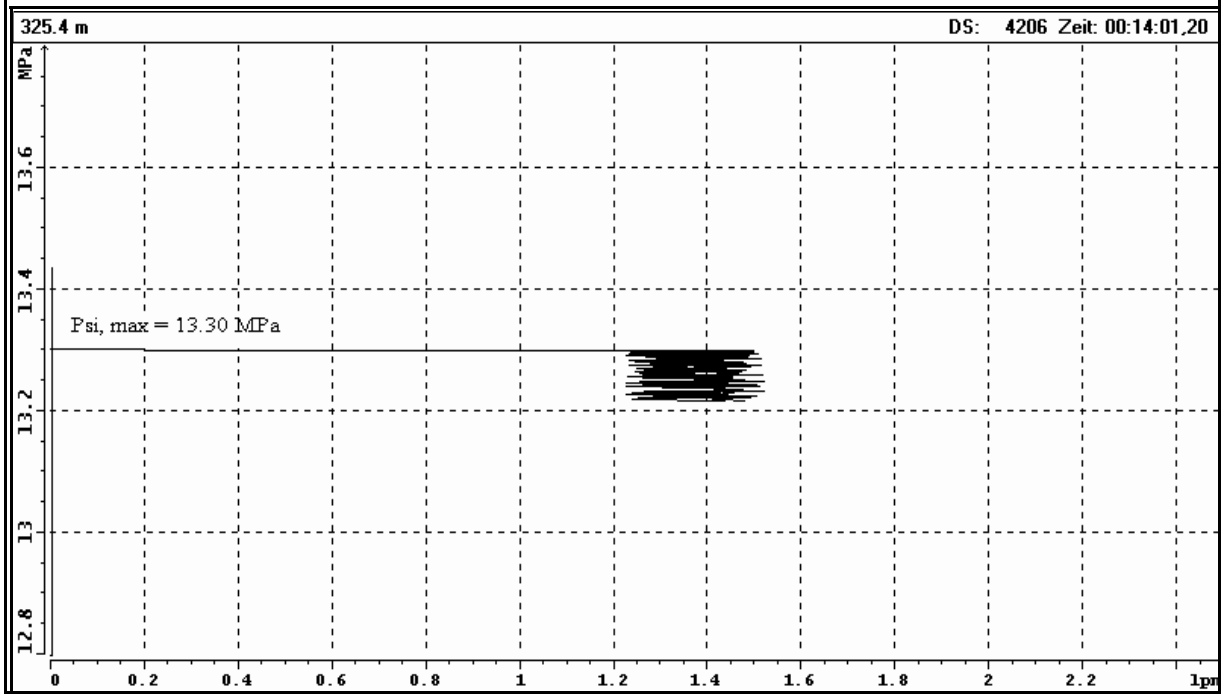

Test at 325.4 m MD: Estimation of $P_{si, min}$ (1. Refrac - Cycle)

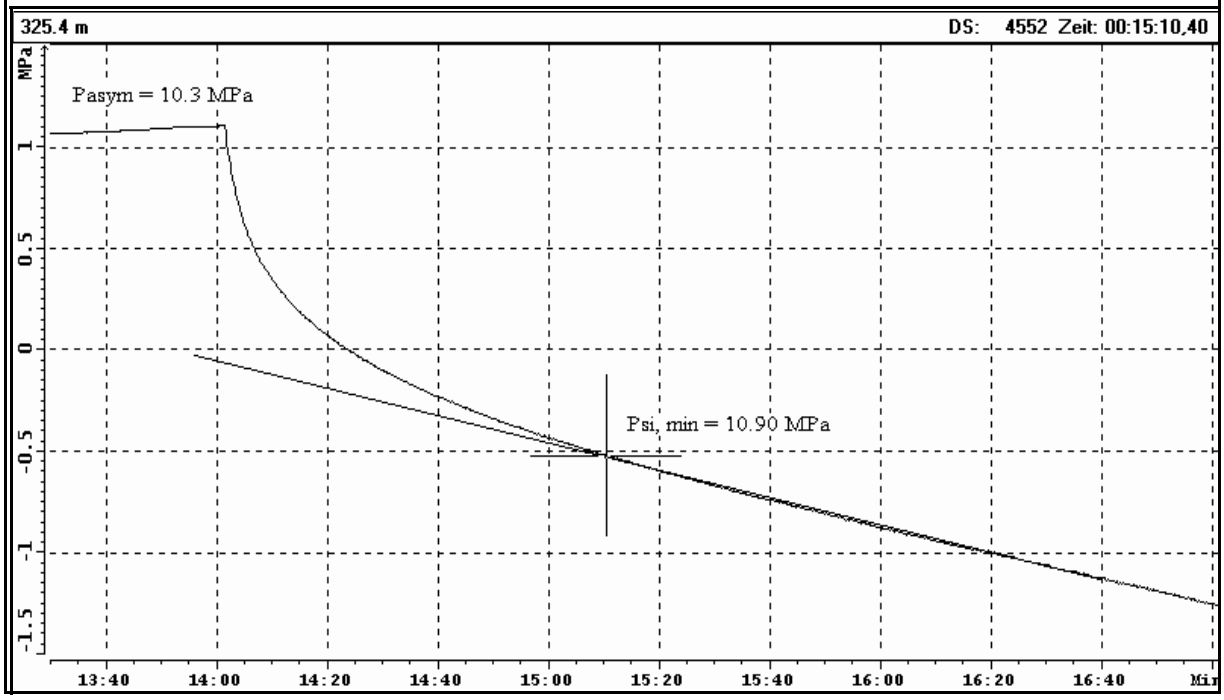

Test at 325.4 m MD: Estimation of P_{si} (1. Refrac - Cycle)

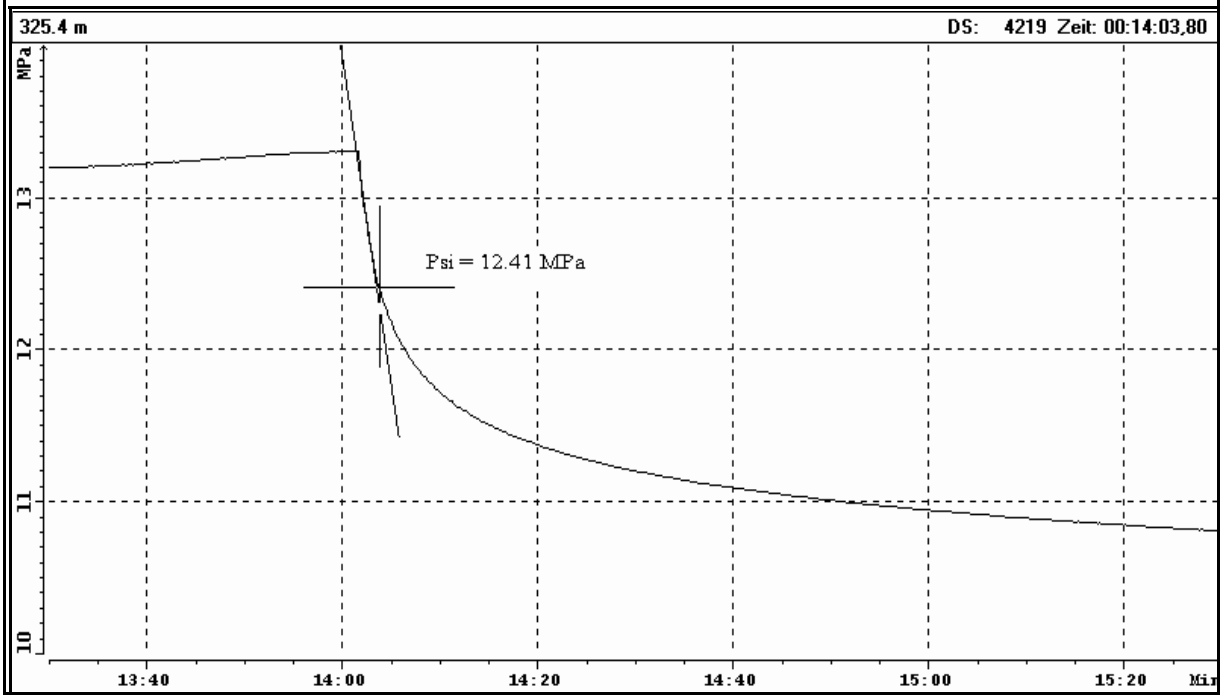

Test at 325.4 m MD: Analysis of Slow - Pump / Step - Rate - Test

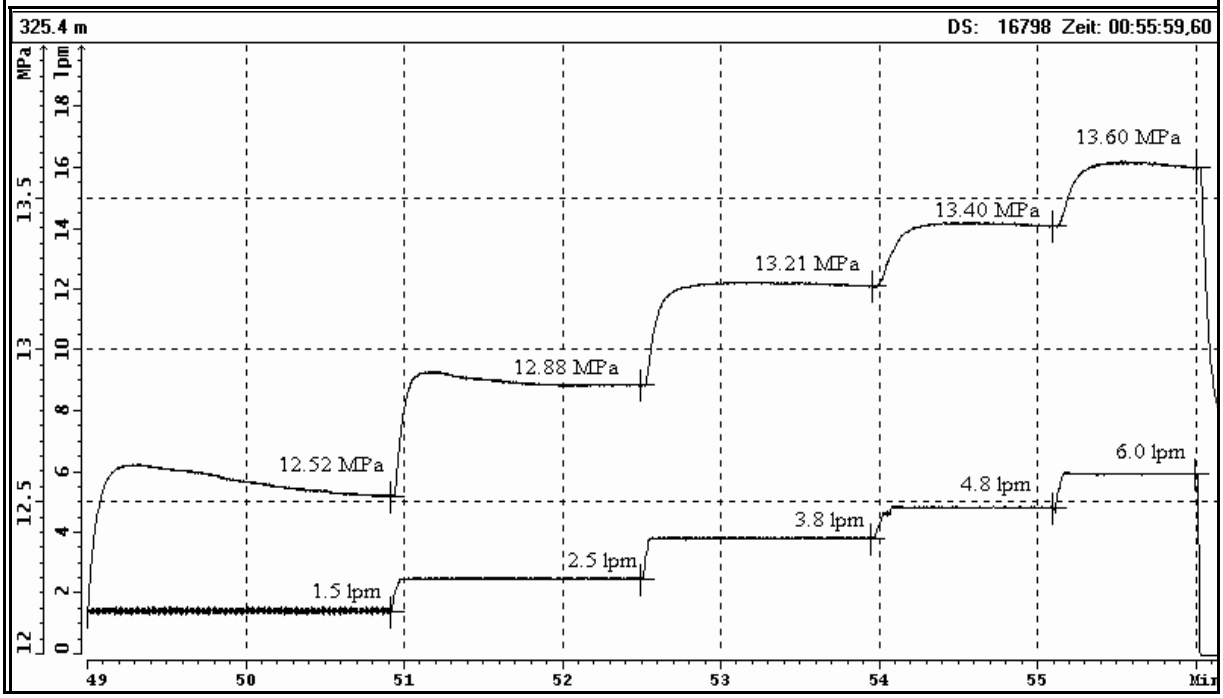

Test at 325.4 m MD: Examination of P_{si} (Step - Rate - Test)

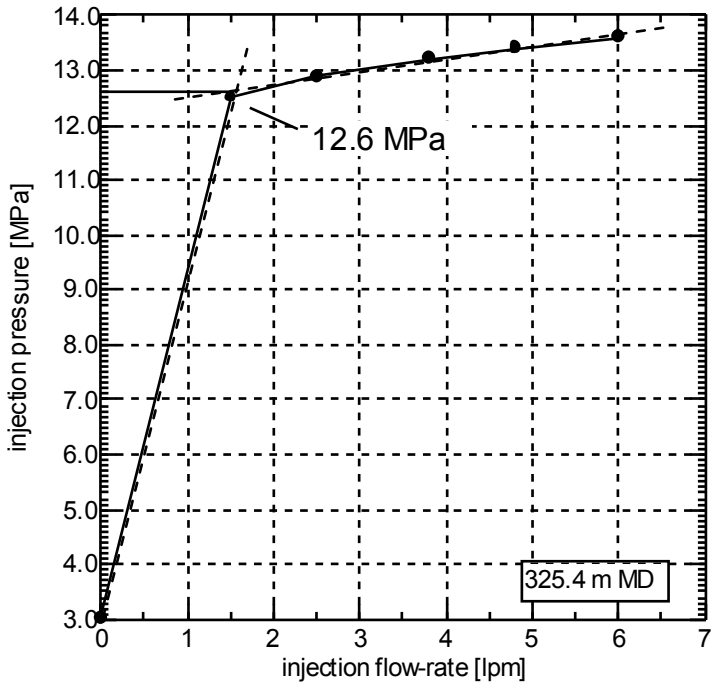

TEST AT 331.5 m MD / 314.2 m TVD

Test at 331.5 m MD: Overview - Plot

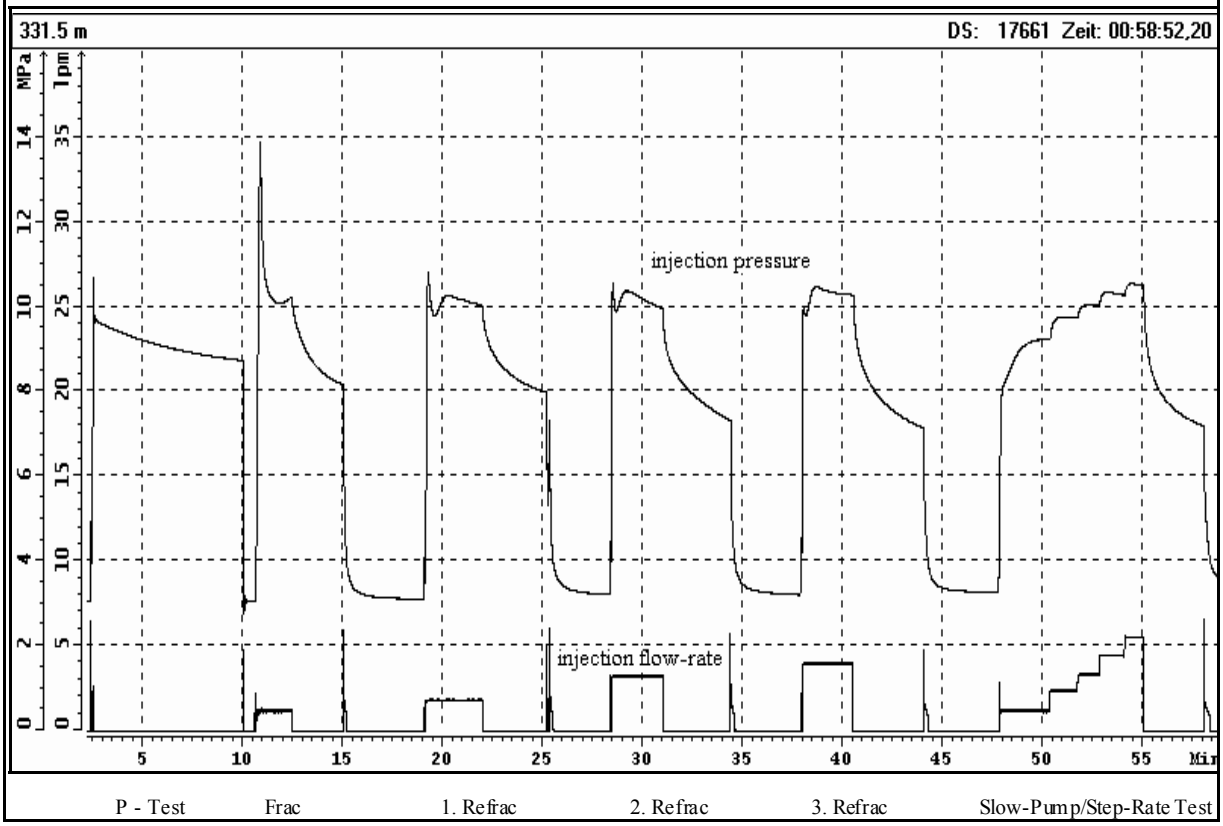

TEST SUMMARY

P - Test :	pressure decrease: 0.9 MPa in 7 min. 23 sec.
Frac - Cycle :	injection-rate Q_i= 1.2 lpm, injected volume V_i = 2.2 l, back-flow volume V_r = 0.3 l clear fracture initiation (breakdown event)
1. Refrac - Cycle :	Q_i = 1.8 lpm, V_i = 5.2 l, V_r = 0.4 l
2. Refrac - Cycle :	Q_i = 3.2 lpm, V_i = 8.3 l, V_r = 0.3 l
3. Refrac - Cycle :	Q_i = 4.0 lpm, V_i = 10.1 l, V_r = 0.3 l
Step-Rate Test :	Q_i = 1.2-5.5 lpm, V_i = 20.8 l, V_r = 0.5 l

total injected volume = 46.6 l, recovered volume = 1.8 l (3.9 %)

Test at 331.5 m MD: Estimation of P_c (Frac - Cycle)

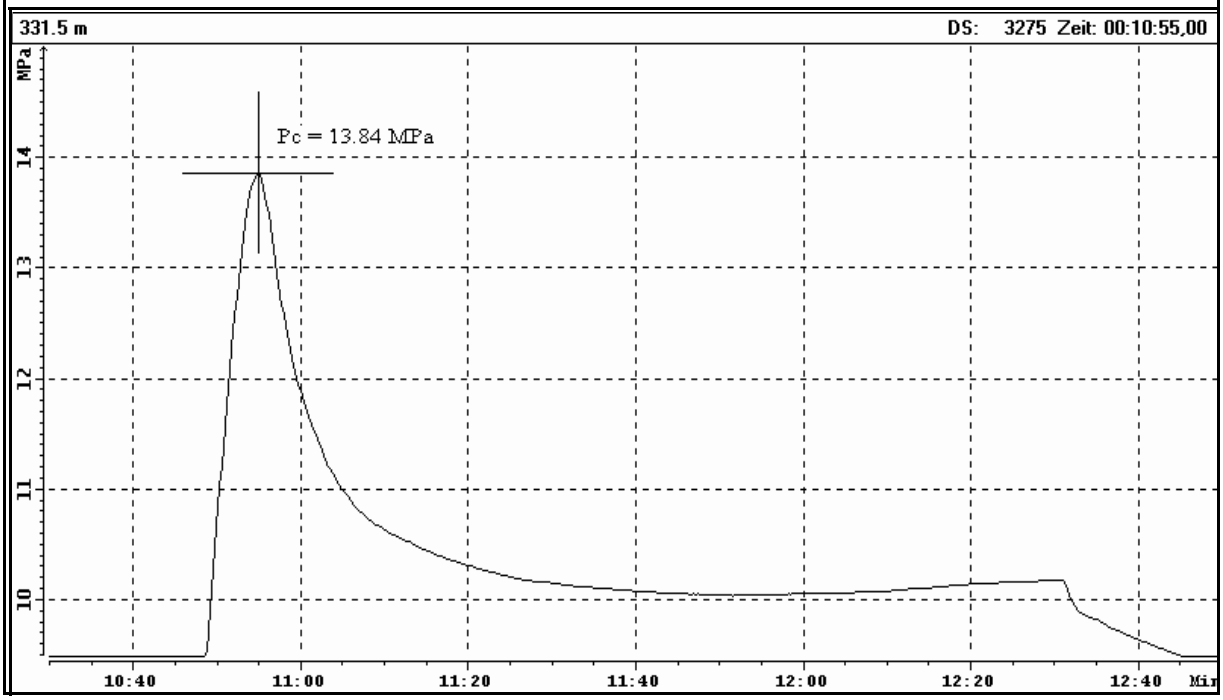

Test at 331.5 m MD: Estimation of P_r (1. Refrac - Cycle)

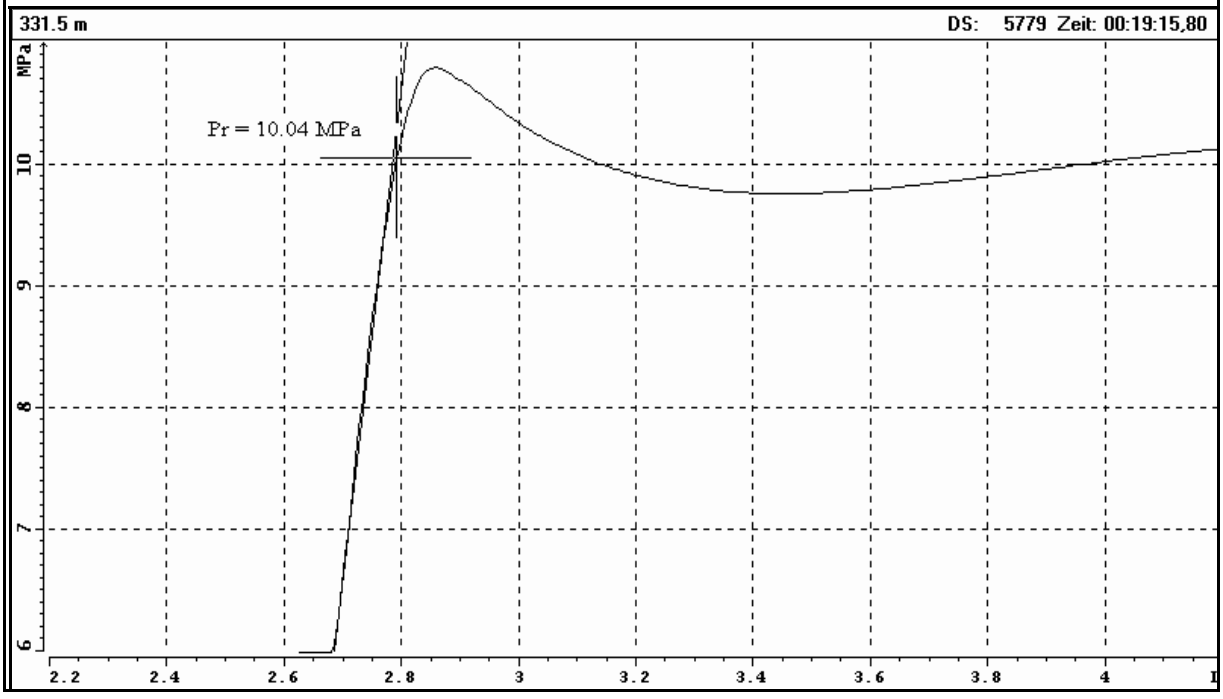

Test at 331.5 m MD: Estimation of $P_{si, max}$ (3. Refrac - Cycle)

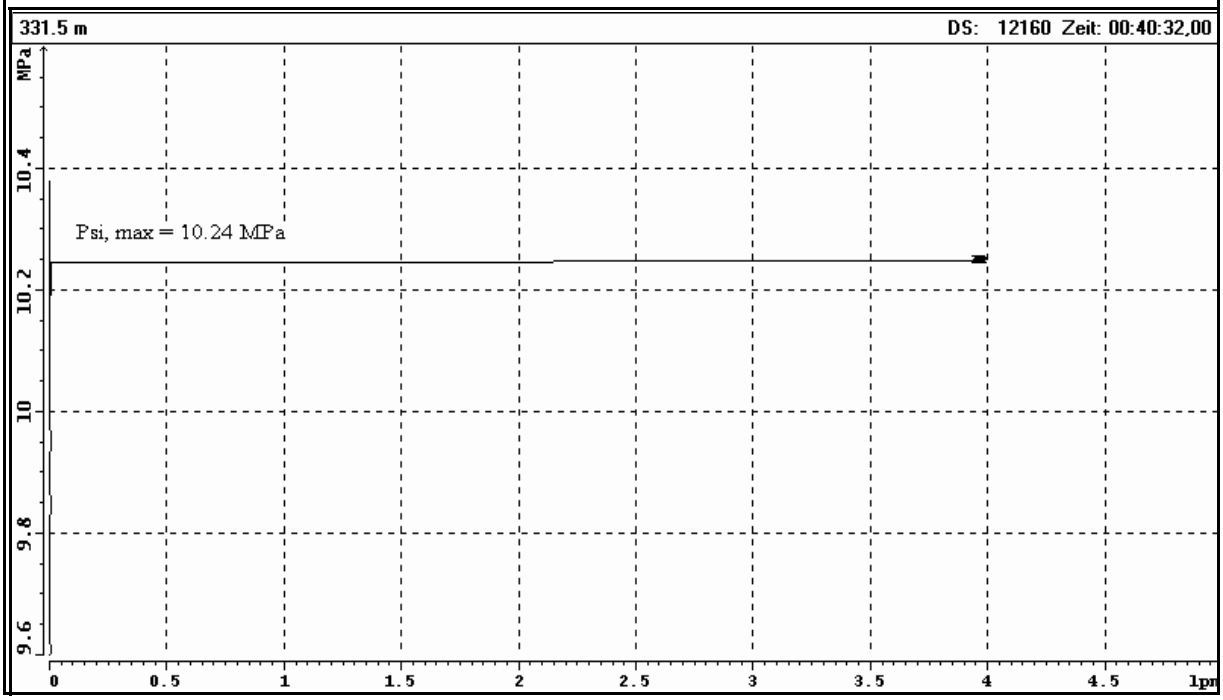

Test at 331.5 m MD: Estimation of $P_{si, min}$ (3. Refrac - Cycle)

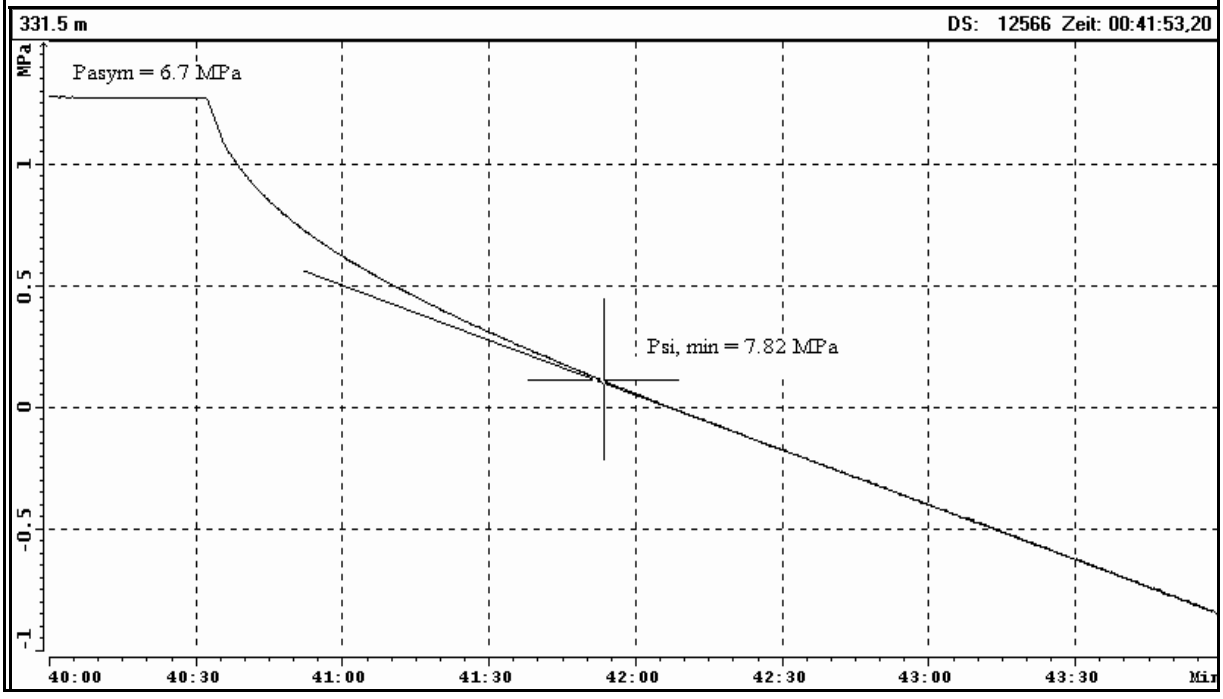

Test at 331.5 m MD: Estimation of P_{si} (3. Refrac - Cycle)

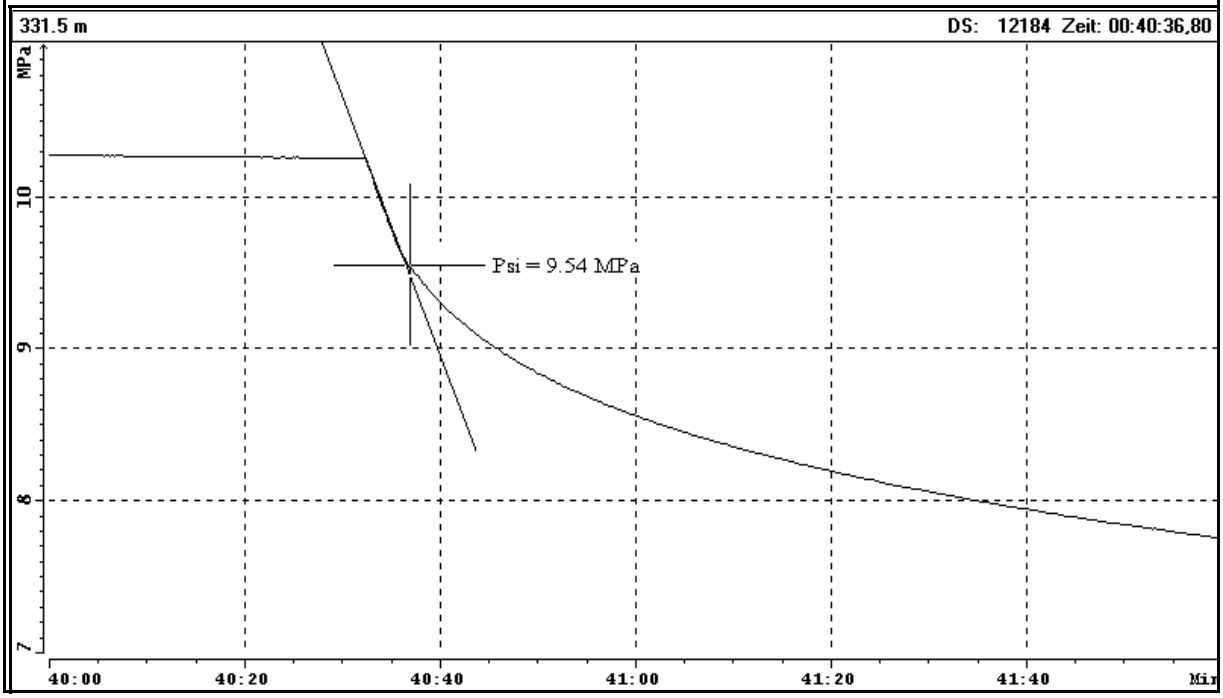

Test at 331.5 m MD: Analysis of Slow - Pump / Step - Rate - Test

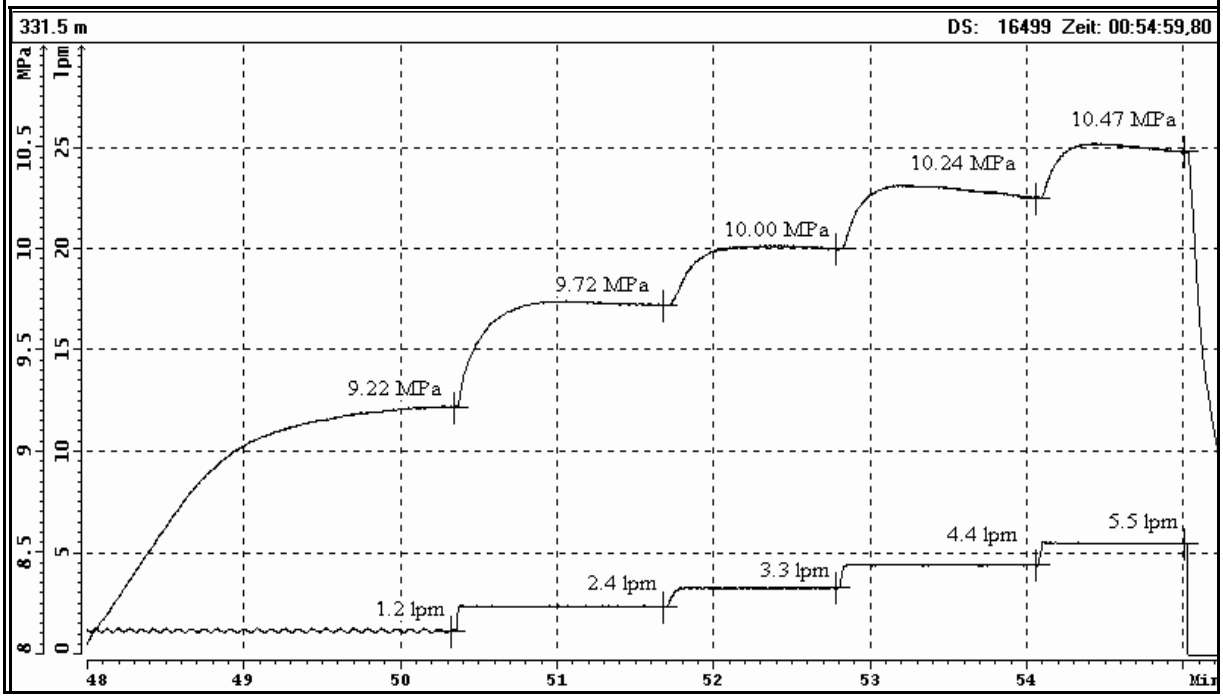

Test at 331.5 m MD: Examination of P_{si} (Step - Rate - Test)

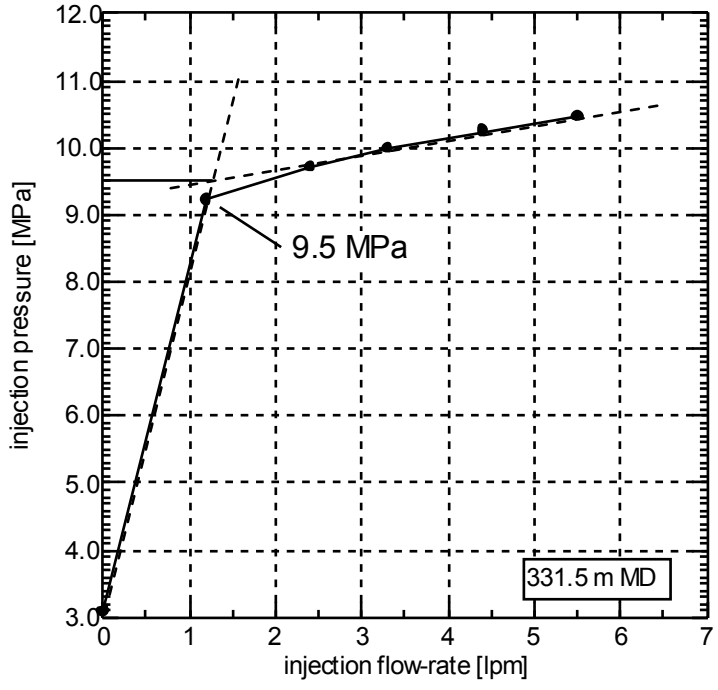

TEST AT 383.5 m MD / 363.0 m TVD

Test at 383.5 m MD: Overview - Plot

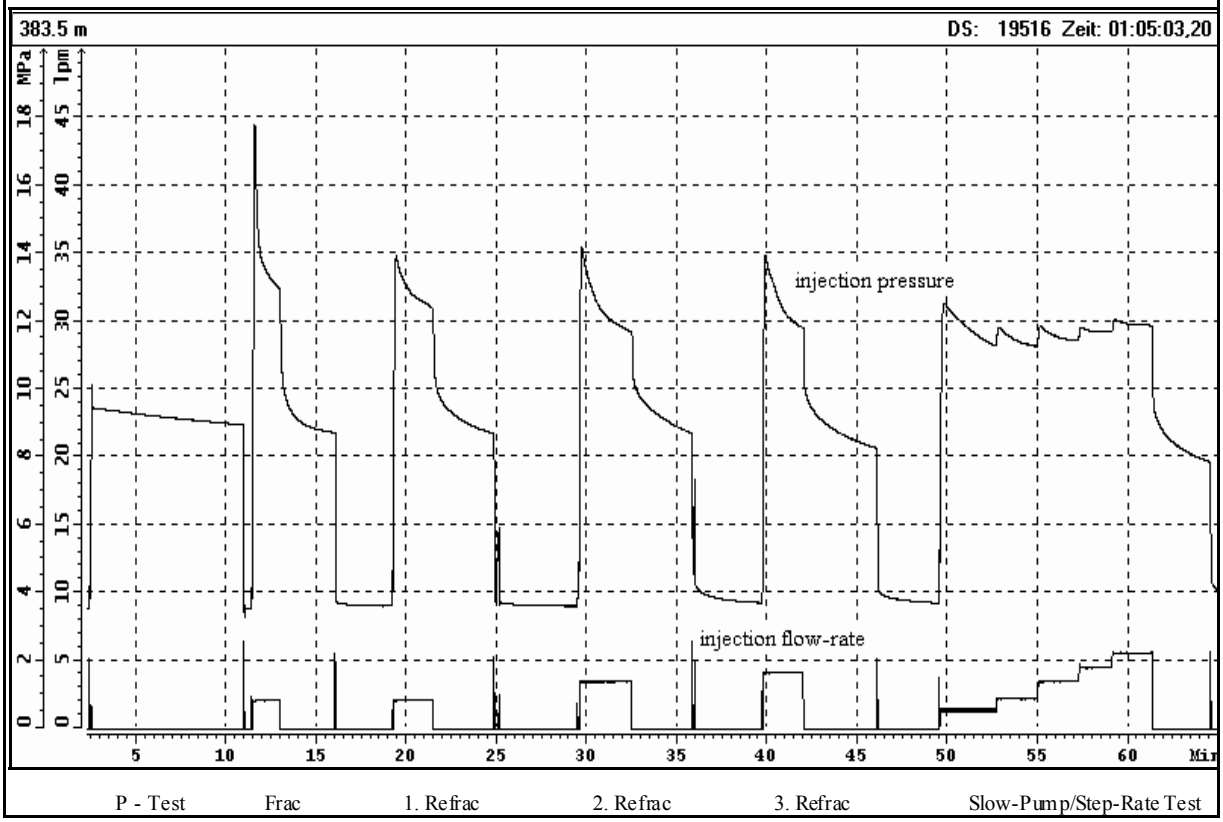

TEST SUMMARY

P - Test :	pressure decrease: 0.5 MPa in 8 min. 12 sec.
Frac - Cycle :	injection-rate Q_i= 2.1 lpm, injected volume V_i = 3.3 l, back-flow volume V_r = 0.1 l clear fracture initiation (breakdown event)
1. Refrac - Cycle :	Q_i = 2.1 lpm, V_i = 3.3 l, V_r = 0.2 l
2. Refrac - Cycle :	Q_i = 3.5 lpm, V_i = 10.2 l, V_r = 0.2 l
3. Refrac - Cycle :	Q_i = 4.2 lpm, V_i = 9.3 l, V_r = 0.1 l
Step-Rate Test :	Q_i = 1.4-5.6 lpm, V_i = 38.2 l, V_r = 0.1 l

total injected volume = 65.8 l, recovered volume = 0.7 l (1.1 %)

Test at 383.5 m MD: Estimation of P_c (Frac - Cycle)

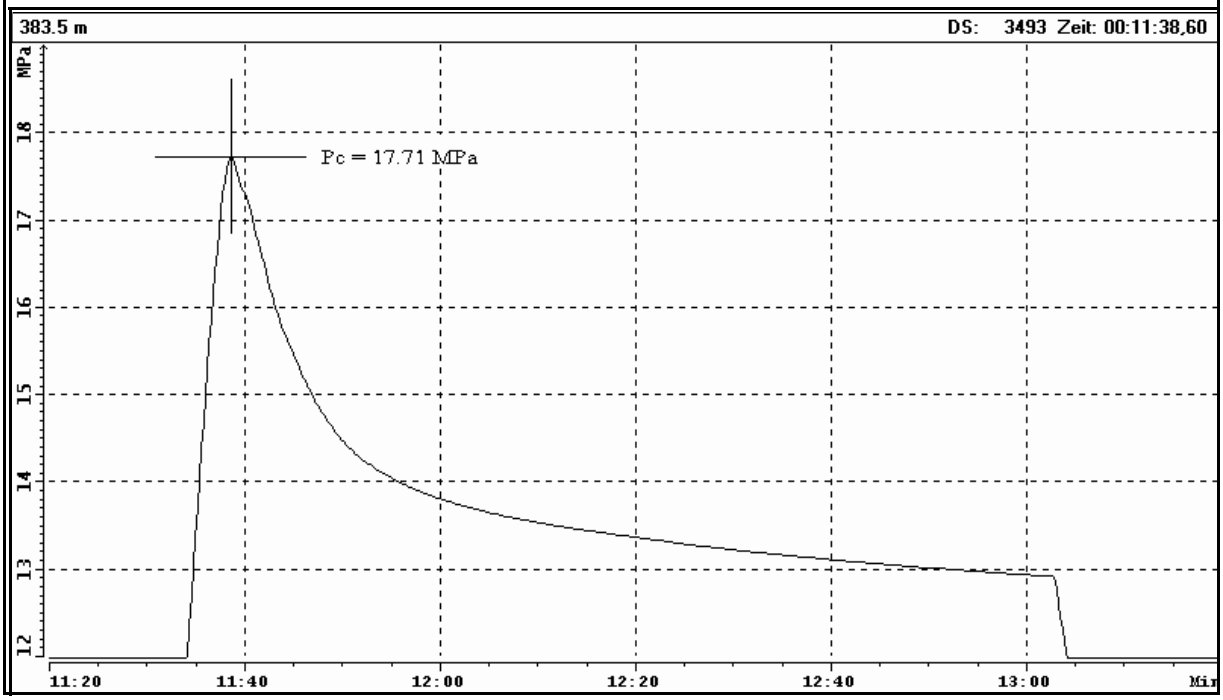

Test at 383.5 m MD: Estimation of P_r (1. Refrac - Cycle)

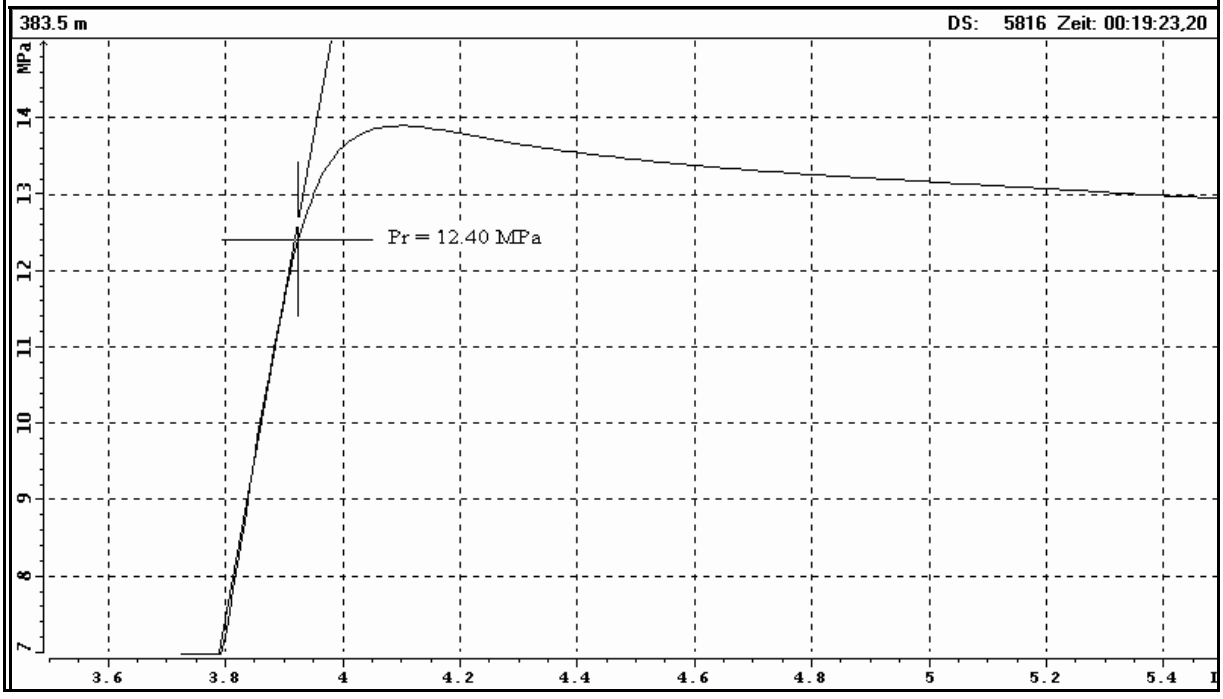

Test at 383.5 m MD: Estimation of $P_{si,\,max}$ (3. Refrac - Cycle)

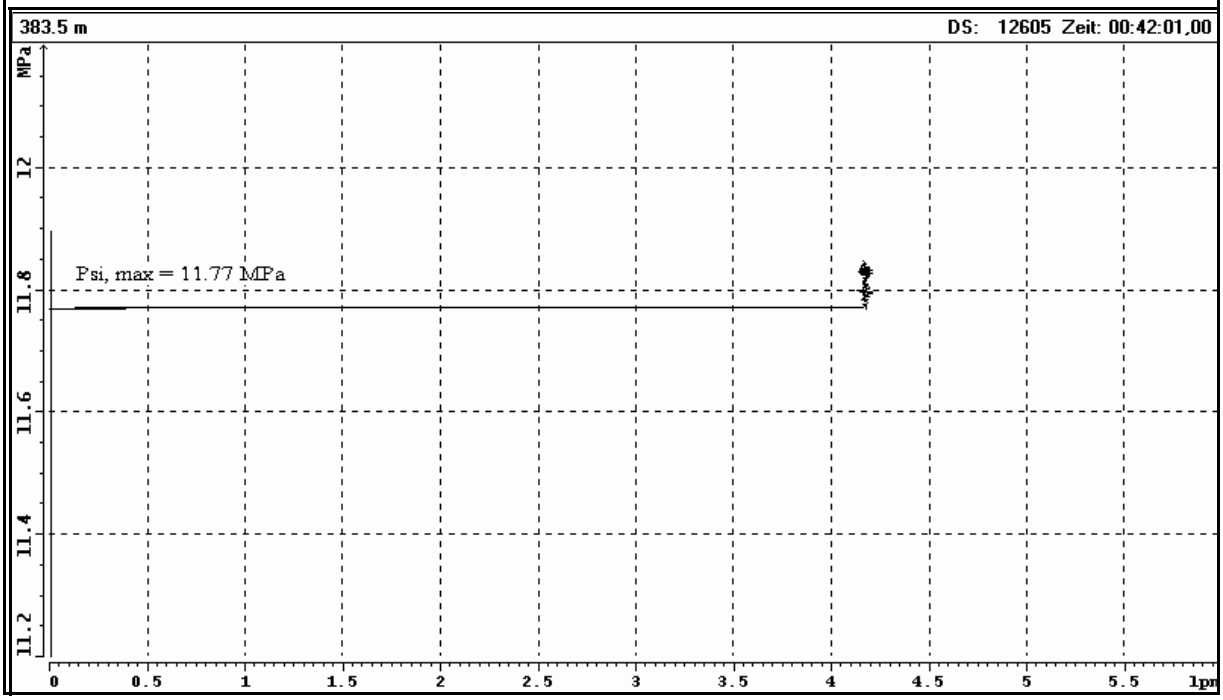

Test at 383.5 m MD: Estimation of $P_{si,\,min}$ (3. Refrac - Cycle)

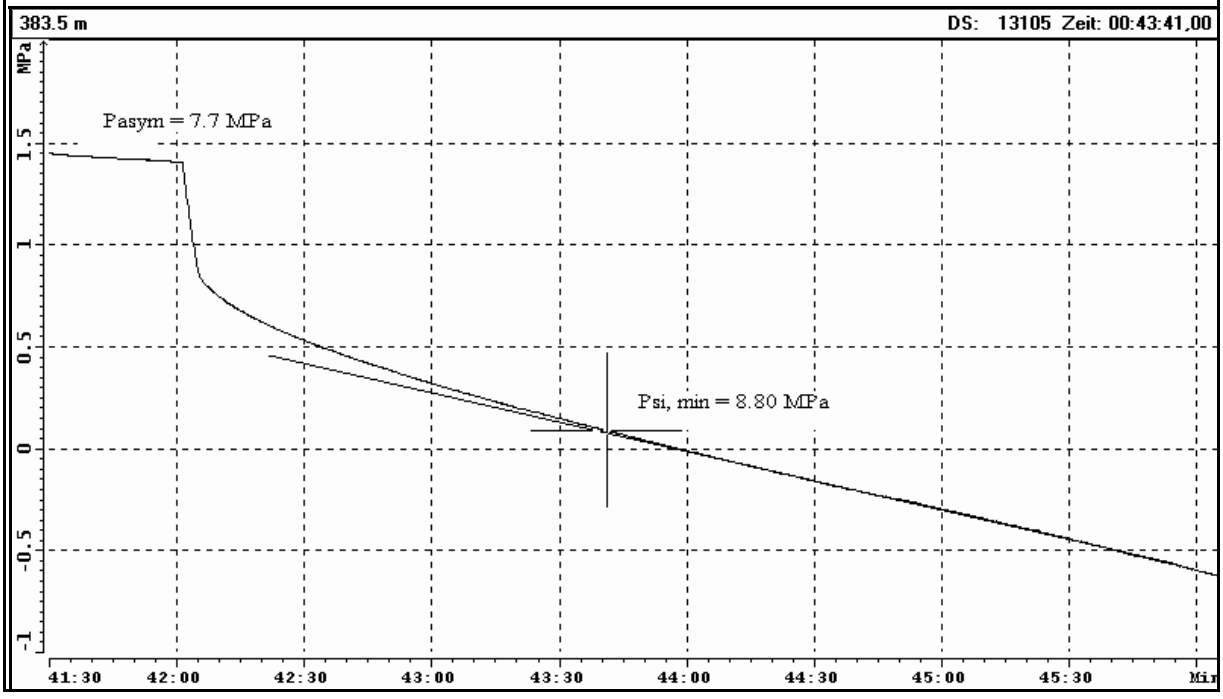

Test at 383.5 m MD: Estimation of P_{si} (3. Refrac - Cycle)

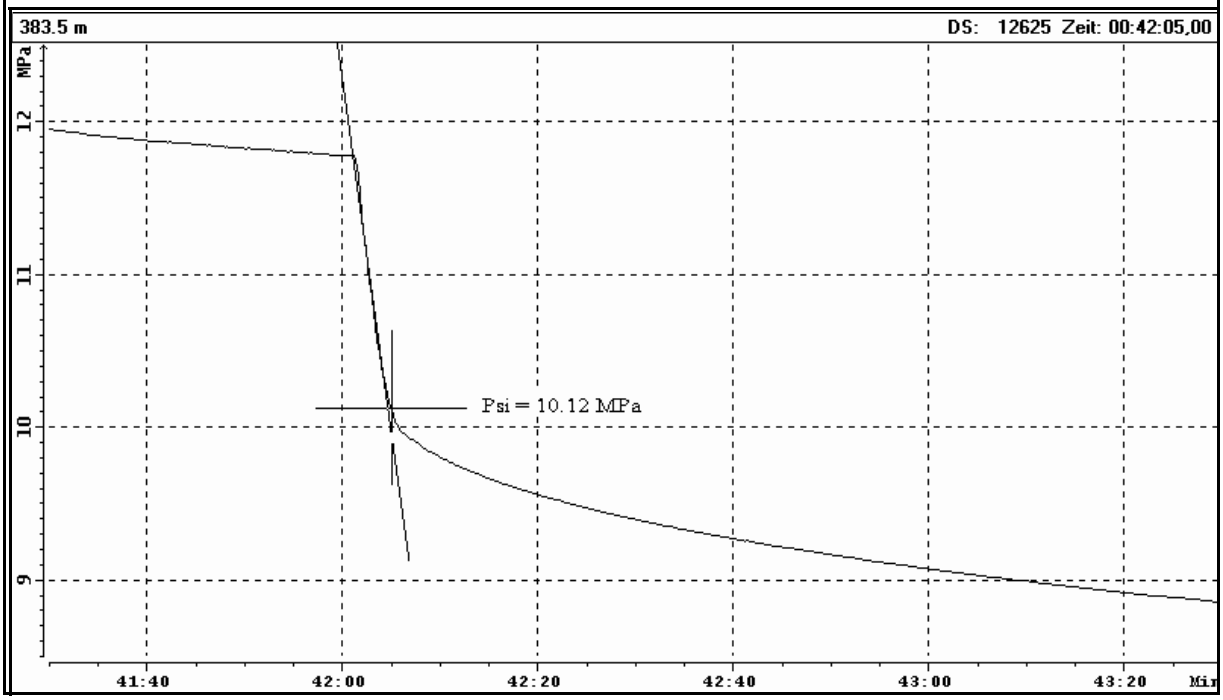

Test at 383.5 m MD: Analysis of Slow - Pump / Step - Rate - Test

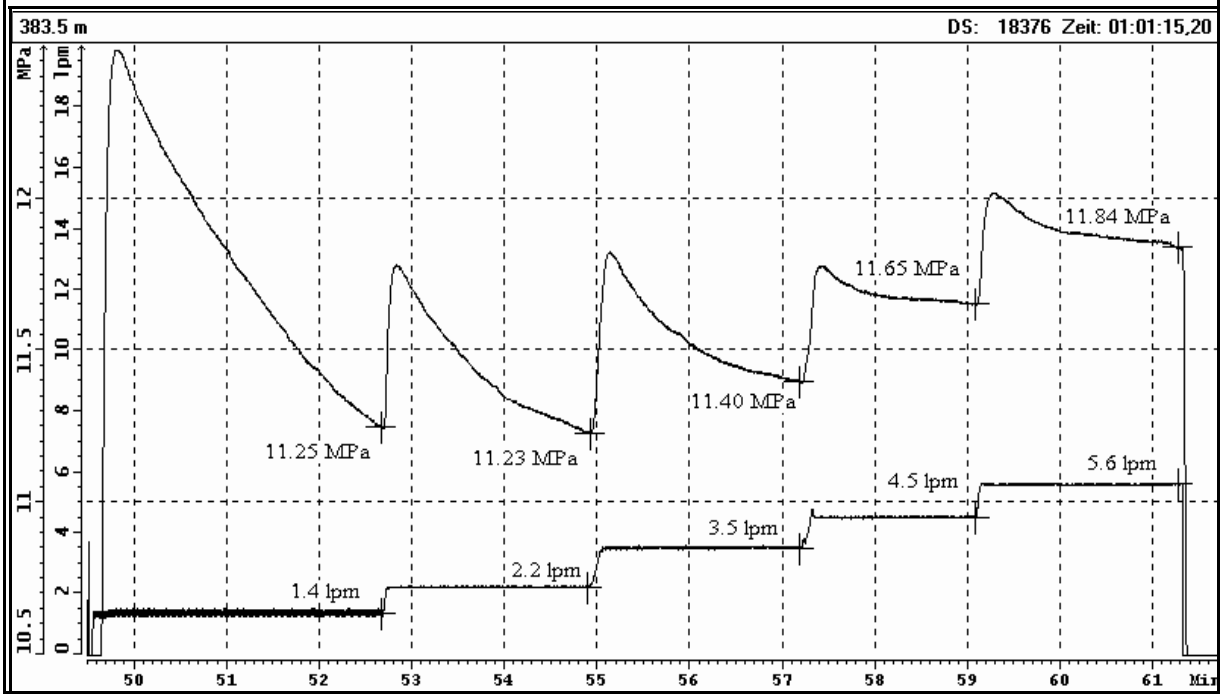

Test at 383.5 m MD: Examination of P_{si} (Step - Rate - Test)

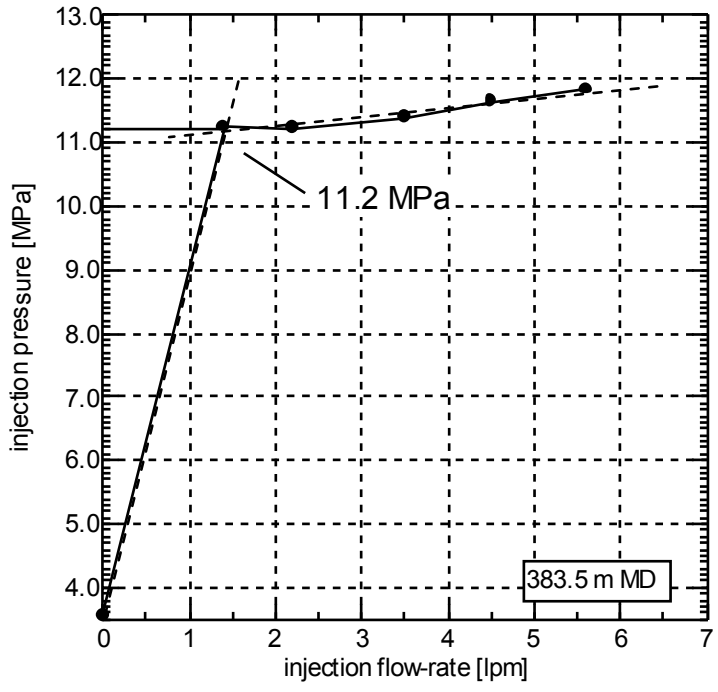

TEST AT 416.0 m MD / 393.8 m TVD

Test at 416.0 m MD : Overview - Plot

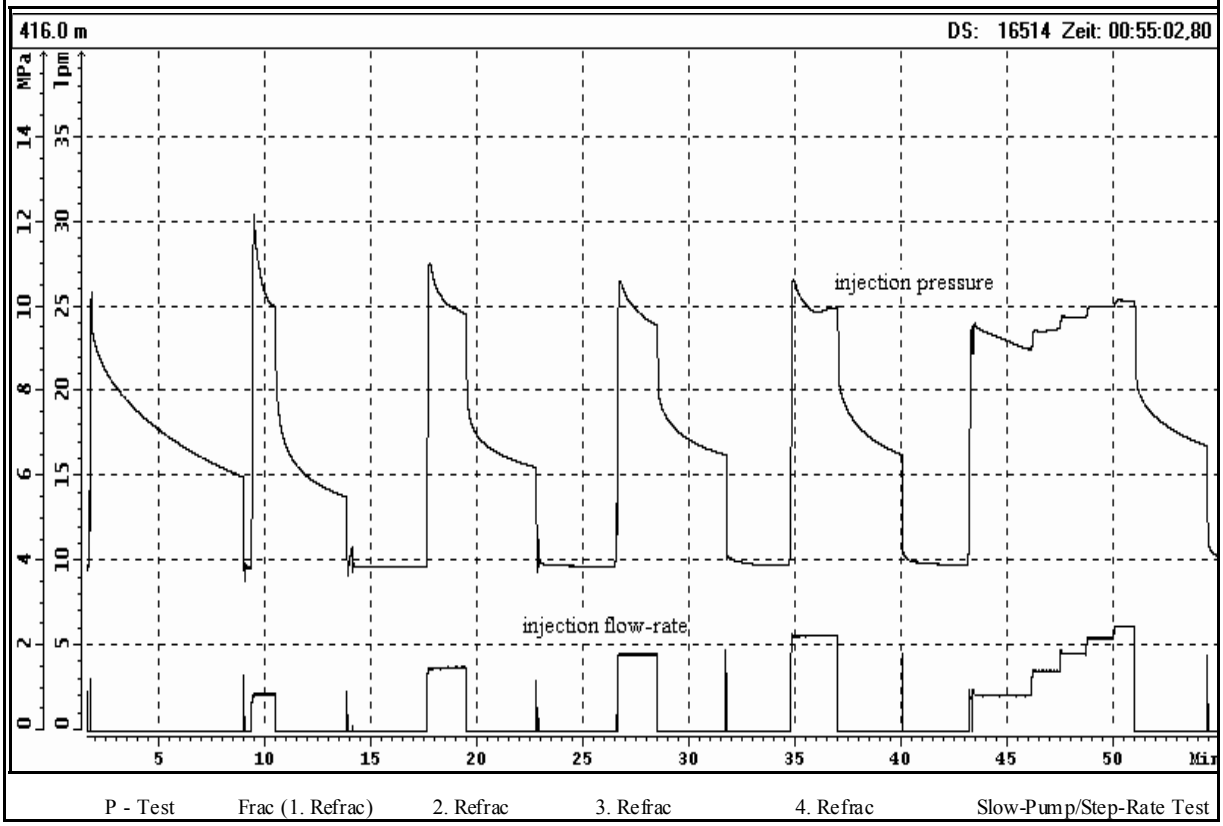

TEST SUMMARY

P - Test :	pressure decrease: 3.4 MPa in 7 min. 5 sec.
Frac (1. Refrac) - Cycle :	injection-rate Q_i= 2.2 lpm, injected volume V_i = 2.4 l, back-flow volume V_r = 0 l stimulation of an existing fracture (no breakdown event)
2. Refrac - Cycle :	Q_i = 3.7 lpm, V_i = 6.8 l, V_r = 0.1 l
3. Refrac - Cycle :	Q_i = 4.5 lpm, V_i = 8.3 l, V_r = 0.1 l
4. Refrac - Cycle :	Q_i = 5.6 lpm, V_i = 12.3 l, V_r = 0.1 l
Step-Rate Test :	Q_i = 2.1-6.2 lpm, V_i = 29.6 l, V_r = 0.1 l

total injected volume = 59.4 l, recovered volume = 0.4 l (0.7 %)

Test at 416.0 m MD: Estimation of P_r (Frac (1. Refrac) - Cycle)

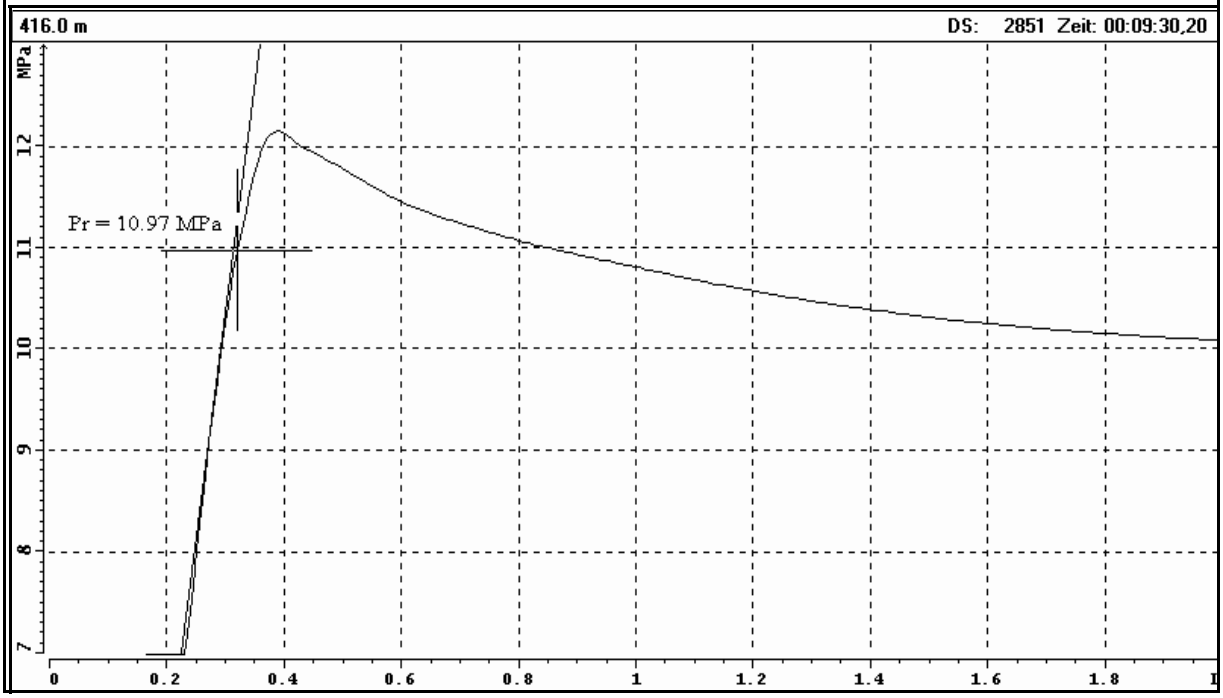

Test at 416.0 m MD: Estimation of $P_{si,\,max}$ (4. Refrac - Cycle)

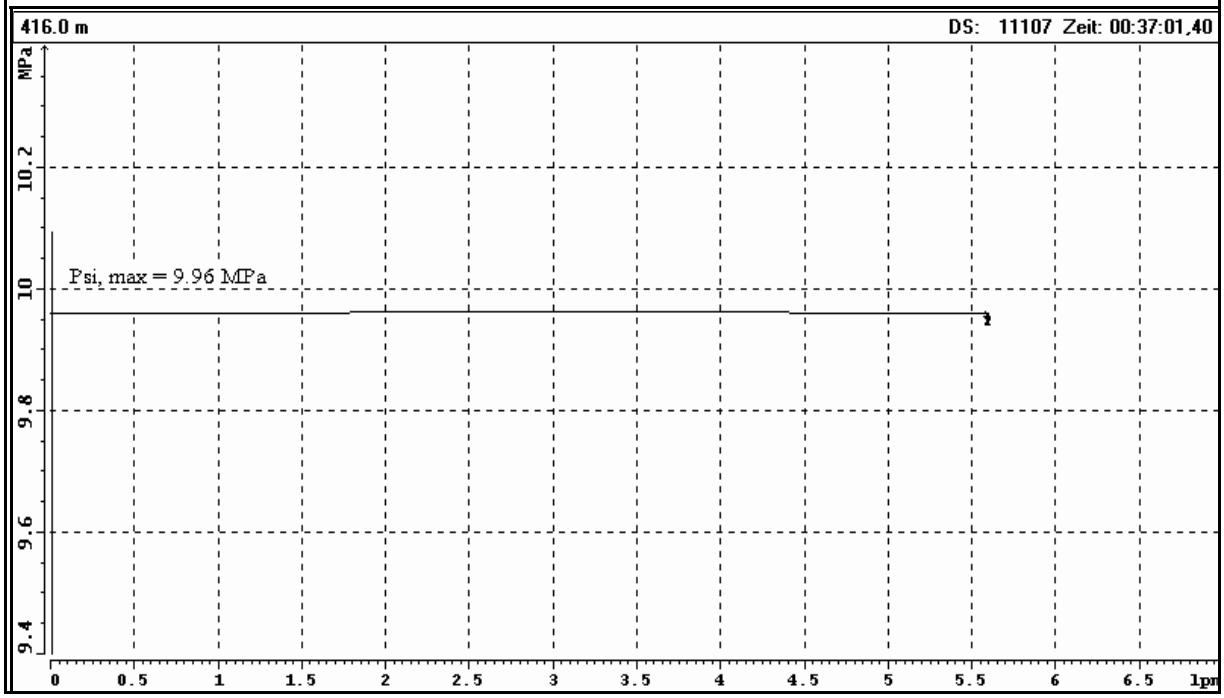

Test at 416.0 m MD: Estimation of $P_{si,\,min}$ (4. Refrac - Cycle)

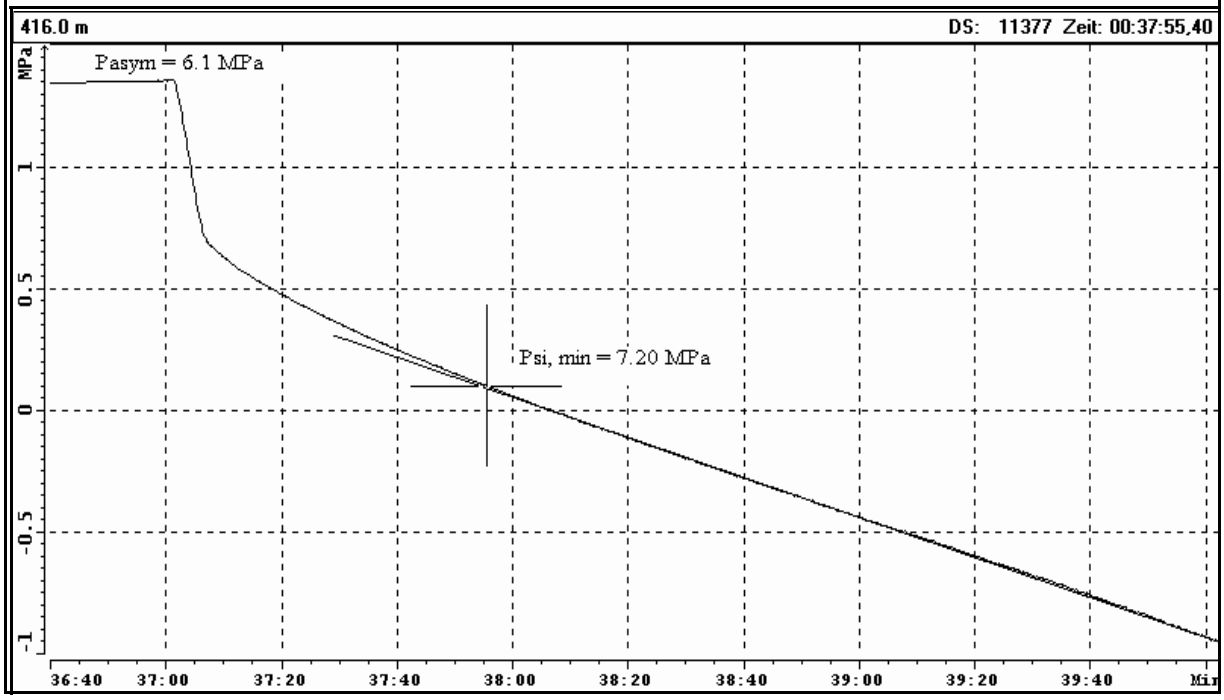

Test at 416.0 m MD: Estimation of P_{si} (4. Refrac - Cycle)

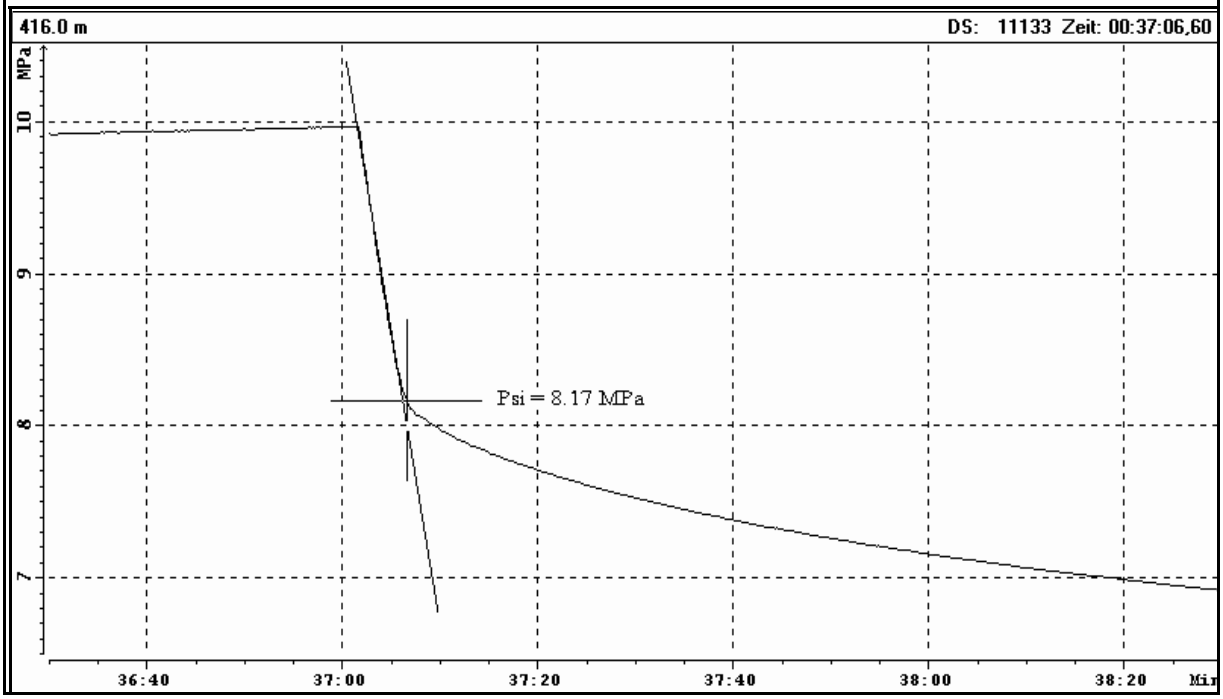

Test at 416.0 m MD: Analysis of Slow - Pump / Step - Rate - Test

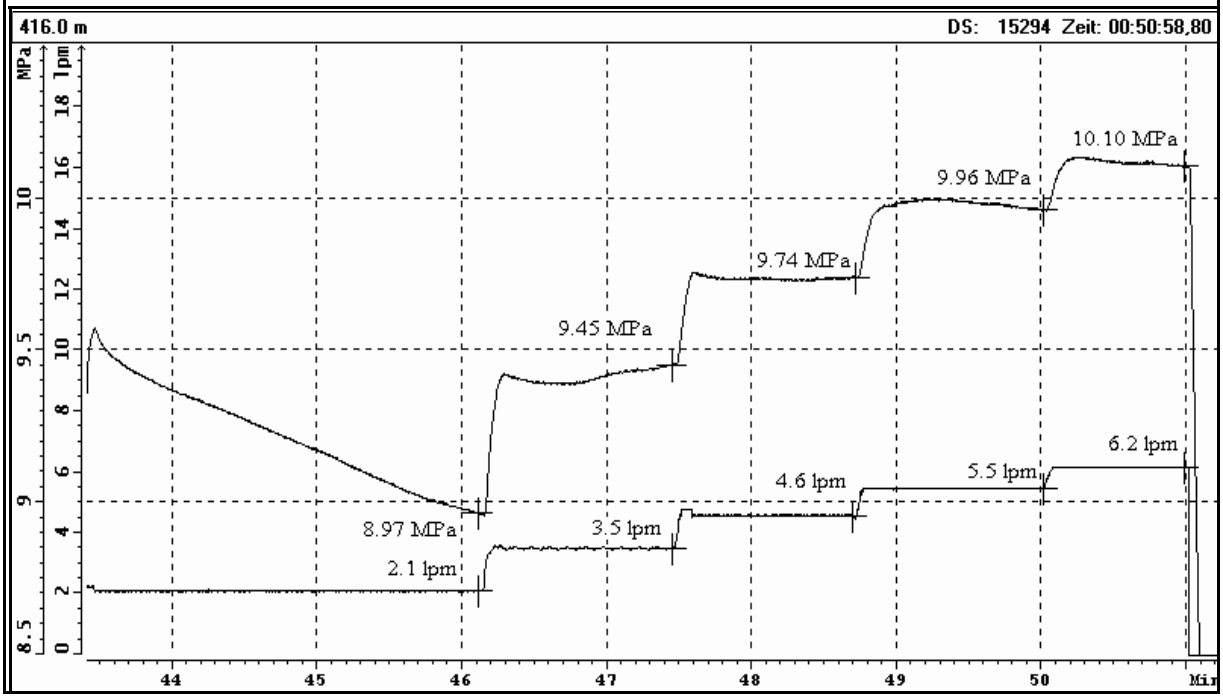

Test at 416.0 m MD: Examination of P_{si} (Step - Rate - Test)

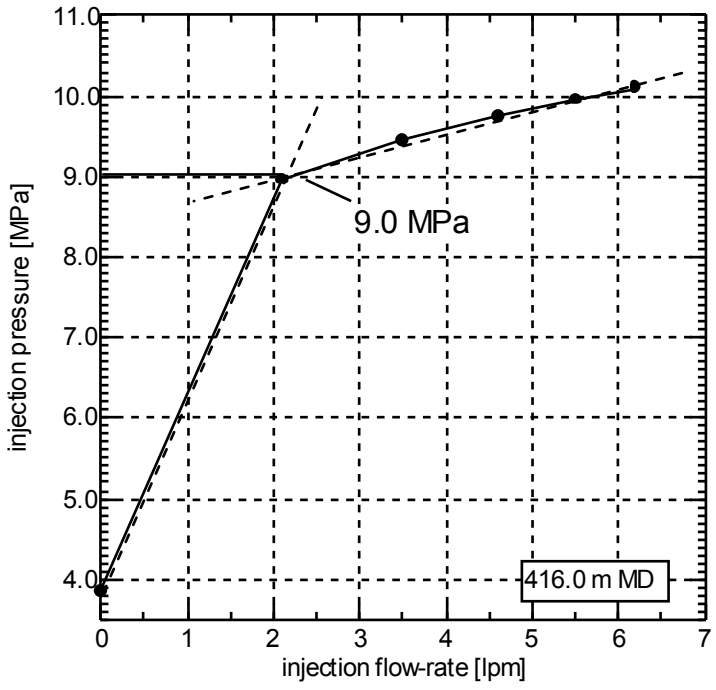

TEST ATTEMPT AT 417.7 m MD / 395.5 m TVD

Test at 417.7 m MD : Overview - Plot

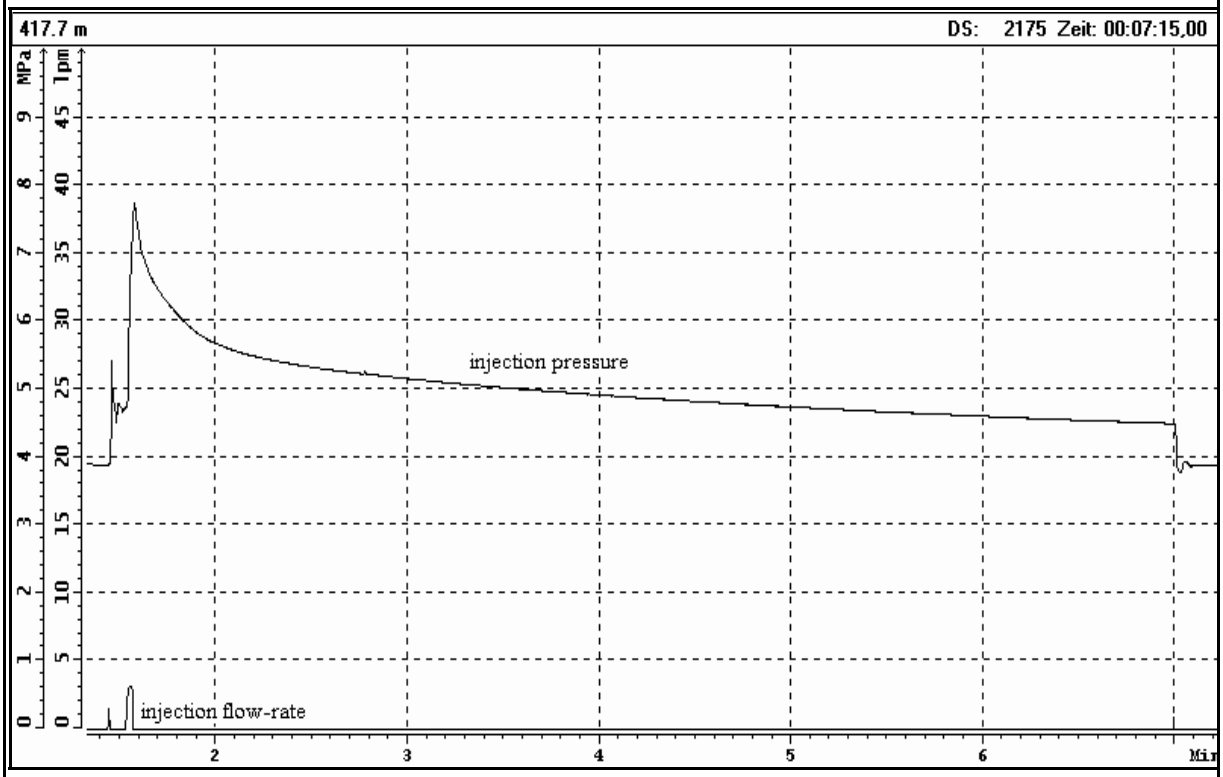

P - Test

TEST SUMMARY

P - Test : pressure decrease: 3.2 MPa in 5 min. 24 sec.

Remark: Test abandoned due to the high rock-mass permeability.

TEST AT 471.0 m MD / 446.9 m TVD

Test at 471.0 m MD : Overview - Plot

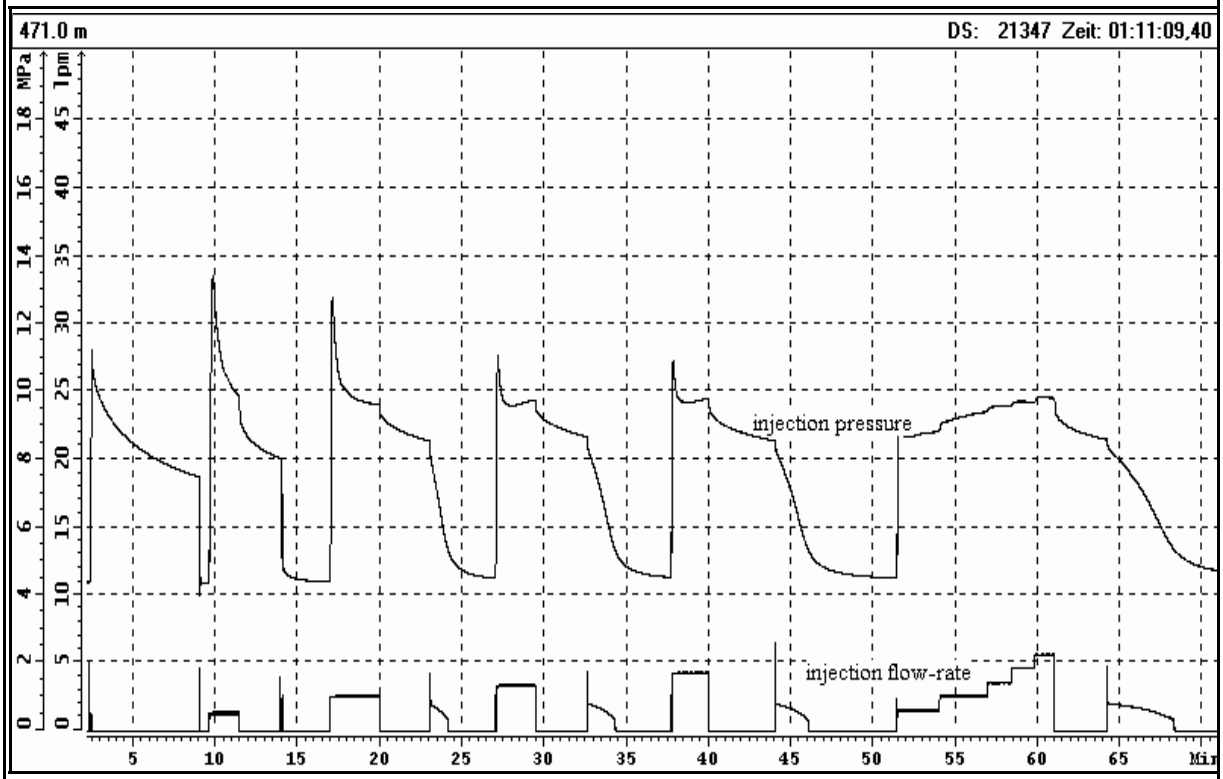

TEST SUMMARY

P - Test :	pressure decrease: 3.0 MPa in 6 min. 26 sec.
Frac (1. Refrac) - Cycle :	injection-rate Q_i= 1.3 lpm, injected volume V_i = 2.4 l, back-flow volume V_r = 0.1 l stimulation of an existing fracture (no breakdown event)
2. Refrac - Cycle :	Q_i = 2.6 lpm, V_i = 7.6 l, V_r = 1.6 l
3. Refrac - Cycle :	Q_i = 3.3 lpm, V_i = 7.9 l, V_r = 2.7 l
4. Refrac - Cycle :	Q_i = 4.3 lpm, V_i = 9.6 l, V_r = 3.1 l
Step-Rate Test :	Q_i = 1.5-5.6 lpm, V_i = 29.9 l, V_r = 6.6 l

total injected volume = 57.4 l, recovered volume = 14.1 l (24.6 %)

Test at 471.0 m MD: Estimation of P_r (Frac (1. Refrac) - Cycle)

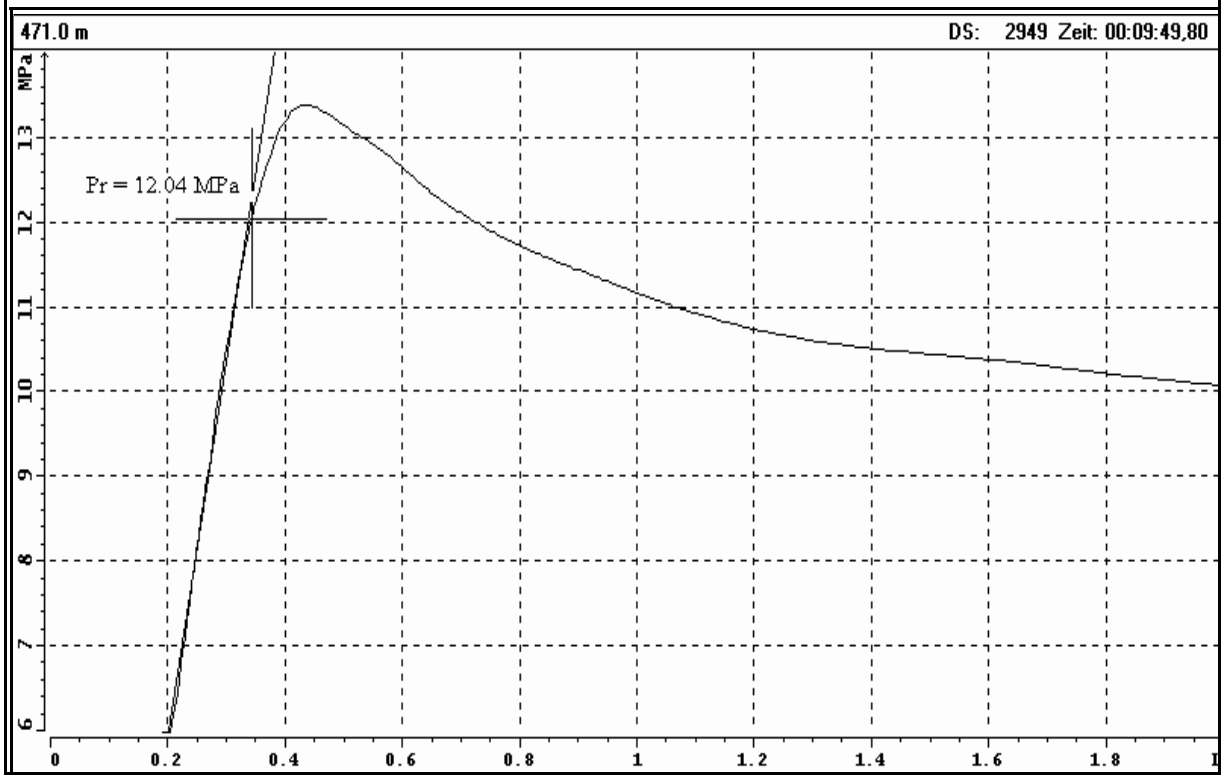

Test at 471.0 m MD: Estimation of $P_{si,\,max}$ (4. Refrac - Cycle)

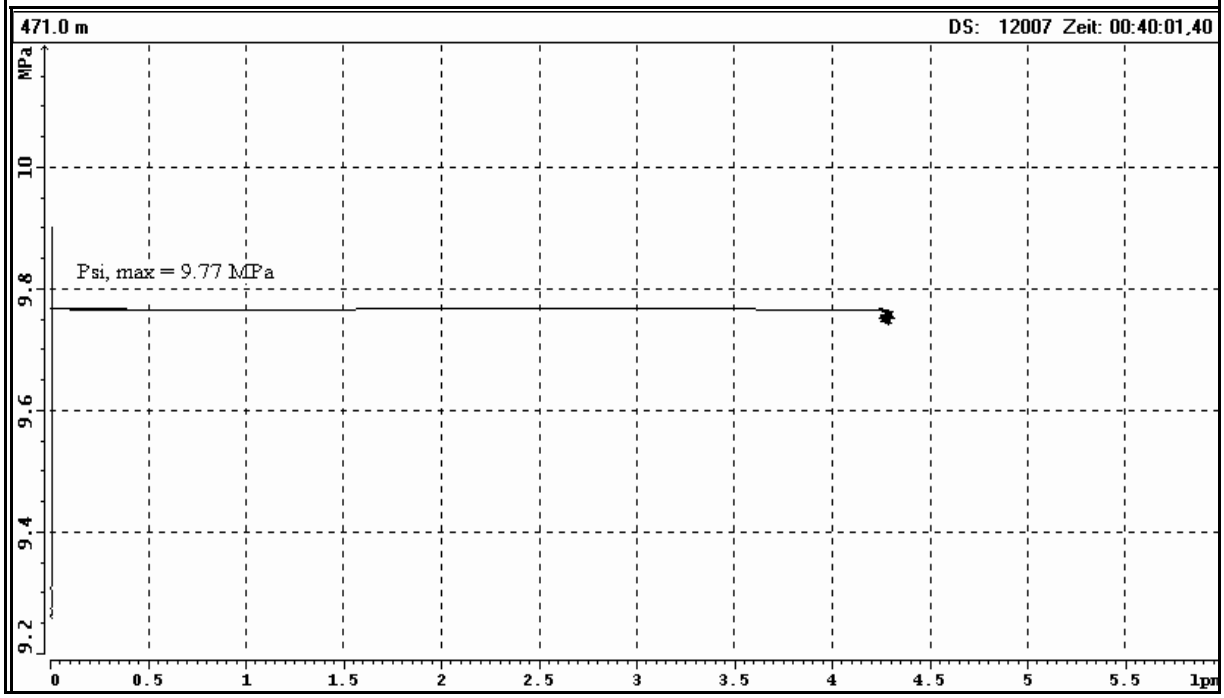

Test at 471.0 m MD: Estimation of $P_{si,\,min}$ (4. Refrac - Cycle)

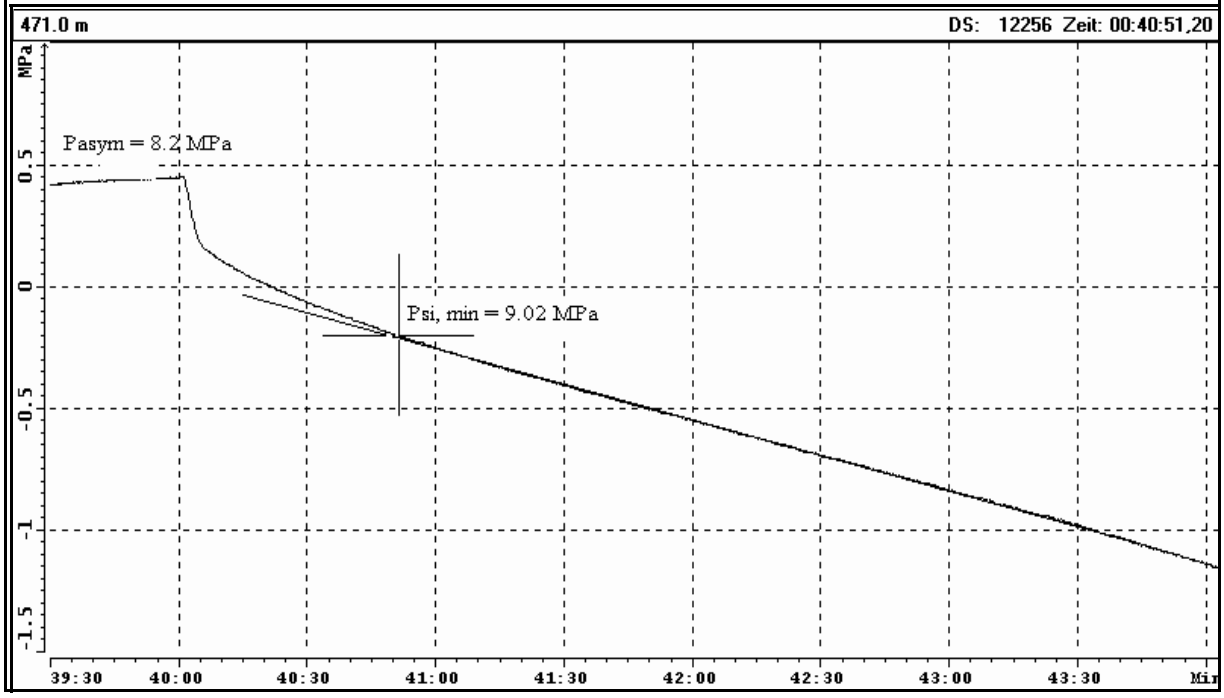

Test at 471.0 m MD: Estimation of P_{si} (4. Refrac - Cycle)

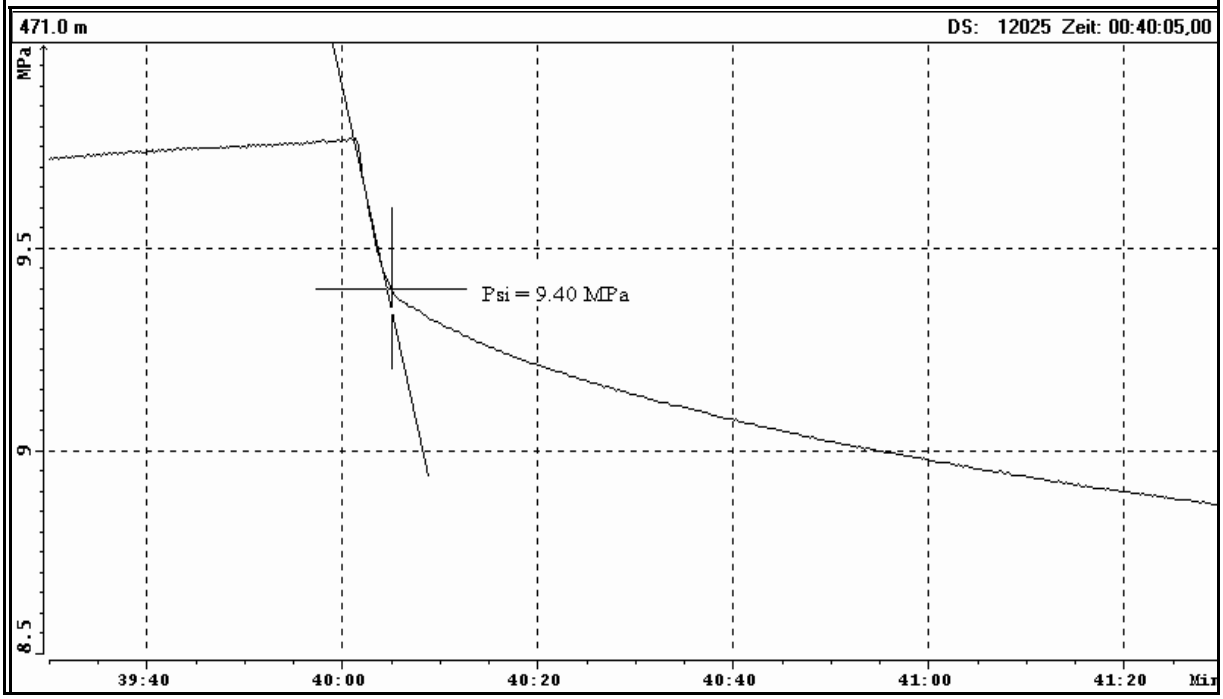

Test at 471.0 m MD: Analysis of Slow - Pump / Step - Rate - Test

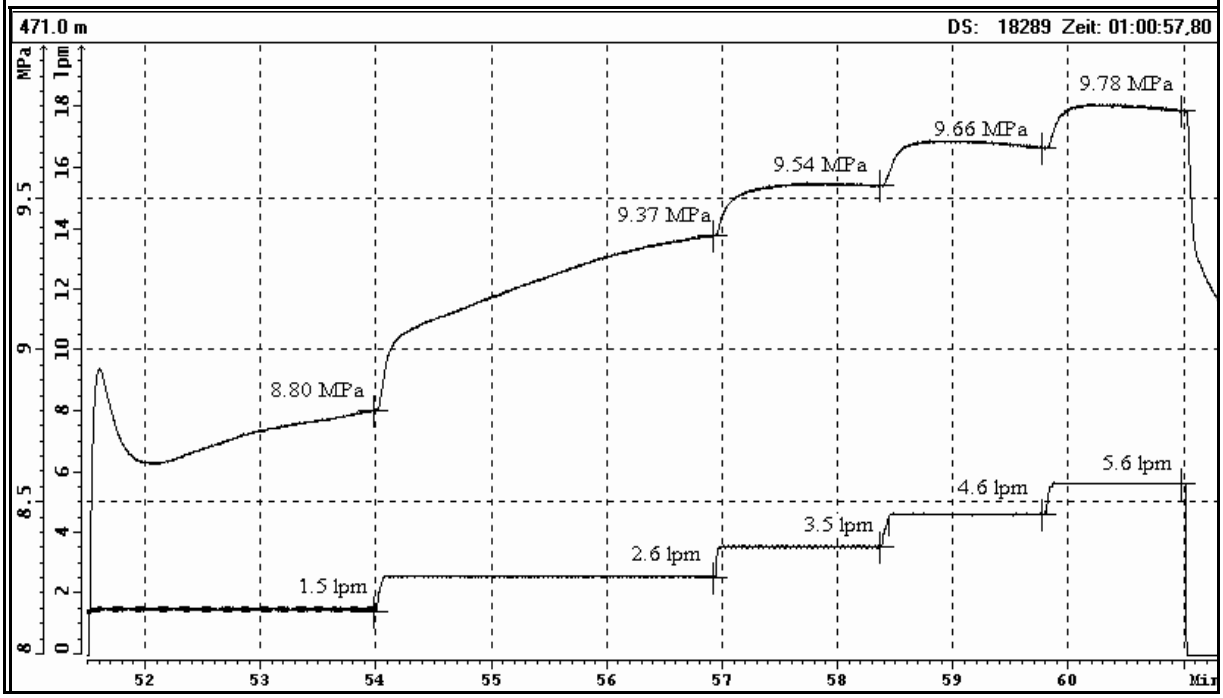

Test at 471.0 m MD: Examination of P_{si} (Step - Rate - Test)

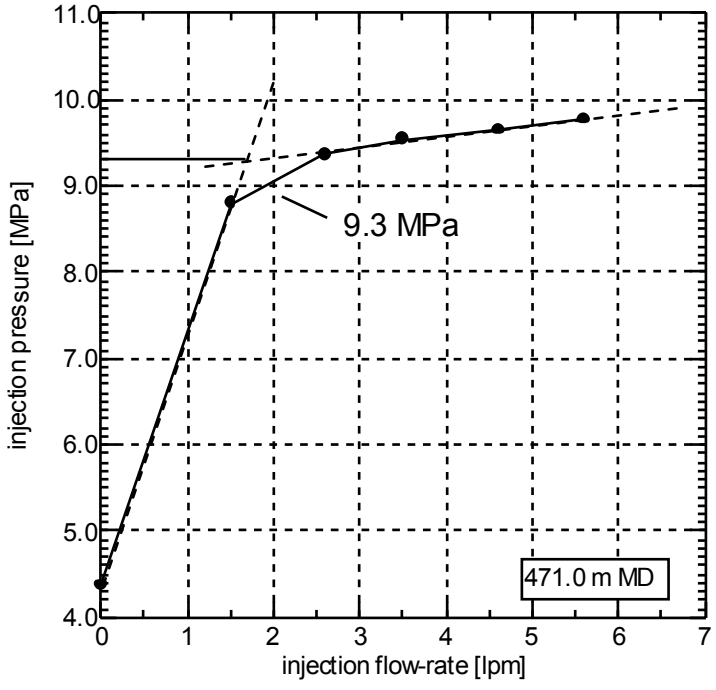

TEST AT 490.5 m MD / 465.8 m TVD

Test at 490.5 m MD: Overview - Plot

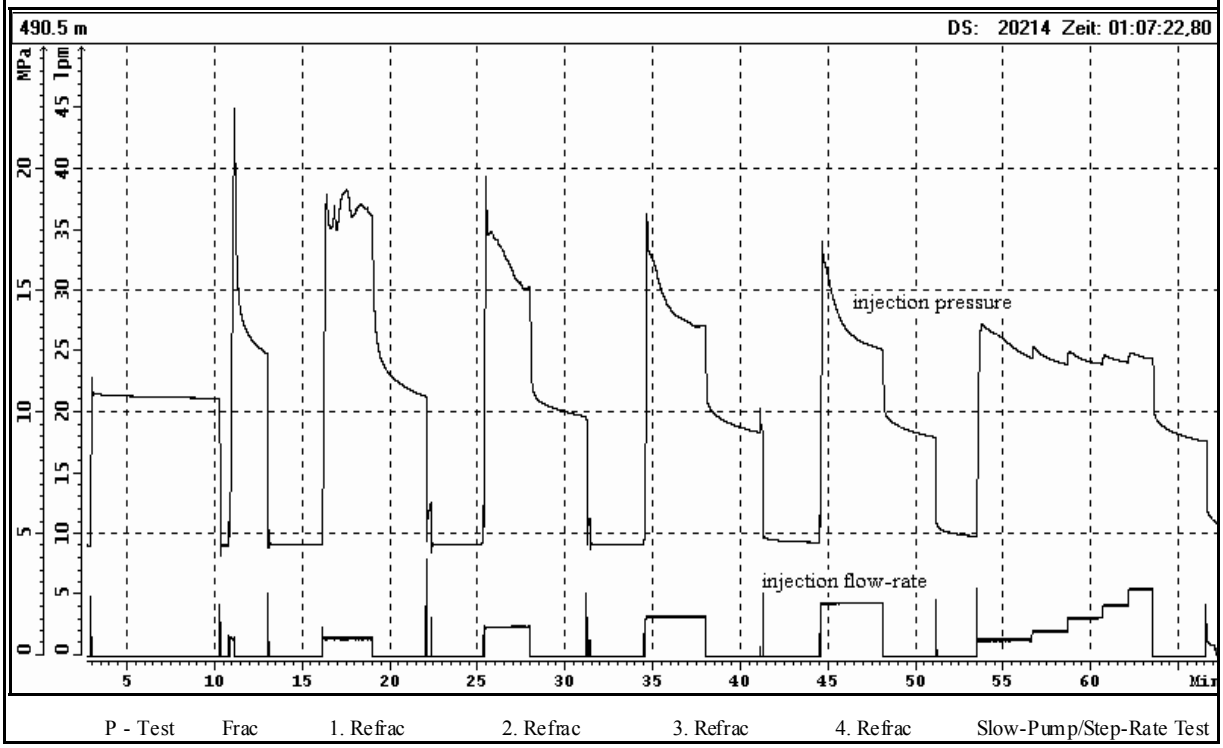

TEST SUMMARY

P - Test :	pressure decrease: 0.2 MPa in 7 min. 10 sec.
Frac - Cycle :	injection-rate Q_i= 1.5 lpm, injected volume V_i = 0.4 l, back-flow volume V_r = 0.1 l clear fracture initiation (breakdown event)
1. Refrac - Cycle :	Q_i = 1.5 lpm, V_i = 4.3 l, V_r = 0.1 l
2. Refrac - Cycle :	Q_i = 2.4 lpm, V_i = 6.4 l, V_r = 0.1 l
3. Refrac - Cycle :	Q_i = 3.3 lpm, V_i = 11.2 l, V_r = 0.1 l
4. Refrac - Cycle :	Q_i = 4.3 lpm, V_i = 15.4 l, V_r = 0.1 l
Step-Rate Test :	Q_i = 1.4-5.5 lpm, V_i = 28.7 l, V_r = 0.6 l

total injected volume = 66.4 l, recovered volume = 1.1 l (1.7 %)

Remark: During the test, a significant decrease of the shut-in pressure from 15.3 MPa (1. refrac-cycle) to 10.3 MPa (4. refrac-cycle) was observed.

Test at 490.5 m MD: Estimation of P_c (Frac - Cycle)

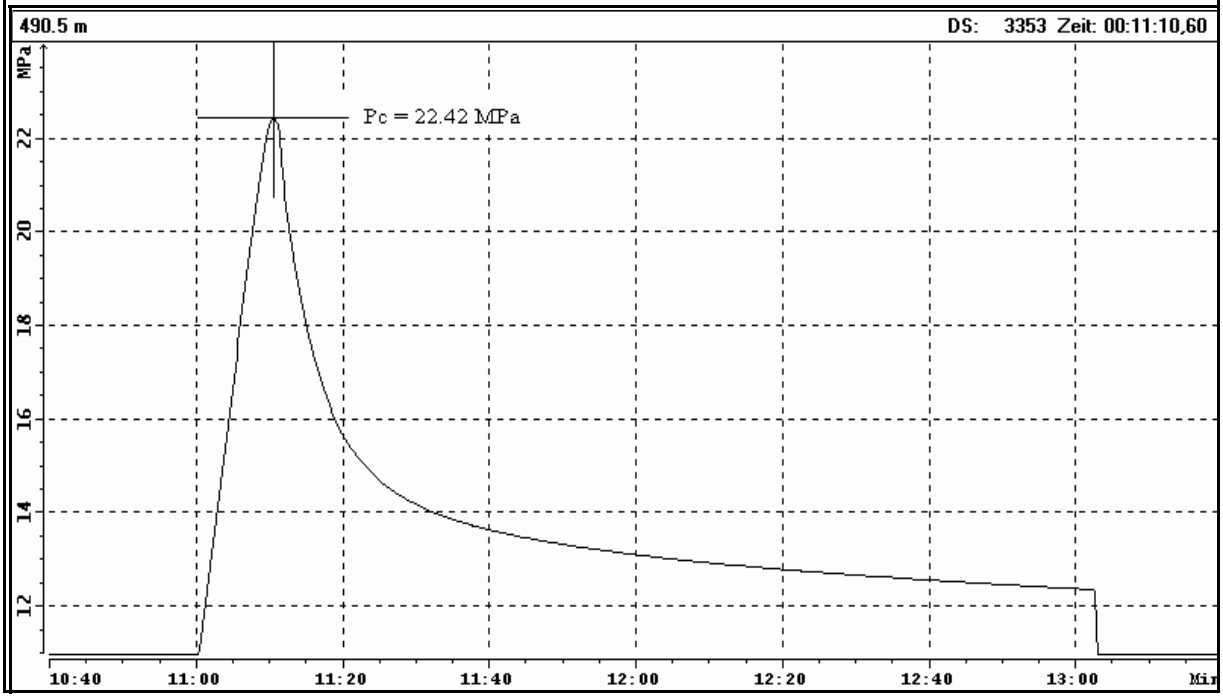

Test at 490.5 m MD: Estimation of P_r (1. Refrac - Cycle)

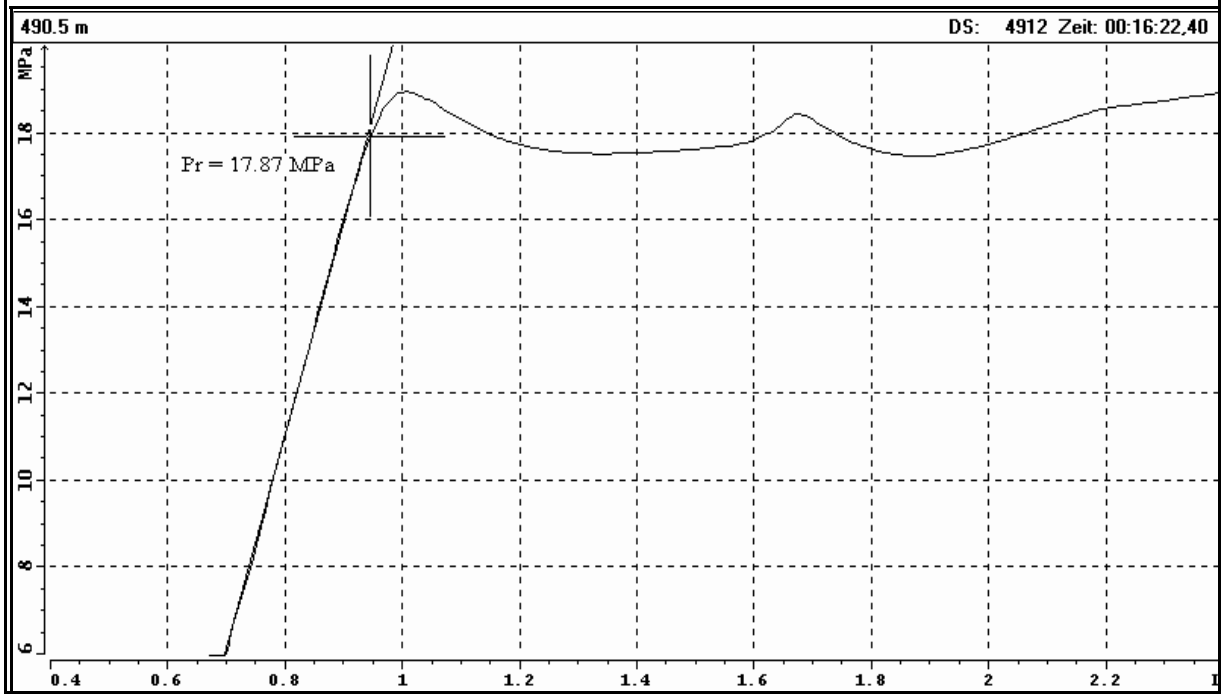

Test at 490.5 m MD: Estimation of P_r (2. Refrac - Cycle)

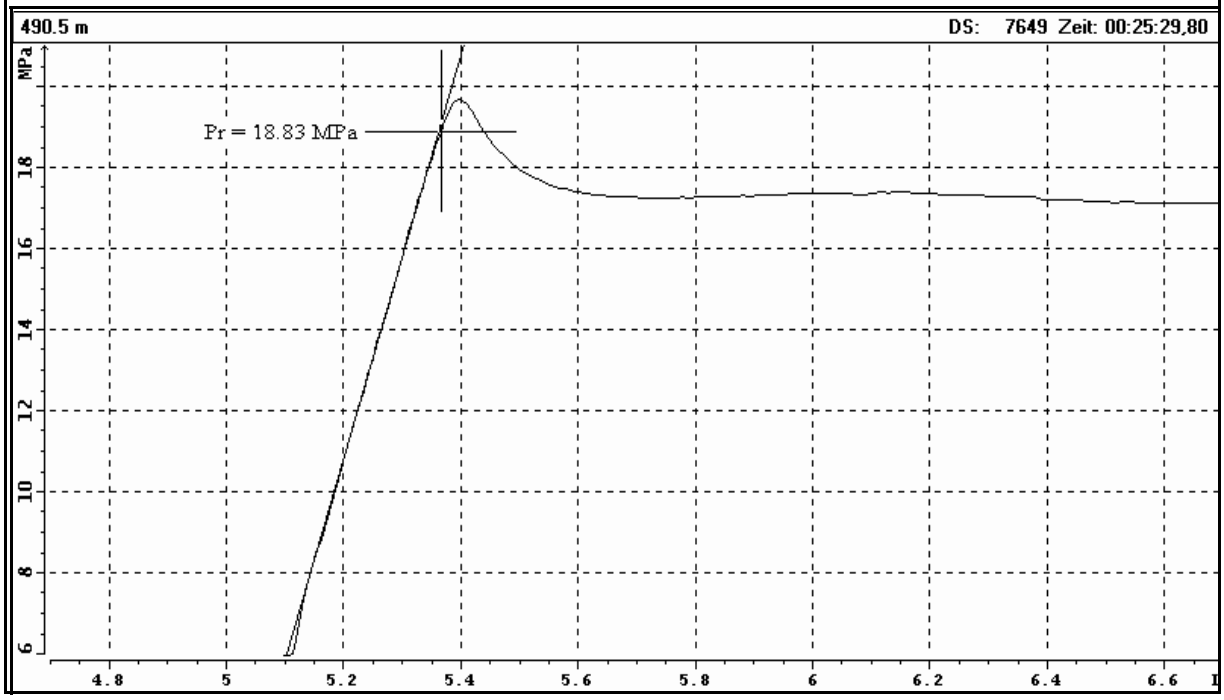

Test at 490.5 m MD: Estimation of $P_{si,\,max}$ (4. Refrac - Cycle)

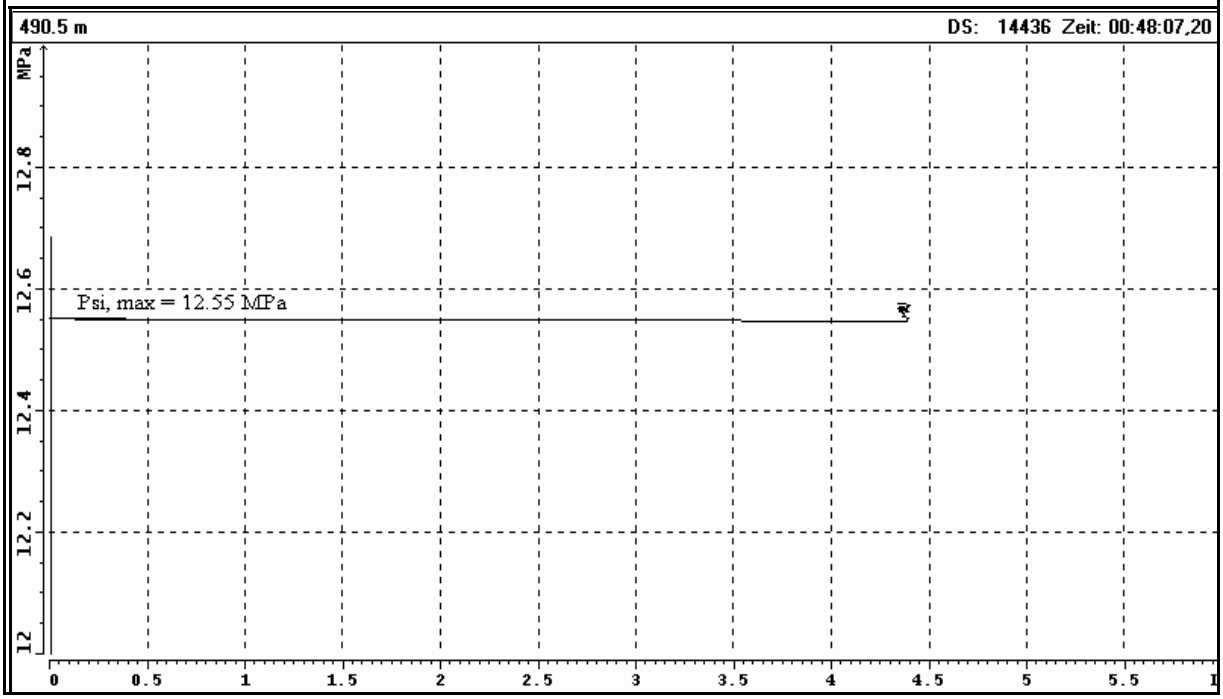

Test at 490.5 m MD: Estimation of $P_{si,\,min}$ (4. Refrac - Cycle)

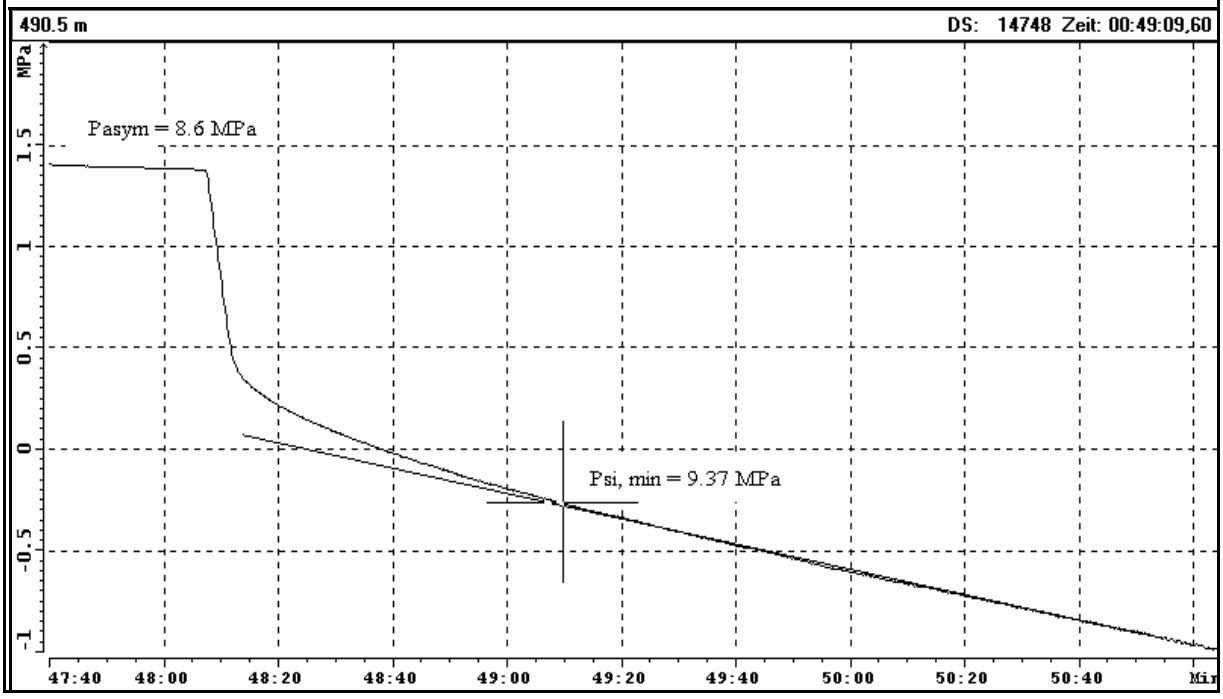

Test at 490.5 m MD: Estimation of P_{si} (4. Refrac - Cycle)

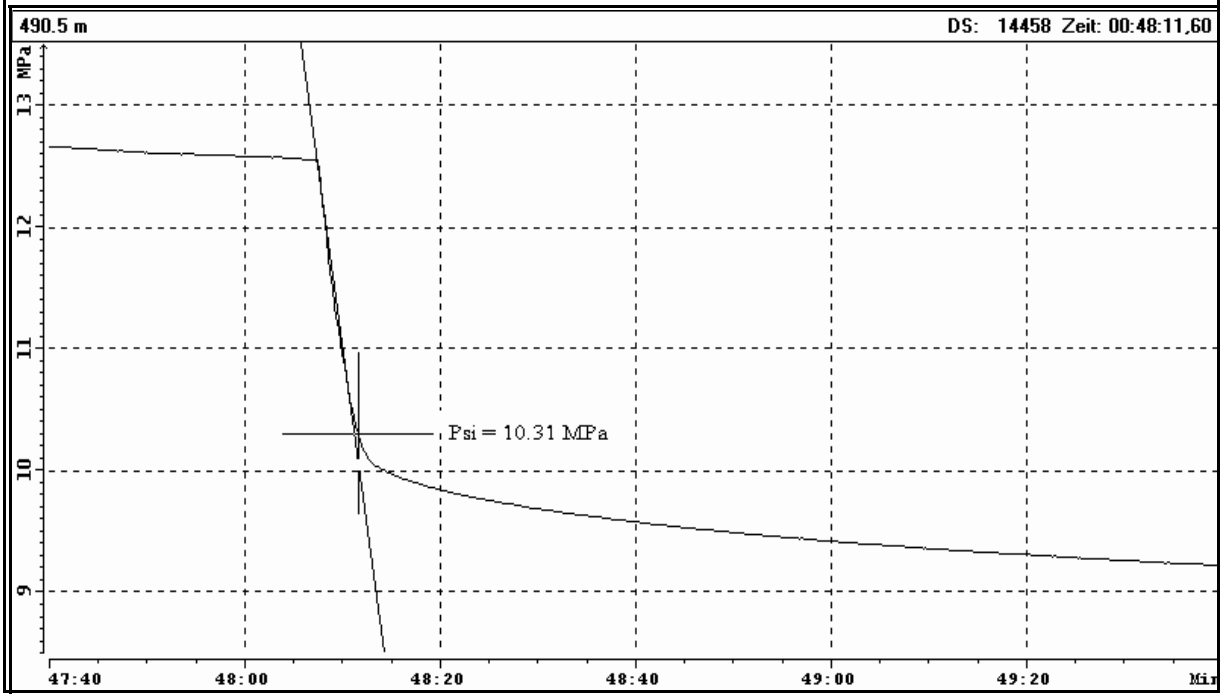

Test at 490.5 m MD: Analysis of Slow - Pump / Step - Rate - Test

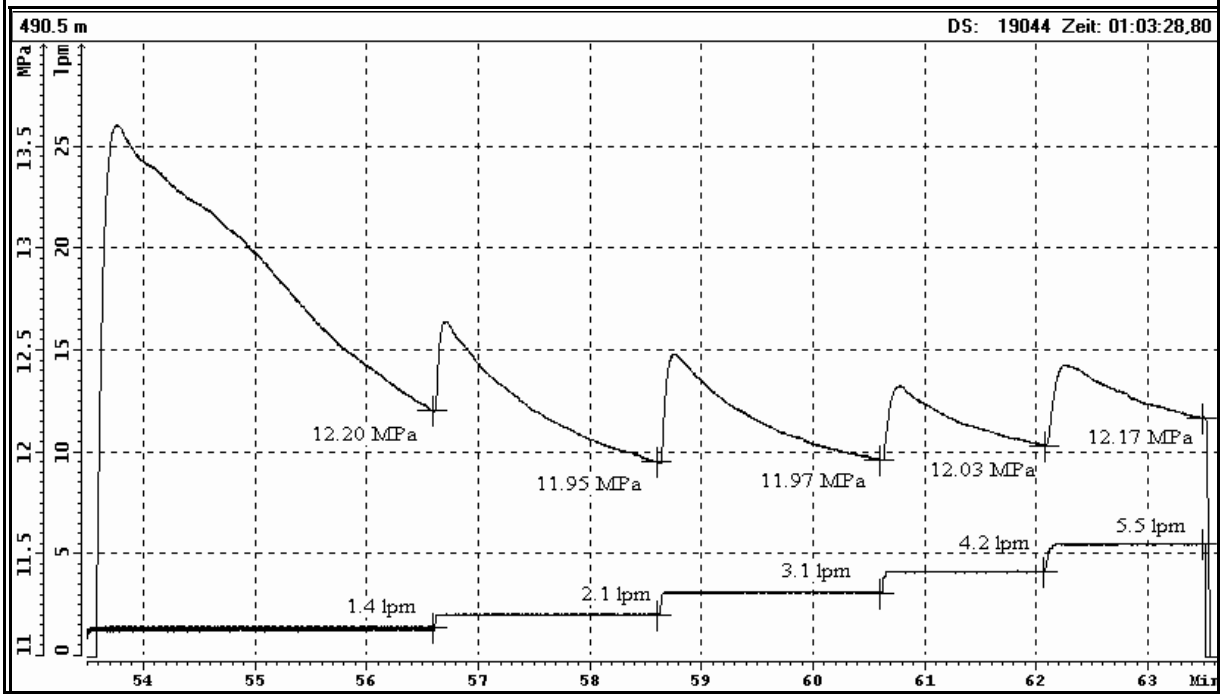

Test at 490.5 m MD: Examination of P_{si} (Step - Rate - Test)

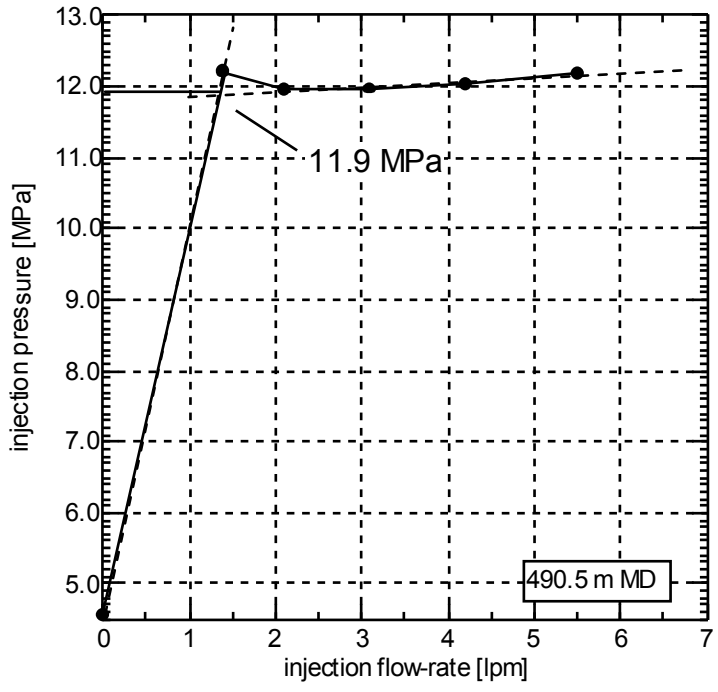

TEST AT 499.8 m MD / 474.8 m TVD

Test at 499.8 m MD : Overview - Plot

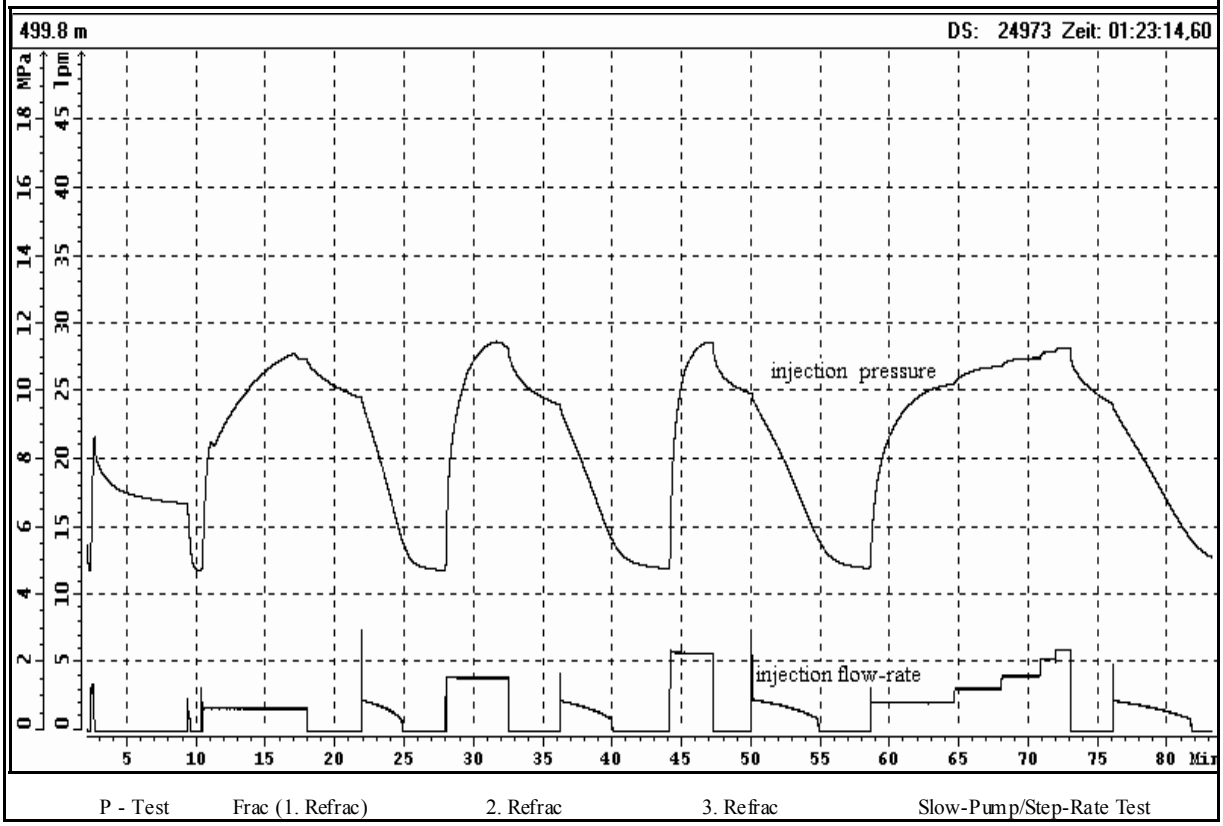

TEST SUMMARY

P - Test :	pressure decrease: 1.9 MPa in 6 min. 42 sec.
Frac (1. Refrac) - Cycle :	injection-rate Q_i= 1.7 lpm, injected volume V_i = 12.6 l, back-flow volume V_r = 5.1 l stimulation of an existing fracture (no breakdown event)
2. Refrac - Cycle :	Q_i = 3.9 lpm, V_i = 17.6 l, V_r = 6.4 l
3. Refrac - Cycle :	Q_i = 5.7 lpm, V_i = 17.8 l, V_r = 8.5 l
Step-Rate Test :	Q_i = 2.1-6.0 lpm, V_i = 46.9 l, V_r = 9.5 l

total injected volume = 94.9 l, recovered volume = 29.5 l (31.1 %)

Remark: The system-stiffness (dP/dV) observed during the opening of the pre-existing fracture is only 6.6 MPa/L compared to the general stiffness of approx. 42 MPa/L.

Test at 499.8 m MD: Estimation of P_r (Frac (1. Refrac) - Cycle)

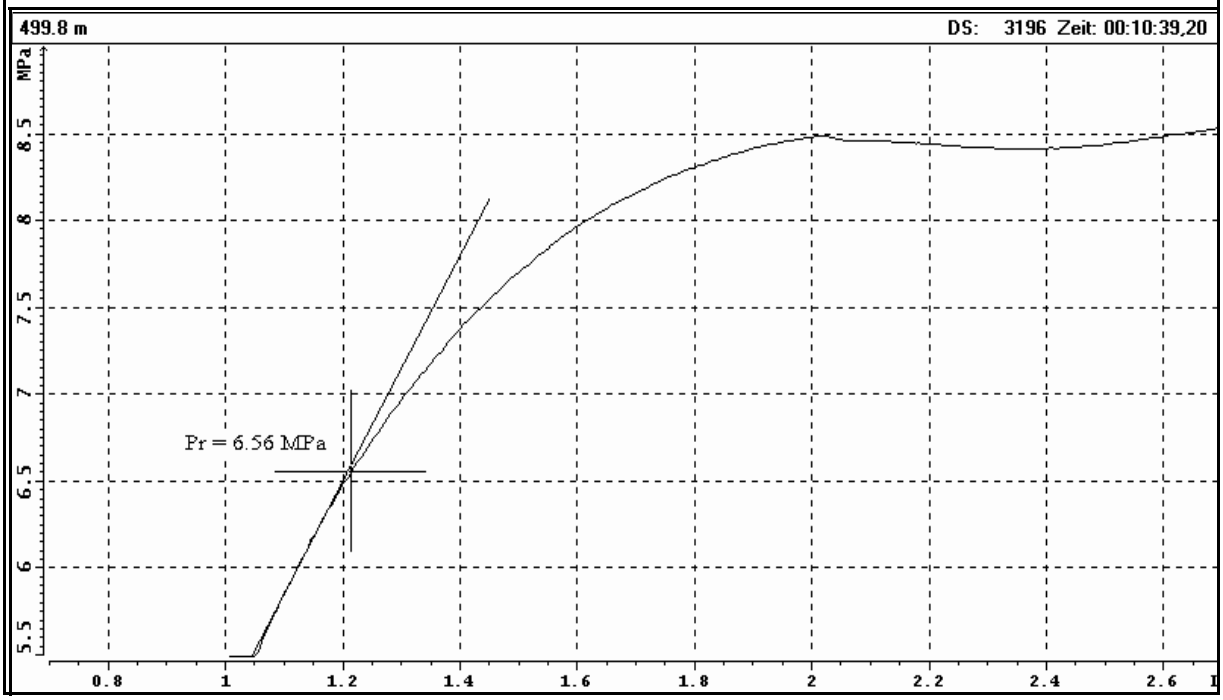

Test at 499.8 m MD: Estimation of P_r (2. Refrac - Cycle, for comparison)

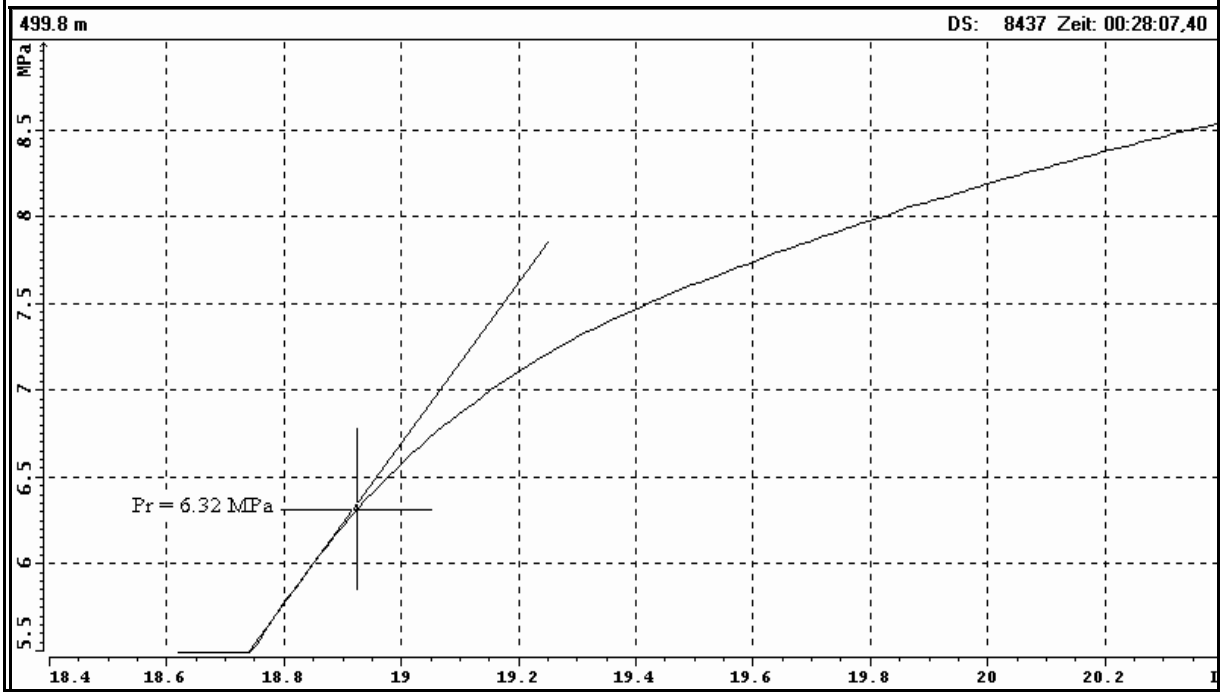

Test at 499.8 m MD: Estimation of $P_{si,\,max}$ (3. Refrac - Cycle)

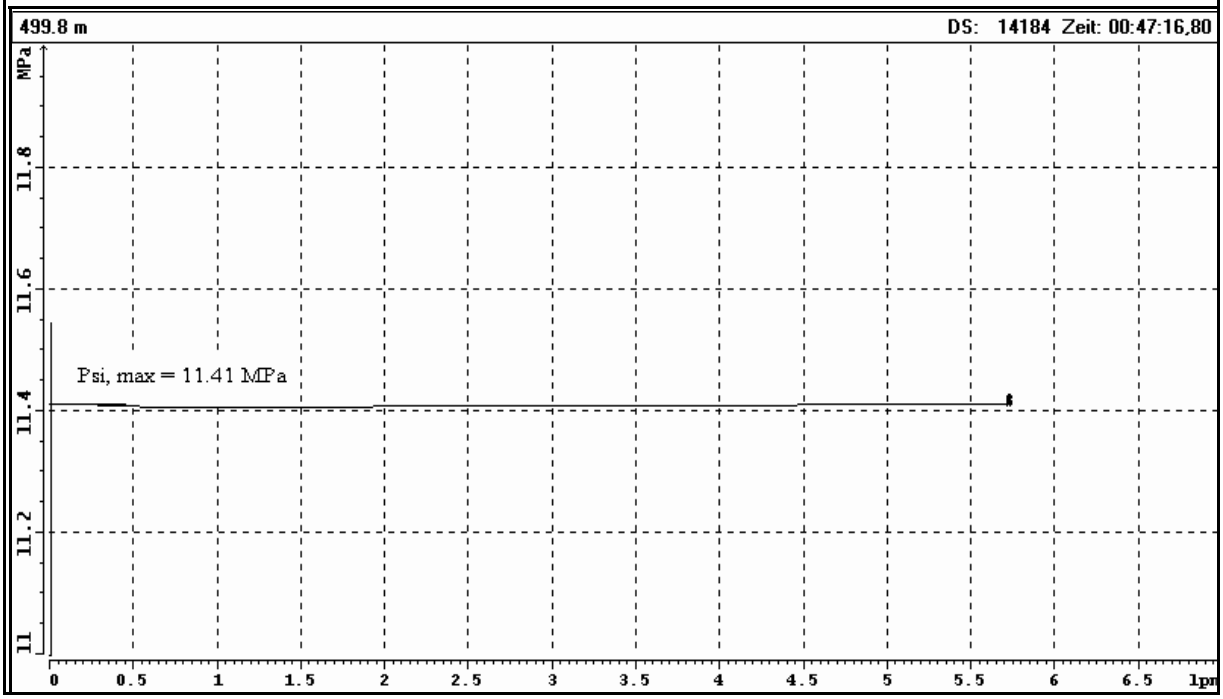

Test at 499.8 m MD: Estimation of $P_{si,\,min}$ (3. Refrac - Cycle)

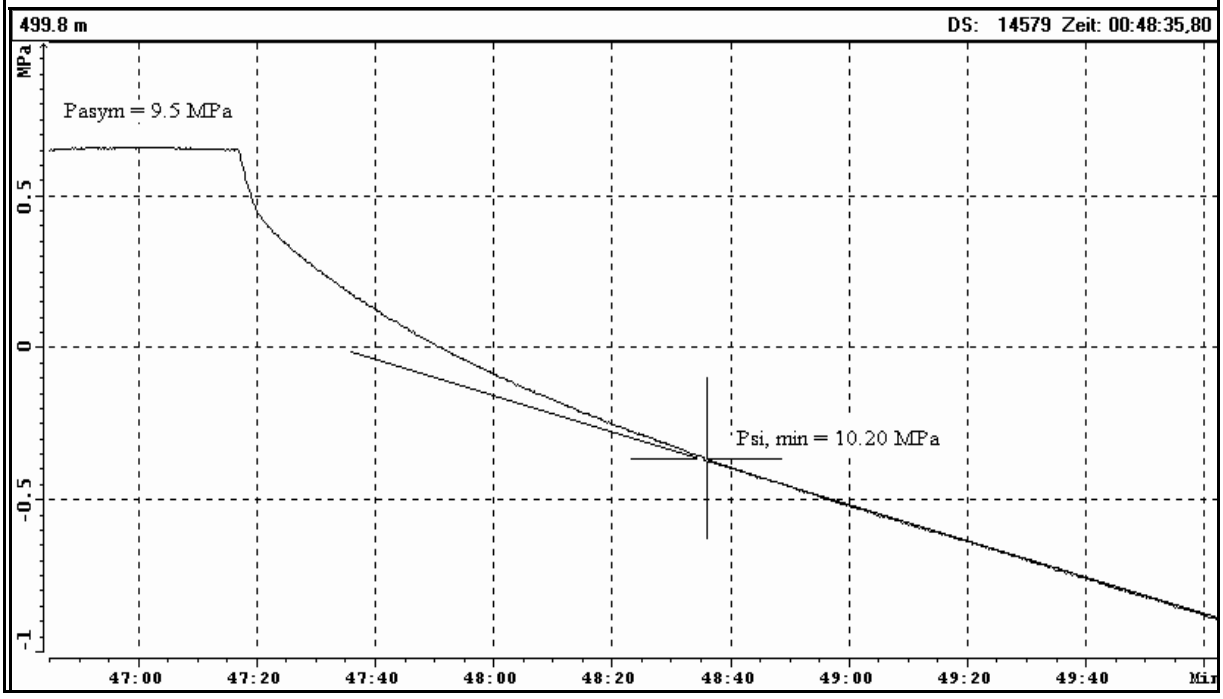

Test at 499.8 m MD: Estimation of P_{si} (3. Refrac - Cycle)

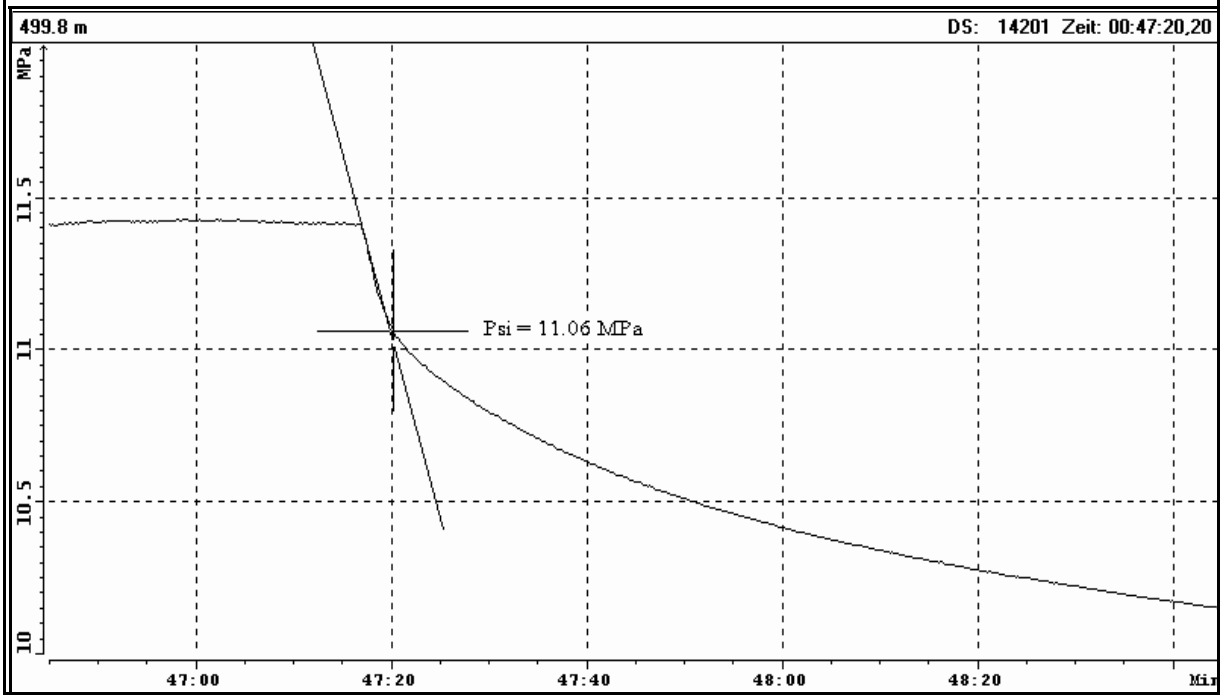

Test at 499.8 m MD: Analysis of Slow - Pump / Step - Rate - Test

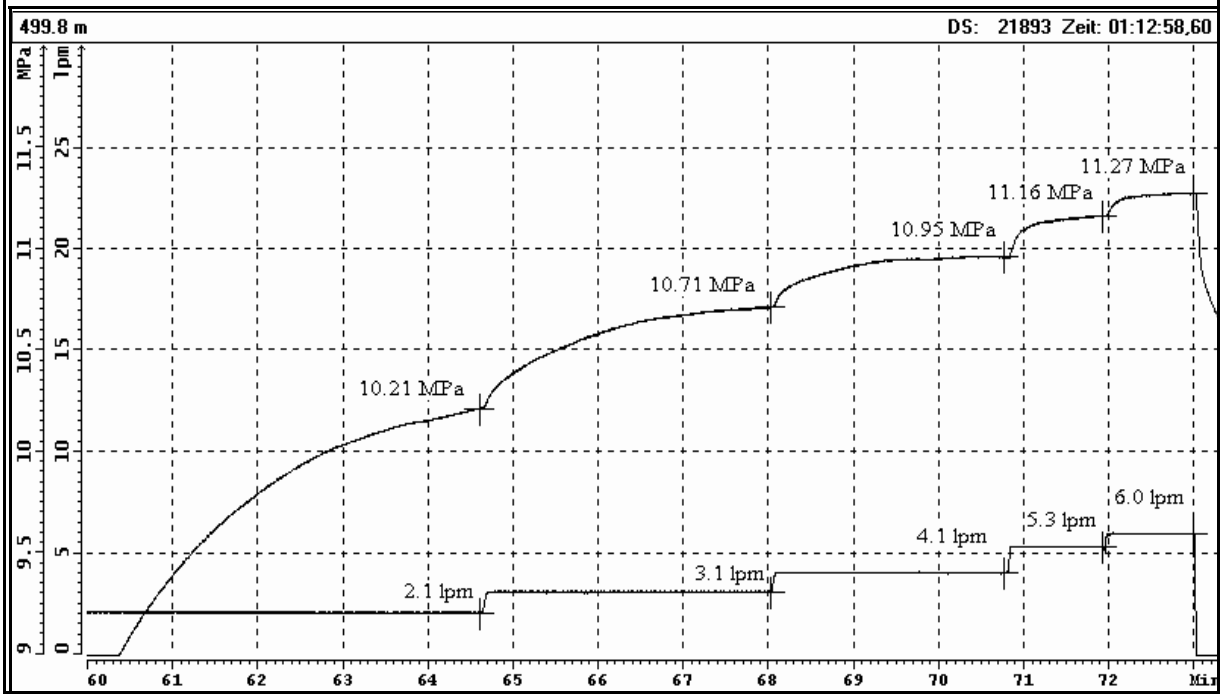

Test at 499.8 m MD: Examination of P_{si} (Step - Rate - Test)

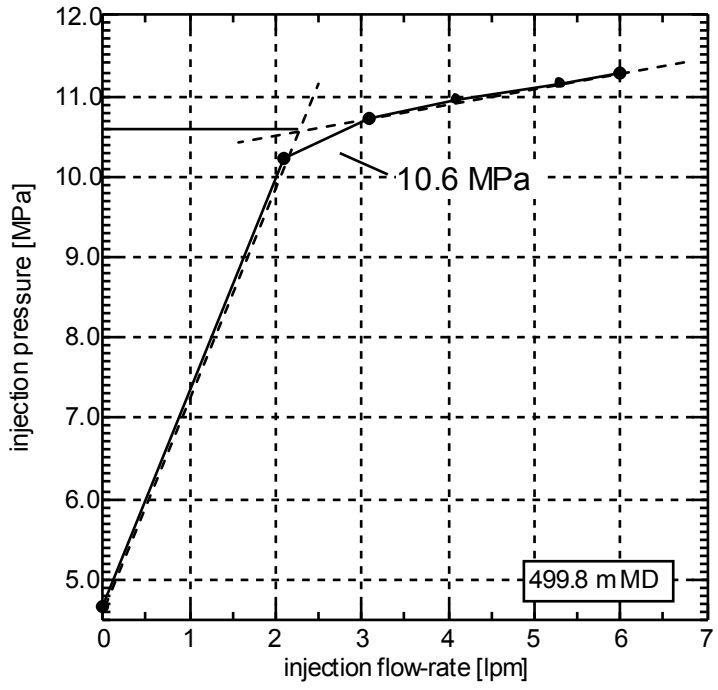

TEST AT 510.8 m MD / 485.6 m TVD

Test at 510.8 m MD: Overview - Plot

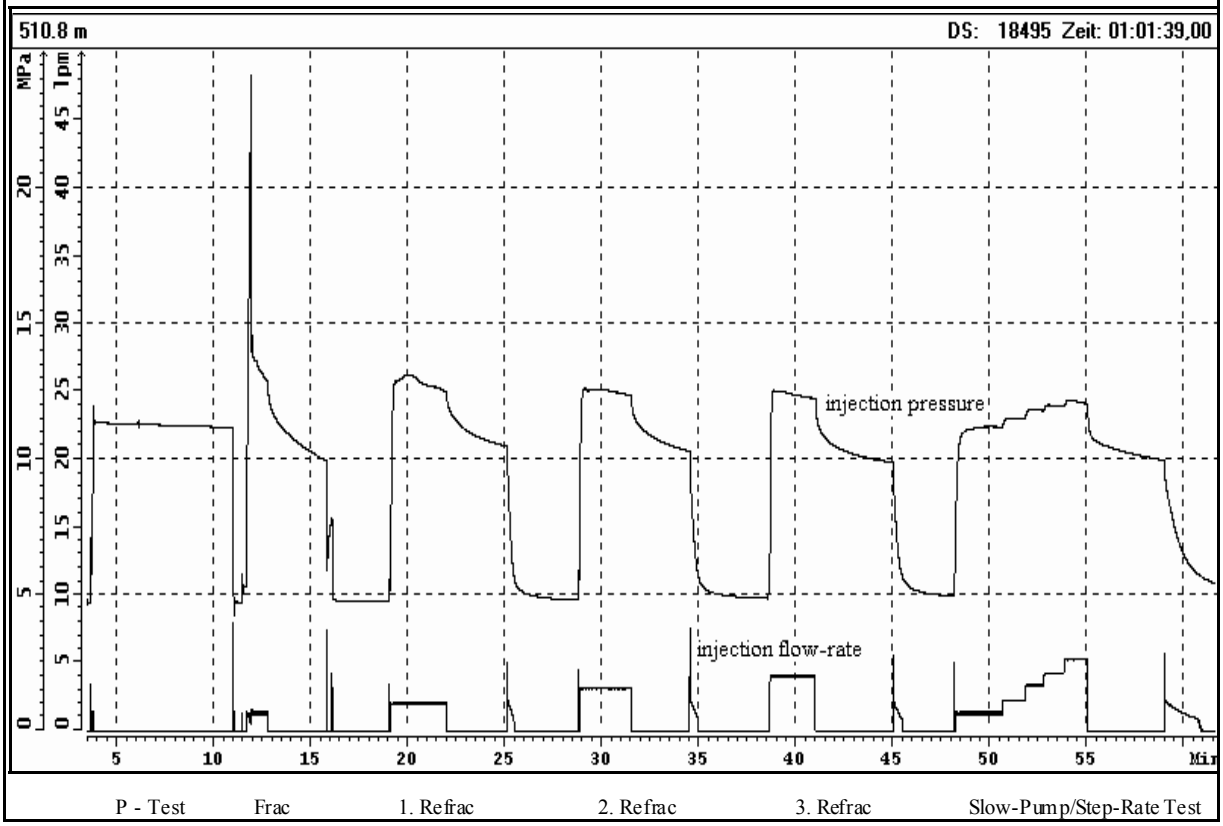

TEST SUMMARY

P - Test :	pressure decrease: 0.2 MPa in 7 min. 10 sec.
Frac - Cycle :	injection-rate Q_i= 1.3 lpm, injected volume V_i = 1.4 l, back-flow volume V_r = 0.2 l clear fracture initiation (breakdown event)
1. Refrac - Cycle :	Q_i = 2.1 lpm, V_i = 6.0 l, V_r = 0.6 l
2. Refrac - Cycle :	Q_i = 3.2 lpm, V_i = 8.4 l, V_r = 0.8 l
3. Refrac - Cycle :	Q_i = 4.0 lpm, V_i = 9.5 l, V_r = 0.7 l
Step-Rate Test :	Q_i = 1.3-5.3 lpm, V_i = 19.8 l, V_r = 2.7 l

total injected volume = 45.1 l, recovered volume = 5.0 l (11.1 %)

Test at 510.8 m MD: Estimation of P_c (Frac - Cycle)

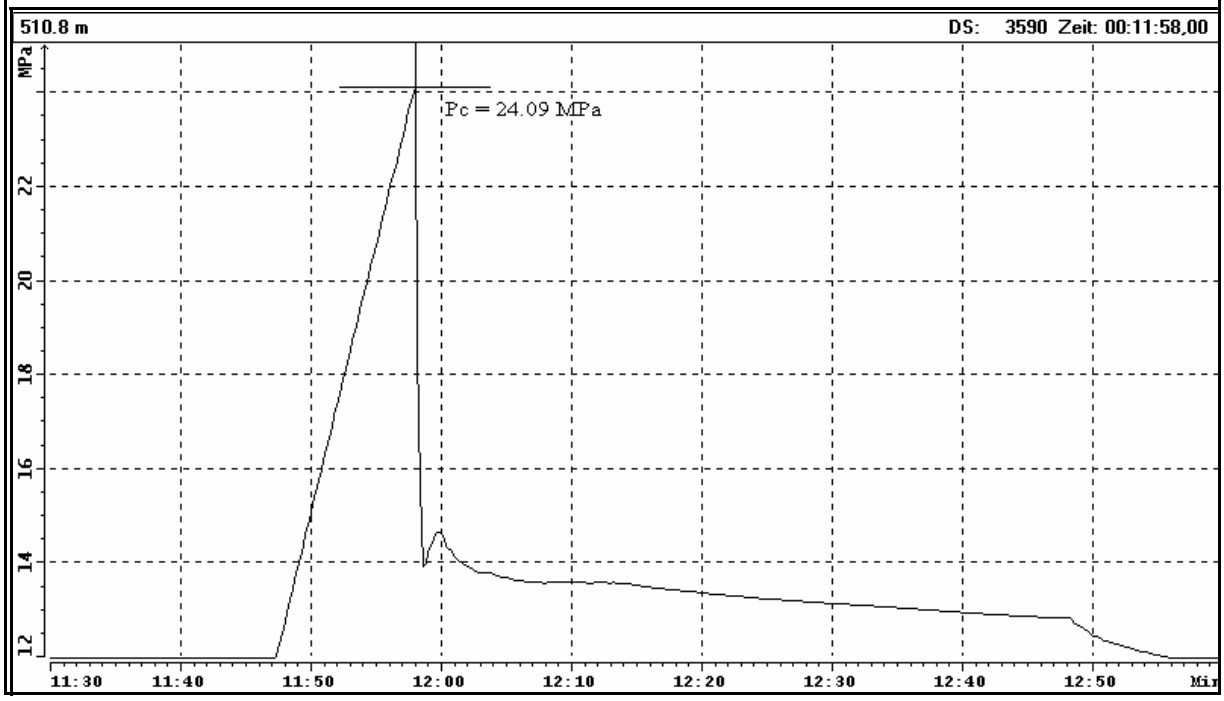

Test at 510.8 m MD: Estimation of P_r (1. Refrac - Cycle)

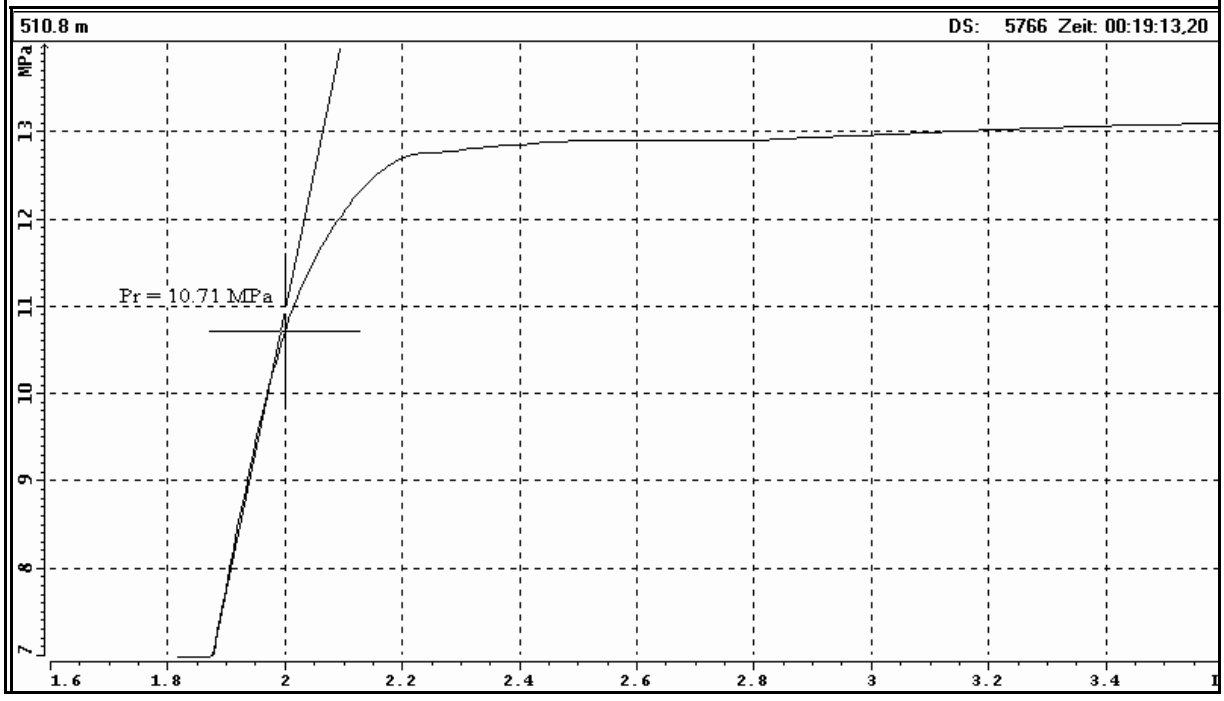

Test at 510.8 m MD: Estimation of $P_{si, max}$ (3. Refrac - Cycle)

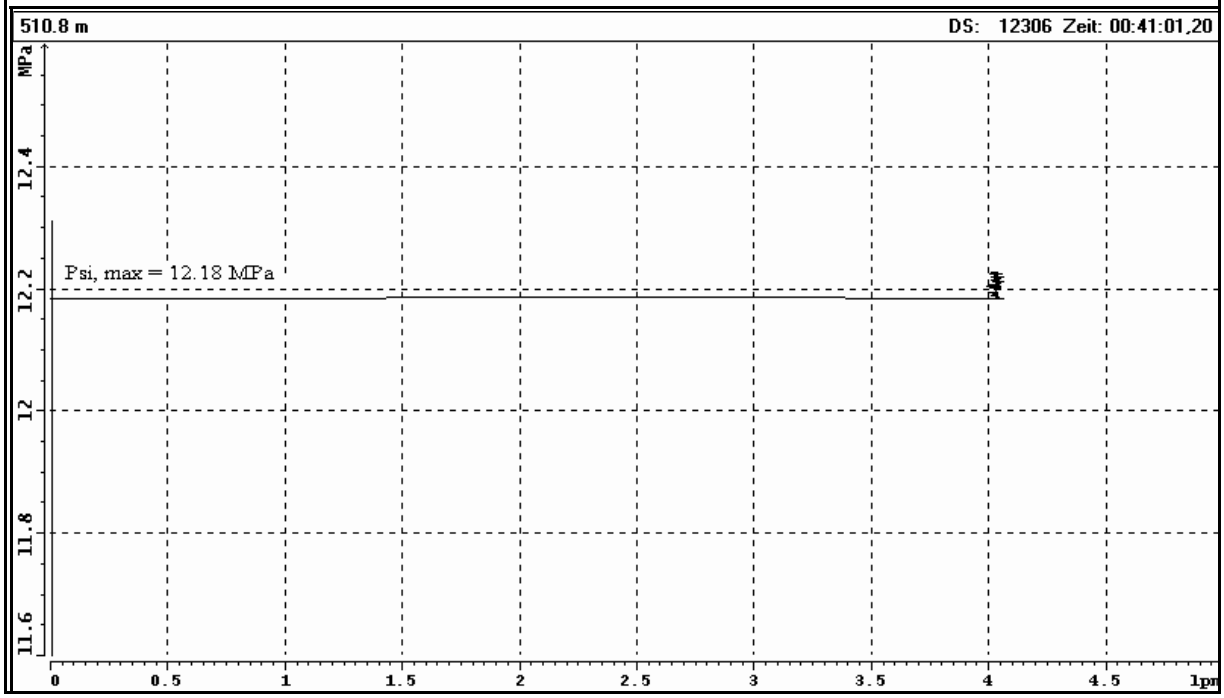

Test at 510.8 m MD: Estimation of $P_{si, min}$ (3. Refrac - Cycle)

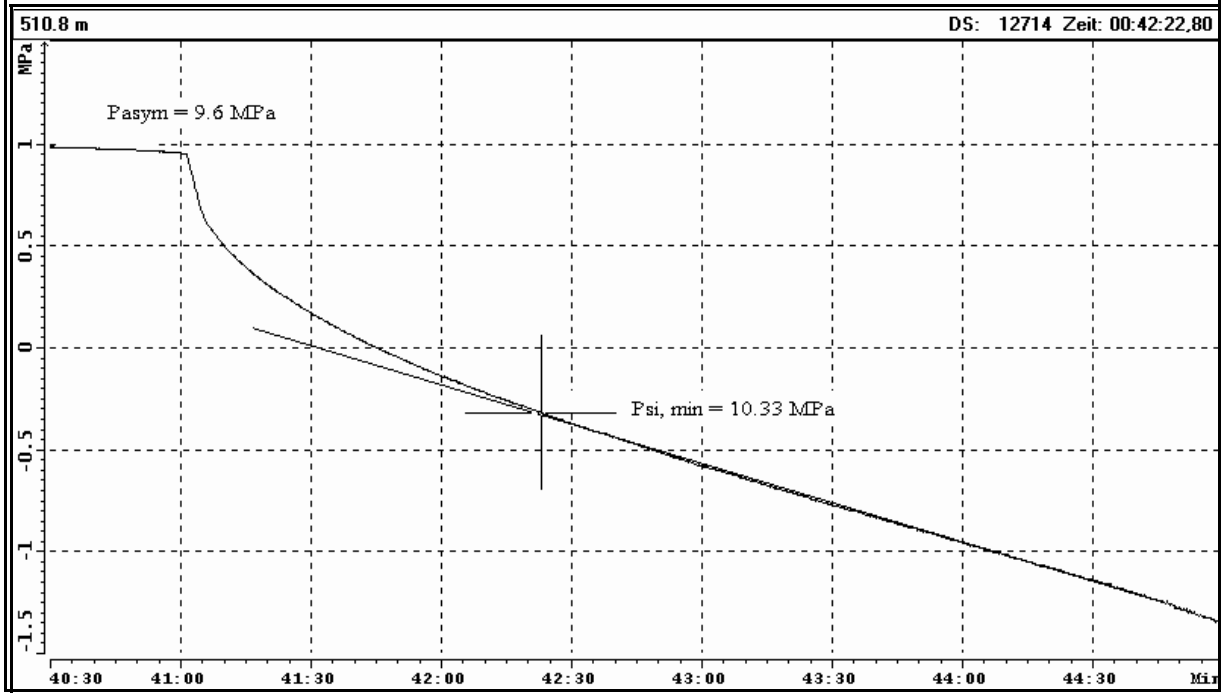

Test at 510.8 m MD: Estimation of P_{si} (3. Refrac - Cycle)

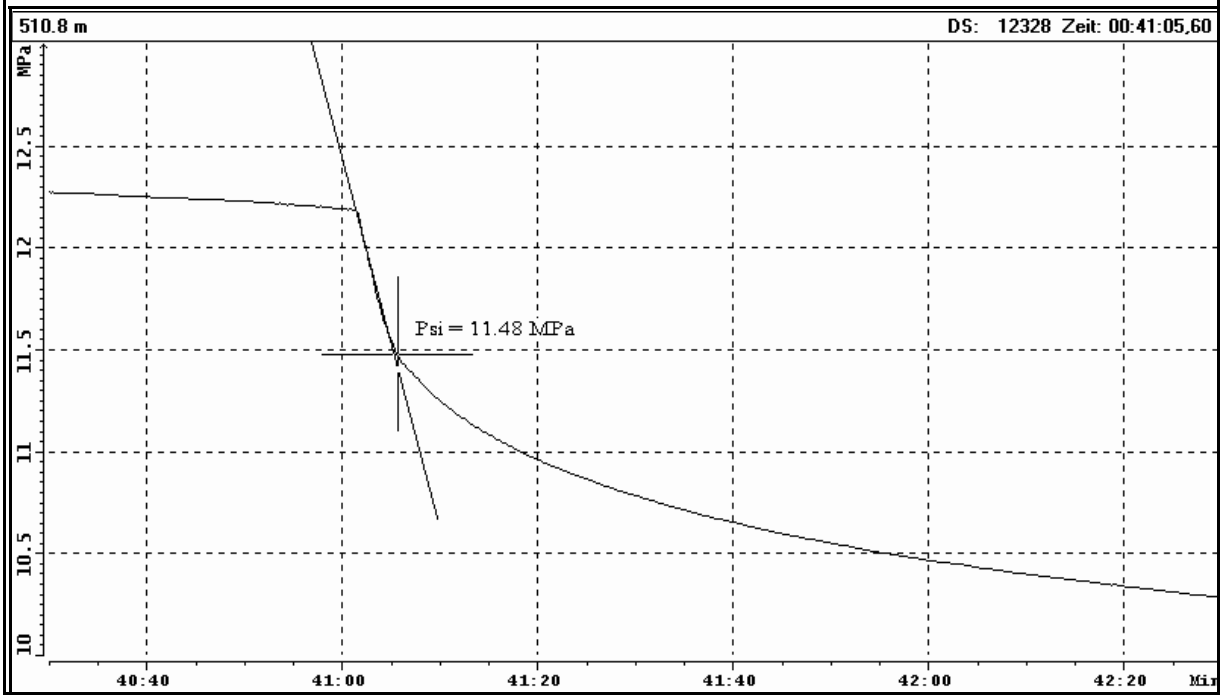

Test at 510.8 m MD: Analysis of Slow - Pump / Step - Rate - Test

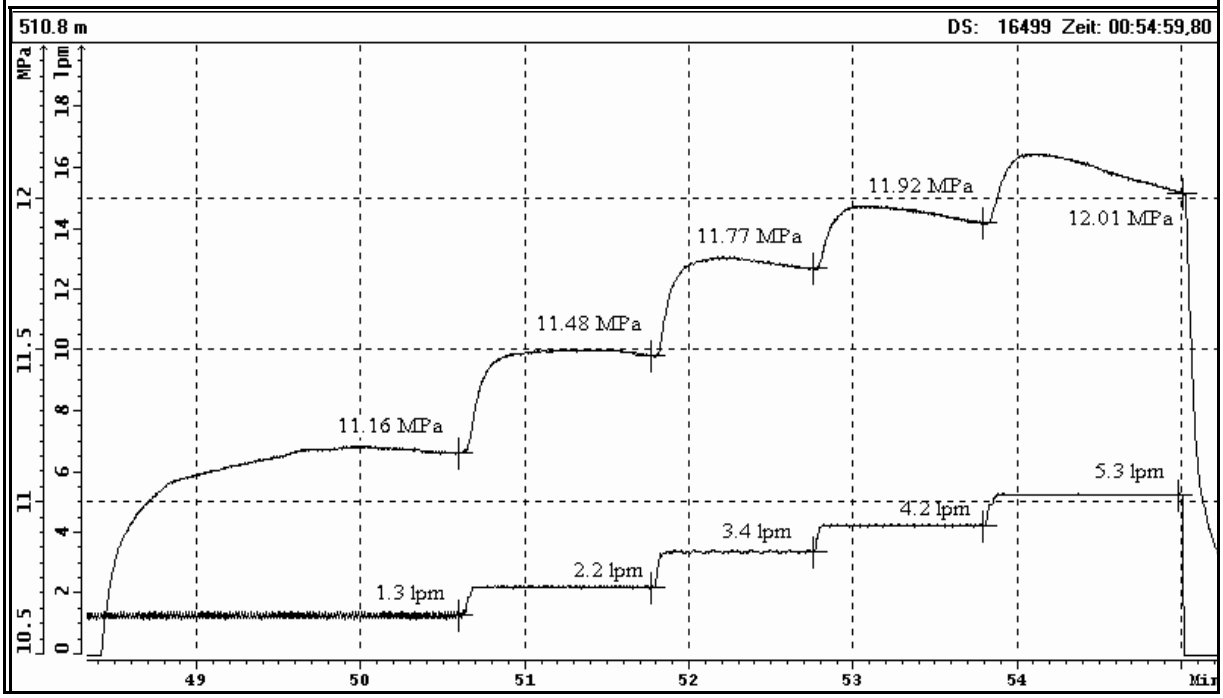

Test at 510.8 m MD: Examination of P_{si} (Step - Rate - Test)

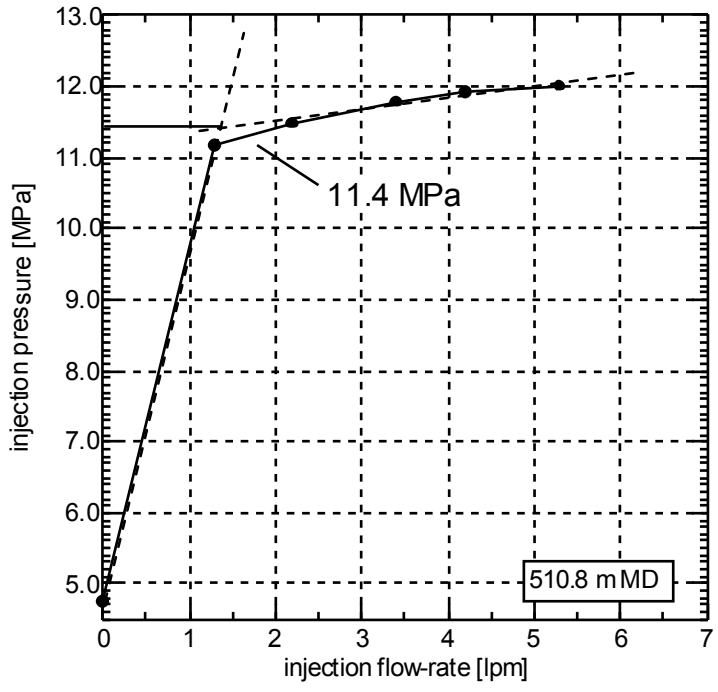

TEST AT 517.0 m MD / 491.6 m TVD

Test at 517.0 m MD : Overview - Plot

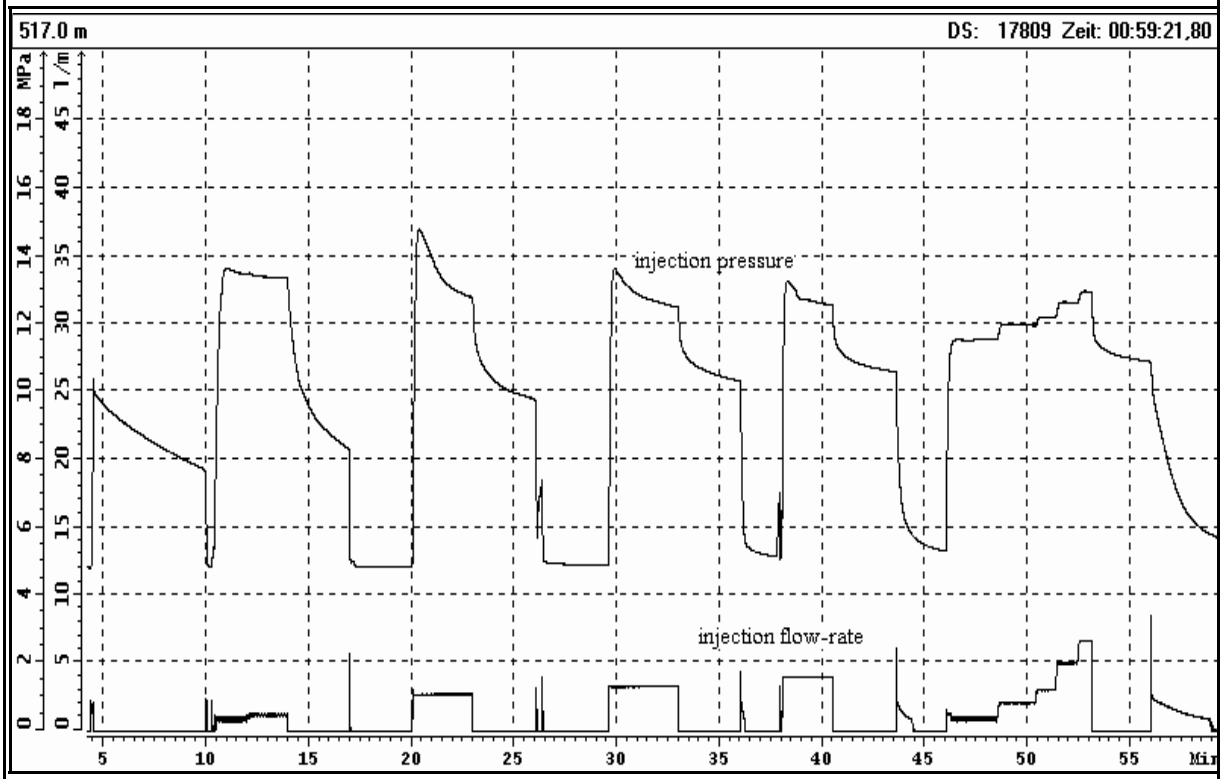

TEST SUMMARY

P - Test :	pressure decrease: 2.3 MPa in 5 min. 19 sec.
Frac (1. Refrac) - Cycle :	injection-rate Q_i= 1.1 lpm, injected volume V_i = 3.9 l, back-flow volume V_r = 0.1 l stimulation of an existing fracture (no breakdown event)
2. Refrac - Cycle :	Q_i = 2.7 lpm, V_i = 7.9 l, V_r = 0.2 l
3. Refrac - Cycle :	Q_i = 3.3 lpm, V_i = 11.1 l, V_r = 0.3 l
4. Refrac - Cycle :	Q_i = 4.0 lpm, V_i = 9.8 l, V_r = 1.2 l
Step-Rate Test :	Q_i = 1.0-6.6 lpm, V_i = 18.9 l, V_r = 4.4 l

total injected volume = 51.6 l, recovered volume = 6.2 l (12.0 %)

Test at 517.0 m MD: Estimation of P_r (Frac (1. Refrac) - Cycle)

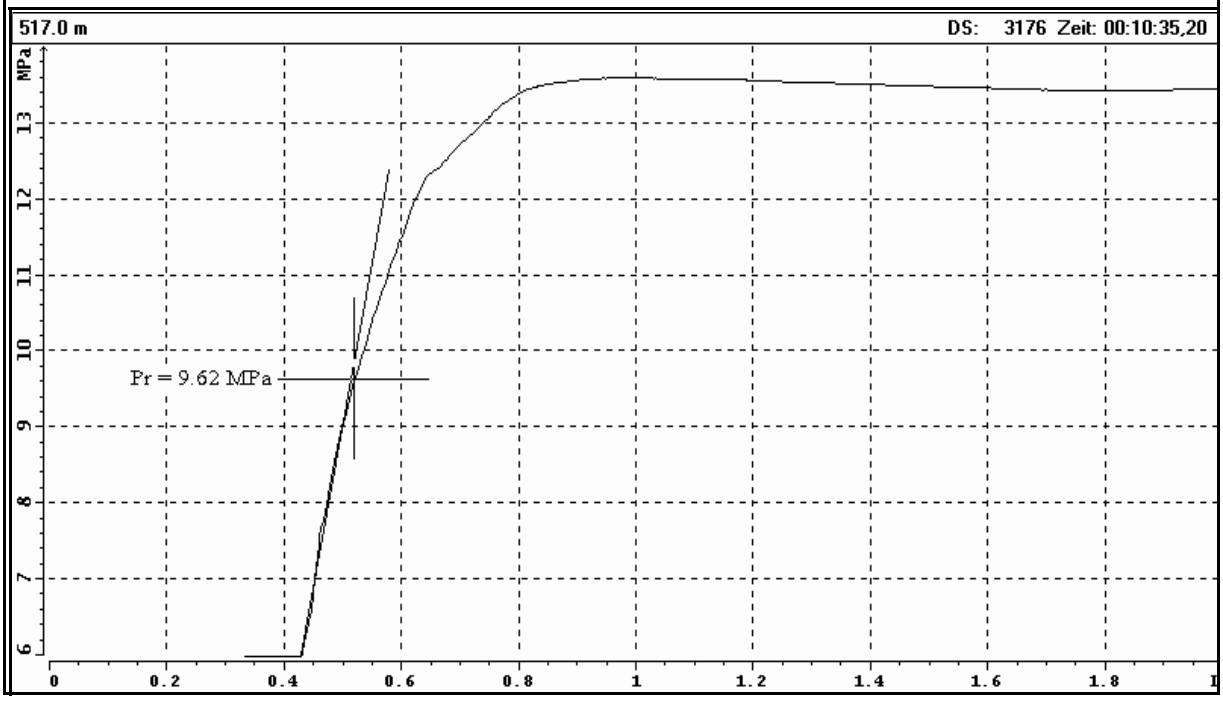

Test at 517.0 m MD: Estimation of P_r (2. Refrac - Cycle, for comparison)

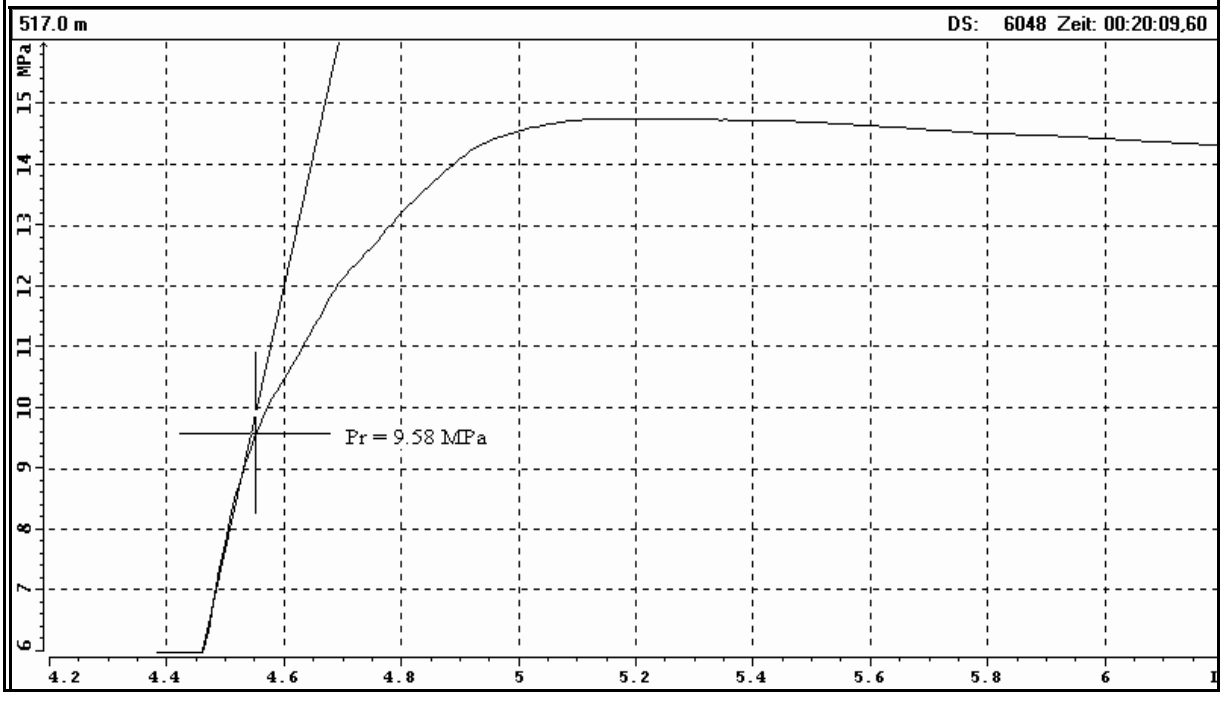

Test at 517.0 m MD: Estimation of $P_{si,\,max}$ (4. Refrac - Cycle)

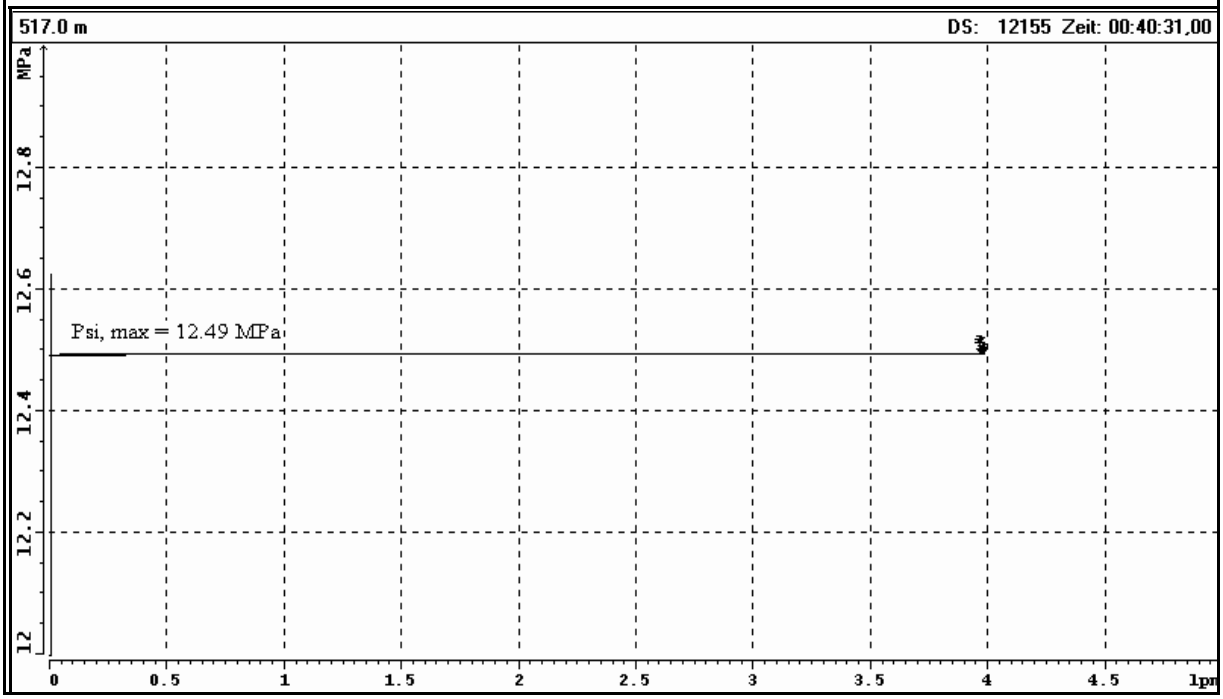

Test at 517.0 m MD: Estimation of $P_{si,\,min}$ (4. Refrac - Cycle)

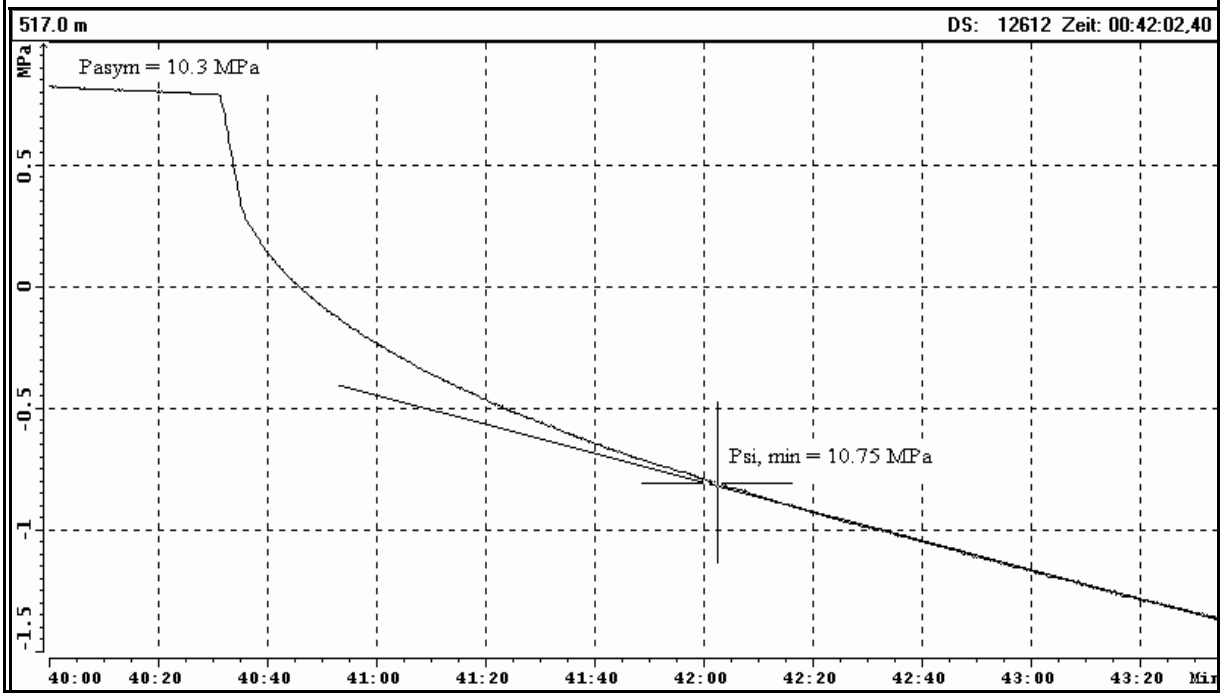

Test at 517.0 m MD: Estimation of P_{si} (4. Refrac - Cycle)

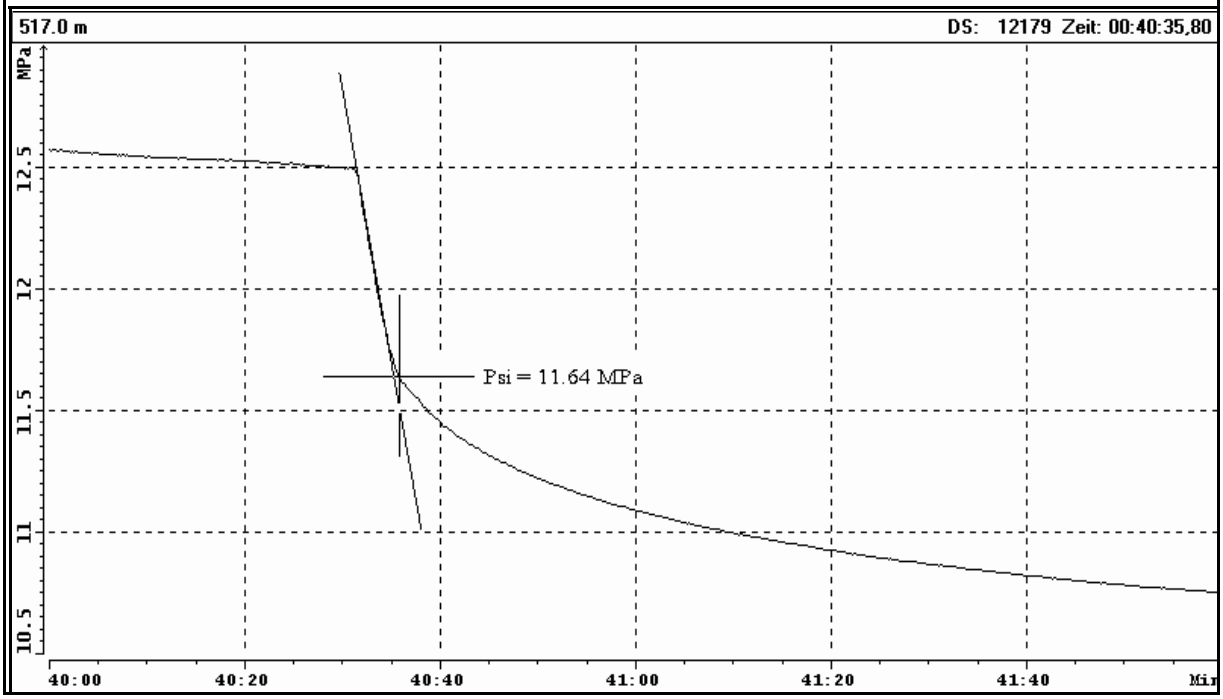

Test at 517.0 m MD: Analysis of Slow - Pump / Step - Rate - Test

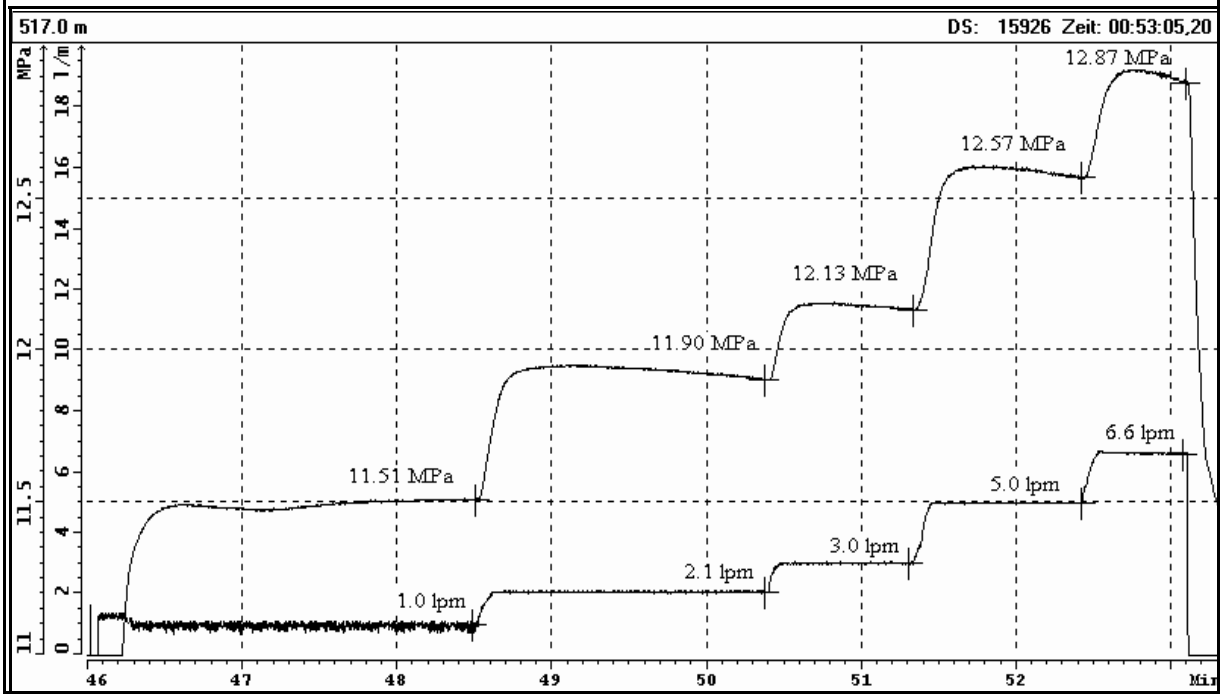

Test at 517.0 m MD: Examination of P_{si} (Step - Rate - Test)

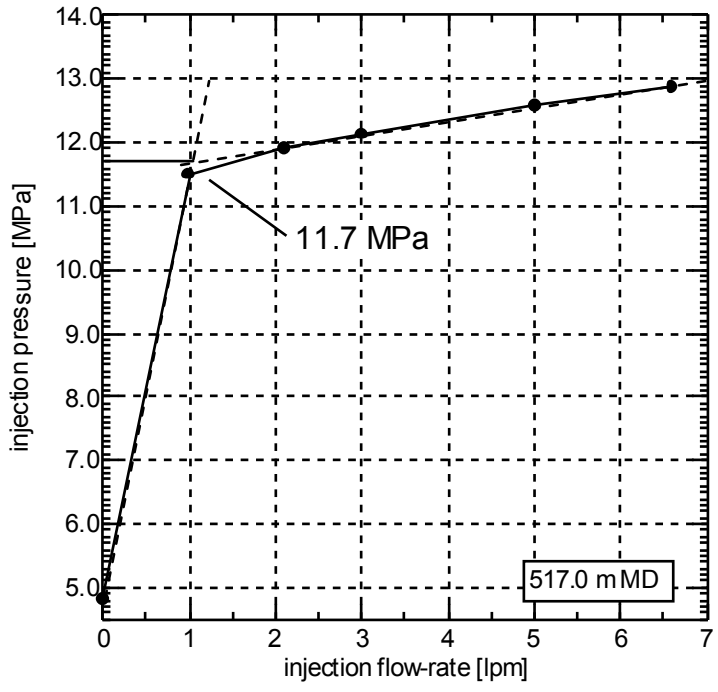

TEST AT 579.0 m MD / 552.2 m TVD

Test at 579.0 m MD: Overview - Plot

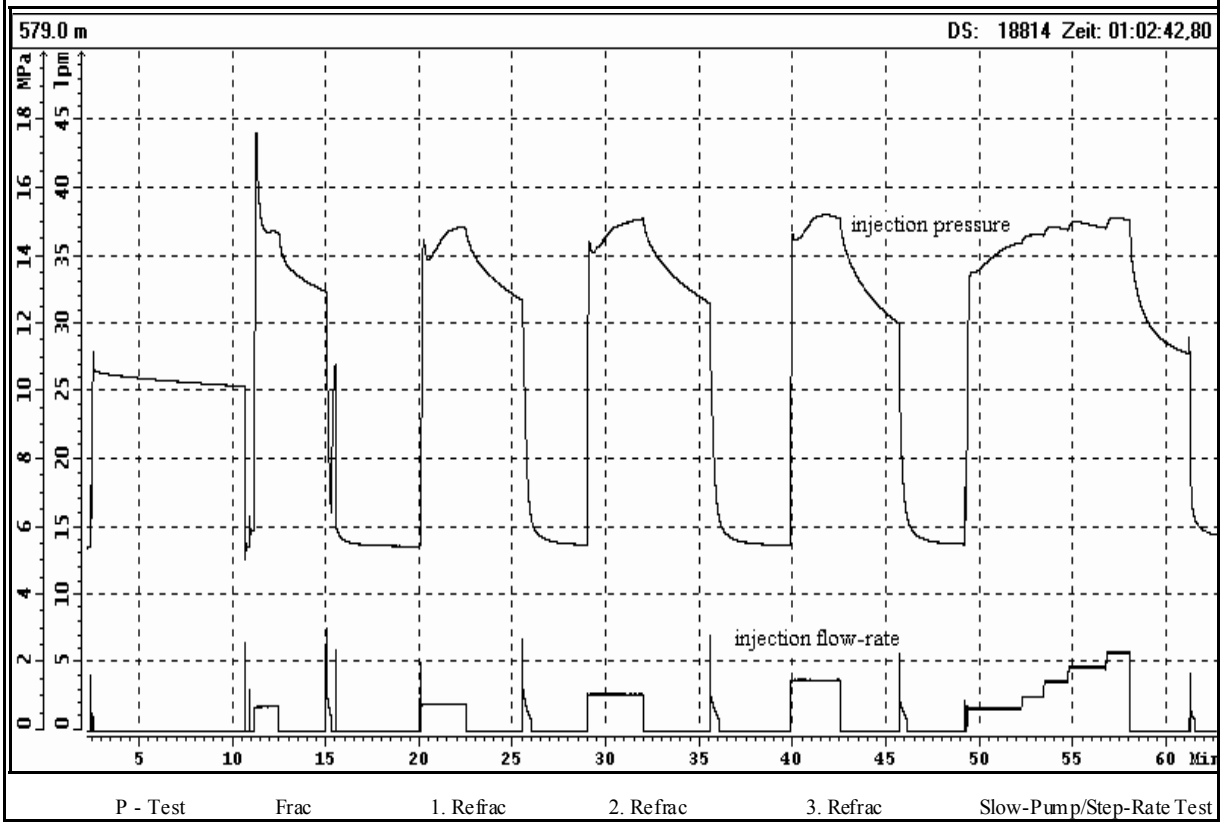

TEST SUMMARY

P - Test :	pressure decrease: 0.45 MPa in 7 min. 59 sec.
Frac - Cycle :	injection-rate Q_i= 1.8 lpm, injected volume V_i = 2.4 l, back-flow volume V_r = 0.7 l clear fracture initiation (breakdown event)
1. Refrac - Cycle :	Q_i = 2.0 lpm, V_i = 4.8 l, V_r = 0.8 l
2. Refrac - Cycle :	Q_i = 2.7 lpm, V_i = 8.1 l, V_r = 0.9 l
3. Refrac - Cycle :	Q_i = 3.7 lpm, V_i = 9.9 l, V_r = 0.7 l
Step-Rate Test :	Q_i = 1.6-5.8 lpm, V_i = 29.4 l, V_r = 0.4 l

total injected volume = 54.9 l, recovered volume = 3.5 l (6.4 %)

Test at 579.0 m MD: Estimation of P_c (Frac - Cycle)

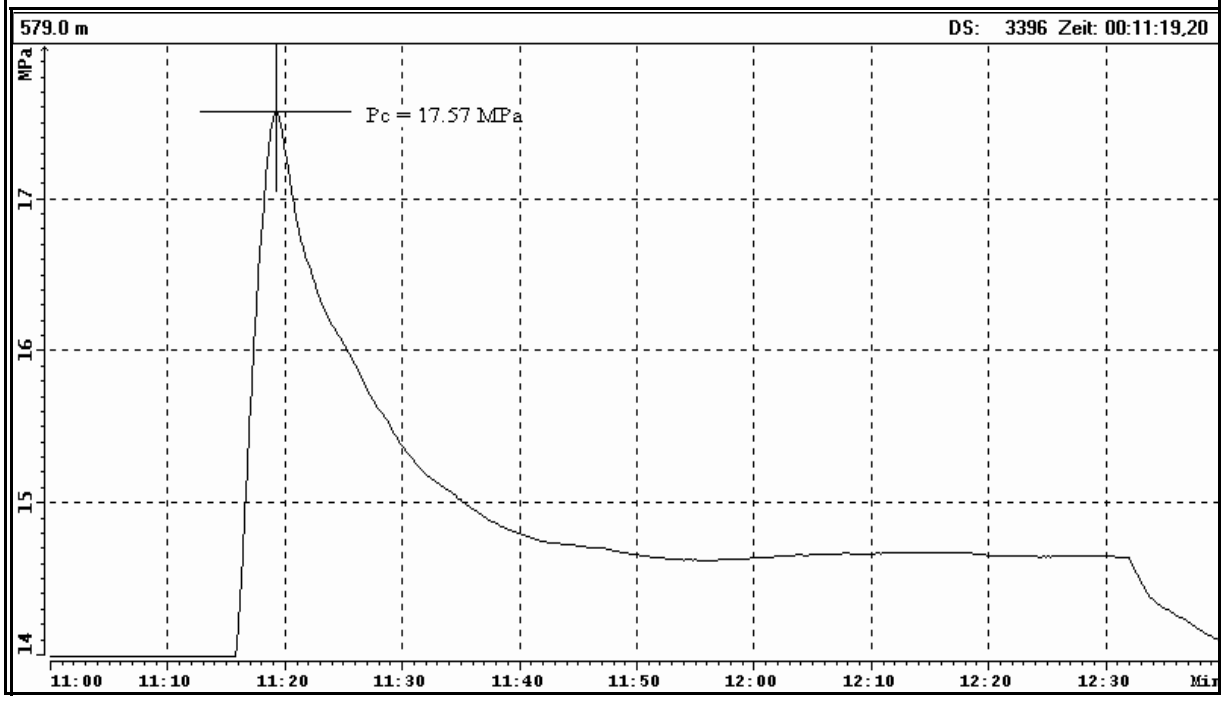

Test at 579.0 m MD: Estimation of P_r (1. Refrac - Cycle)

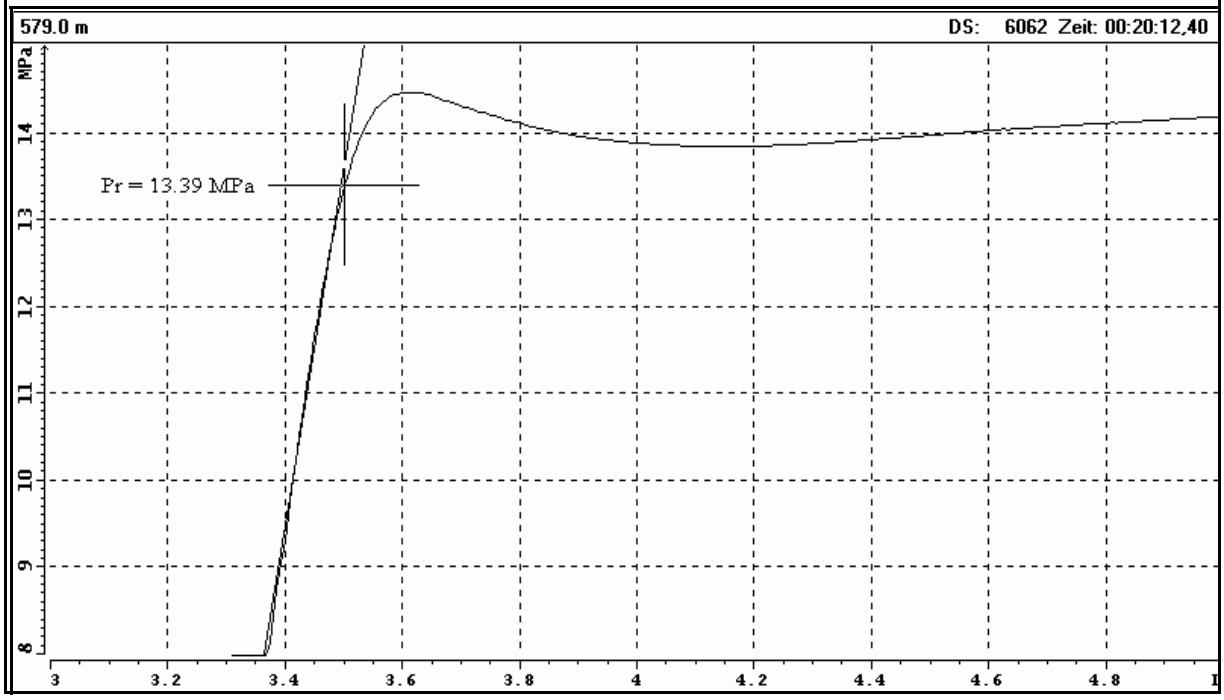

Test at 579.0 m MD: Estimation of $P_{si,\,max}$ (3. Refrac - Cycle)

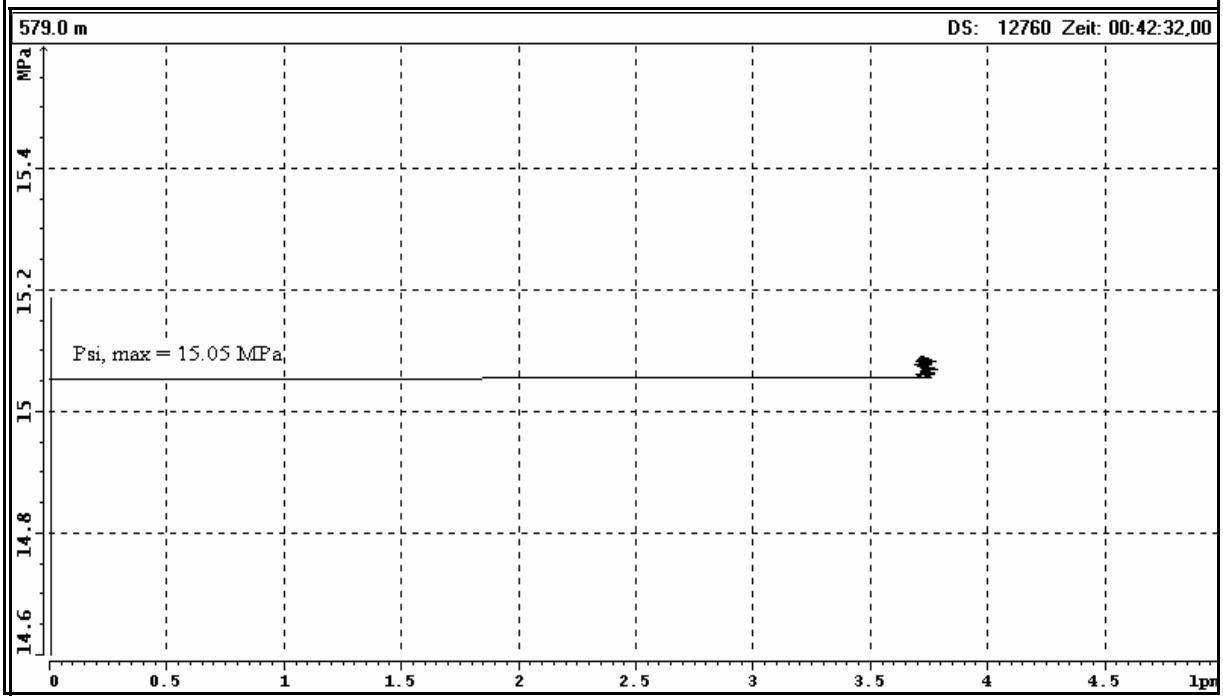

Test at 579.0 m MD: Estimation of $P_{si,\,min}$ (3. Refrac - Cycle)

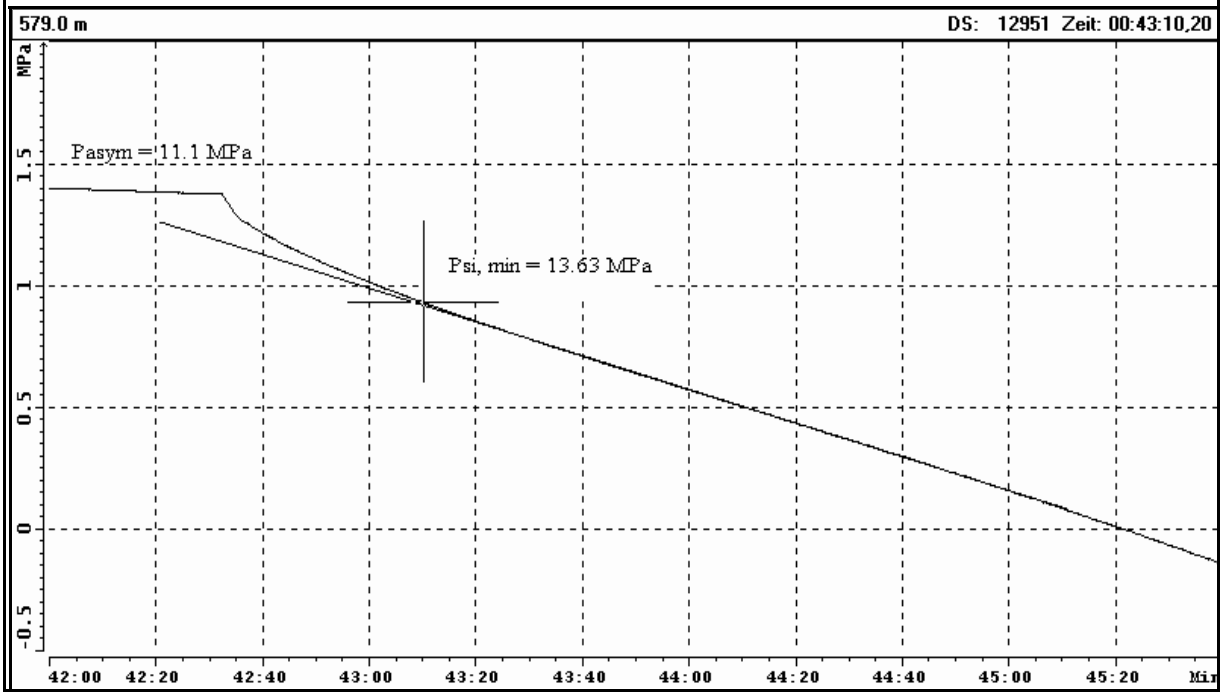

Test at 579.0 m MD: Estimation of P_{si} (3. Refrac - Cycle)

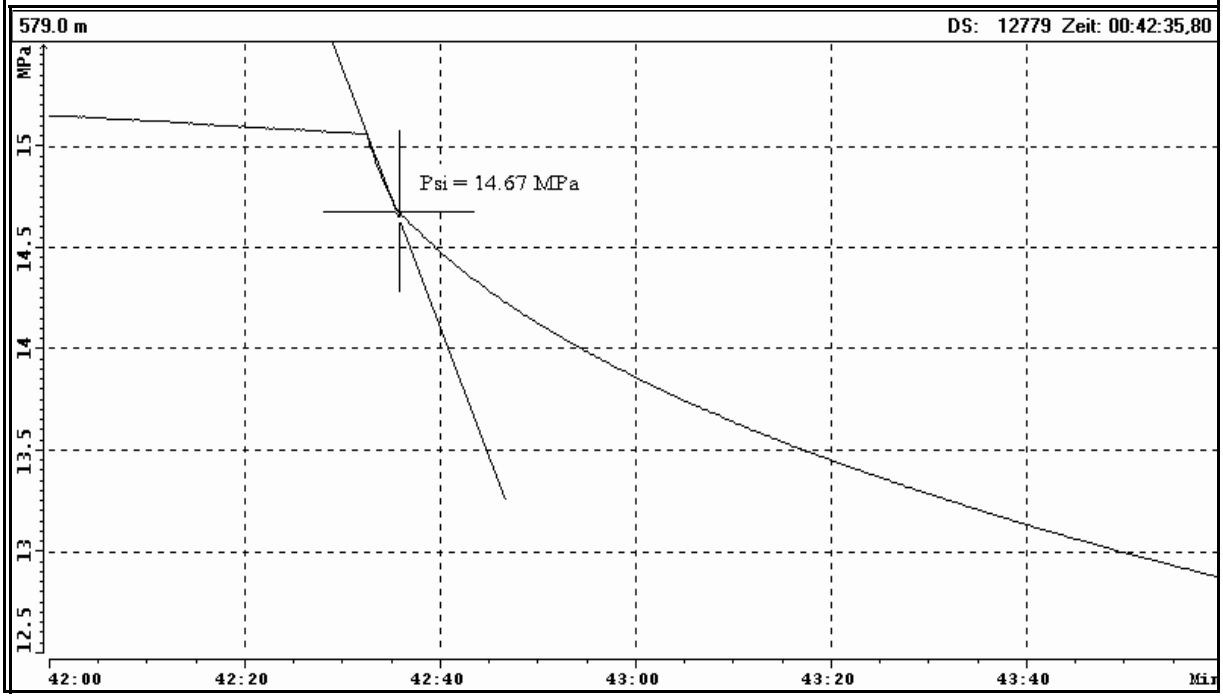

Test at 579.0 m MD: Analysis of Slow - Pump / Step - Rate - Test

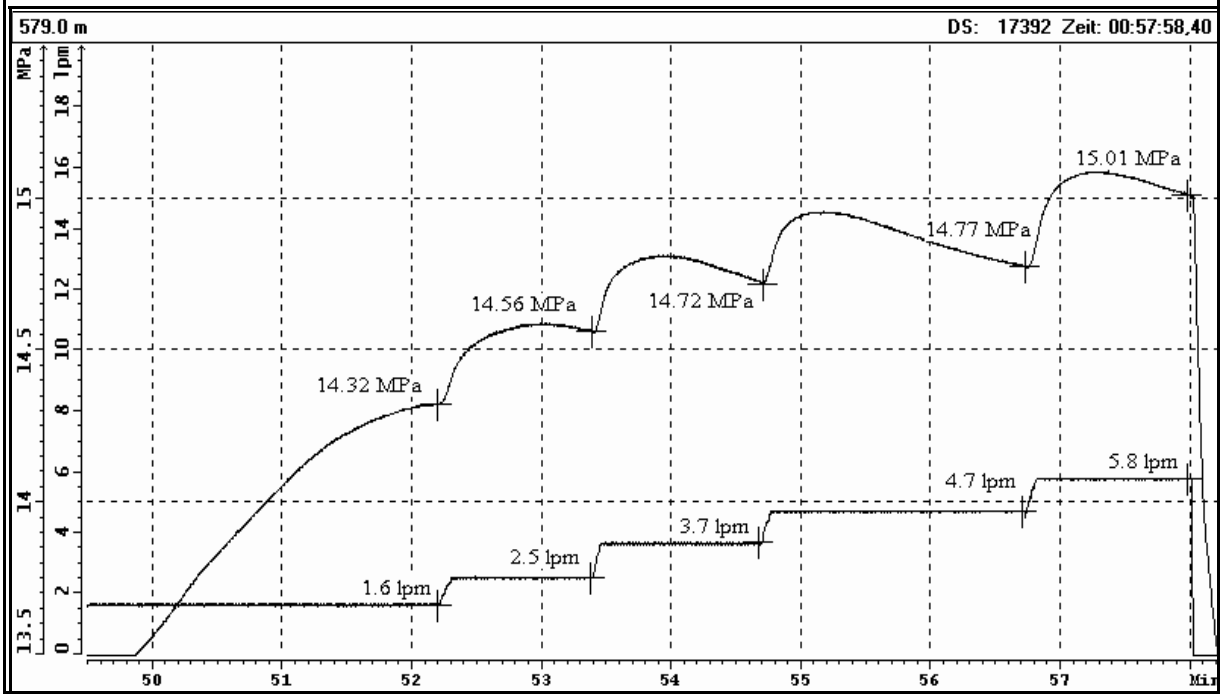

Test at 579.0 m MD: Examination of P_{si} (Step - Rate - Test)

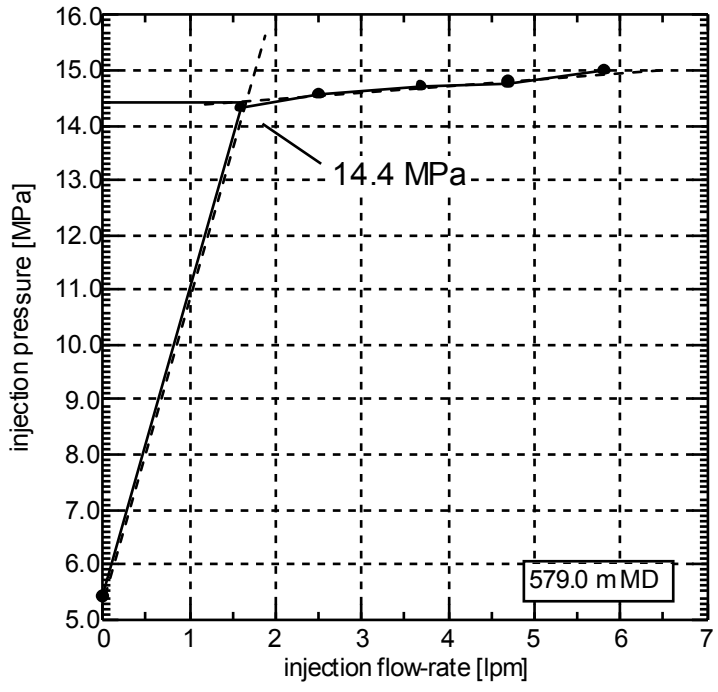

TEST AT 604.2 m MD / 577.0 m TVD

Test at 604.2 m MD : Overview - Plot

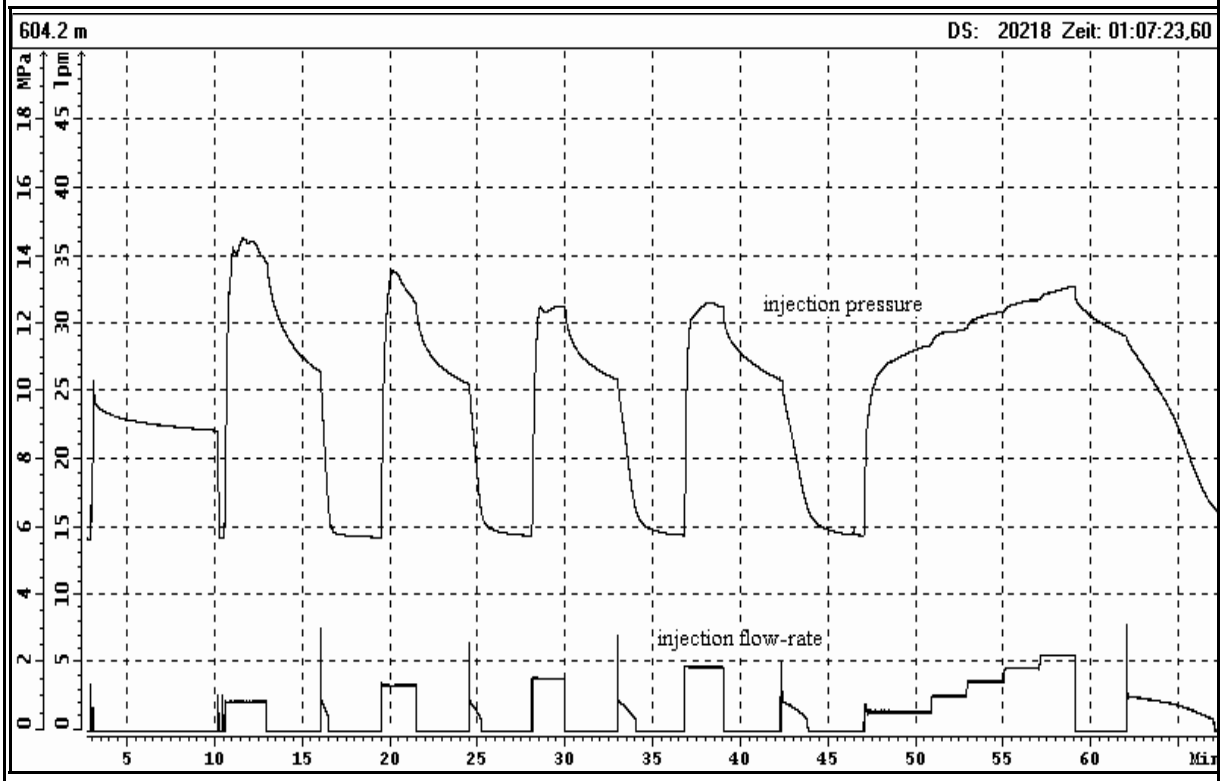

TEST SUMMARY

P - Test :	pressure decrease: 1.3 MPa in 7 min. 0 sec.
Frac (1. Refrac) - Cycle :	injection-rate Q_i= 2.1 lpm, injected volume V_i = 5.1 l, back-flow volume V_r = 0.8 l stimulation of an existing fracture (no breakdown event)
2. Refrac - Cycle :	Q_i = 3.3 lpm, V_i = 6.6 l, V_r = 1.1 l
3. Refrac - Cycle :	Q_i = 3.9 lpm, V_i = 7.2 l, V_r = 1.7 l
4. Refrac - Cycle :	Q_i = 4.7 lpm, V_i = 10.3 l, V_r = 2.4 l
Step-Rate Test :	Q_i = 1.4-5.6 lpm, V_i = 38.9 l, V_r = 9.5 l

total injected volume = 68.1 l, recovered volume = 15.5 l (22.8 %)

Remark: The system-stiffness (dP/dV) observed during the opening of the pre-existing fracture is only 25 MPa/L compared to the general stiffness of approx. 42 MPa/L.

Test at 604.2 m MD: Estimation of P_r (Frac (1. Refrac) - Cycle)

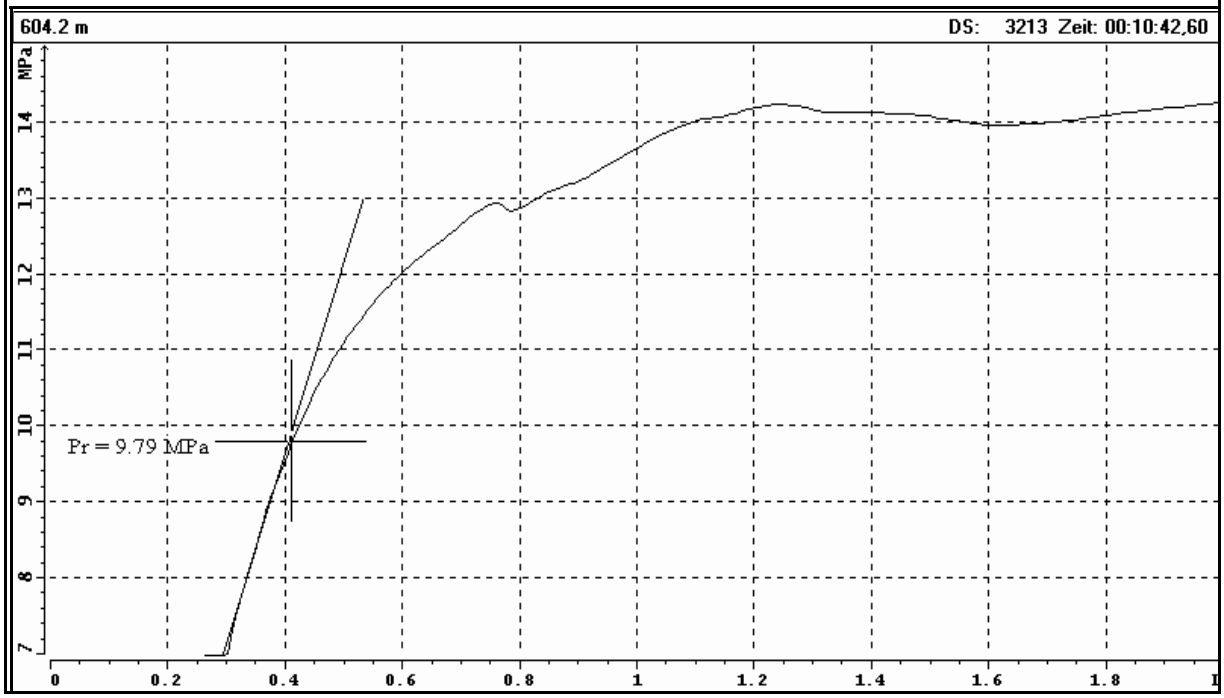

Test at 604.2 m MD: Estimation of P_r (2. Refrac - Cycle, for comparison)

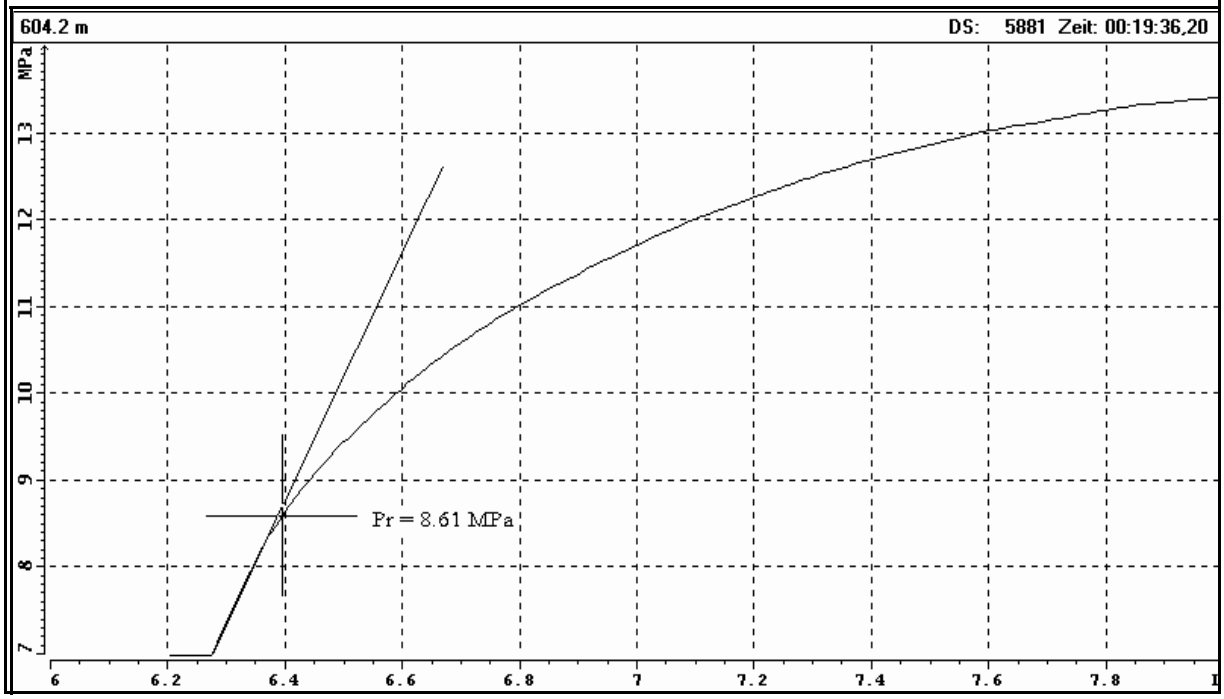

Test at 604.2 m MD: Estimation of $P_{si,\,max}$ (4. Refrac - Cycle)

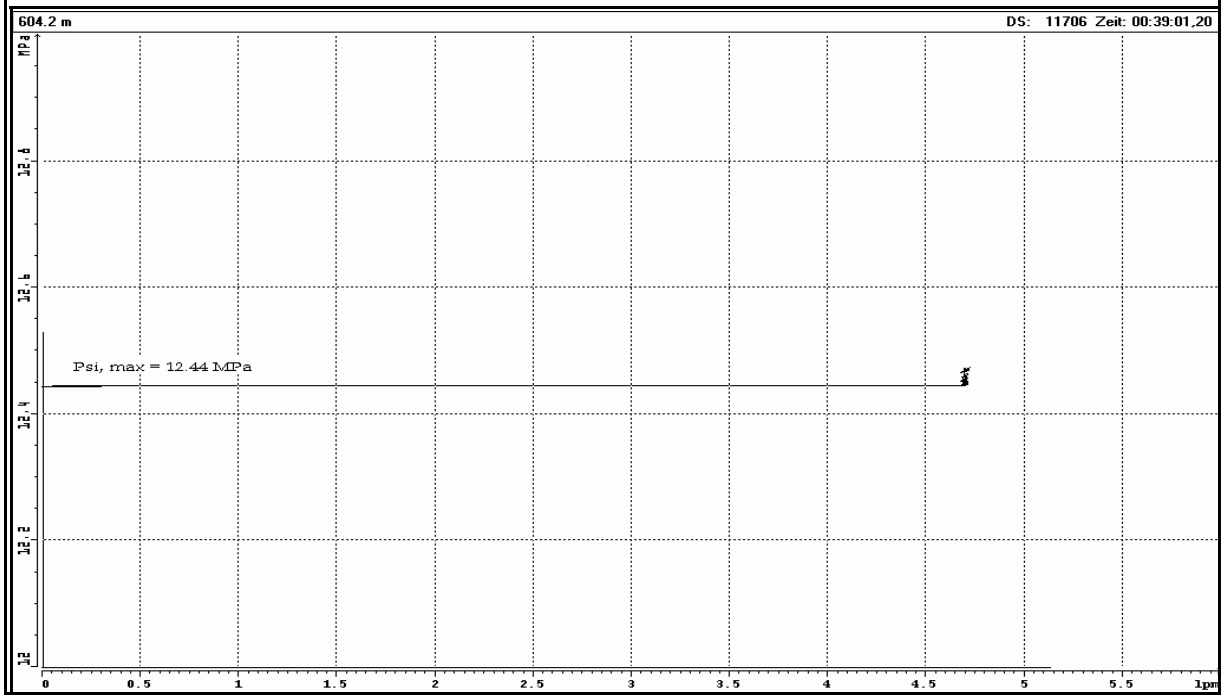

Test at 604.2 m MD: Estimation of $P_{si,\,min}$ (4. Refrac - Cycle)

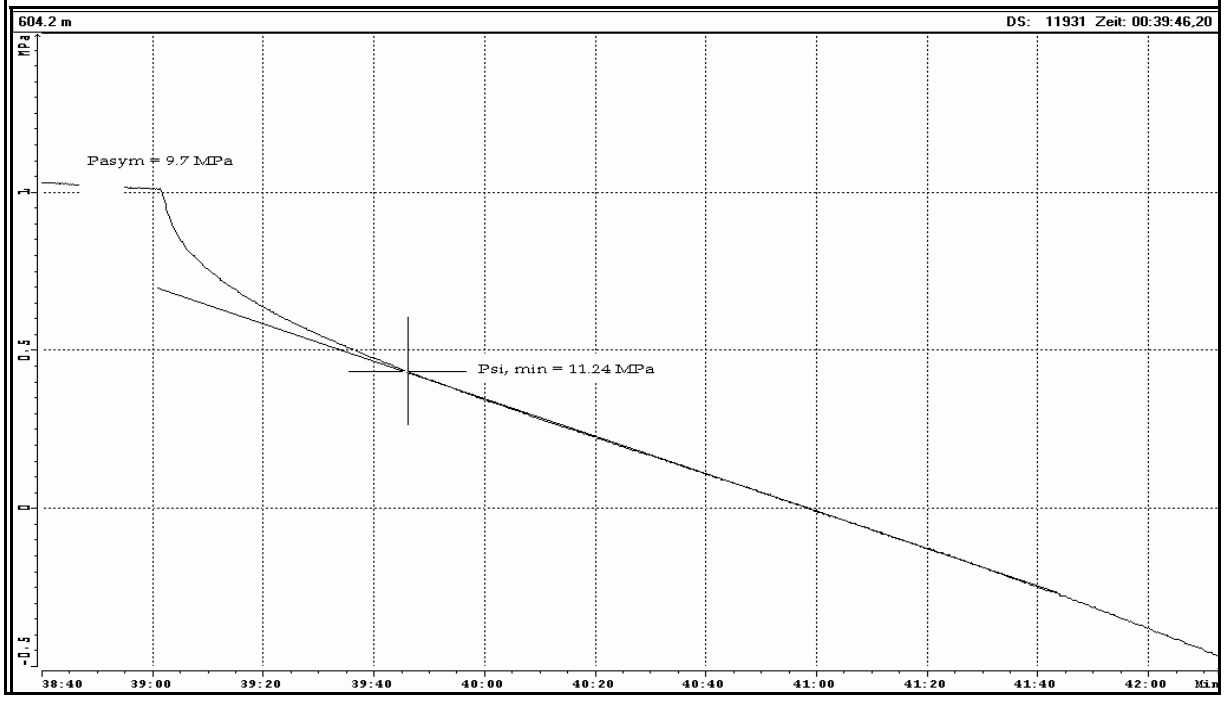

Test at 604.2 m MD: Estimation of P_{si} (4. Refrac - Cycle)

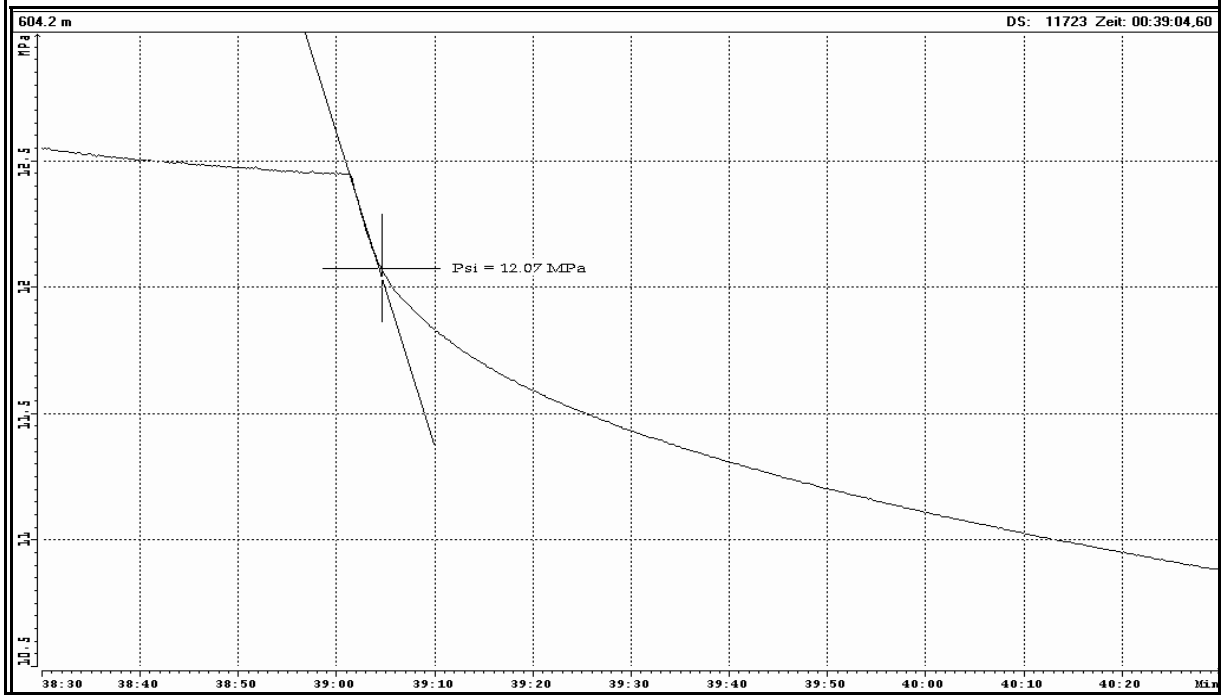

Test at 604.2 m MD: Analysis of Slow - Pump / Step - Rate - Test

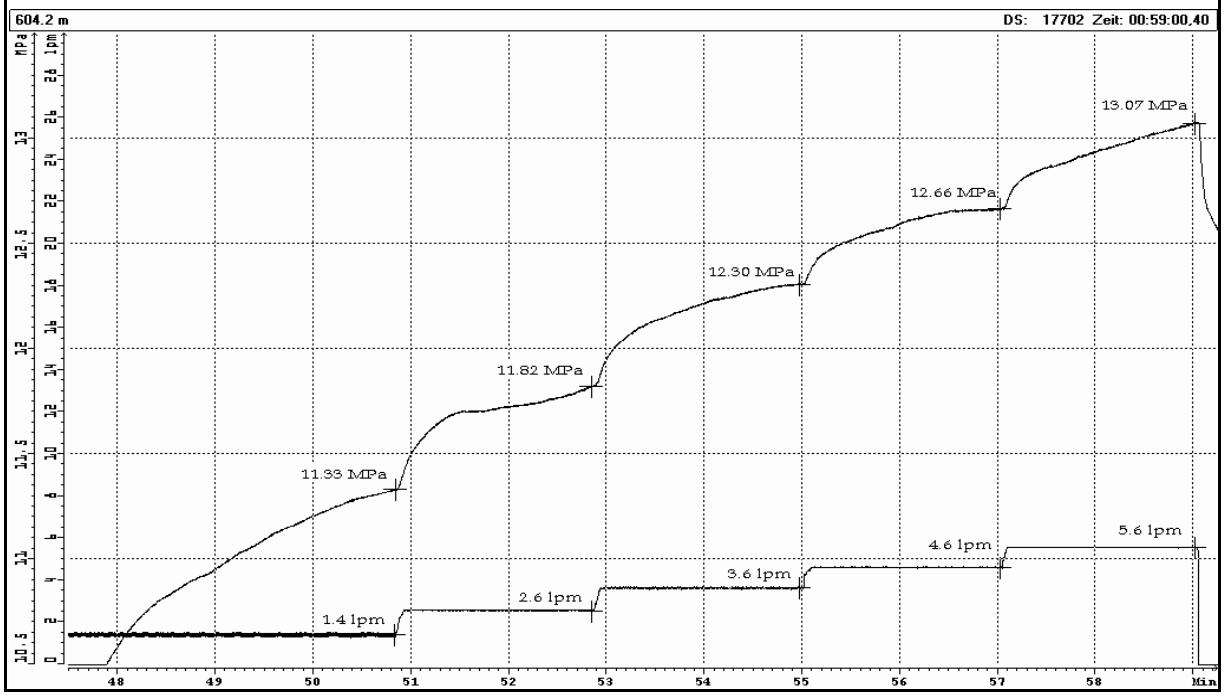

Test at 604.2 m MD: Examination of P_{si} (Step - Rate - Test)

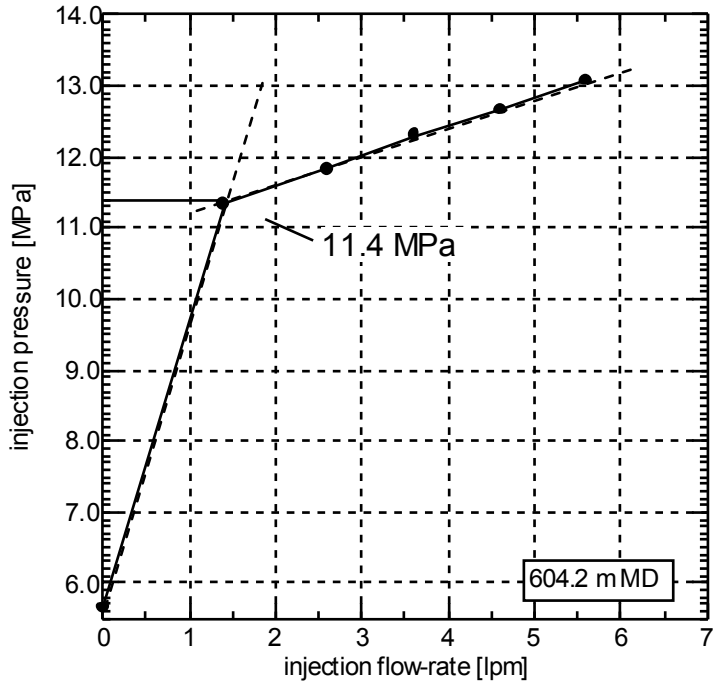

TEST AT 681.0 m MD / 652.9 m TVD

Test at 681.0 m MD : Overview - Plot

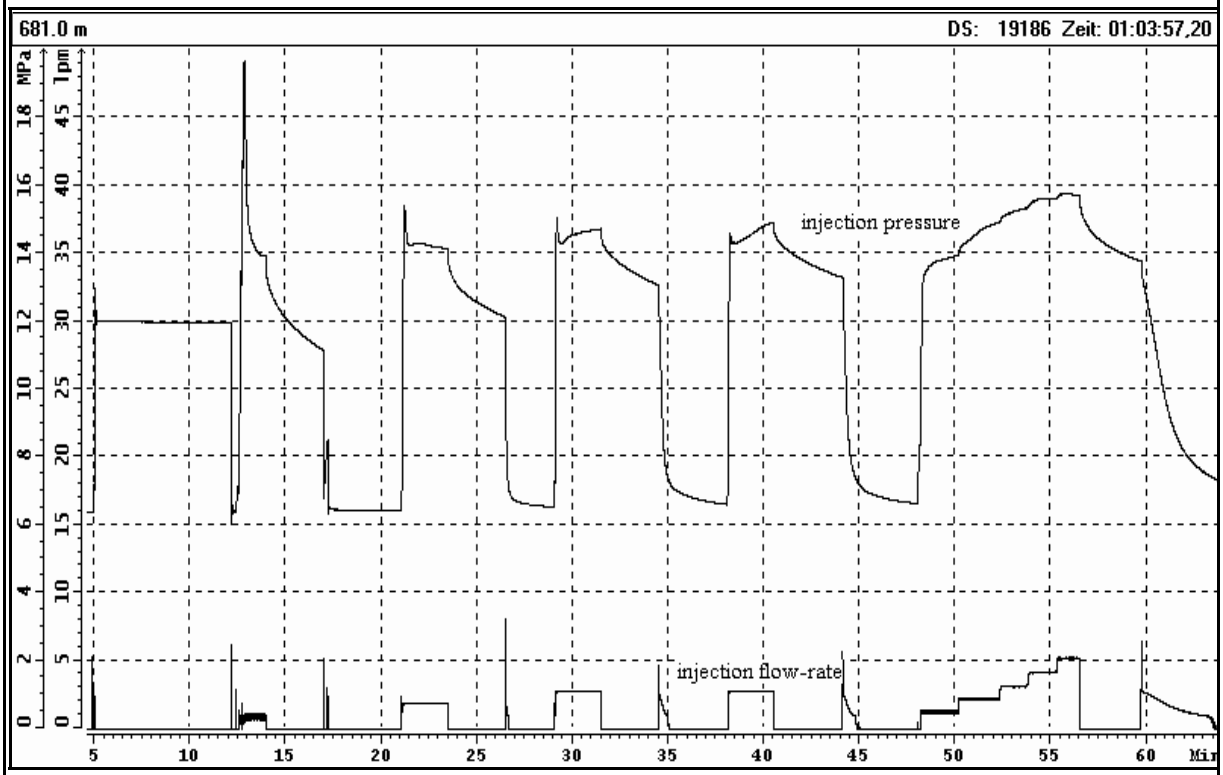

TEST SUMMARY

P - Test :	pressure decrease: 0.1 MPa in 6 min. 58 sec.
Frac - Cycle :	injection - rate Q_i= 1.0 lpm, injected volume V_i = 1.3 l, back-flow volume V_r = 0.2 l clear fracture initiation (breakdown event)
1. Refrac - Cycle :	Q_i = 1.9 lpm, V_i = 4.6 l, V_r = 0.3 l
2. Refrac - Cycle :	Q_i = 2.8 lpm, V_i = 6.7 l, V_r = 0.8 l
3. Refrac - Cycle :	Q_i = 2.8 lpm, V_i = 6.5 l, V_r = 1.1 l
Step-Rate Test :	Q_i = 1.3-5.2 lpm, V_i = 24.5 l, V_r = 6.2 l

total injected volume = 43.6 l, recovered volume = 8.6 l (19.7 %)

Remark: During the injection - cycles, an increase of the shut-in pressure was observed. The P_{si} - value was therefore determined from the 1. refrac - cycle.

Test at 681.0 m MD: Estimation of P_c (Frac - Cycle)

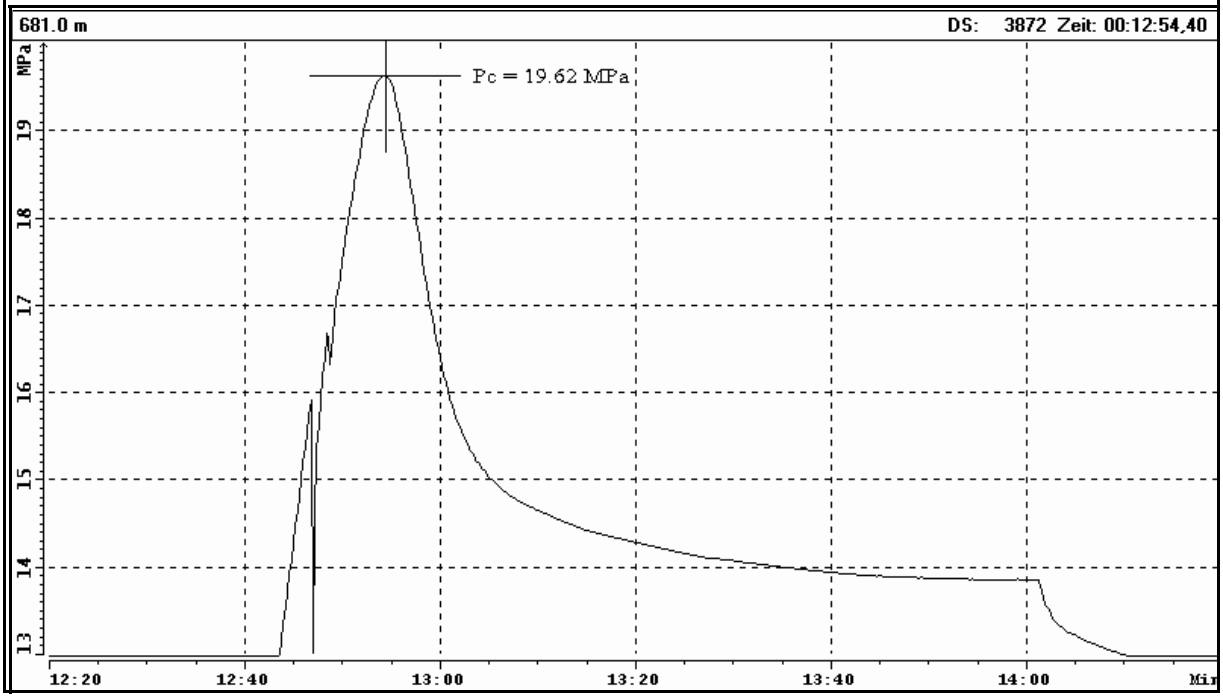

Test at 681.0 m MD: Estimation of P_r (1. Refrac - Cycle)

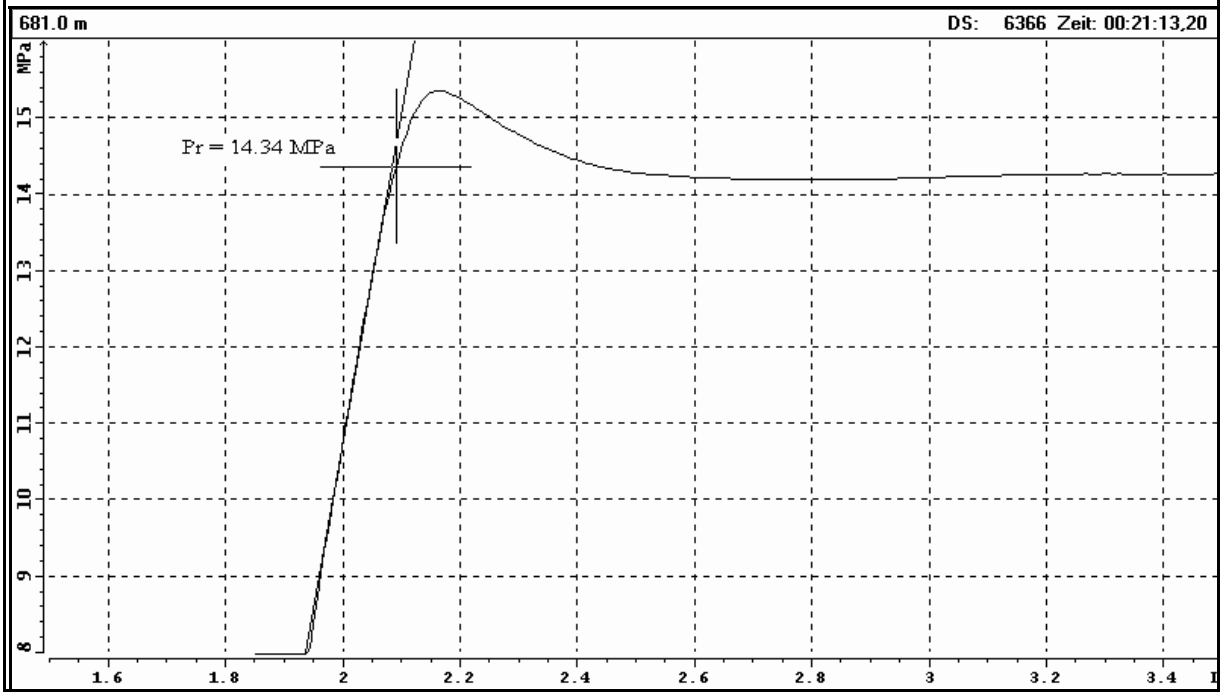

Test at 681.0 m MD: Estimation of $P_{si,\,max}$ (1. Refrac - Cycle)

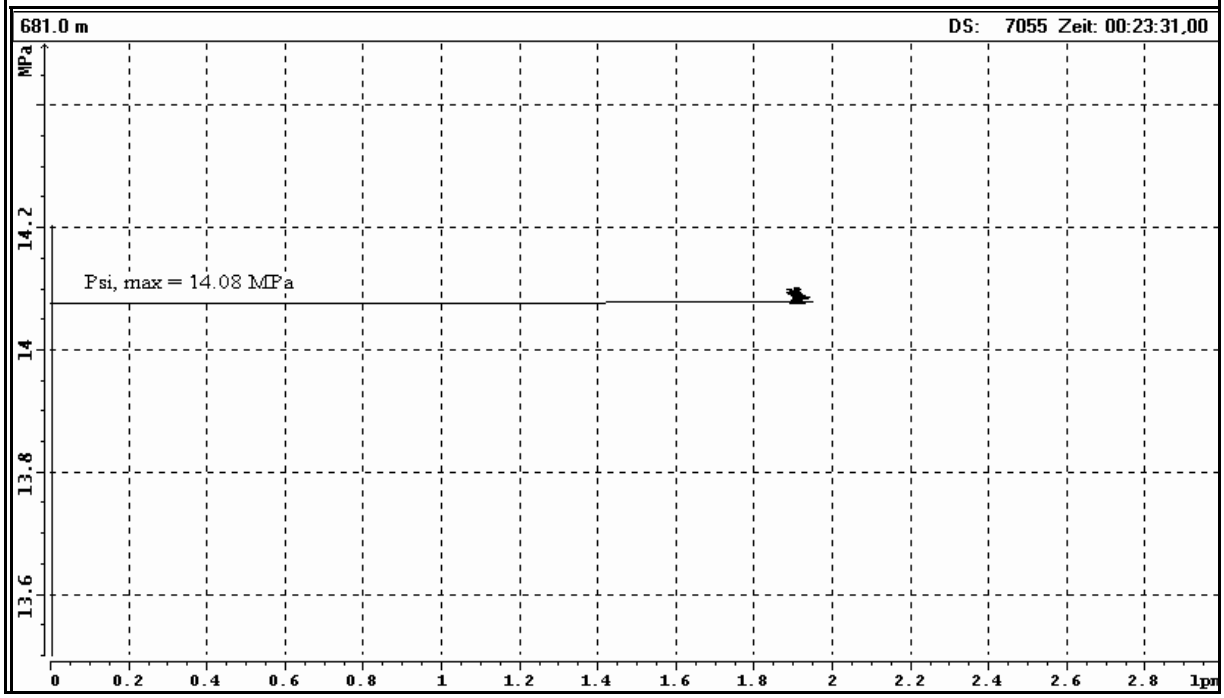

Test at 681.0 m MD: Estimation of $P_{si,\,min}$ (1. Refrac - Cycle)

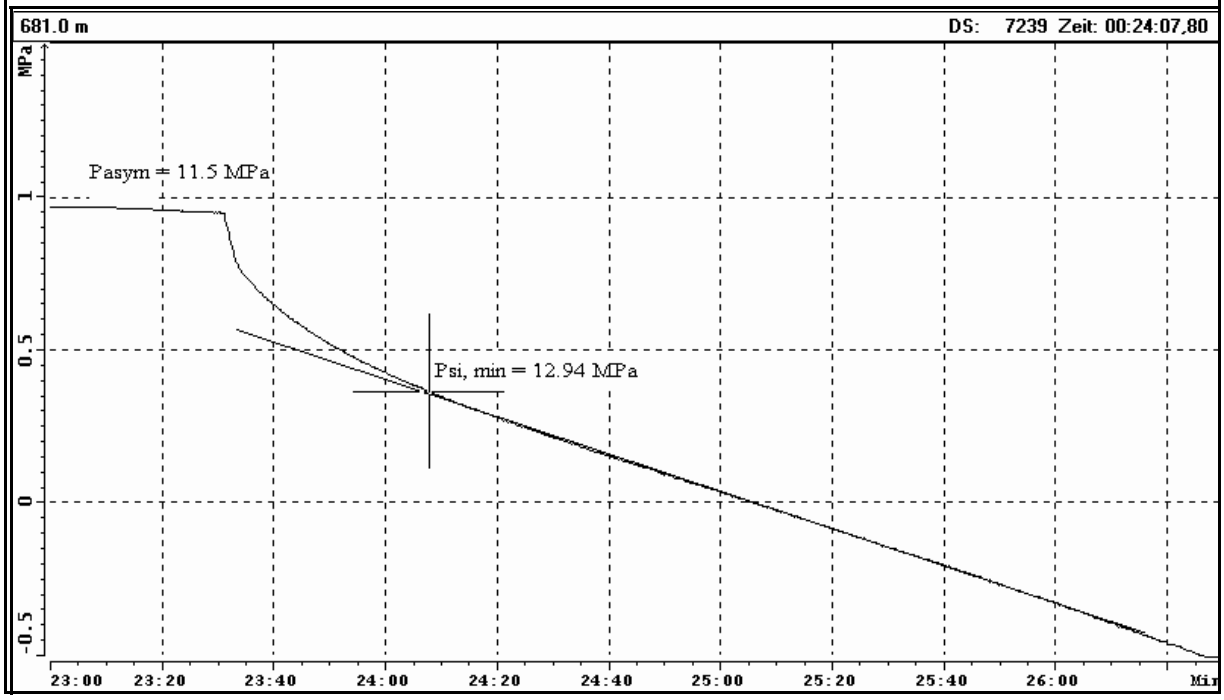

Test at 681.0 m MD: Estimation of P_{si} (1. Refrac - Cycle)

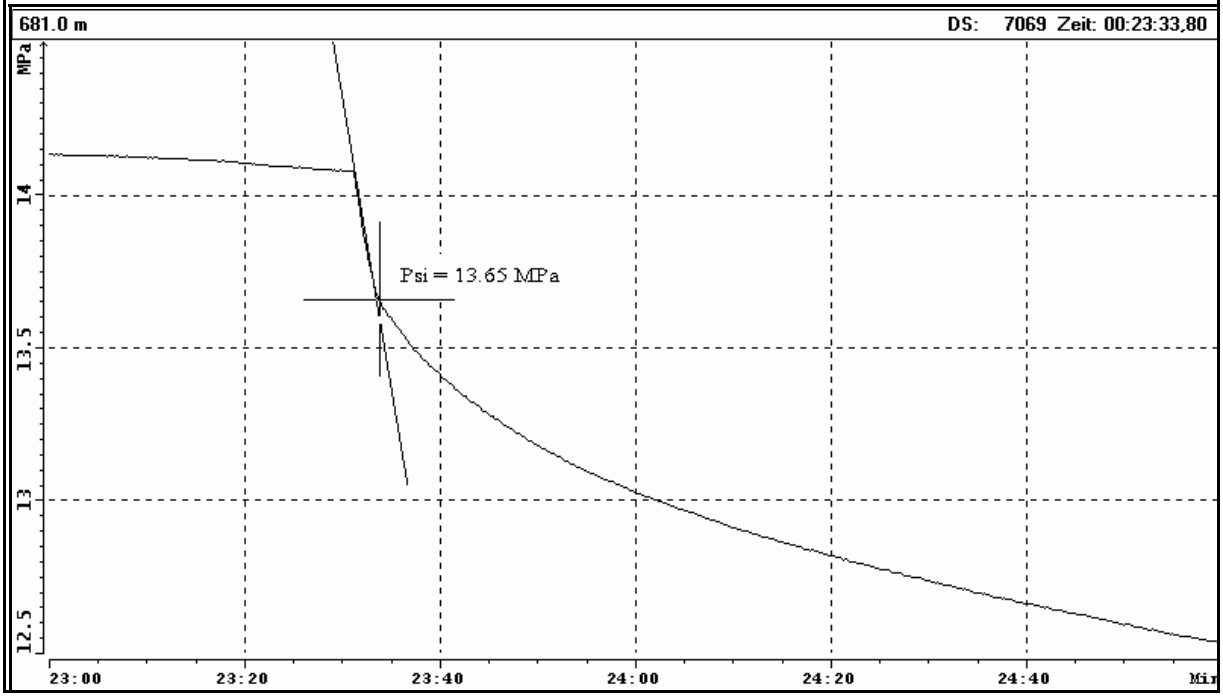

Test at 681.0 m MD: Analysis of Slow - Pump / Step - Rate - Test

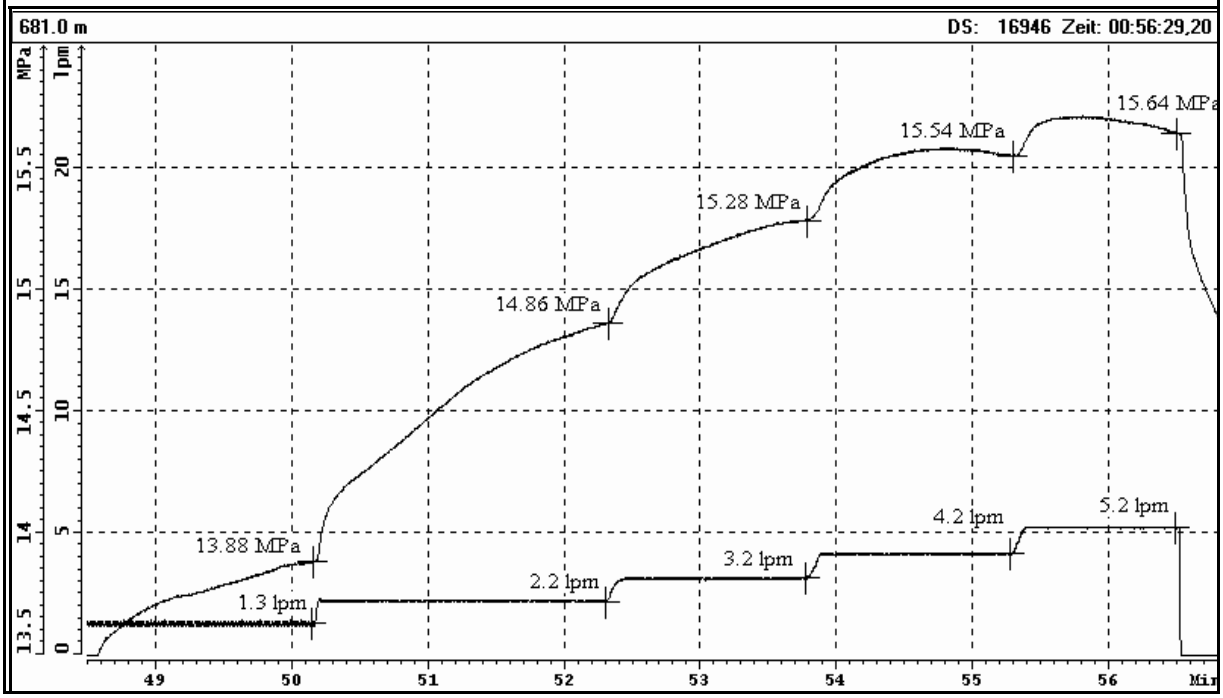

Test at 681.0 m MD: Examination of P_{si} (Step - Rate - Test)

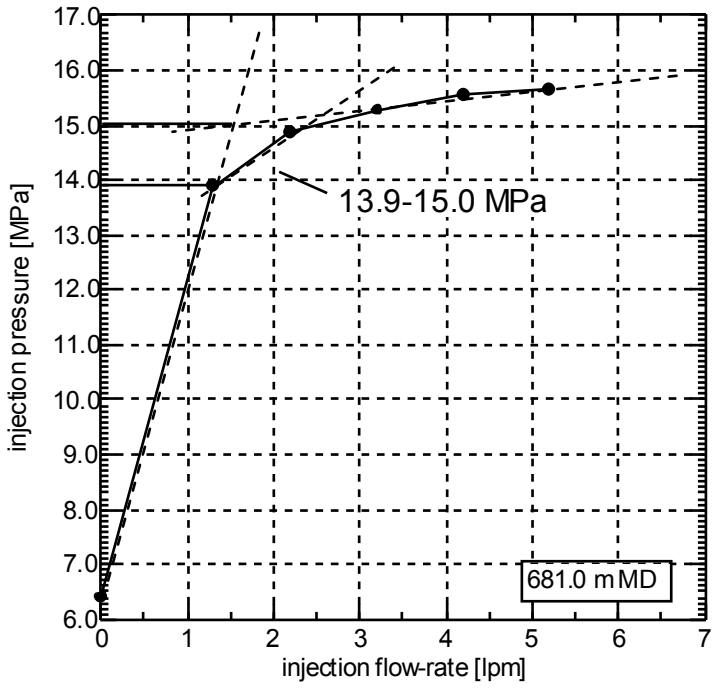

TEST AT 689.5 m MD / 661.3 m TVD

Test at 689.5 m MD : Overview - Plot

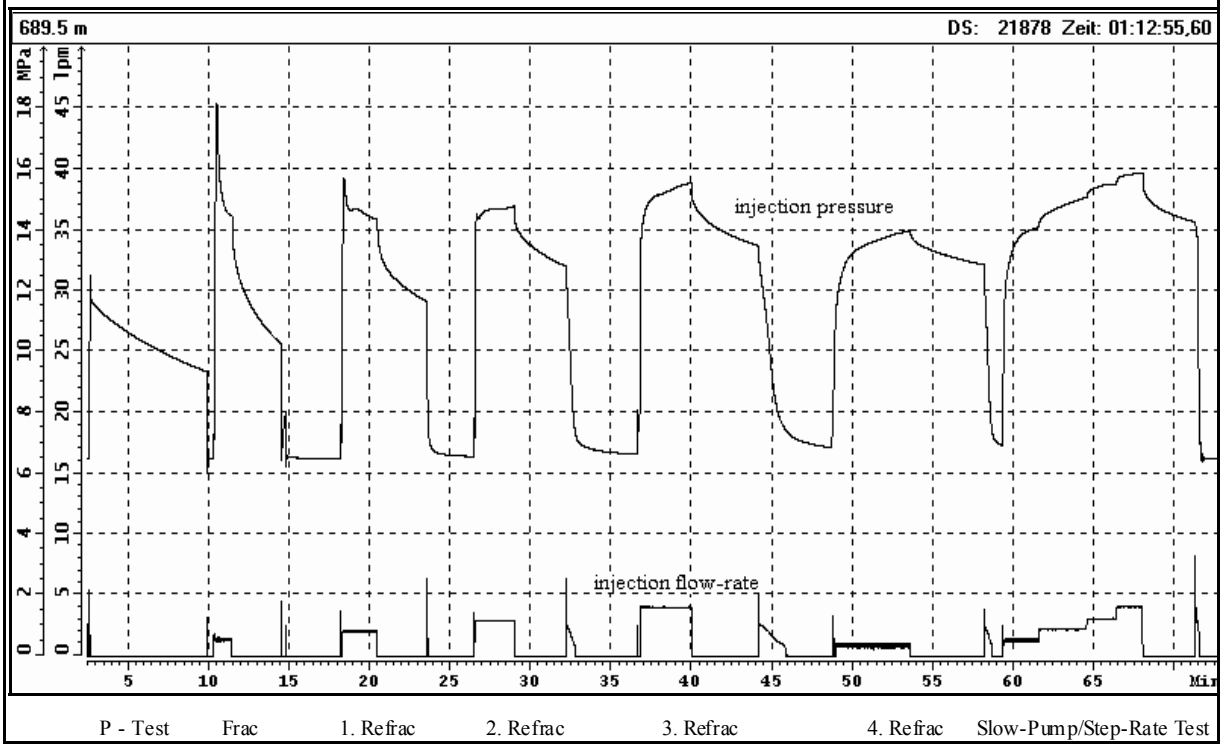

TEST SUMMARY

P - Test :	pressure decrease: 2.3 MPa in 7 min. 9 sec.
Frac - Cycle :	injection - rate Q_i= 1.4 lpm, injected volume V_i = 1.6 l, back-flow volume V_r = 0.1 l clear fracture initiation (breakdown event)
1. Refrac - Cycle :	Q_i = 2.1 lpm, V_i = 4.6 l, V_r = 0.2 l
2. Refrac - Cycle :	Q_i = 2.9 lpm, V_i = 7.2 l, V_r = 1.0 l
3. Refrac - Cycle :	Q_i = 4.0 lpm, V_i = 12.8 l, V_r = 3.0 l
4. Refrac - Cycle :	Q_i = 1.0 lpm, V_i = 4.5 l, V_r = 1.0 l
Step-Rate Test :	Q_i = 1.3-4.1 lpm, V_i = 21.8 l, V_r = 0.7 l

total injected volume = 52.5 l, recovered volume = 6.0 l (11.4 %)

Remark: During the injection - cycles, an increase of the shut-in pressure was observed. The P_{si} - value was therefore determined from the 1. refrac - cycle.

Test at 689.5 m MD: Estimation of P_c (Frac - Cycle)

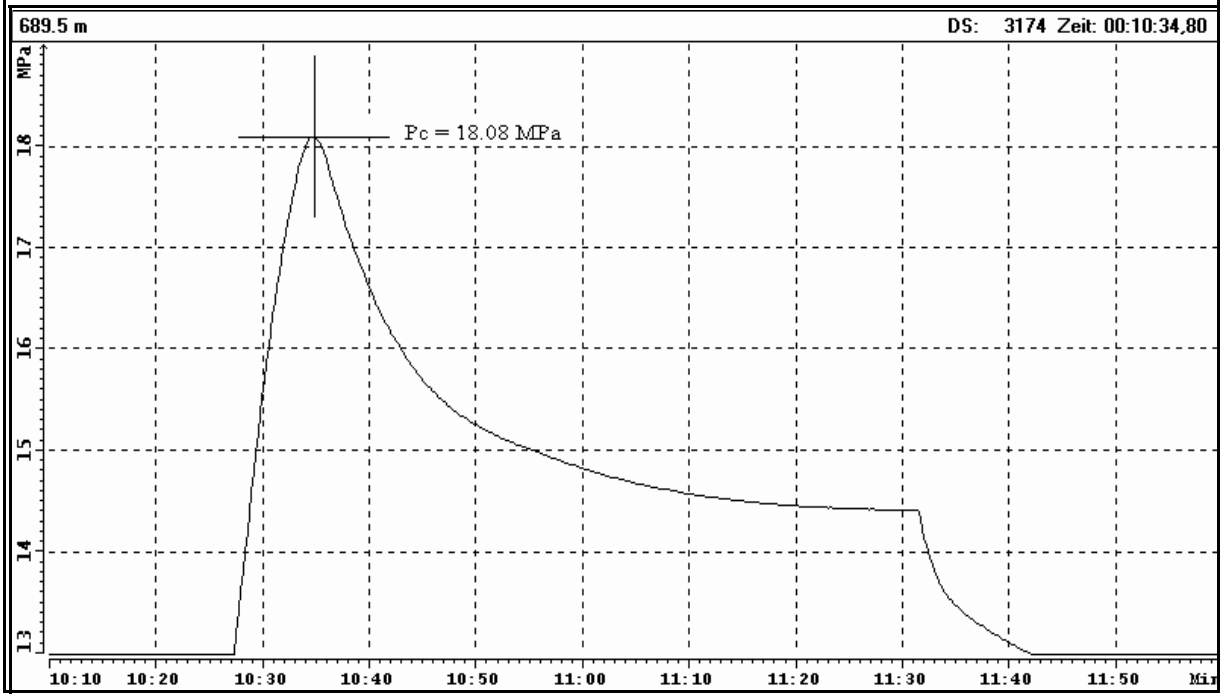

Test at 689.5 m MD: Estimation of P_r (1. Refrac - Cycle)

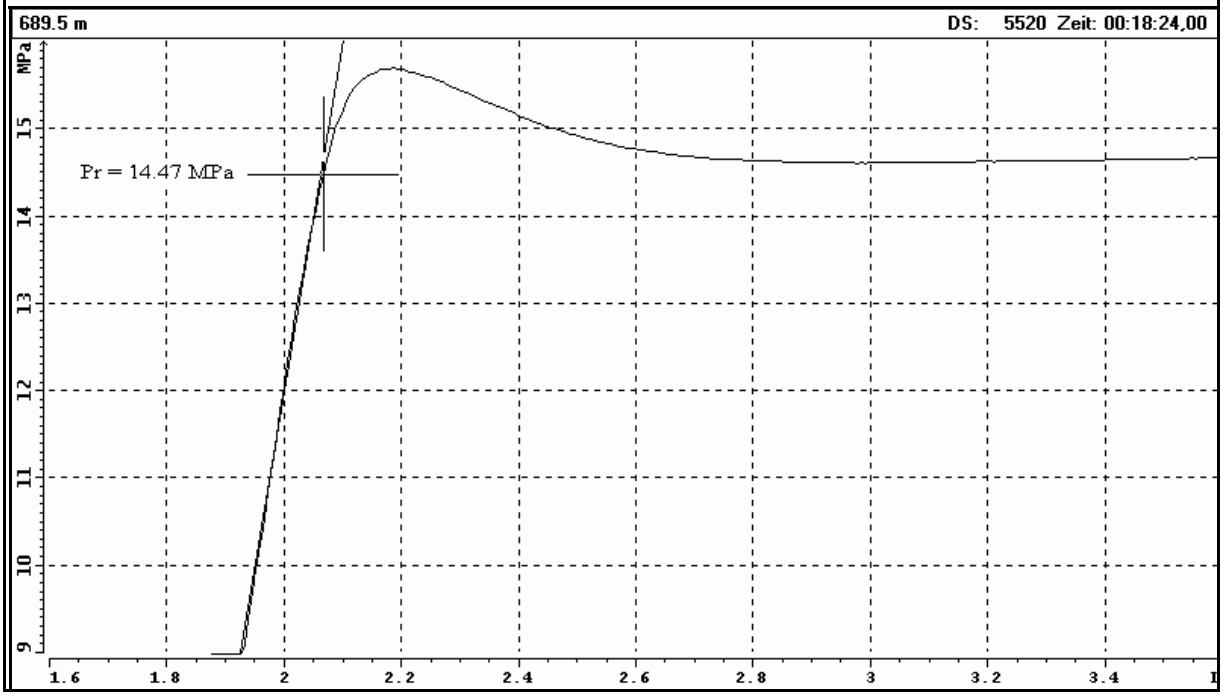

Test at 689.5 m MD: Estimation of $P_{si,\,max}$ (1. Refrac - Cycle)

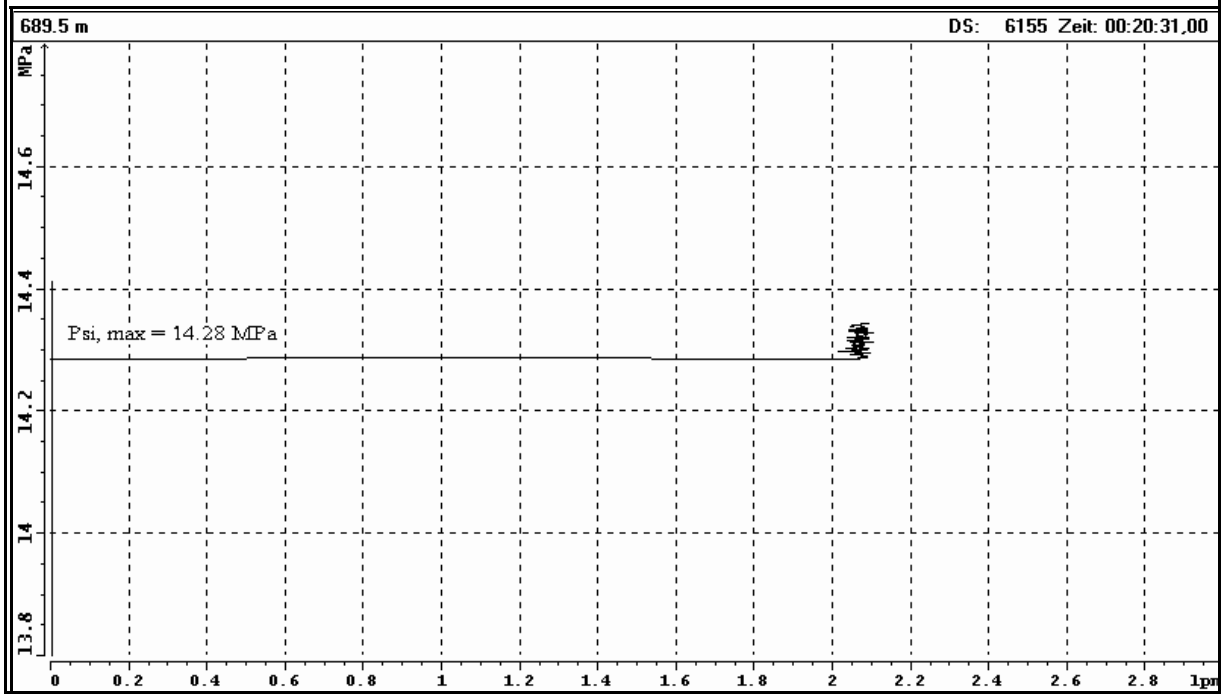

Test at 689.5 m MD: Estimation of $P_{si,\,min}$ (1. Refrac - Cycle)

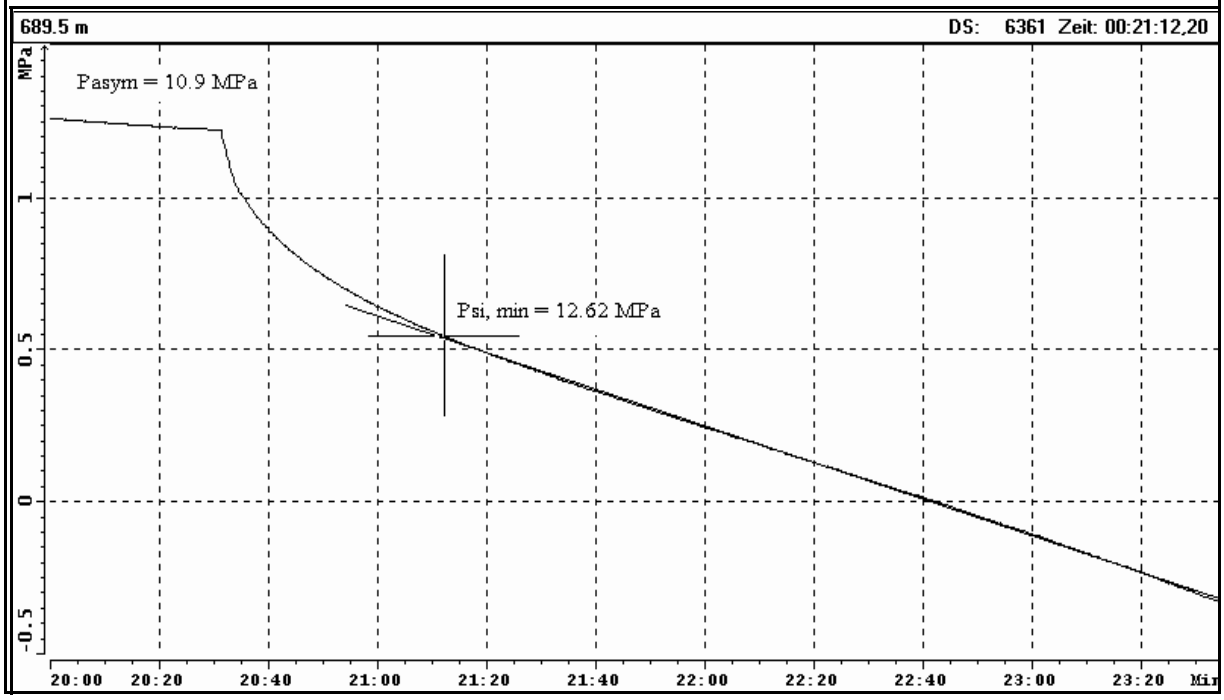

Test at 689.5 m MD: Estimation of P_{si} (1. Refrac - Cycle)

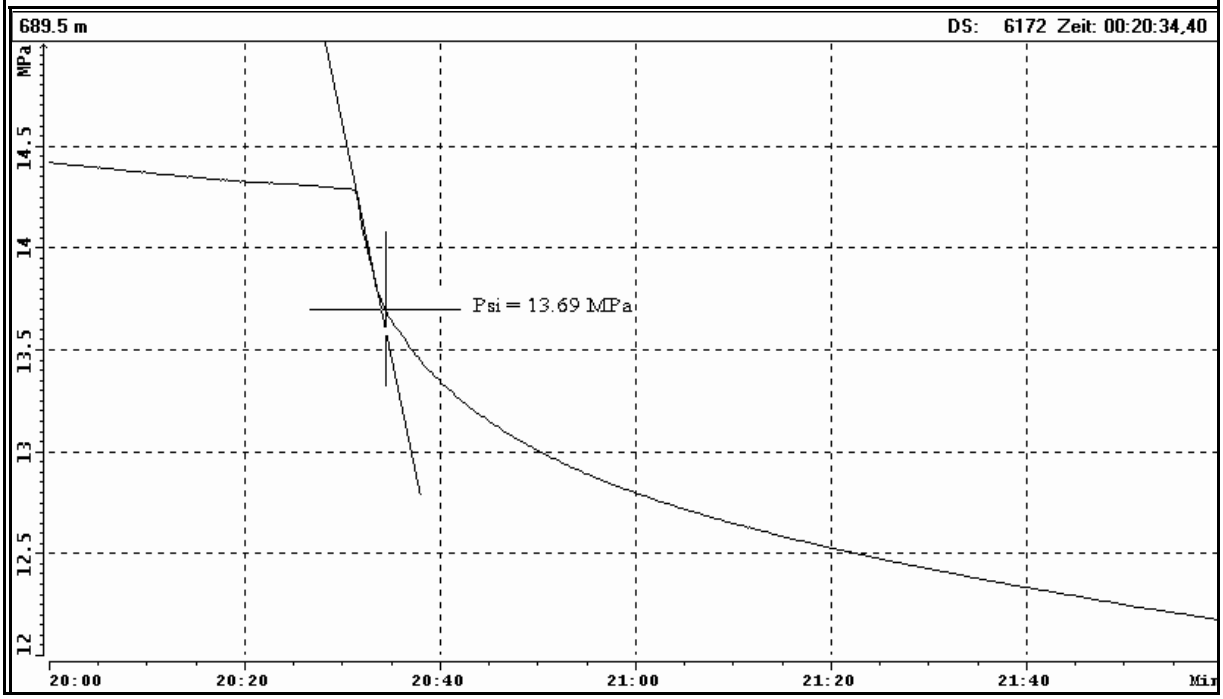

Test at 689.5 m MD: Analysis of Slow - Pump / Step - Rate - Test

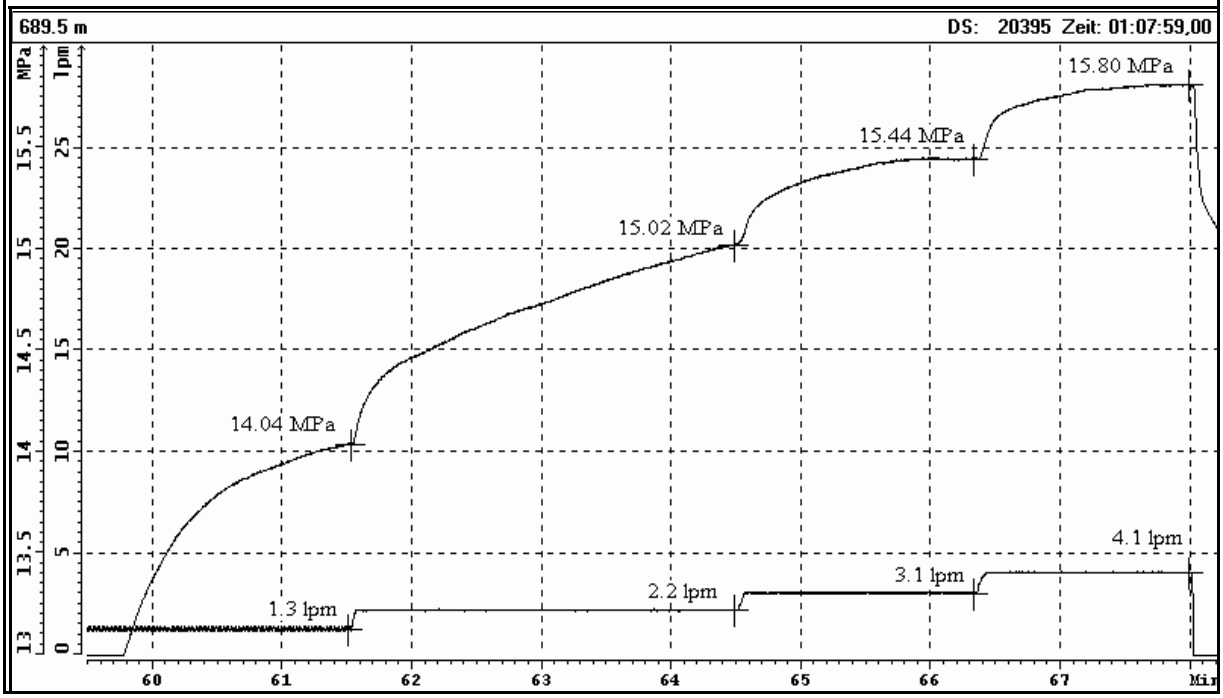

Test at 689.5 m MD: Examination of P_{si} (Step - Rate - Test)

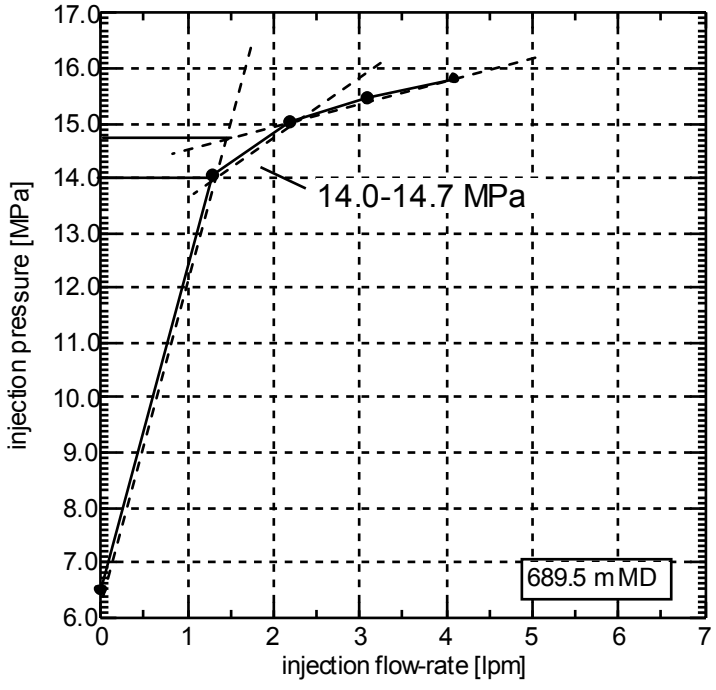

TEST AT 702.5 m MD / 674.2 m TVD

Test at 702.5 m MD : Overview - Plot

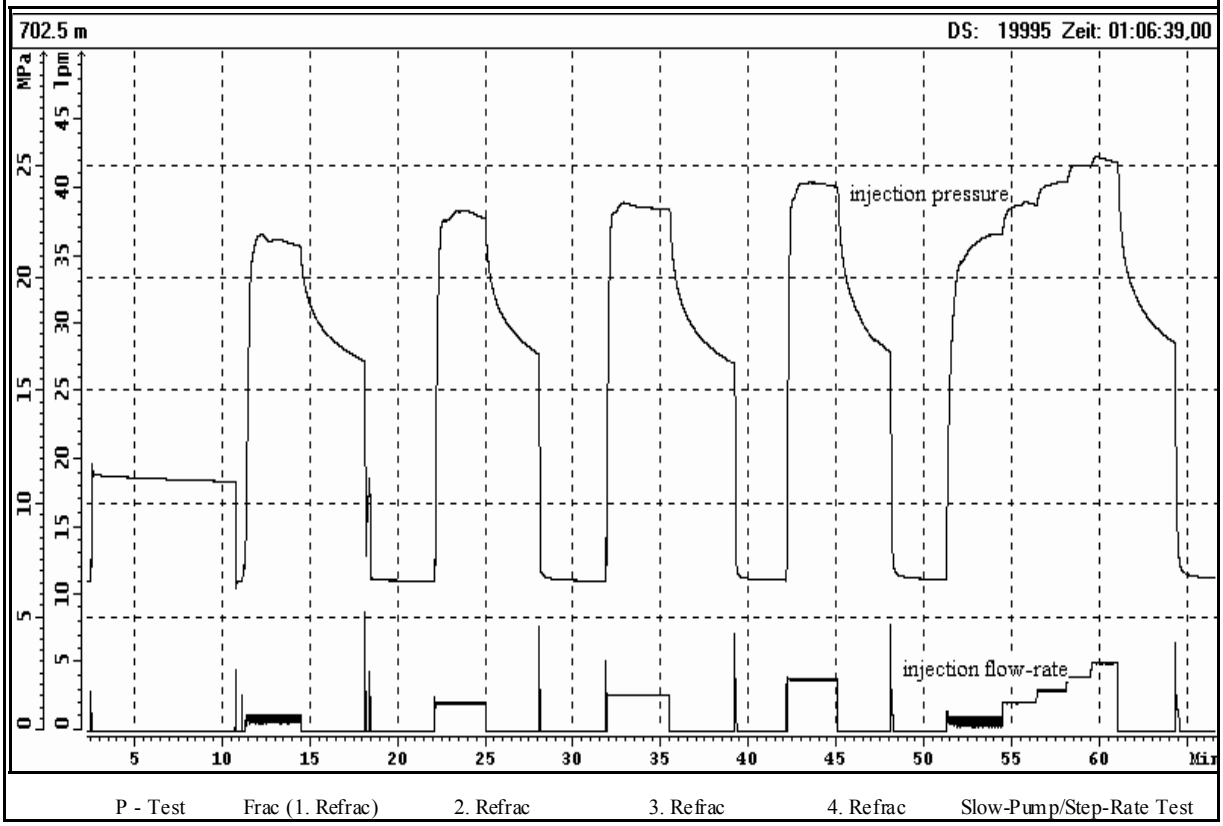

TEST SUMMARY

P - Test :	pressure decrease: 0.3 MPa in 8 min. 1 sec.
Frac (1. Refrac) - Cycle :	injection-rate Q_i= 1.1 lpm, injected volume V_i = 3.0 l, back-flow volume V_r = 0.3 l stimulation of an existing fracture (no breakdown event)
2. Refrac - Cycle :	Q_i = 2.0 lpm, V_i = 5.9 l, V_r = 0.3 l
3. Refrac - Cycle :	Q_i = 2.7 lpm, V_i = 9.5 l, V_r = 0.3 l
4. Refrac - Cycle :	Q_i = 3.8 lpm, V_i = 10.9 l, V_r = 0.4 l
Step-Rate Test :	Q_i = 0.9-5.0 lpm, V_i = 24.8 l, V_r = 0.6 l

total injected volume = 54.1 l, recovered volume = 1.9 l (3.5 %)

Remark: During the injection - cycles, an increase of the shut-in pressure was observed. The P_{si} - value was therefore determined from the 1. refrac - cycle.

Test at 702.5 m MD: Estimation of P_r (Frac (1. Refrac) - Cycle)

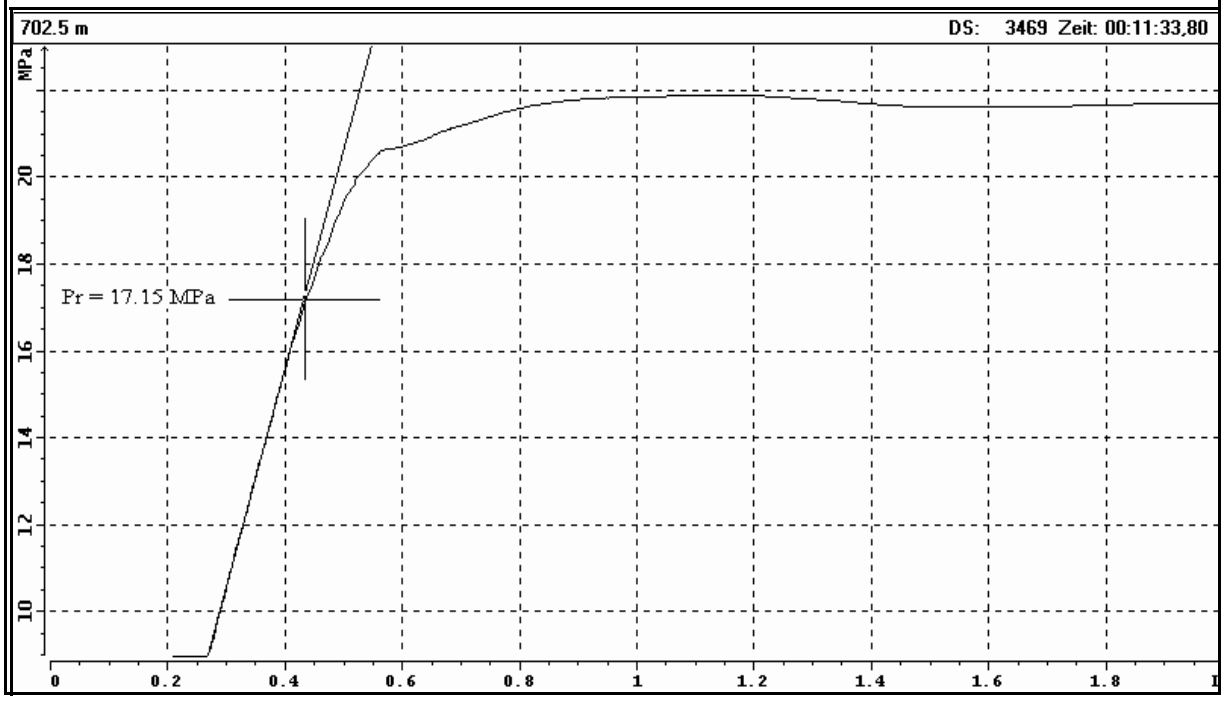

Test at 702.5 m MD: Estimation of P_r (2. Refrac - Cycle, for comparison)

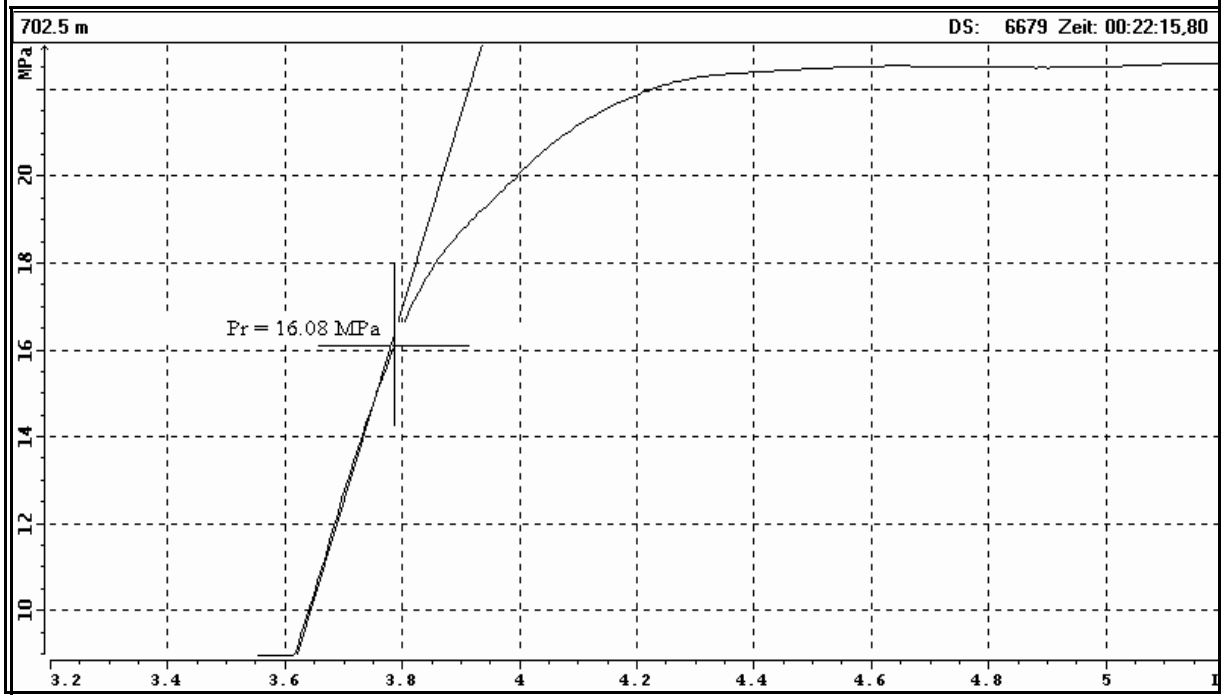

Test at 702.5 m MD: Estimation of $P_{si,\,max}$ (1. Refrac - Cycle)

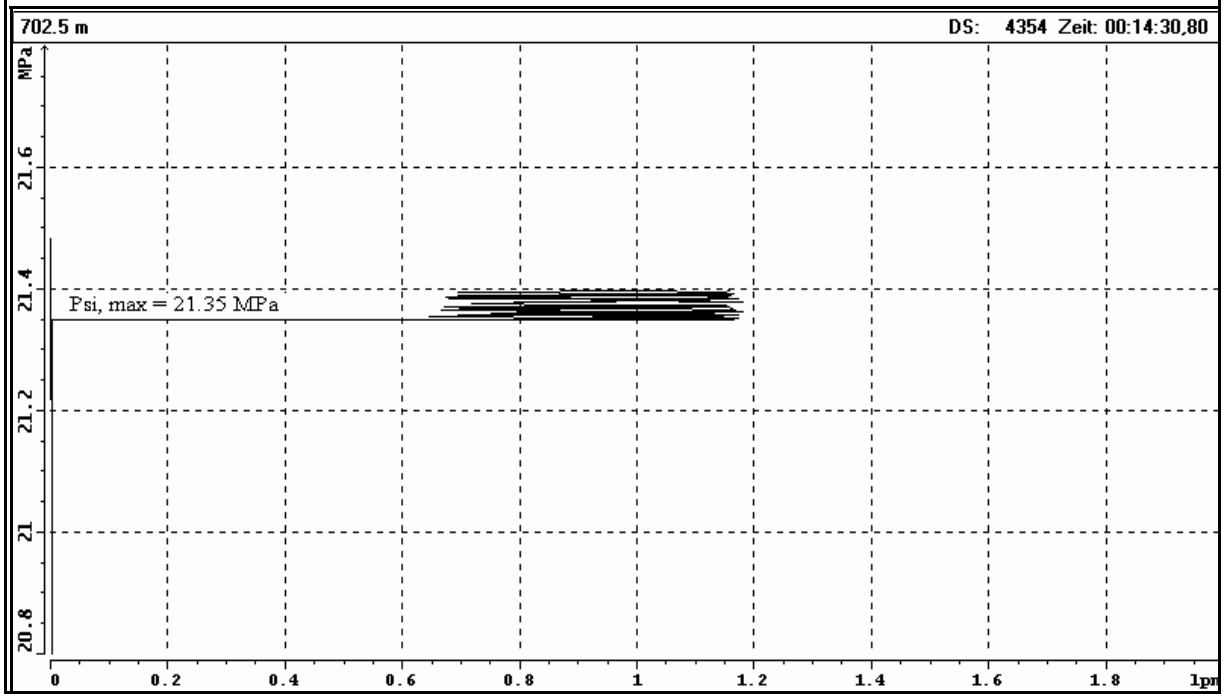

Test at 702.5 m MD: Estimation of $P_{si,\,min}$ (1. Refrac - Cycle)

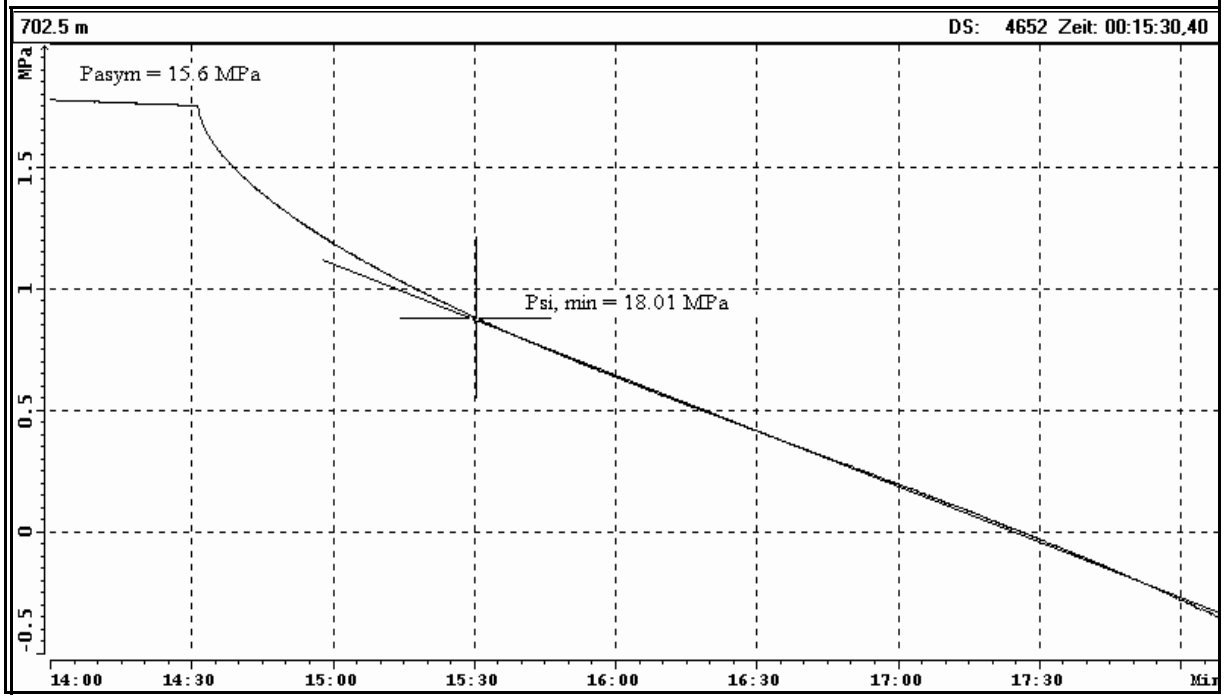

Test at 702.5 m MD: Estimation of P_{si} (1. Refrac - Cycle)

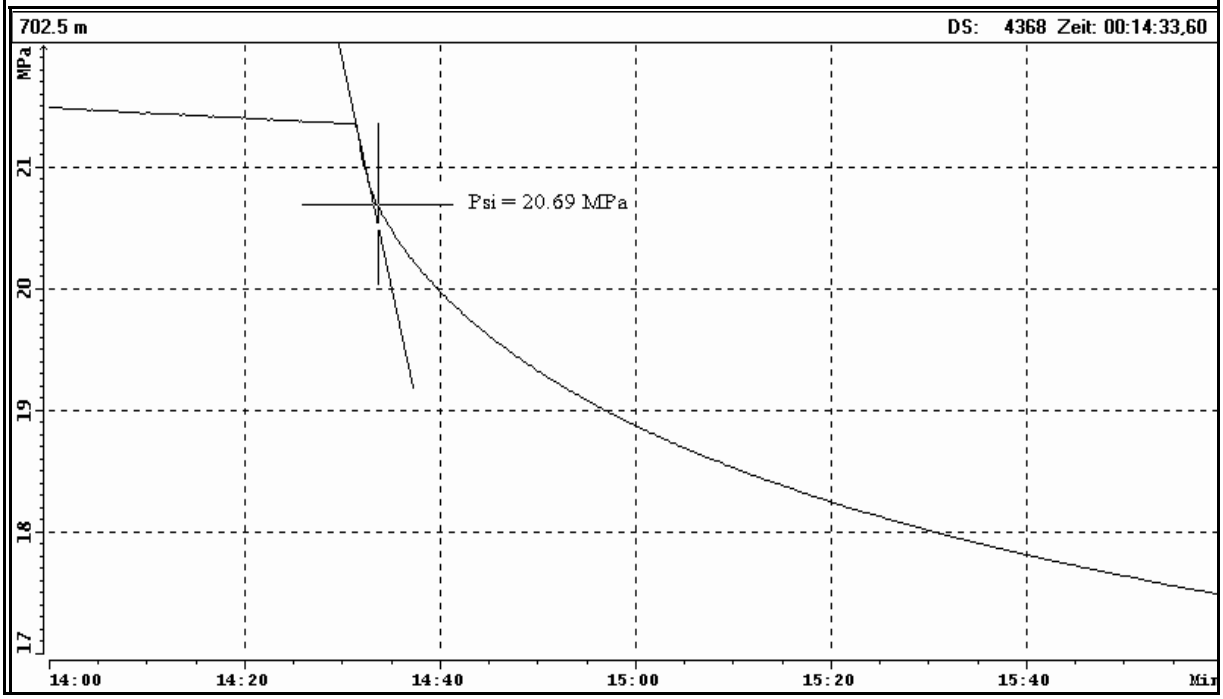

Test at 702.5 m MD: Analysis of Slow - Pump / Step - Rate - Test

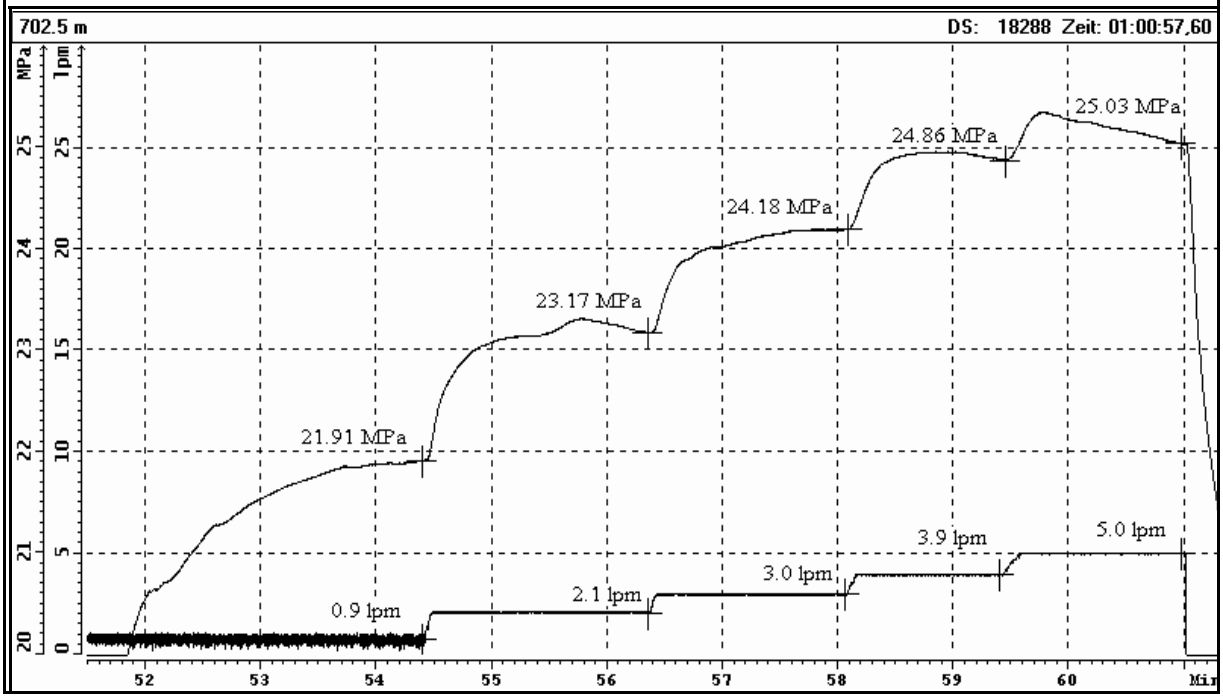

Test at 702.5 m MD: Examination of P_{si} (Step - Rate - Test)

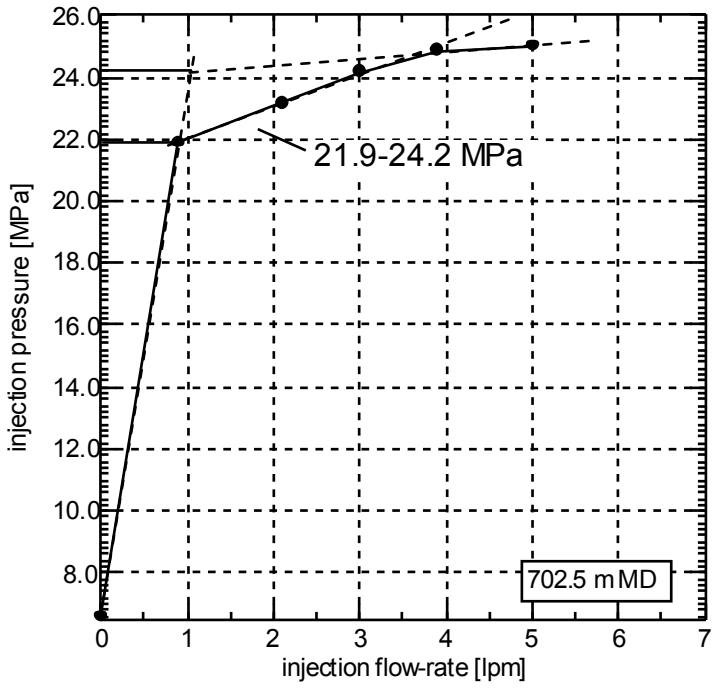

TEST AT 708.0 m MD / 679.6 m TVD

Test at 708.0 m MD: Overview - Plot

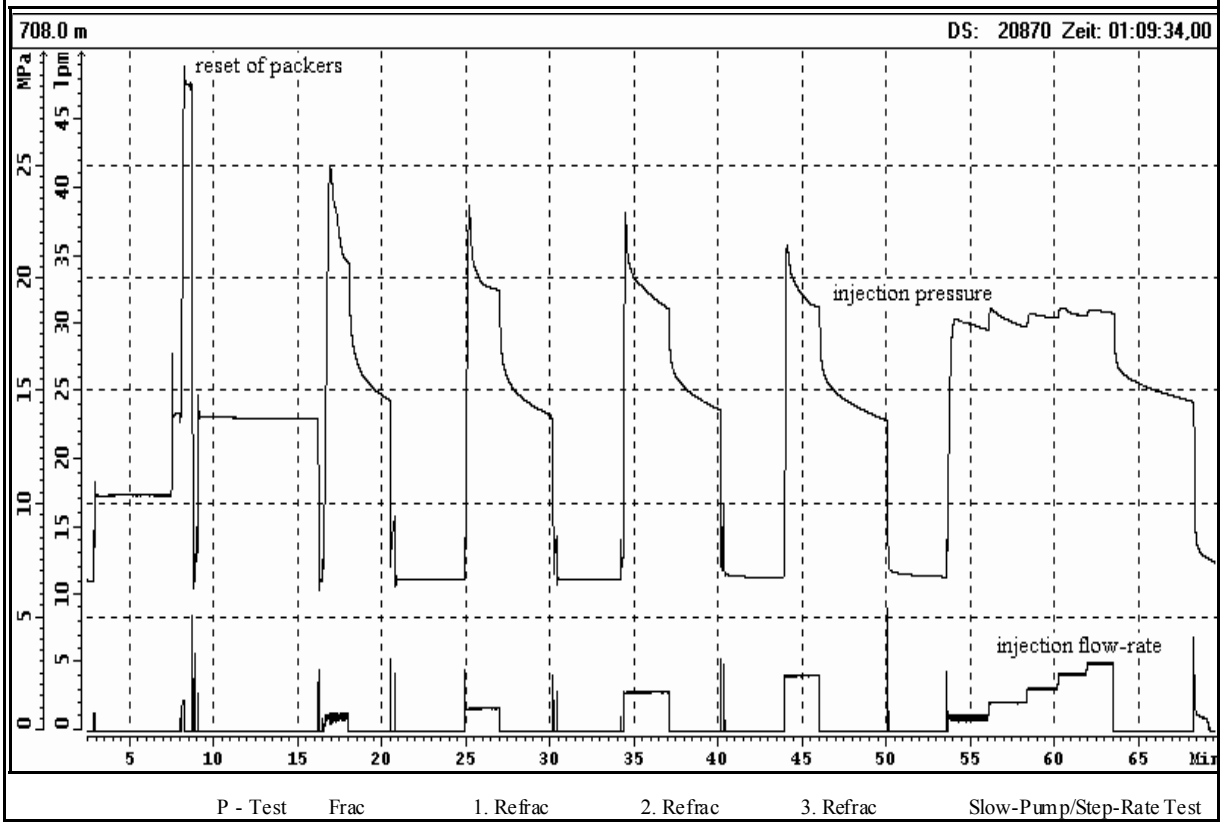

TEST SUMMARY

P - Test :	pressure decrease: 0.1 MPa in 6 min. 58 sec.
Frac - Cycle :	injection-rate Q_i= 1.1 lpm, injected volume V_i = 2.0 l, back-flow volume V_r = 0.1 l clear fracture initiation (breakdown event)
1. Refrac - Cycle :	Q_i = 1.7 lpm, V_i = 3.4 l, V_r = 0.2 l
2. Refrac - Cycle :	Q_i = 2.9 lpm, V_i = 7.7 l, V_r = 0.2 l
3. Refrac - Cycle :	Q_i = 4.1 lpm, V_i = 8.4 l, V_r = 0.2 l
Step-Rate Test :	Q_i = 1.0-5.0 lpm, V_i = 28.2 l, V_r = 1.1 l

total injected volume = 49.7 l, recovered volume = 1.8 l (3.6 %)

Test at 708.0 m MD: Estimation of P_c (Frac - Cycle)

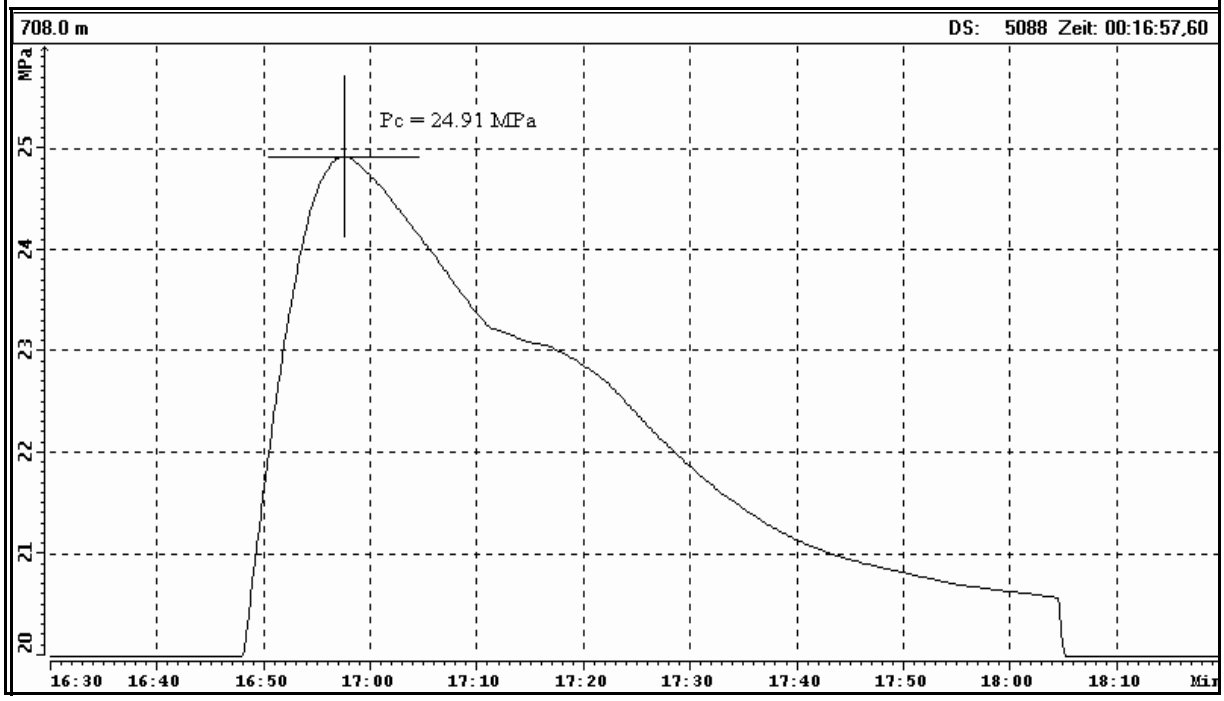

Test at 708.0 m MD: Estimation of P_r (1. Refrac - Cycle)

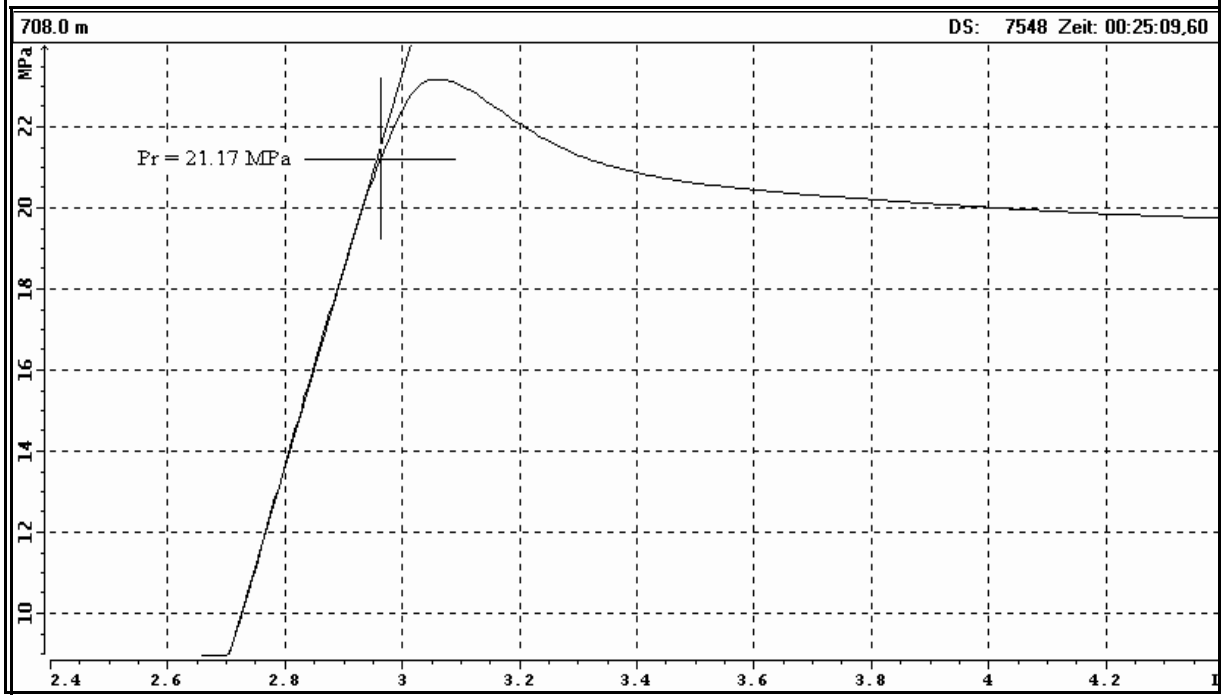

Test at 708.0 m MD: Estimation of $P_{si,\,max}$ (3. Refrac - Cycle)

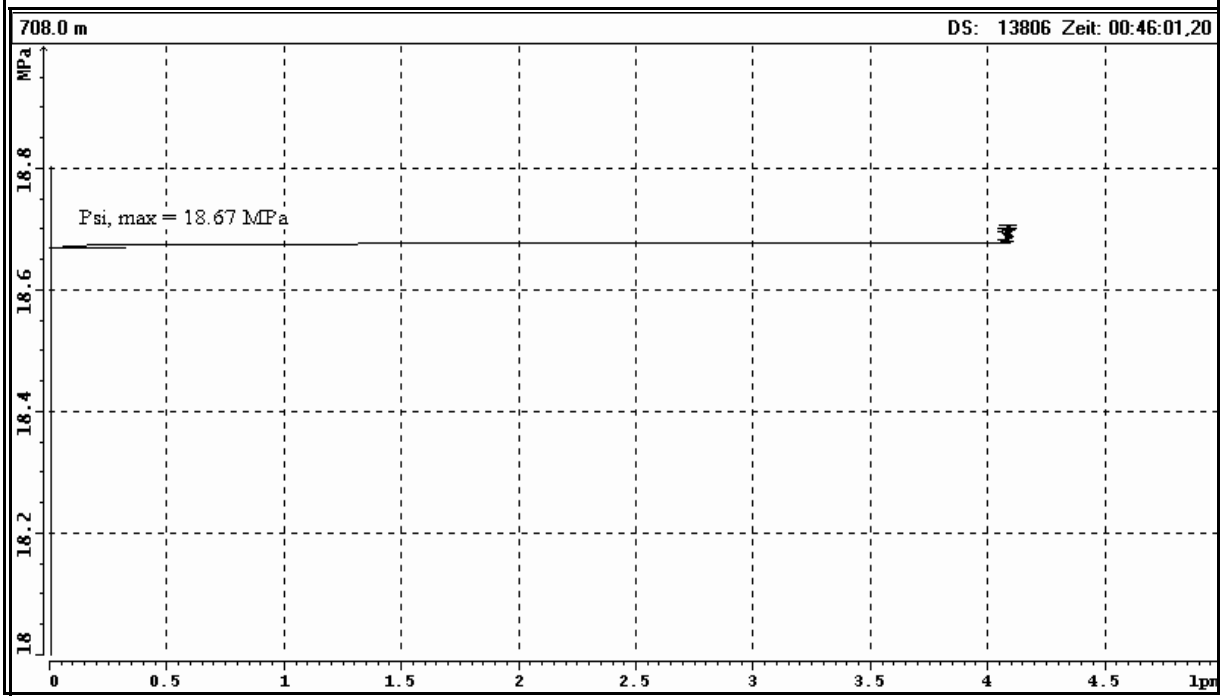

Test at 708.0 m MD: Estimation of $P_{si,\,min}$ (3. Refrac - Cycle)

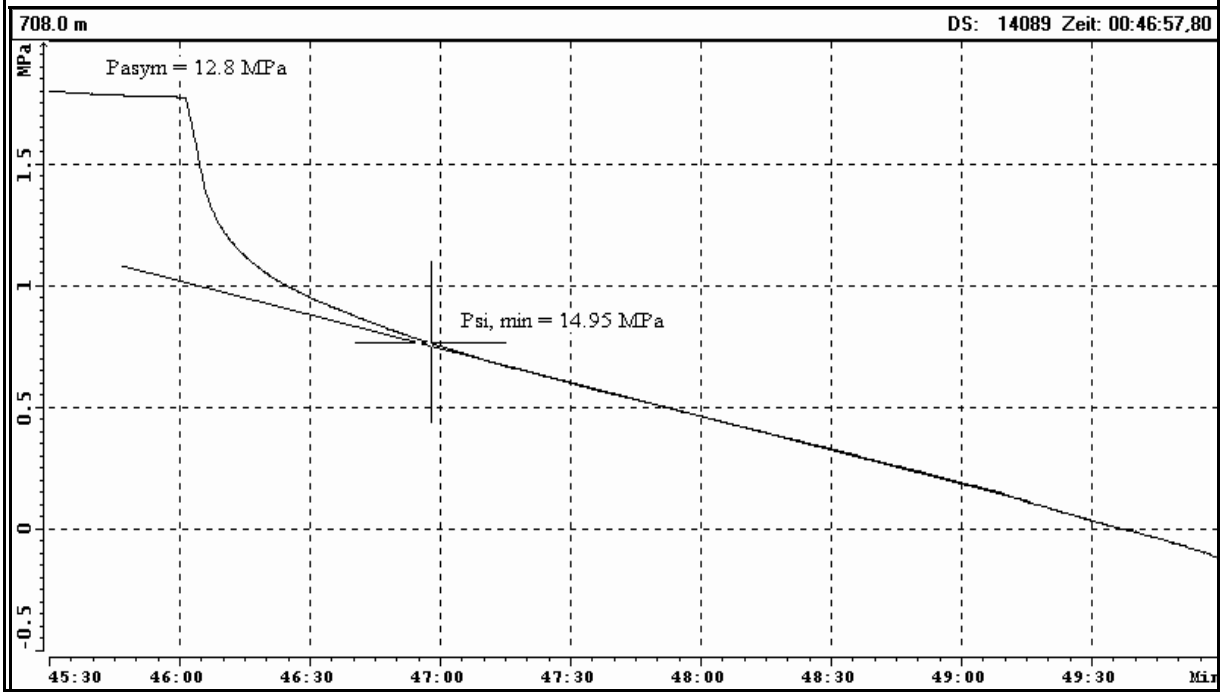

Test at 708.0 m MD: Estimation of P_{si} (3. Refrac - Cycle)

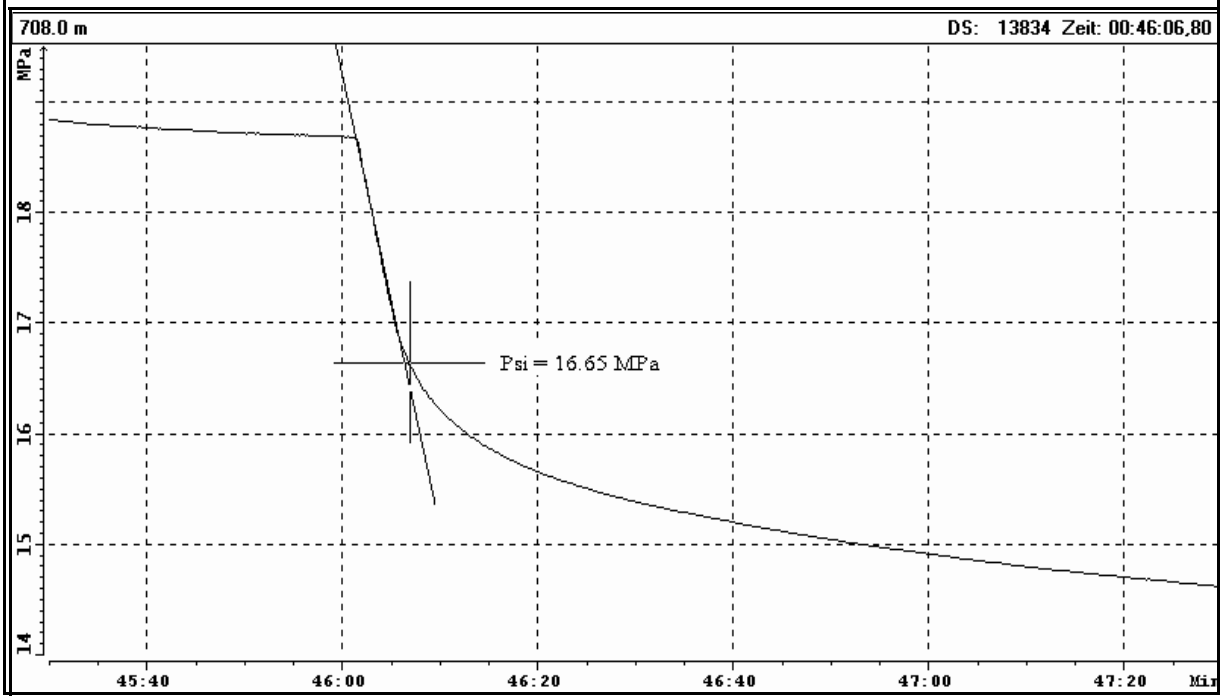

Test at 708.0 m MD: Analysis of Slow - Pump / Step - Rate - Test

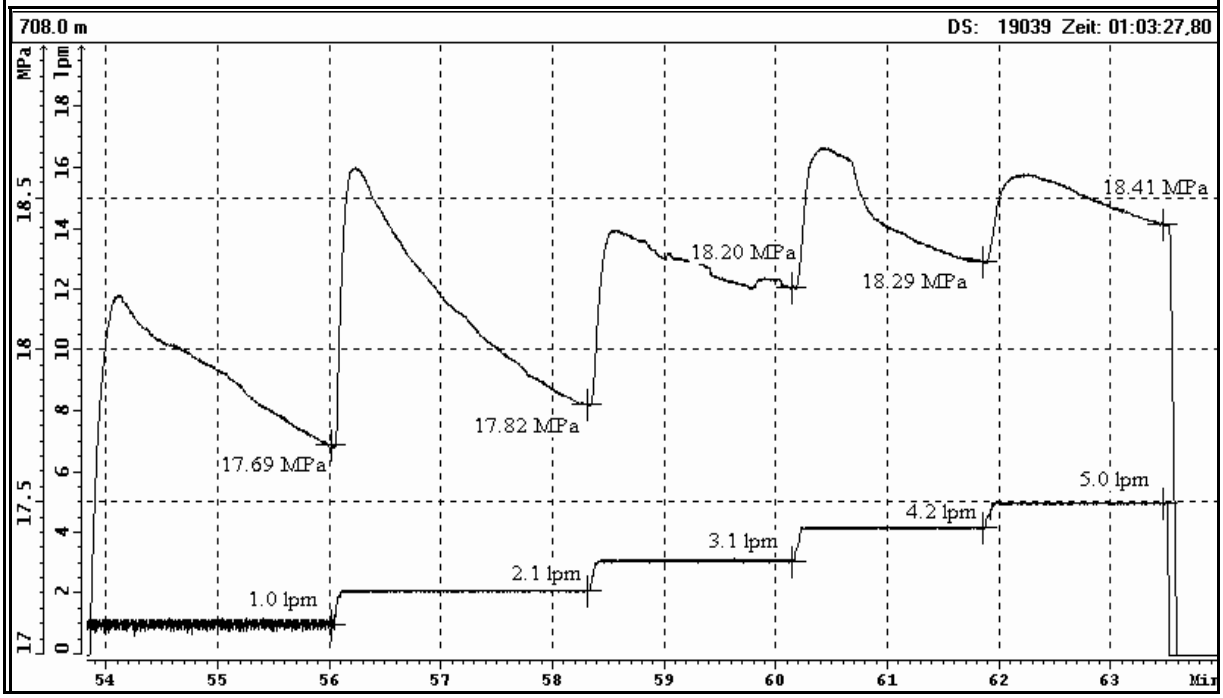

Test at 708.0 m MD: Examination of P_{si} (Step - Rate - Test)

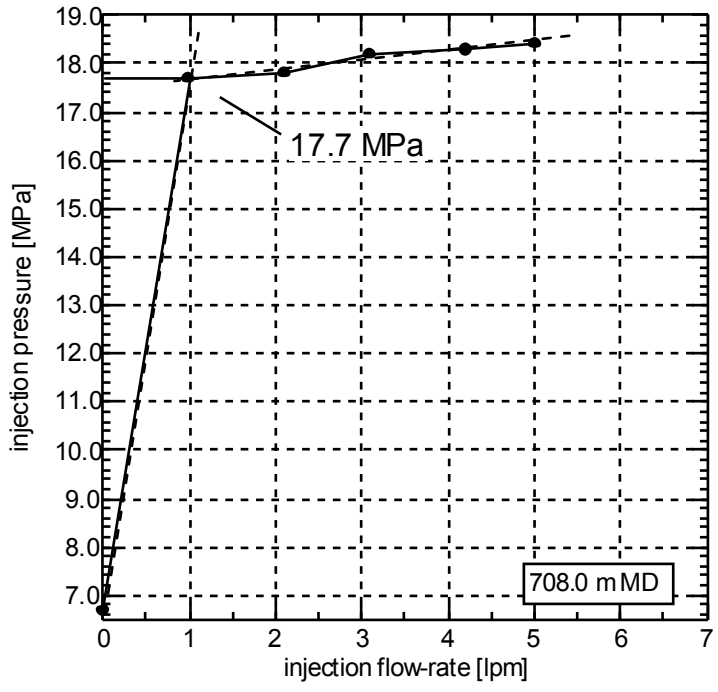

TEST AT 712.8 m MD / 684.4 m TVD

Test at 712.8 m MD : Overview - Plot

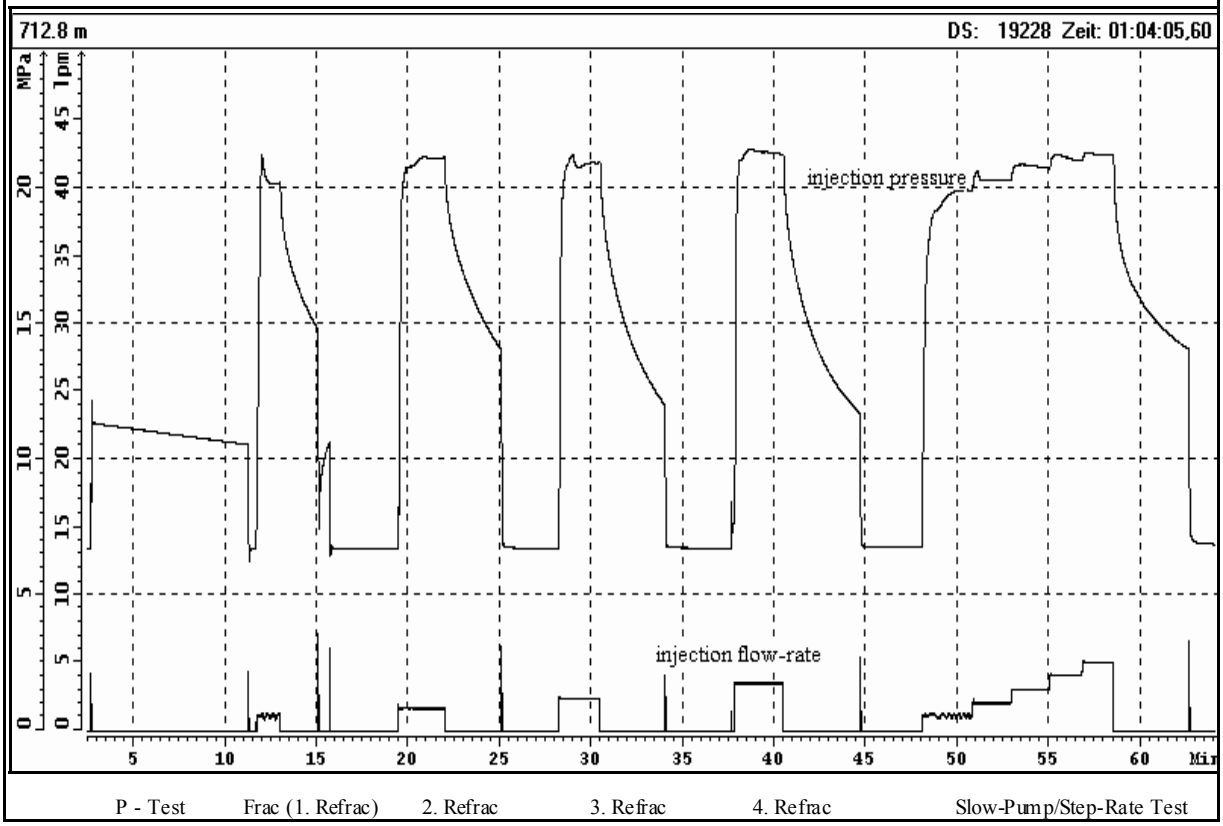

TEST SUMMARY

P - Test :	pressure decrease: 0.8 MPa in 8 min. 24 sec.
Frac (1. Refrac) - Cycle :	injection-rate Q_i= 1.0 lpm, injected volume V_i = 1.5 l, back-flow volume V_r = 0.2 l stimulation of an existing fracture (no breakdown event)
2. Refrac - Cycle :	Q_i = 1.7 lpm, V_i = 4.2 l, V_r = 0.2 l
3. Refrac - Cycle :	Q_i = 2.4 lpm, V_i = 5.4 l, V_r = 0.1 l
4. Refrac - Cycle :	Q_i = 3.5 lpm, V_i = 9.2 l, V_r = 0.1 l
Step-Rate Test :	Q_i = 1.1-5.0 lpm, V_i = 29.9 l, V_r = 0.2 l

total injected volume = 50.2 l, recovered volume = 0.8 l (1.6 %)

Test at 712.8 m MD: Estimation of P_r (Frac (1. Refrac) - Cycle)

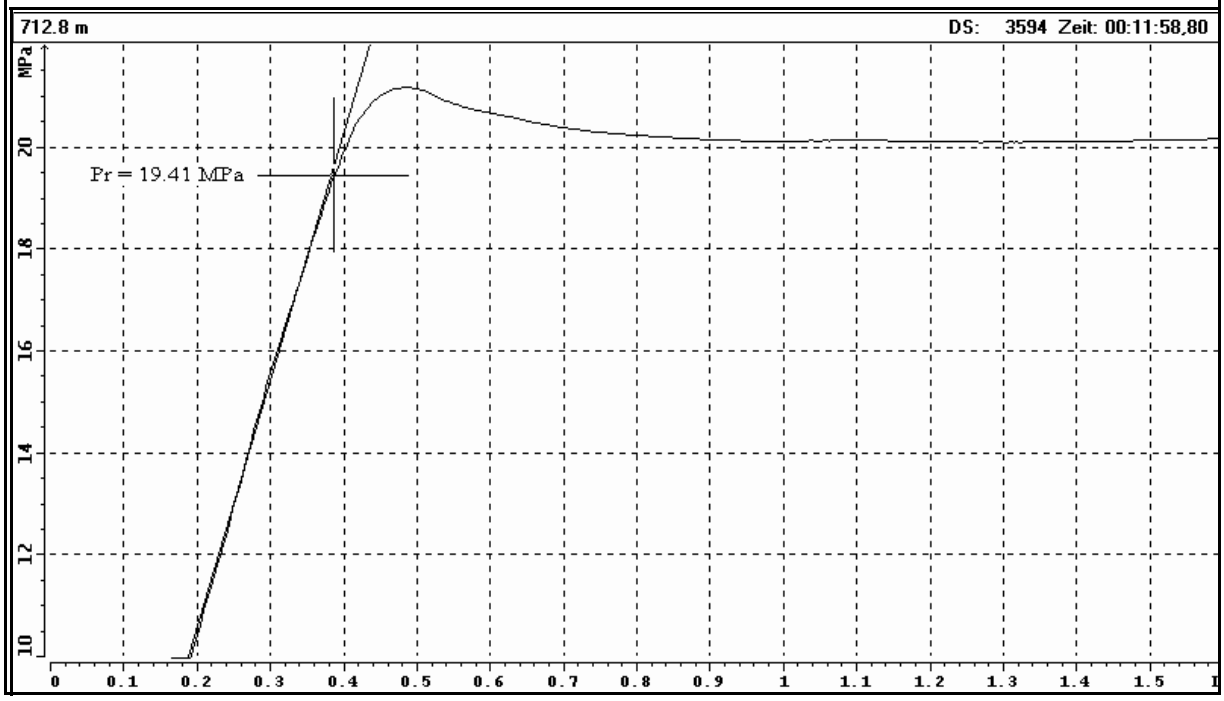

Test at 712.8 m MD: Estimation of P_r (2. Refrac - Cycle, for comparison)

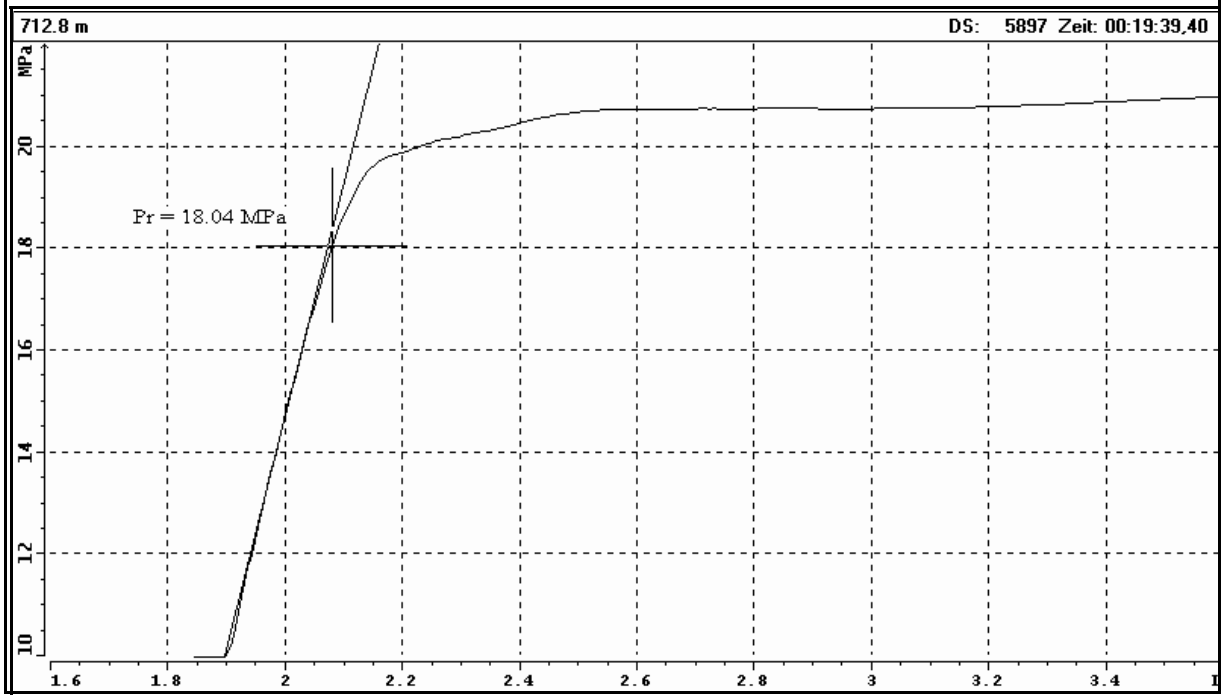

Test at 712.8 m MD: Estimation of $P_{si, max}$ (4. Refrac - Cycle)

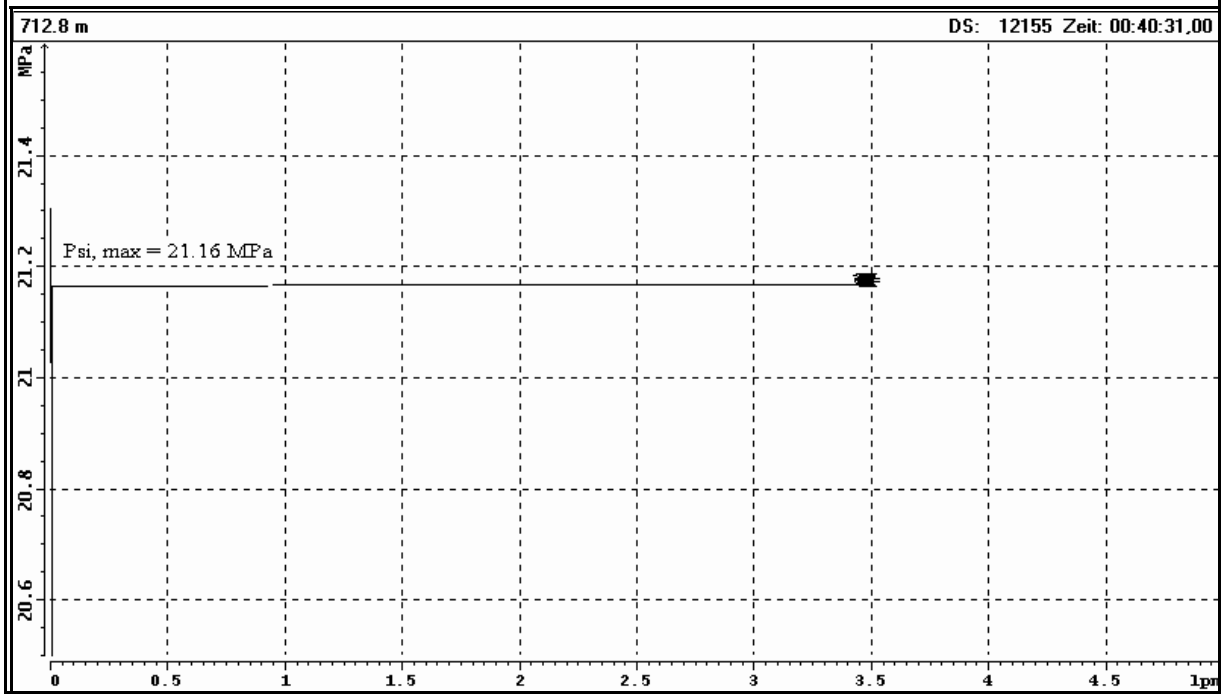

Test at 712.8 m MD: Estimation of $P_{si, min}$ (4. Refrac - Cycle)

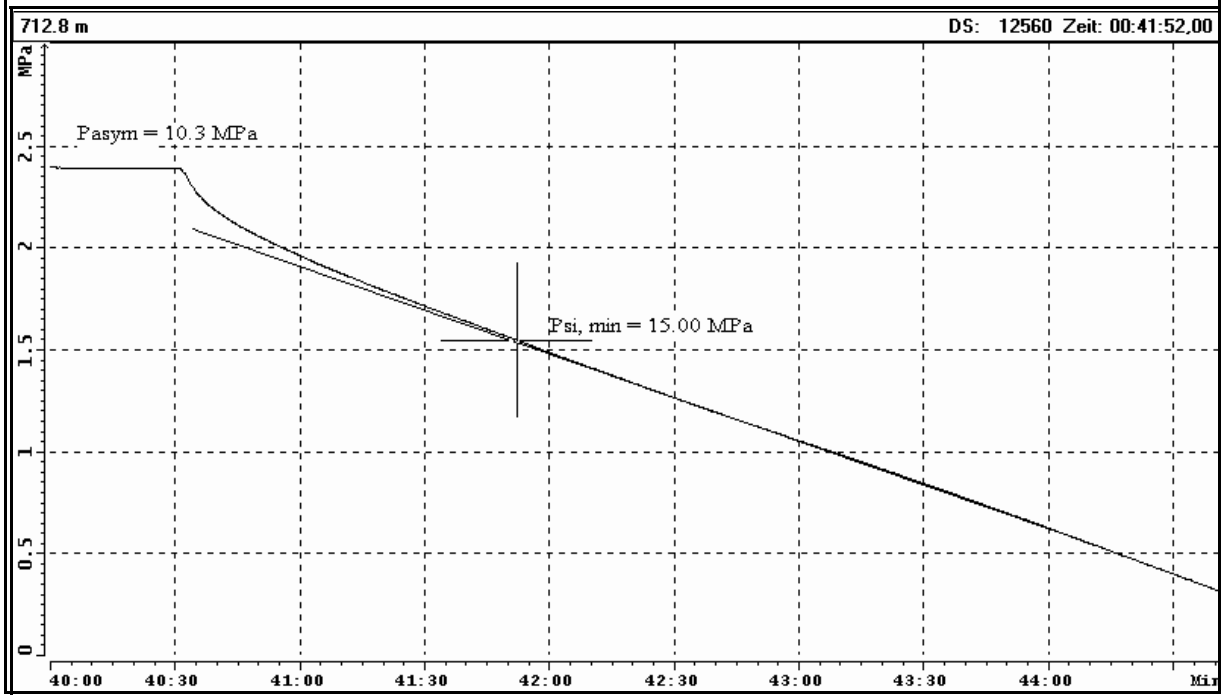

Test at 712.8 m MD: Estimation of P_{si} (4. Refrac - Cycle)

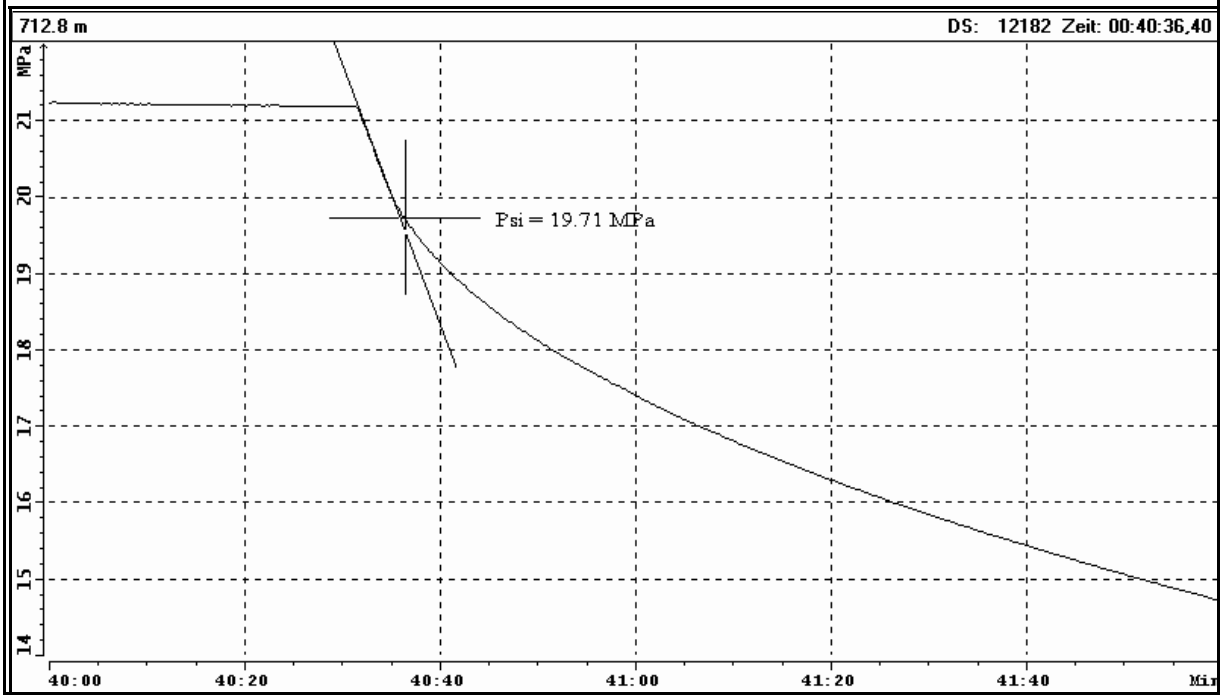

Test at 712.8 MD: Analysis of Slow - Pump / Step - Rate - Test

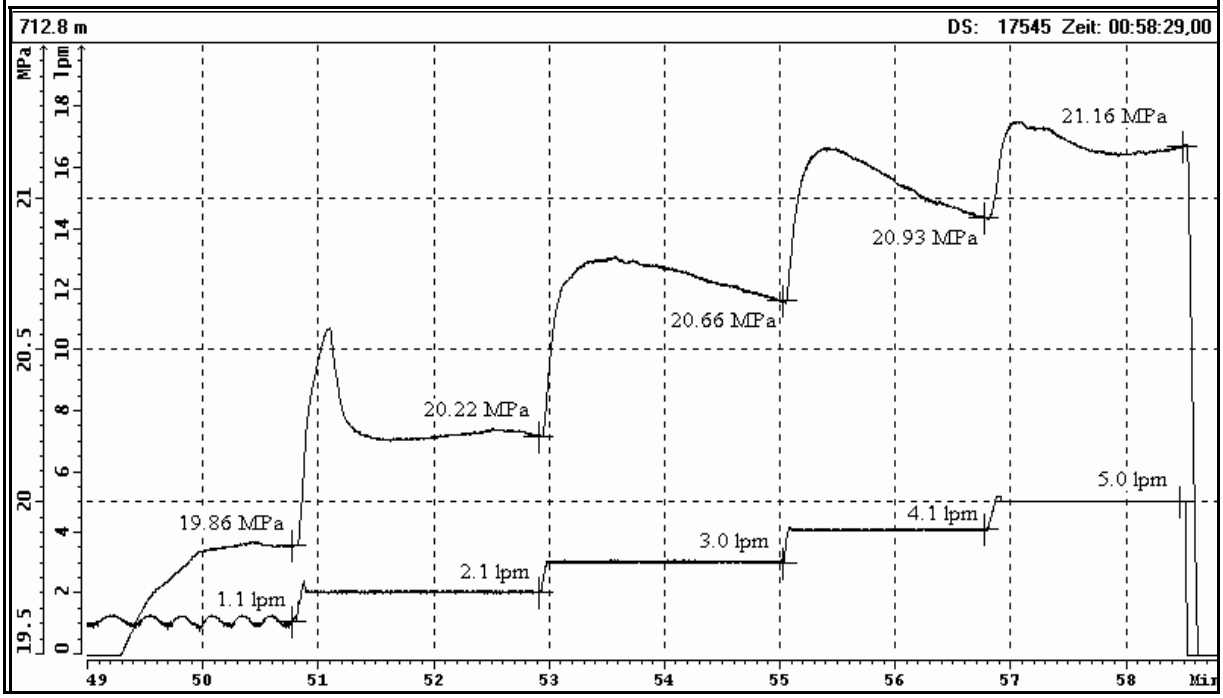

Test at 712.8 MD: Examination of P_{si} (Step - Rate - Test)

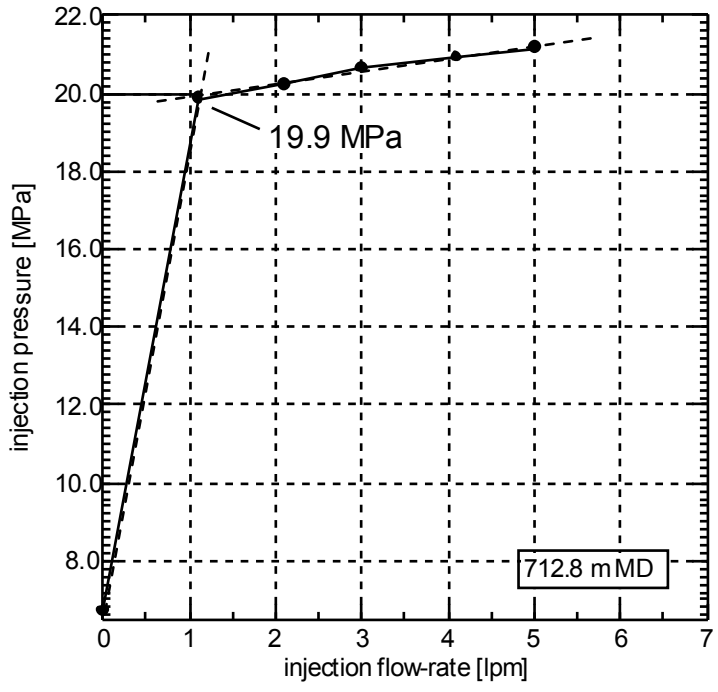

APPENDIX B

Fracture traces on the impression packer sleeve

Test at 296.0 m MD / 280.9 m TVD

borehole dip / direction: 20° / N 206°

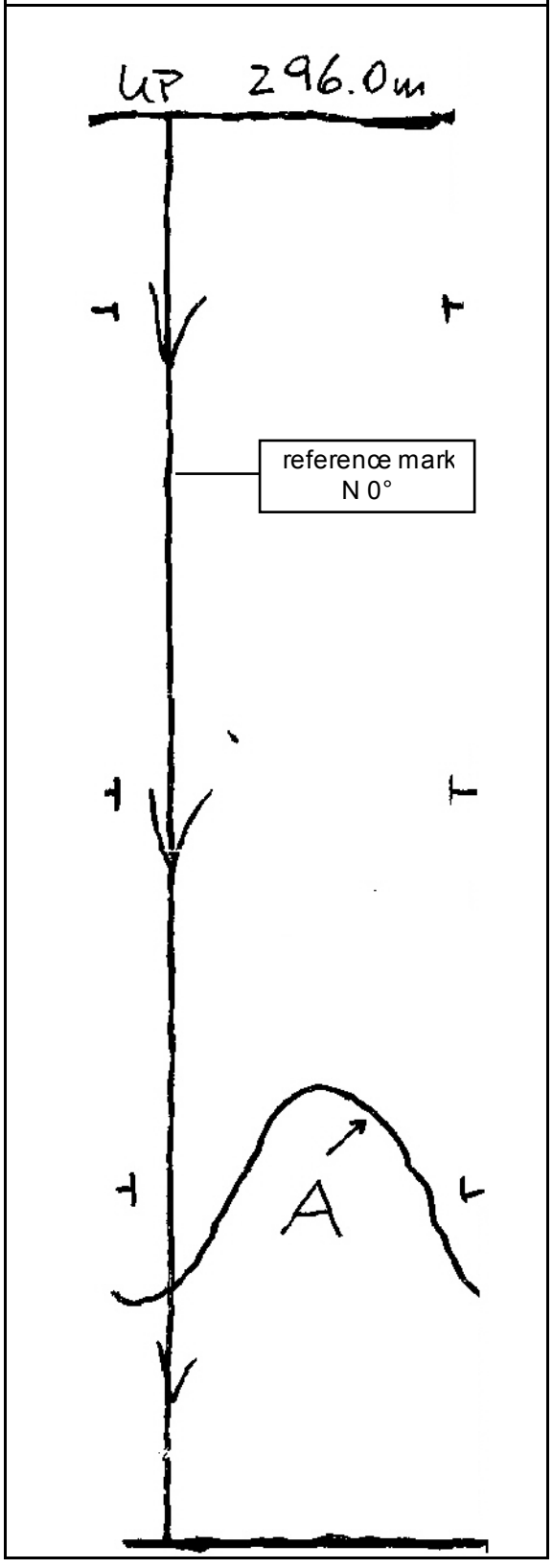

Test at 303.5 m MD / 288.0 m TVD

borehole dip / direction: 21° / N 206°

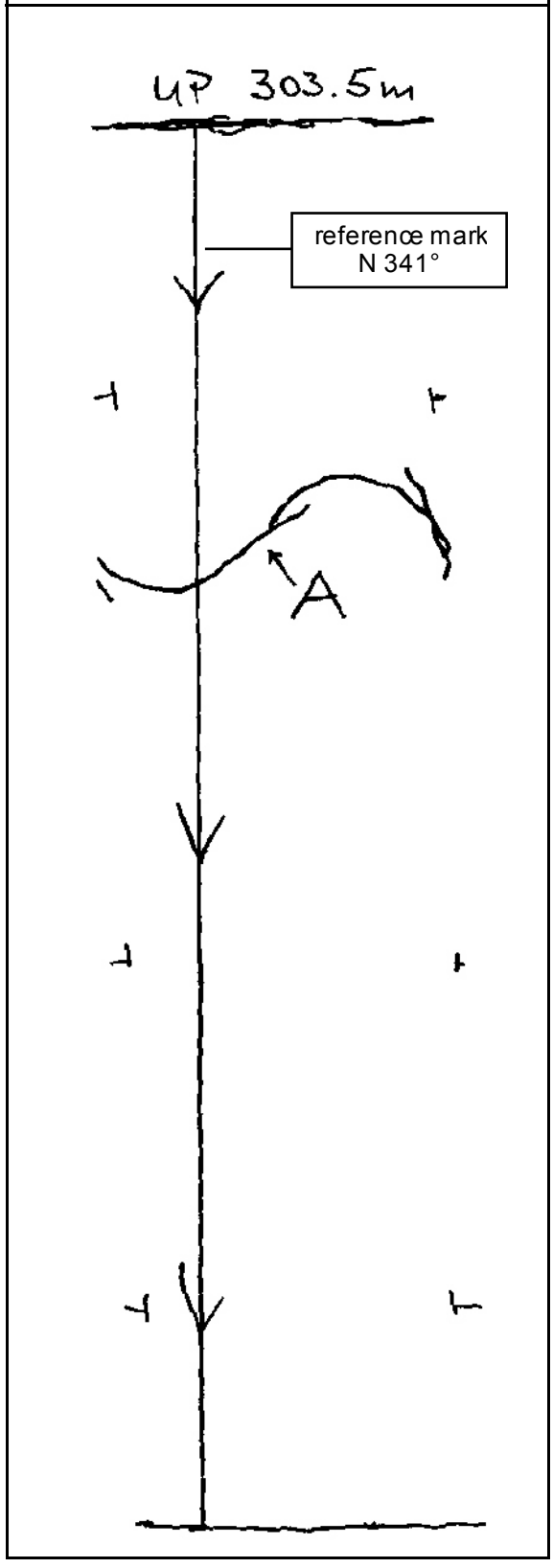

Test at 319.3 m MD / 302.8 m TVD

borehole dip / direction: 21° / N 206°

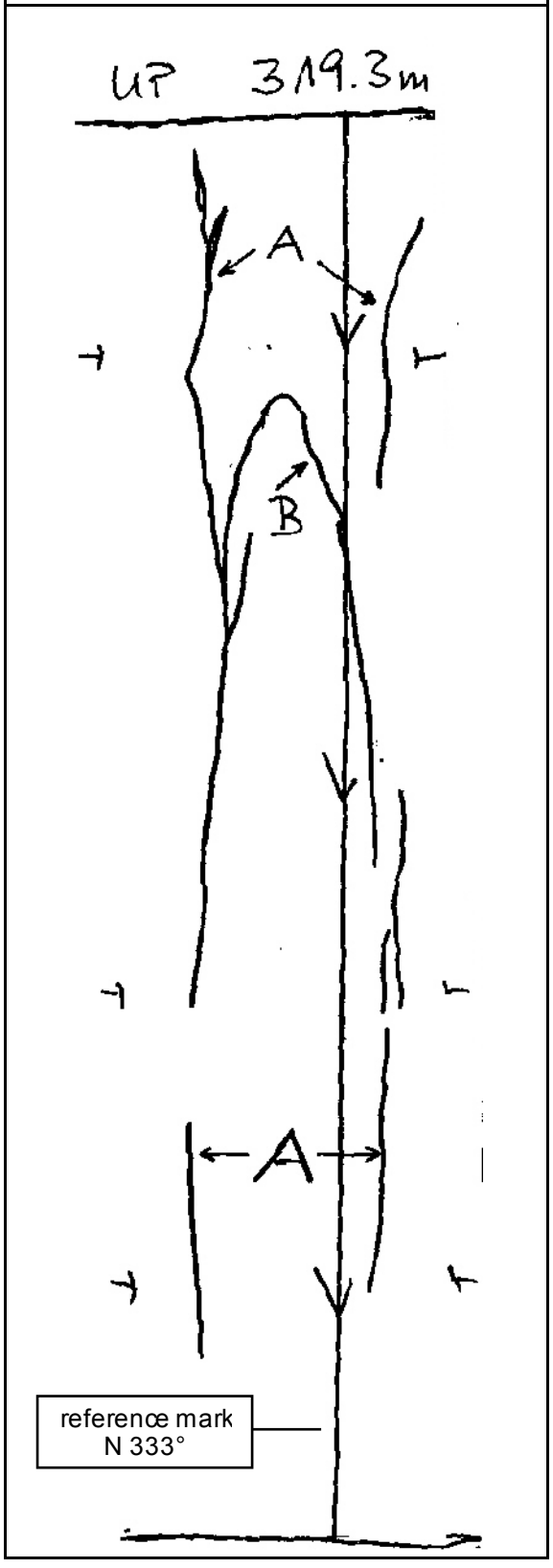

Test at 325.4 m MD / 308.5 m TVD

borehole dip / direction: 21° / N 206°

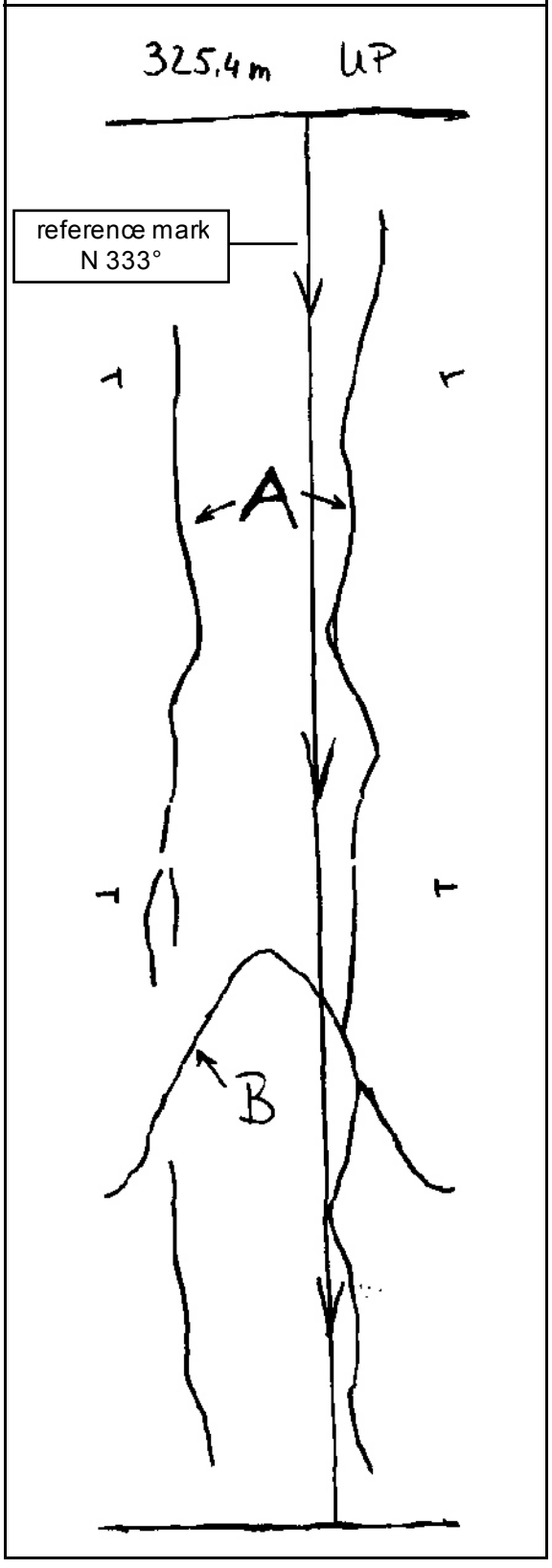

Test at 331.5 m MD / 314.2 m TVD

borehole dip / direction: 21° / N 206°

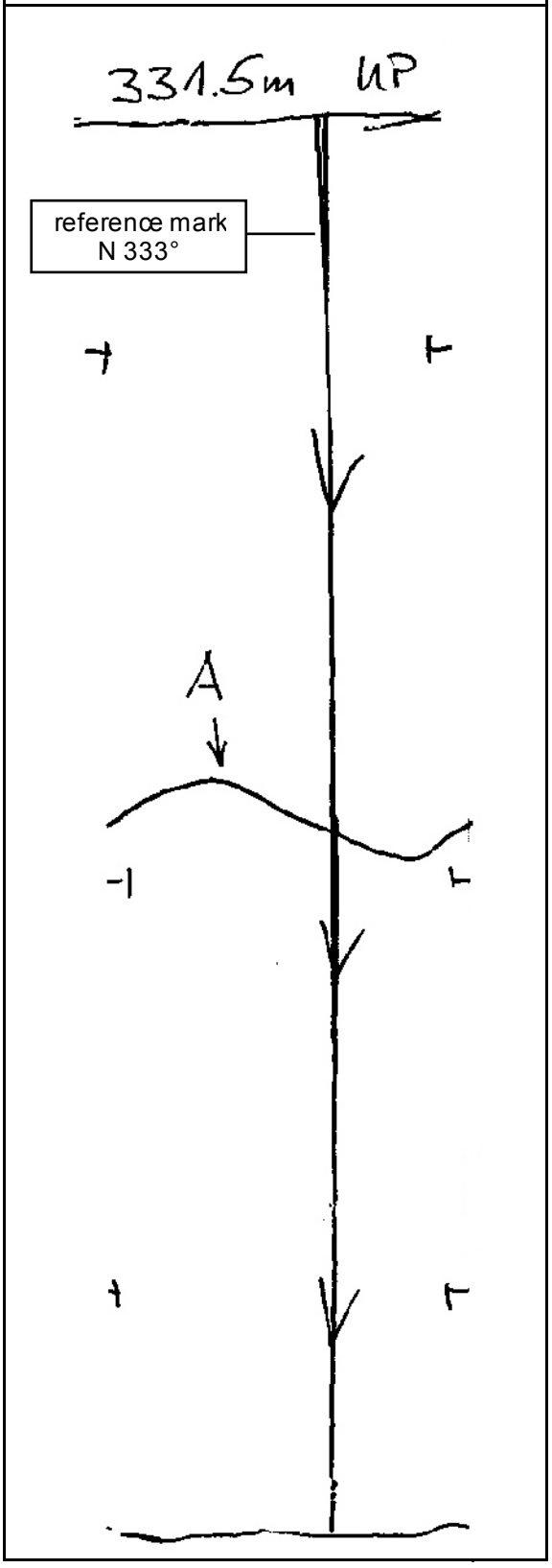

Test at 383.5 m MD / 363.0 m TVD

borehole dip / direction: 20° / N 210°

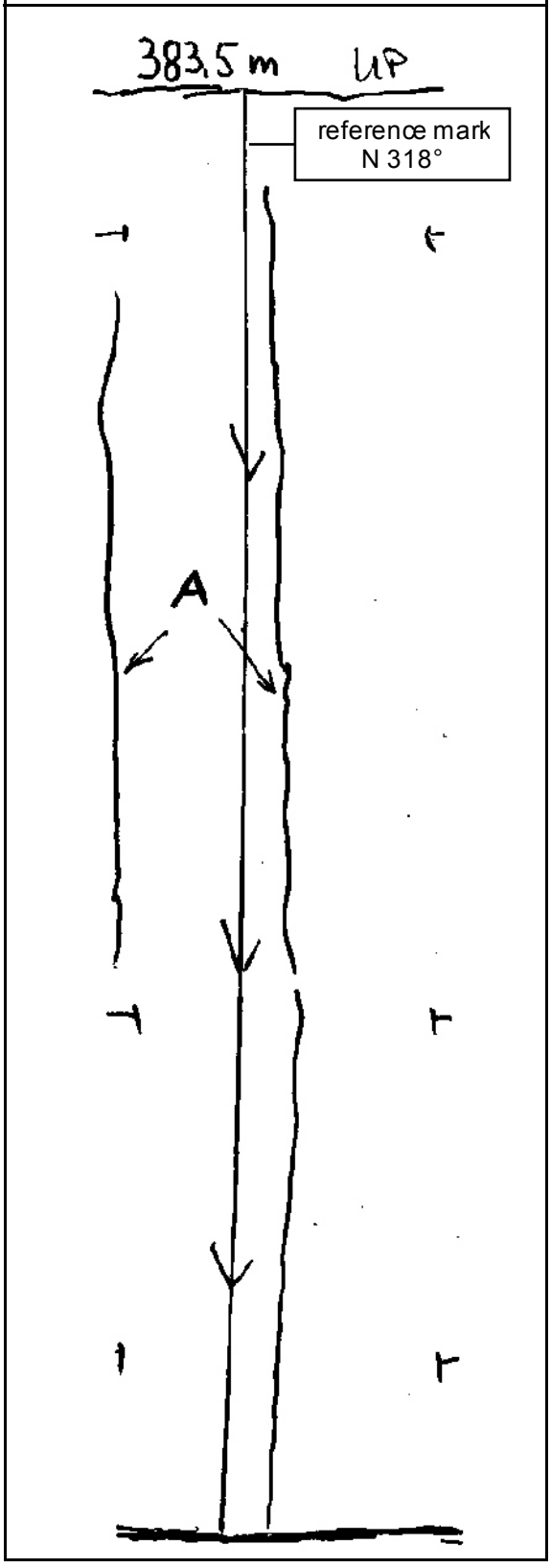

Test at 416.0 m MD / 393.8 m TVD

borehole dip / direction: 17° / N 213°

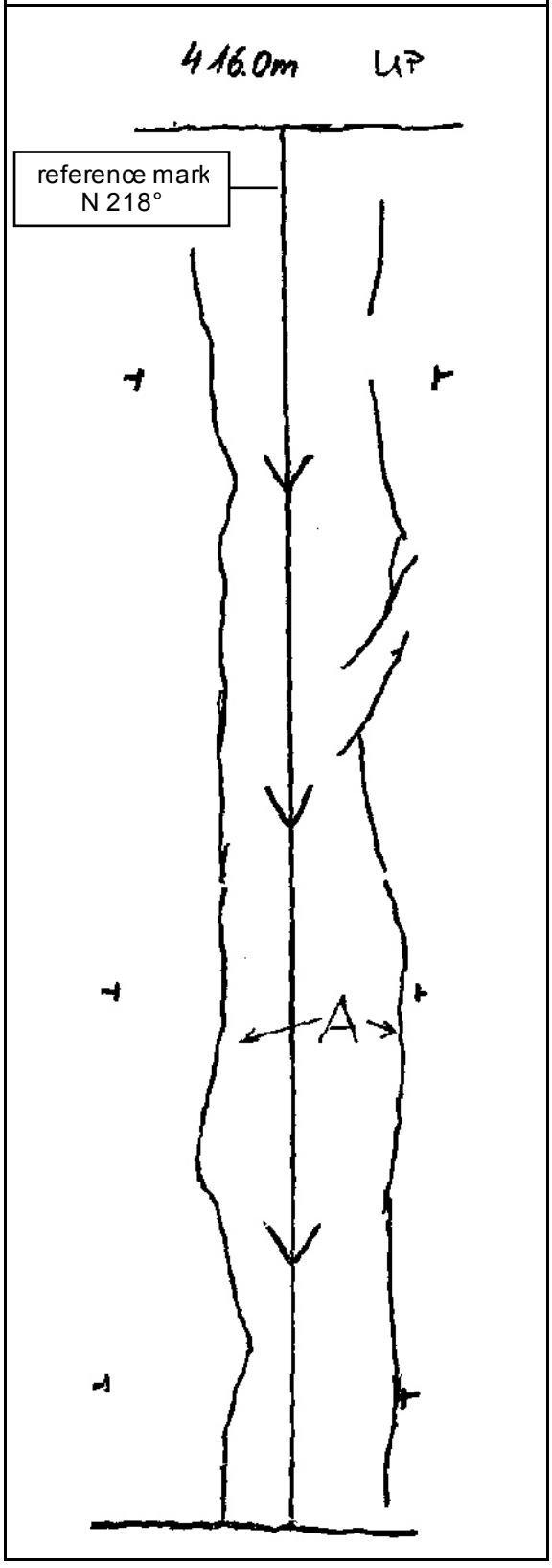

Test at 471.0 m MD / 446.9 m TVD

borehole dip / direction: 14° / N 214°

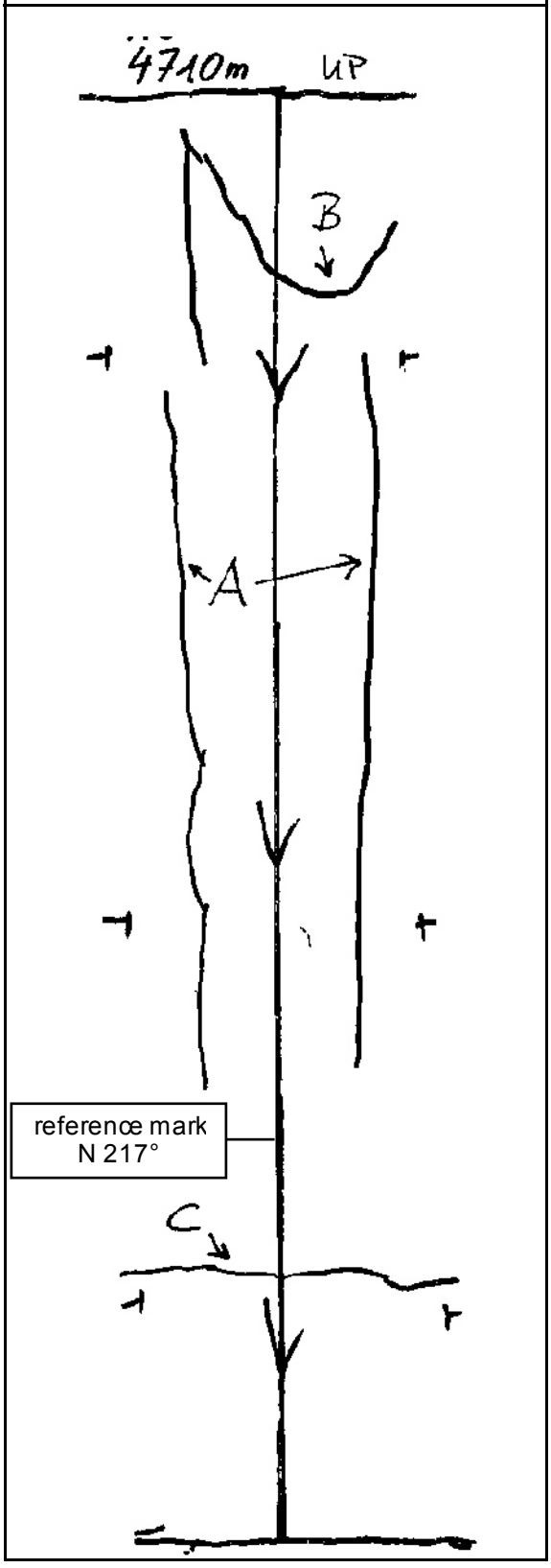

Test at 490.5 m MD / 465.8 m TVD

borehole dip / direction: 14° / N 216°

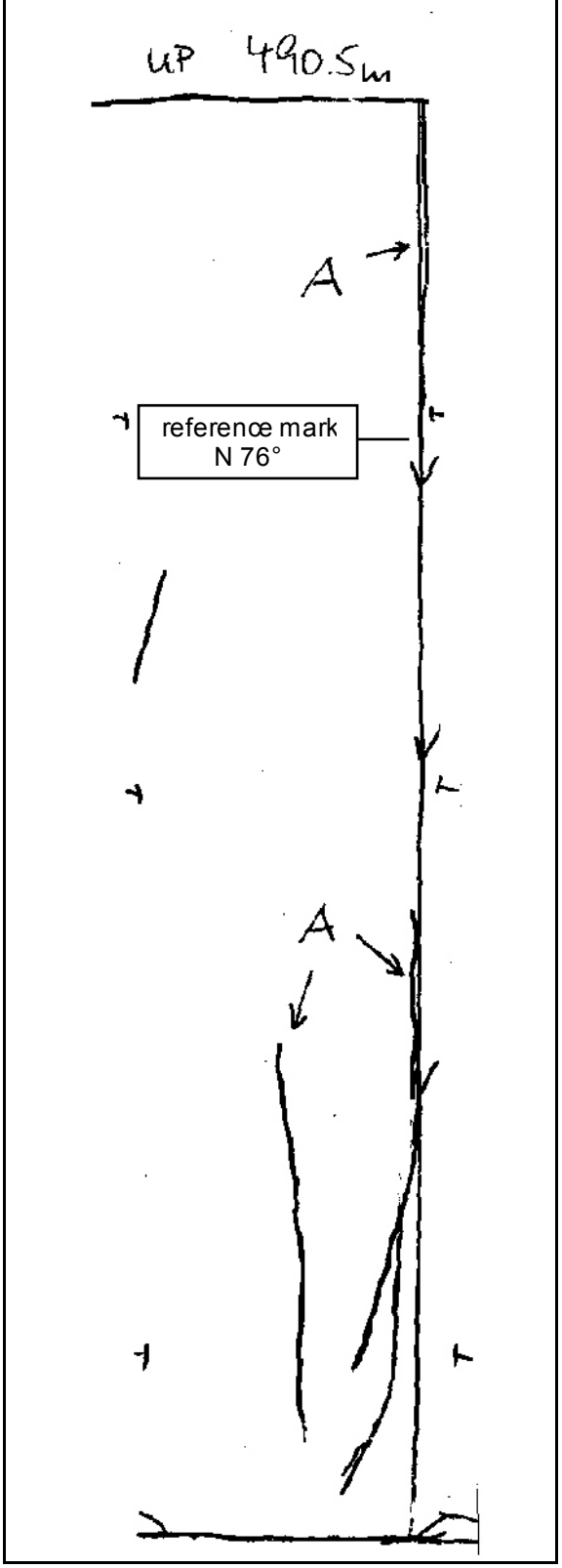

Test at 499.8 m MD / 474.8 m TVD

borehole dip / direction: 13° / N 216°

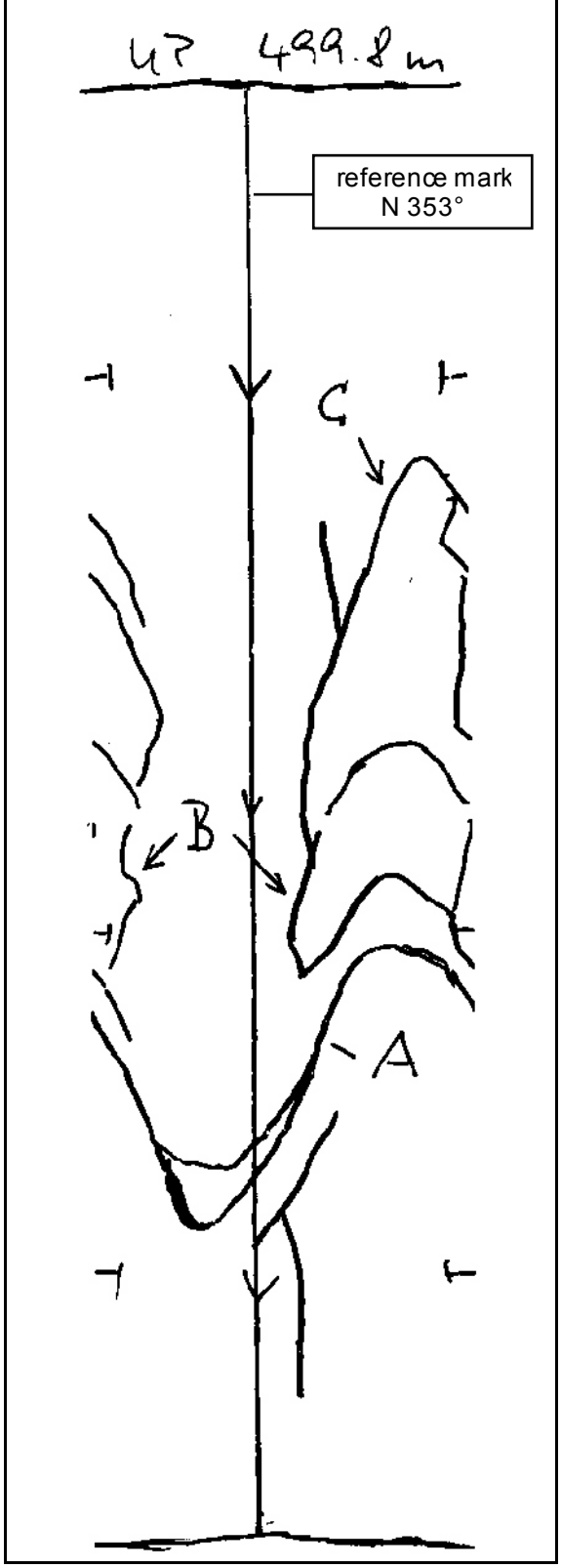

Test at 510.8 m MD / 485.6 m TVD

borehole dip / direction: 13° / N 217°

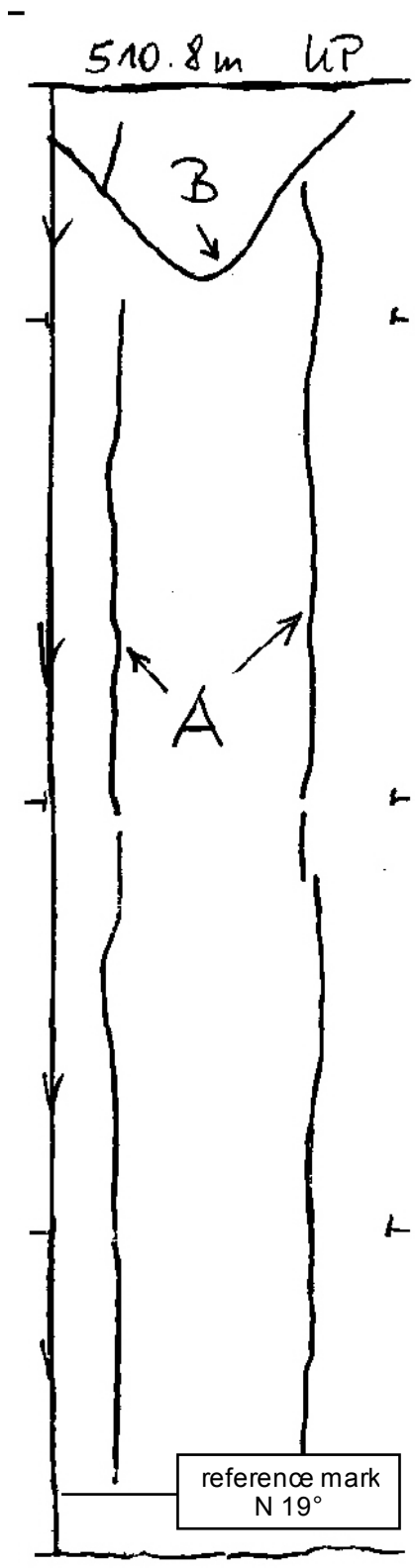

Test at 517.0 m MD / 491.6 m TVD

borehole dip / direction: 13° / N 217°

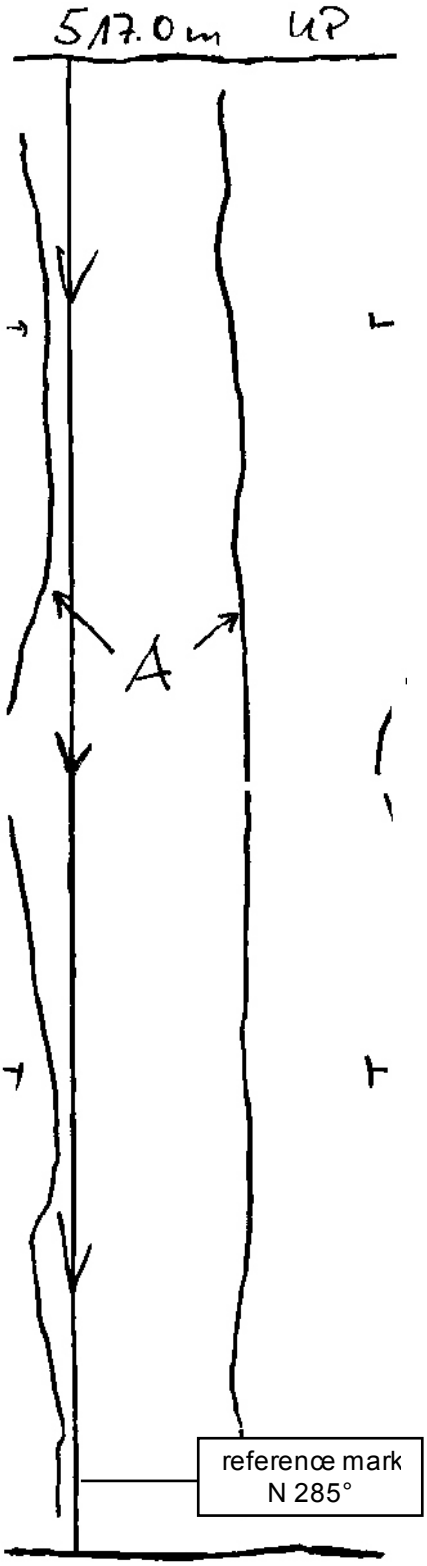

Test at 579.0 m MD / 552.2 m TVD

borehole dip / direction: 11° / N 216°

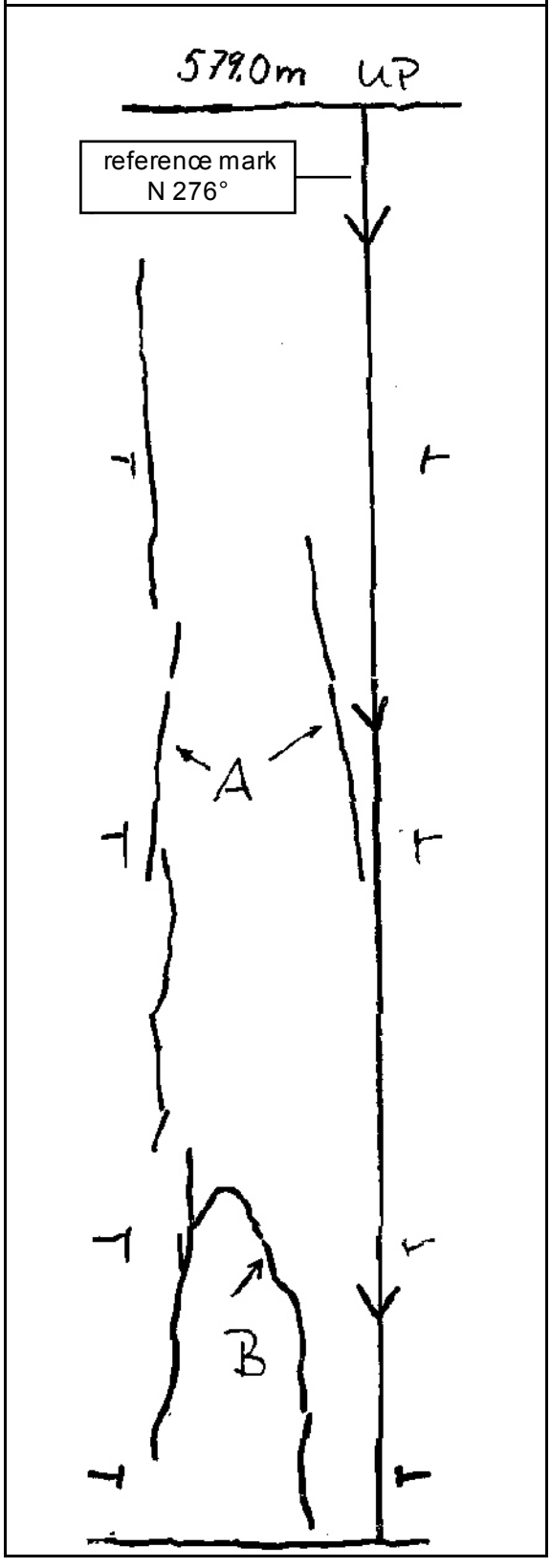

Test at 604.2 m MD / 577.0 m TVD

borehole dip / direction: 10° / N 206°

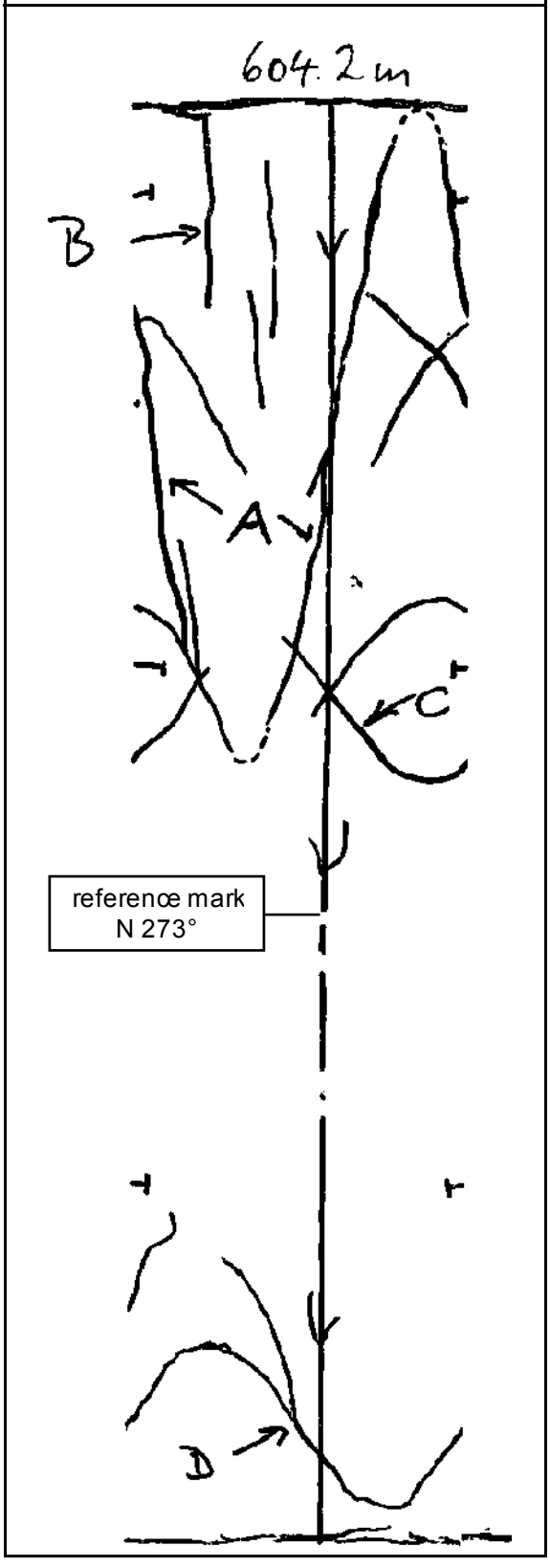

Test at 681.0 m MD / 652.9 m TVD

borehole dip / direction: 8° / N 201°

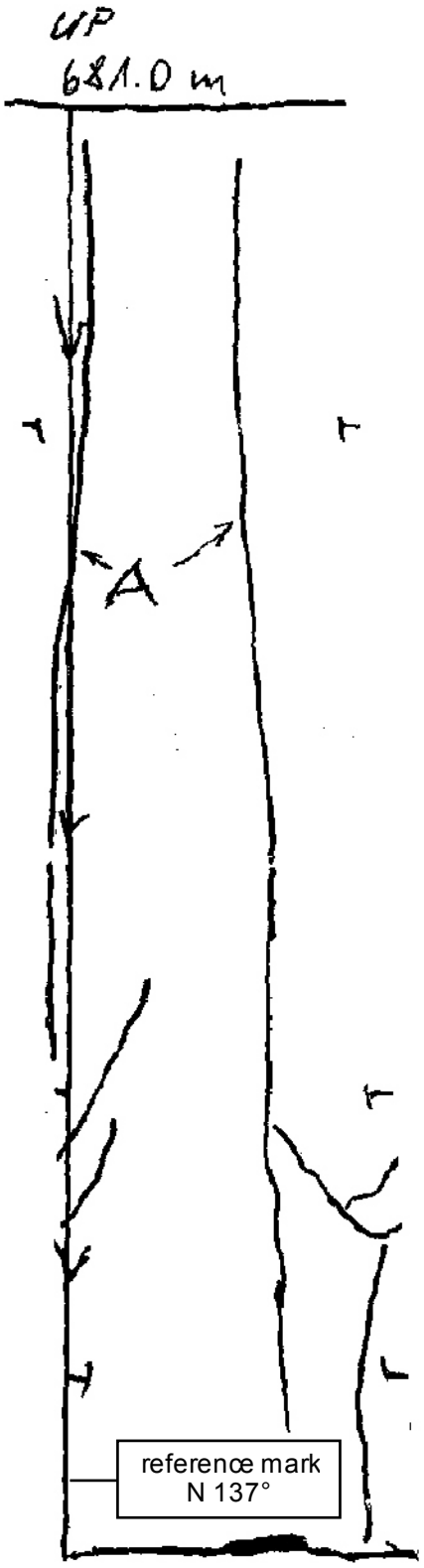

Test at 689.5 m MD / 661.3 m TVD

borehole dip / direction: 8° / N 201°

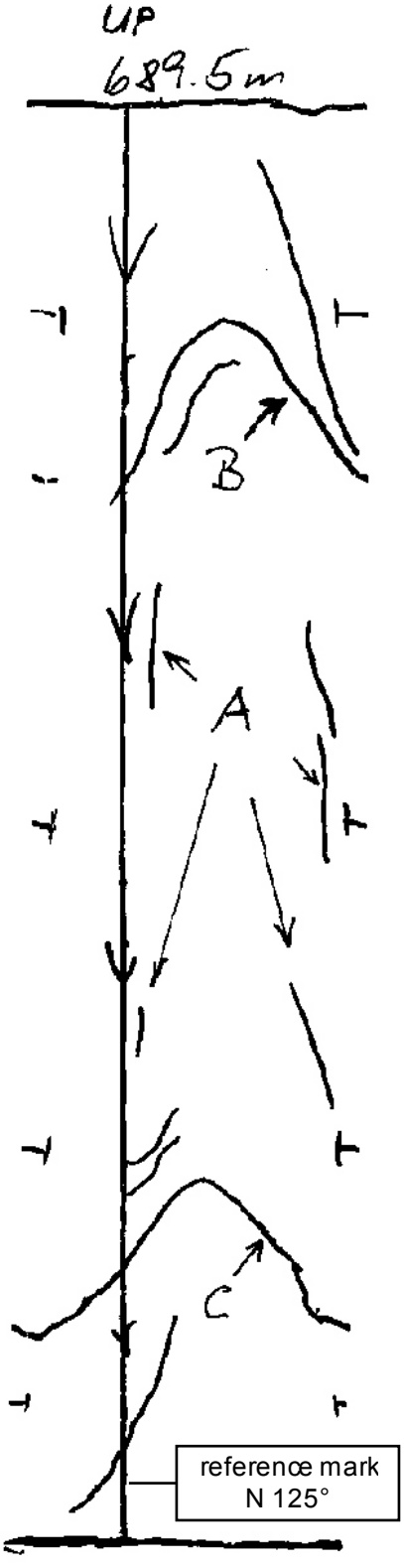

Test at 702.5 m MD / 674.2 m TVD

borehole dip / direction: 8° / N 202°

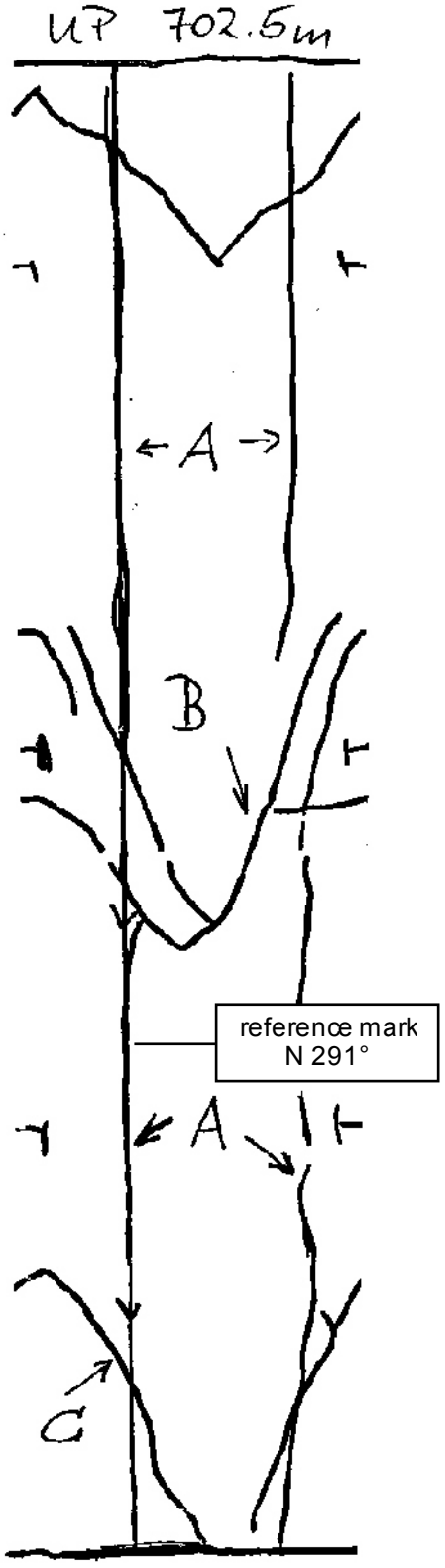

Test at 708.0 m MD / 679.6 m TVD

borehole dip / direction: 8° / N 203°

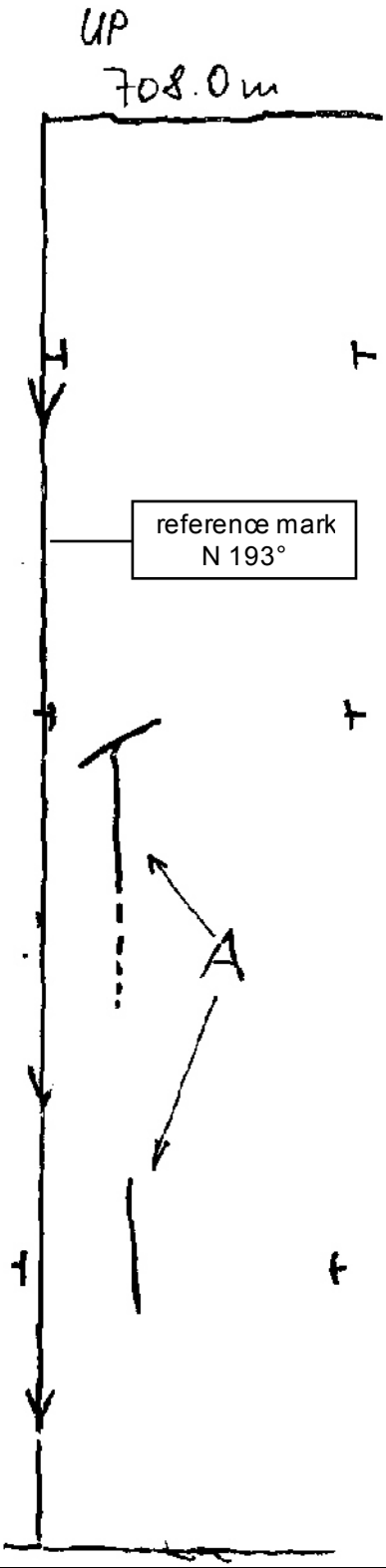

Test at 712.8 m MD / 684.4 m TVD

borehole dip / direction: 8° / N 204°

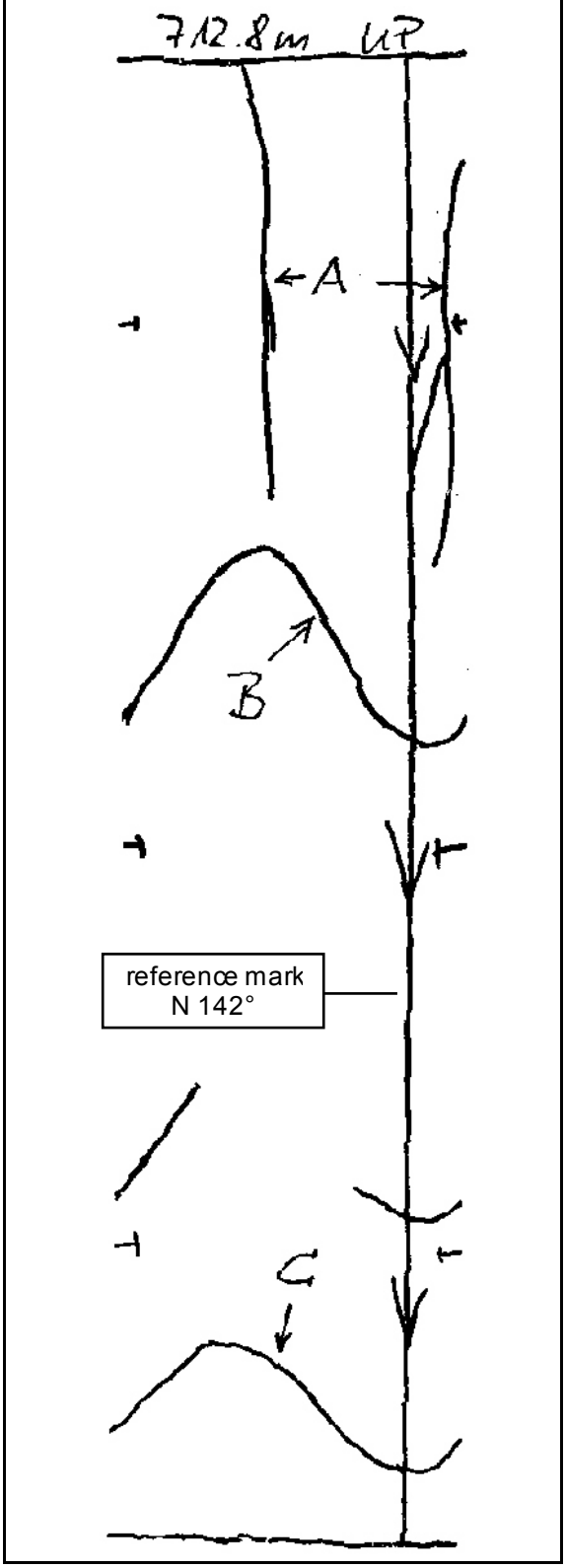

APPENDIX C

Core piece data sheets

Core Piece Data Sheet

Client:	**SKB**	
Project:	**5561**	
Core Container No.:		
SKB Core No.:		
MeSy Core No.:	**1**	
Core unconditioned from container	**date :** **operator :**	
Number of core pieces:	**2**	
Core piece dimensions: **length (min), mm:** **A 300, B 168** **length (max), mm:** **A 328, B 190**	**diameter (min), mm: 47.6** **diameter (max), mm: 47.6**	
Core piece(s) mass, g	**A 1486.5 B 863.7**	
Depth of origin: **Geological Facies:**	**min., m: 333.55** **max., m: 334.03**	

Photo

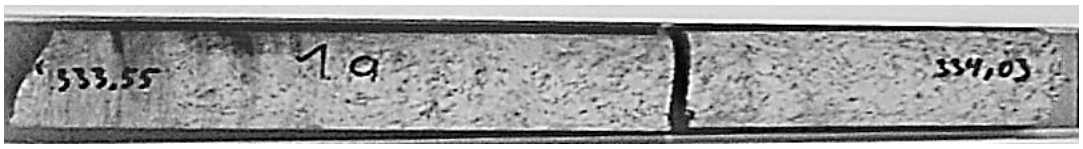

Core Piece Data Sheet

Client:		**SKB**	
Project:		**5561**	
Core Container No.:			
SKB Core No.:			
MeSy Core No.:		**2**	
Core unconditioned from container		**date :** **operator :**	
Number of core pieces:		**1**	
Core piece dimensions:			
length (min), mm:	**390**	**diameter (min), mm:**	**47.4**
length (max), mm:	**402**	**diameter (max), mm:**	**47.4**
Core piece(s) mass, g		**1880.8**	
Depth of origin:		**min., m:**	**382.96**
		max., m:	**383.35**
Geological Facies:			

Photo

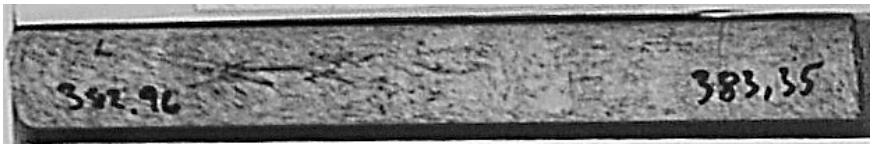

Core Piece Data Sheet

Client:	**SKB**	
Project:	**5561**	
Core Container No.:		
SKB Core No.:		
MeSy Core No.:	**3**	
Core unconditioned from container	**date :** **operator :**	
Number of core pieces:	**3**	
Core piece dimensions: **length (min), mm:** **A 140, B 145, C 105** **length (max), mm:** **A 150, B 165, C 120**	**diameter (min), mm: 47.4** **diameter (max), mm: 47.4**	
Core piece(s) mass, g	**A 689.5, B 729.2, C 539.2**	
Depth of origin: **Geological Facies:**	**min., m: 438.12** **max., m: 438.53**	

Photo

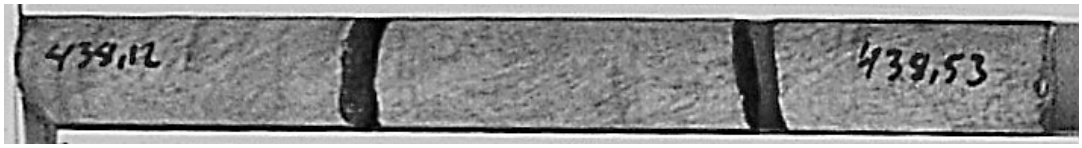

Core Piece Data Sheet

Client:	**SKB**	
Project:	**5561**	
Core Container No.:		
SKB Core No.:		
MeSy Core No.:	**4**	
Core unconditioned from container	**date :** **operator :**	
Number of core pieces:	**3**	
Core piece dimensions: **length (min), mm:** **A 160, B 175, C 140** **length (max), mm:** **A 175, B 202, C 180**	**diameter (min), mm: 47.4** **diameter (max), mm: 47.4**	
Core piece(s) mass, g	**A 786.7, B 907.6, C 775.5**	
Depth of origin: **Geological Facies:**	**min., m: 463.60** **max., m: 464.10**	

Photo

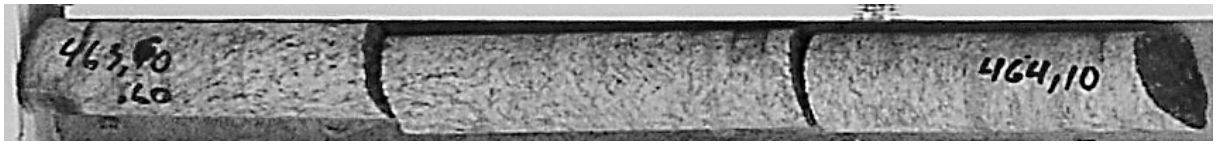

Core Piece Data Sheet

Client:		**SKB**	
Project:		**5561**	
Core Container No.:			
SKB Core No.:			
MeSy Core No.:		**5**	
Core unconditioned from container		**date :** **operator :**	
Number of core pieces:		**1**	
Core piece dimensions:			
length (min), mm:	**390**	**diameter (min), mm:**	**51.7**
length (max), mm:	**425**	**diameter (max), mm:**	**51.7**
Core piece(s) mass, g		**2294.9**	
Depth of origin:		**min., m:**	**500.20**
		max., m:	**500.60**
Geological Facies:			

Photo

Core Piece Data Sheet

Client:		**SKB**	
Project:		**5561**	
Core Container No.:			
SKB Core No.:			
MeSy Core No.:		**6**	
Core unconditioned from container		**date :** **operator :**	
Number of core pieces:		**1**	
Core piece dimensions:			
length (min), mm:	**400**	**diameter (min), mm:**	**47.2**
length (max), mm:	**420**	**diameter (max), mm:**	**47.2**
Core piece(s) mass, g		**1961.4**	
Depth of origin:		**min., m:**	**559.70**
		max., m:	**560.10**
Geological Facies:			

Photo

Core Piece Data Sheet

Client:		**SKB**	
Project:		**5561**	
Core Container No.:			
SKB Core No.:			
MeSy Core No.:		**7**	
Core unconditioned from container		**date :** **operator :**	
Number of core pieces:		**1**	
Core piece dimensions:			
length (min), mm:	**390**	**diameter (min), mm:**	**47.2**
length (max), mm:	**395**	**diameter (max), mm:**	**47.2**
Core piece(s) mass, g		**1837.3**	
Depth of origin:		**min., m:**	**595.46**
		max., m:	**596.85**
Geological Facies:			

Photo

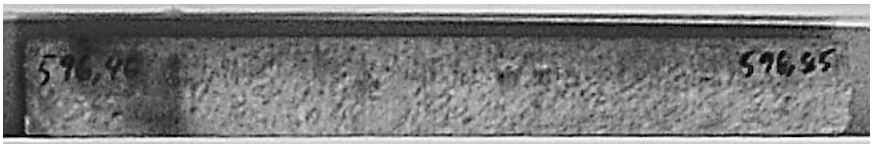

Core Piece Data Sheet

Client:	**SKB**	
Project:	**5561**	
Core Container No.:		
SKB Core No.:		
MeSy Core No.:	**8**	
Core unconditioned from container	**date :** **operator :**	
Number of core pieces:	**2**	
Core piece dimensions: **length (min), mm:** **A 75, B 305** **length (max), mm:** **A 98, B 350**	**diameter (min), mm: 47.2** **diameter (max), mm: 47.2**	
Core piece(s) mass, g	**A 404.7, B 1568.6**	
Depth of origin: **Geological Facies:**	**min., m: 648.68** **max., m: 649.10**	

Photo

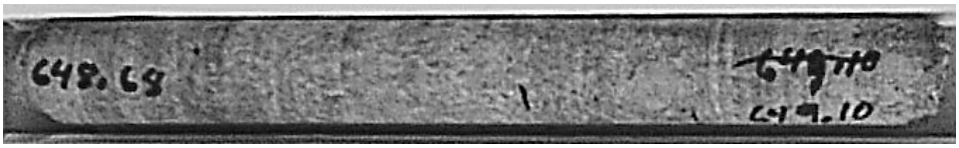

Core Piece Data Sheet

Client:	**SKB**	
Project:	**5561**	
Core Container No.:		
SKB Core No.:		
MeSy Core No.:	**9**	
Core unconditioned from container	**date :** **operator :**	
Number of core pieces:	**2**	
Core piece dimensions: **length (min), mm:** **A 255, B 55** **length (max), mm:** **A 380, B 120**	**diameter (min), mm: 51.9** **diameter (max), mm: 51.9**	
Core piece(s) mass, g	**A 1817.8, B 504.5**	
Depth of origin: **Geological Facies:**	**min., m: 692.58** **max., m: 692.98**	

Photo

Core Piece Data Sheet

Client:	**SKB**	
Project:	**5561**	
Core Container No.:		
SKB Core No.:		
MeSy Core No.:	**10**	
Core unconditioned from container	**date :** **operator :**	
Number of core pieces:	**2**	
Core piece dimensions: **length (min), mm:** **A 204, B 105** **length (max), mm:** **A 308, B 240**	**diameter (min), mm: 51.9** **diameter (max), mm: 51.9**	
Core piece(s) mass, g	**A 1461.3, B 1042.7**	
Depth of origin: **Geological Facies:**	**min., m: 709.33** **max., m: 709.77**	

Photo

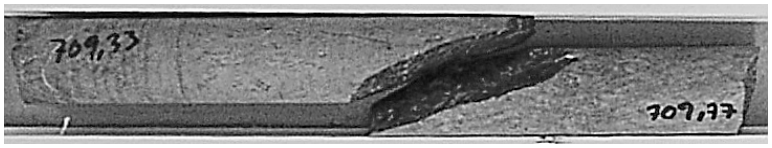

APPENDIX D

Rock density data sheets

MeSy core-no./ sample-no	depth m	weight in air g	weight in water g	density ρ g/cm3
1A1	333.79	465.7	293.2	2.700
1A2		547.3	343.9	2.691
1A2a				2.710
1A2b				2.690
1A3		473.5	297.6	2.692
1B1		438.6	276.9	2.712
1B2		425.1	270.0	2.741
mean				**2.705±.018**
2A1	383.16	452.6	285.0	2.700
2A2		960.8	605.4	2.703
2A3		467.4	294.8	2.708
2A3a				2.703
2A3b				2.635
mean				**2.690±.031**
3A	438.33	689.5	434.5	2.704
3B		729.2	457.8	2.687
3C		539.2	337.6	2.675
3Ca				2.669
3Cb				2.667
mean				**2.680±.015**
4A1	463.85	442.1	278.5	2.702
4A2		344.6	217.4	2.709
4B1		475.9	299.8	2.702
4B1a				2.701
4B1b				2.691
4B2		431.7	271.1	2.688
4C		775.5	488.9	2.706
mean				**2.700±.008**
5A1	500.40	642.2	405.0	2.707
5A1a				2.683
5A1b				2.700
5A2		1068.1	671.2	2.691
5A3		584.6	367.0	2.687
mean				**2.694±.010**
6A1	559.90	501.0	315.7	2.704
6A1a				2.697
6A1b				2.707
6A2		904.4	575.5	2.750
6A3		556.0	354.1	2.753

mean				**2.722±.027**
7A1	596.65	477.1	300.6	2.703
7A1a				2.706
7A1b				2.695
7A2		881.9	556.7	2.712
7A3		478.3	303.0	2.728
mean				**2.709±.012**
8A	648.89	404.7	254.2	2.689
8B1		444.4	280.5	2.711
8B2		659.4	415.0	2.698
8B2a				2.689
8B2b				2.710
8B3		464.8	293.2	2.709
mean				**2.701±.010**
9A1	692.78	889.9	558.7	2.687
9A1a				2.685
9A1b				2.672
9A2		927.9	584.4	2.701
9B		504.5	318.3	2.709
mean				**2.691±.014**
10A1	709.55	611.6	379.2	2.632
10A1a				2.626
10A1b				2.624
10A2		849.7	527.4	2.636
10B		1042.7	651.6	2.666
mean				**2.637±.017**

APPENDIX E

Ultrasonic velocity data sheets

		radial		axial	
MeSy core-no./ sample-no	**depth m**	**v_p km/s**	**v_s km/s**	**v_p km/s**	**v_s km/s**
1A	333.79	5.52	3.19		
1A2a				5.38	2.39
1A2b				5.55	3.05
1B		5.41	3.09		
mean		**5.47±.08**	**3.14±.07**	**5.47±.12**	**2.72±.48**
2A	383.16	5.41	3.07		
2A3a				5.59	3.21
2A3b				5.56	3.09
mean		**5.41**	**3.07**	**5.58±.02**	**3.15±.08**
3A	438.33	5.33	3.08		
3B		5.51	3.10		
3C		5.39	3.06		
3Ca				5.38	3.05
3Cb				5.50	3.08
mean		**5.41±.09**	**3.08±.02**	**5.44±.08**	**3.07±.02**
4A	463.85	5.45	3.12		
4B		5.39	3.10		
4B1a				5.54	3.11
4B1b				5.56	3.22
4C		5.58	3.12		
mean		**5.47±.10**	**3.11±.01**	**5.55±.01**	**3.17±.08**
5A	500.40	5.31	3.01		
5A1a				5.46	3.08
5A1b				5.53	3.16
mean		**5.31**	**3.01**	**5.50±.05**	**3.12±.06**
6A	559.90	5.36	2.99		
6A1a				5.34	3.05
6A1b				5.49	3.19
mean		**5.36**	**2.99**	**5.42±.11**	**3.12±.09**
7A	596.65	5.83	3.05		
7A1a				5.60	3.15
7A1b				5.68	3.25
mean		**5.83**	**3.05**	**5.64±.06**	**3.20±.07**
8A	648.89	5.19	2.99		
8B2a				5.50	3.14
8B2b				5.53	3.17
8B		5.32	3.03		
mean		**5.26±.09**	**3.01±.03**	**5.52±.02**	**3.16±.02**

		radial		axial	
MeSy core-no./ sample-no	**depth m**	**v_p km/s**	**v_s km/s**	**v_p km/s**	**v_s km/s**
9A	692.78	5.30	2.98		
9A1a				5.52	3.14
9A1b				5.35	3.00
9B		5.46	3.04		
mean		**5.38±.11**	**3.01±.04**	**5.44±.12**	**3.07±.10**
10A	709.55	4.90	2.75		
10A1a				5.07	2.94
10A1b				5.02	2.89
10B		5.19	2.97		
mean		**5.05±.21**	**2.86±.16**	**5.05±.04**	**2.92±.04**

APPENDIX F
Elasticity data sheets

		radial		axial	
MeSy core-no./ sample-no	**depth m**	**E_{dyn} GPa**	**ν_{dyn}**	**E_{dyn} GPa**	**ν_{dyn}**
1A	333.79	69	0.25		
1A2a				59	0.29
1A2b				64	0.28
1B		65	0.26		
mean		**67±3**	**0.26±.01**	**62±4**	**0.29±.01**
2A	383.16	64	0.26		
2A3a				70	0.25
2A3b				66	0.28
mean		**64**	**0.26**	**68±3**	**0.27±.02**
3A	438.33	64	0.25		
3B		66	0.27		
3C		64	0.26		
3Ca				63	0.26
3Cb				65	0.27
mean		**65±1**	**0.26±.01**	**64±1**	**0.27±.01**
4A	463.85	66	0.26		
4B		65	0.25		
4B1a				66	0.27
4B1b				70	0.25
4C		67	0.27		
mean		**66±1**	**0.26±.01**	**68±3**	**0.26±.01**
5A	500.40	62	0.26		
5A1a				65	0.27
5A1b				68	0.26
6A	559.90	62	0.28		
6A1a				63	0.26
6A1b				68	0.25
mean		**62**	**0.28**	**66±4**	**0.26±.01**
7A	596.65	64	0.26		
7A1a				68	0.27
7A1b				72	0.26
mean		**64**	**0.26**	**70±3**	**0.27±.01**
8A	648.89	61	0.25		
8B2a		63	0.26		
8B2b				67	0.26
8B				68	0.26
mean		**62±1**	**0.26±.01**	**68±1**	**0.26**

		radial		axial	
MeSy core-no./ sample-no	**depth m**	**E_{dyn} GPa**	**ν_{dyn}**	**E_{dyn} GPa**	**ν_{dyn}**
9A	692.78	61	0.27		
9A1a				67	0.26
9A1b				63	0.26
9B		64	0.28		
mean		**63±2**	**0.28±.01**	**65±3**	**0.26**
10A	709.55	51	0.27		
10A1a				57	0.25
10A1b				55	0.25
10B		59	0.27		
mean		**55±6**	**0.27**	**56±1**	**0.25**

APPENDIX G

Fracture toughness data sheets

FRACTURE TOUGHNESS TEST ISRM standard 1988

borehole:	KOV01
sample - no.:	1A1-1A2
mean depth, m:	333.79
diameter, mm:	47.6
initial crack length, mm:	7.0
date of unpacking / sampling:	08.11.01
sample ready for testing:	09.11.01
date of testing:	09.11.01
operated by	U. Weber
checked by	U. Weber

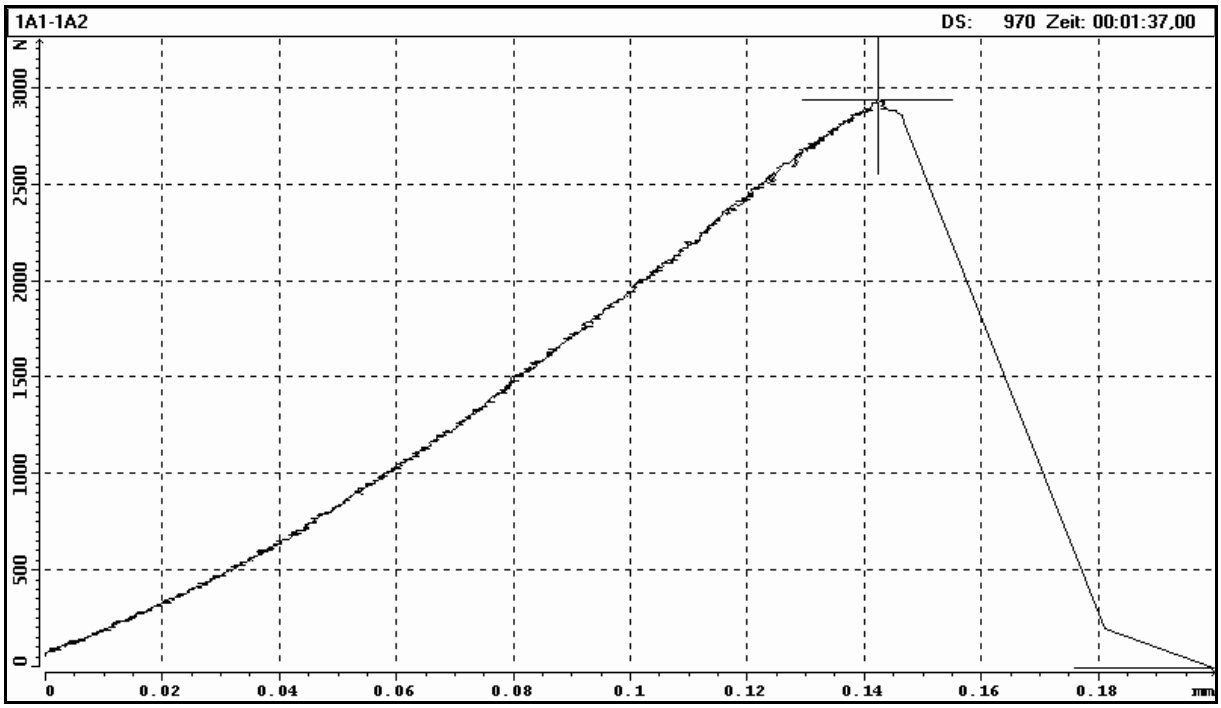

F_{max}, N	2927
K_{IC}, MN·m$^{1/2}$	2.90

FRACTURE TOUGHNESS TEST ISRM standard 1988

borehole:	KOV01
sample - no.:	1A2-1A3
mean depth, m:	333.79
diameter, mm:	47.6
initial crack length, mm:	7.0
date of unpacking / sampling:	08.11.01
sample ready for testing:	09.11.01
date of testing:	09.11.01
operated by	U. Weber
checked by	U. Weber

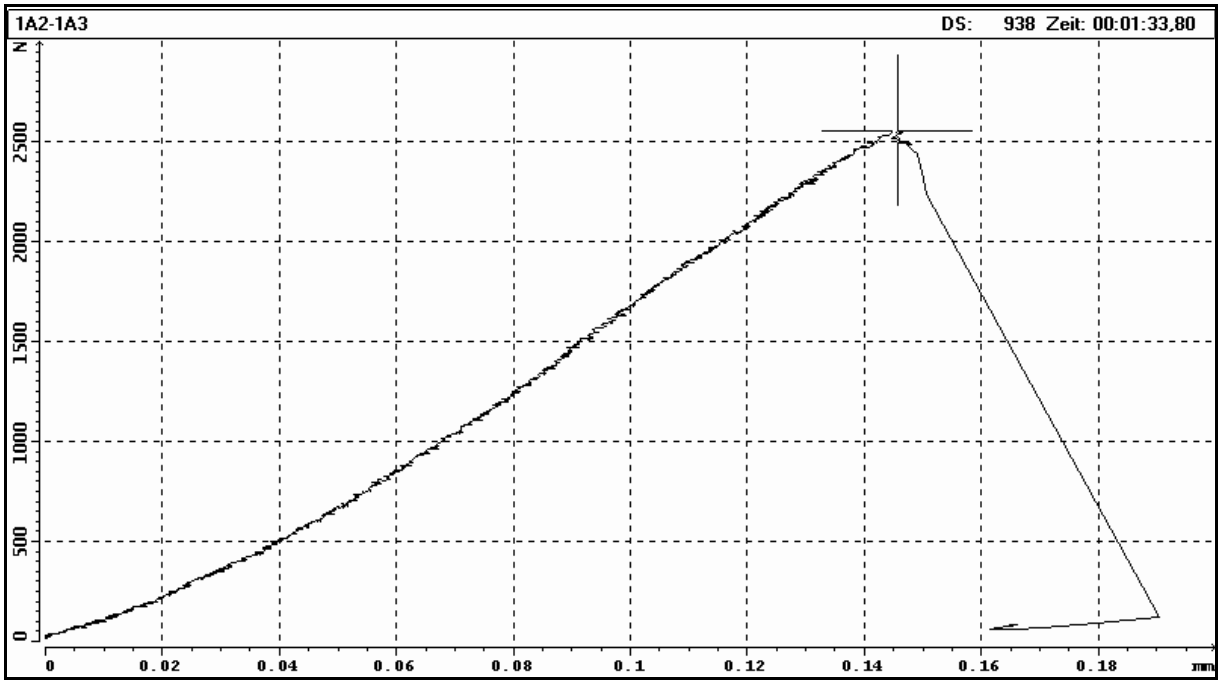

F_{max}, N	2547
K_{IC}, MN·m$^{1/2}$	2.53

FRACTURE TOUGHNESS TEST ISRM standard 1988

borehole:	KOV01
sample - no.:	1B1-1B2
mean depth, m:	333.79
diameter, mm:	47.6
initial crack length, mm:	7.0
date of unpacking / sampling:	08.11.01
sample ready for testing:	09.11.01
date of testing:	09.11.01
operated by	U. Weber
checked by	U. Weber

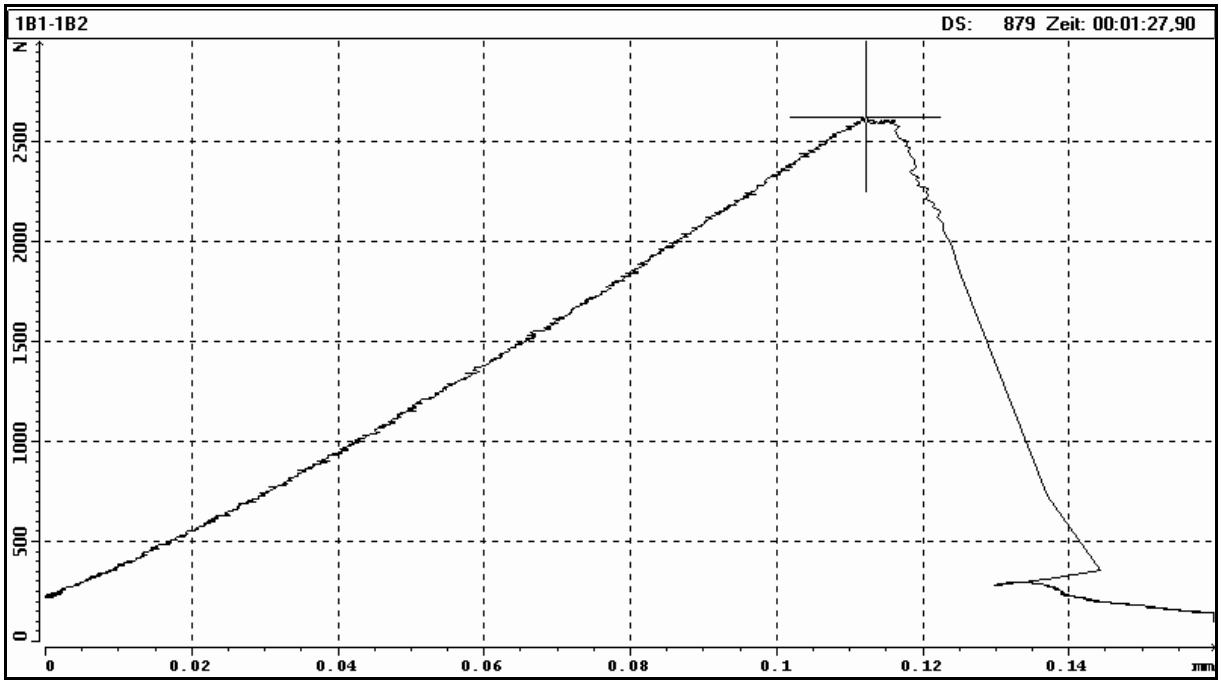

F_{max}, N	2617
K_{IC}, MN·m$^{1/2}$	2.60

FRACTURE TOUGHNESS TEST ISRM standard 1988

borehole:	KOV01
sample - no.:	2A1-2A2
mean depth, m:	383.16
diameter, mm:	47.4
initial crack length, mm:	6.9
date of unpacking / sampling:	08.11.01
sample ready for testing:	09.11.01
date of testing:	09.11.01
operated by	U. Weber
checked by	U. Weber

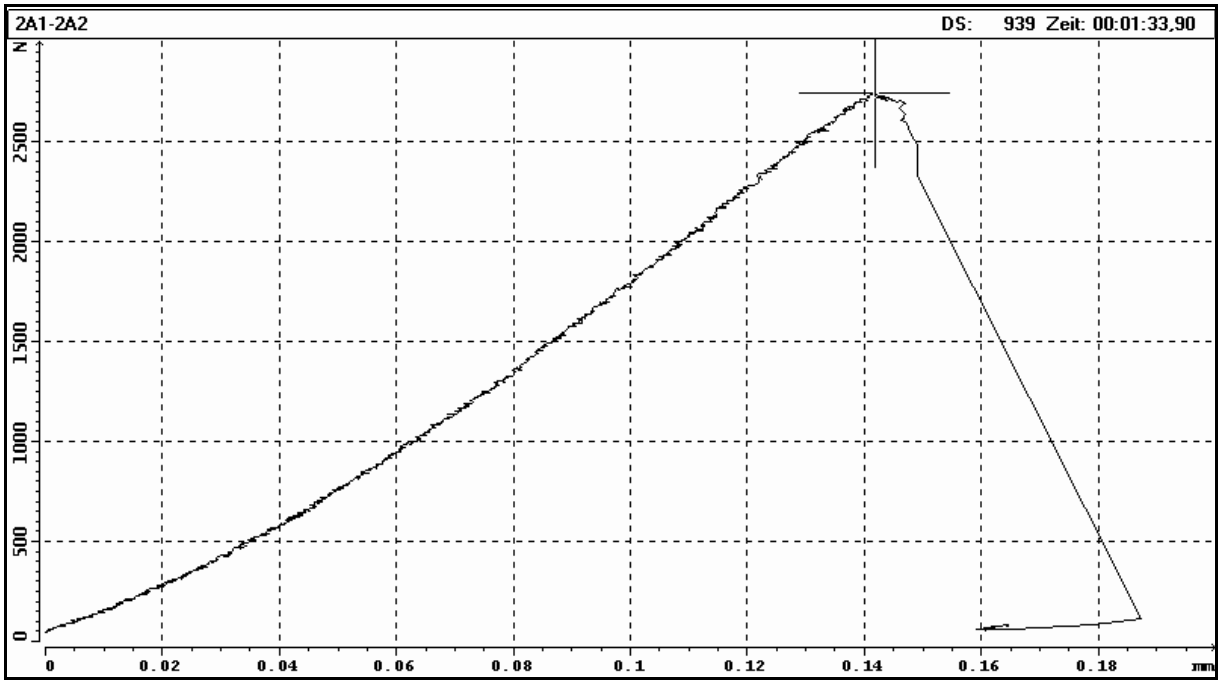

F_{max}, N	2736
K_{IC}, MN·m$^{1/2}$	2.73

FRACTURE TOUGHNESS TEST ISRM standard 1988

borehole:	KOV01
sample - no.:	2A2-2A3
mean depth, m:	383.16
diameter, mm:	47.4
initial crack length, mm:	6.0
date of unpacking / sampling:	08.11.01
sample ready for testing:	09.11.01
date of testing:	09.11.01
operated by	U. Weber
checked by	U. Weber

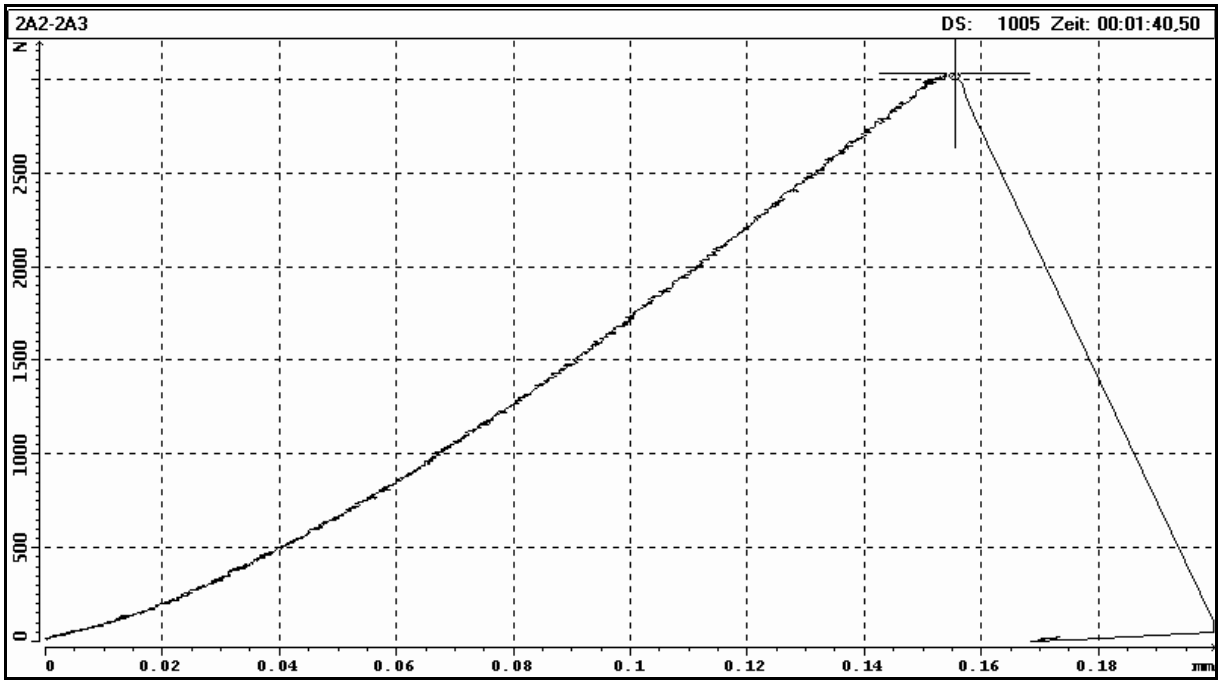

F_{max}, N	3023
K_{IC}, MN·m$^{1/2}$	2.83

FRACTURE TOUGHNESS TEST ISRM standard 1988

borehole:	KOV01
sample - no.:	4A1-4A2
mean depth, m:	463.85
diameter, mm:	47.4
initial crack length, mm:	6.8
date of unpacking / sampling:	08.11.01
sample ready for testing:	09.11.01
date of testing:	09.11.01
operated by	U. Weber
checked by	U. Weber

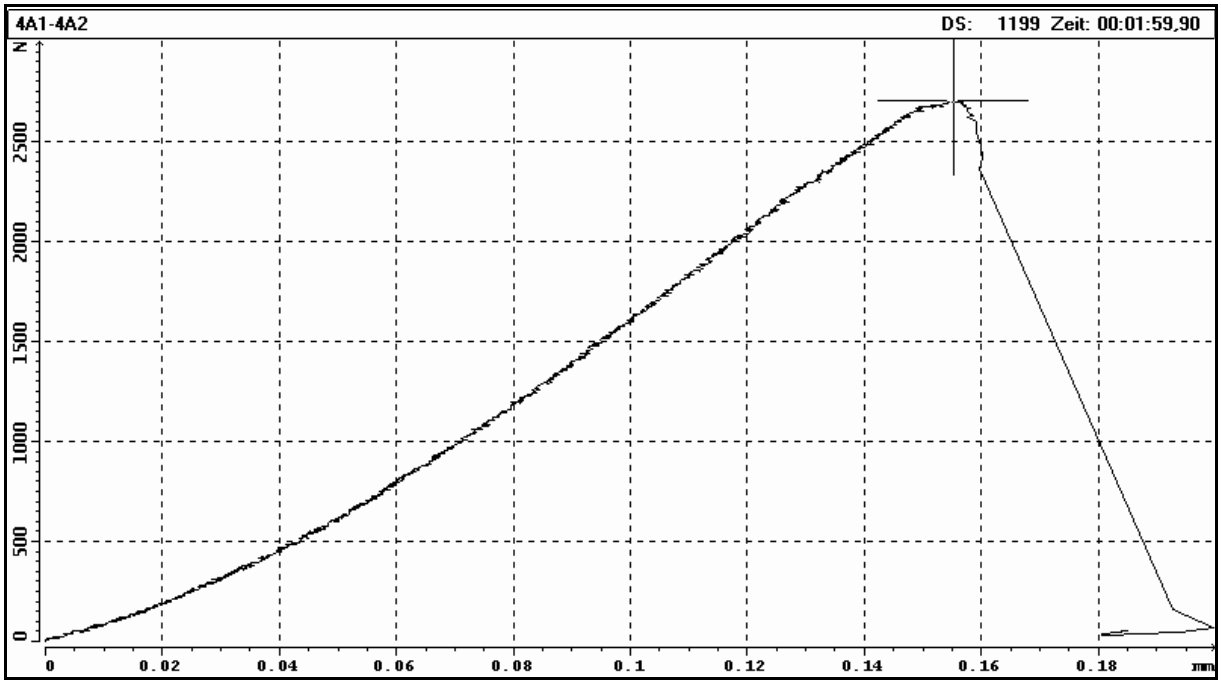

F_{max}, N	2700
K_{IC}, MN·m$^{1/2}$	2.67

FRACTURE TOUGHNESS TEST ISRM standard 1988

borehole:	KOV01
sample - no.:	4B1-4B2
mean depth, m:	463.85
diameter, mm:	47.4
initial crack length, mm:	7.2
date of unpacking / sampling:	08.11.01
sample ready for testing:	09.11.01
date of testing:	09.11.01
operated by	U. Weber
checked by	U. Weber

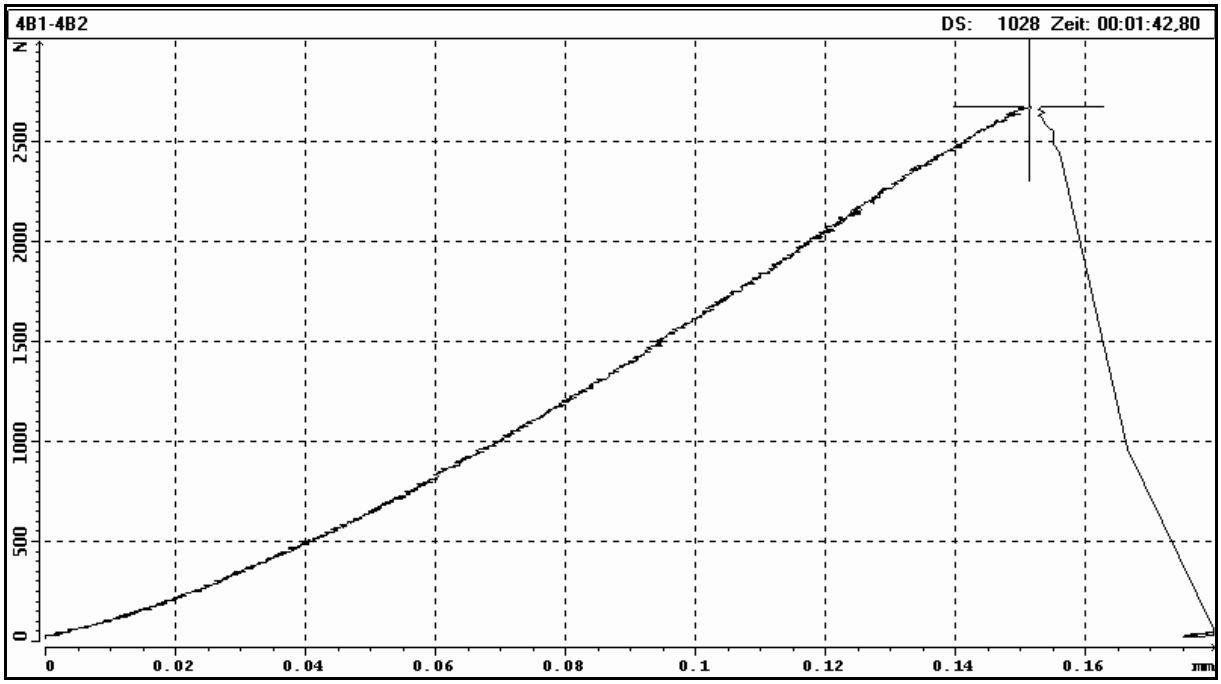

F_{max}, N	2665
K_{IC}, MN·m$^{1/2}$	2.71

FRACTURE TOUGHNESS TEST ISRM standard 1988

borehole:	KOV01
sample - no.:	5A1-5A2
mean depth, m:	500.40
diameter, mm:	51.7
initial crack length, mm:	7.3
date of unpacking / sampling:	08.11.01
sample ready for testing:	09.11.01
date of testing:	09.11.01
operated by	U. Weber
checked by	U. Weber

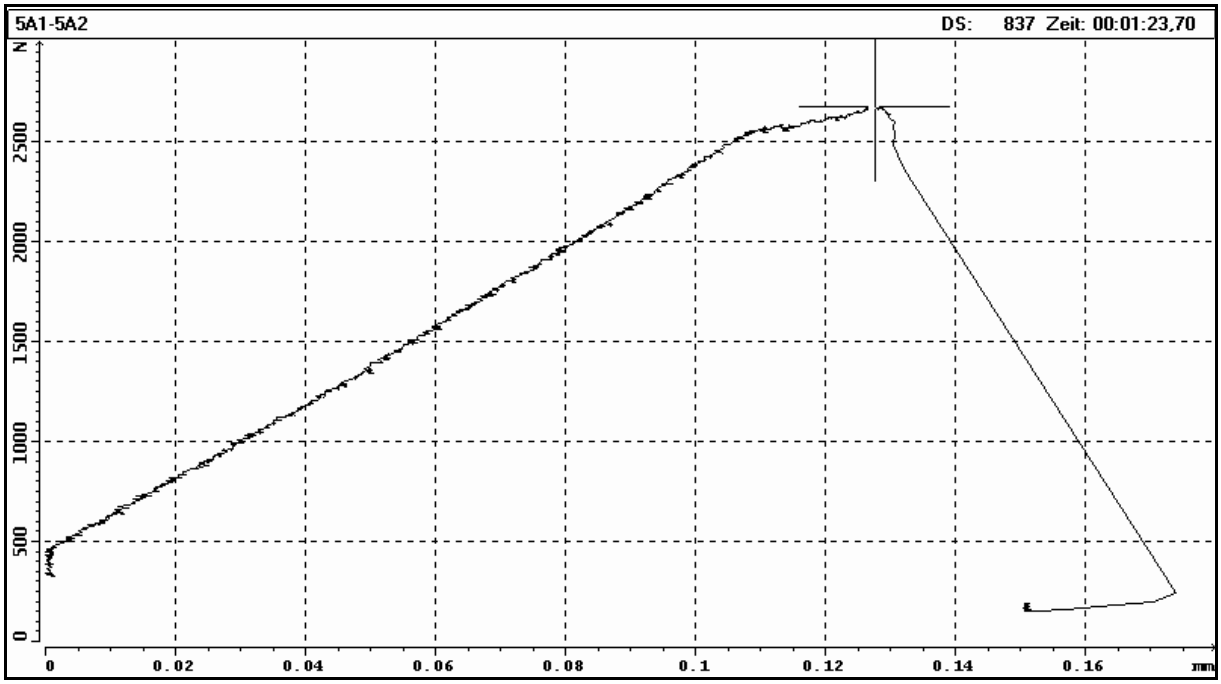

F_{max}, N	2672
K_{IC}, MN·m$^{1/2}$	2.30

FRACTURE TOUGHNESS TEST ISRM standard 1988

borehole:	KOV01
sample - no.:	5A2-5A3
mean depth, m:	500.40
diameter, mm:	51.7
initial crack length, mm:	7.1
date of unpacking / sampling:	08.11.01
sample ready for testing:	09.11.01
date of testing:	09.11.01
operated by	U. Weber
checked by	U. Weber

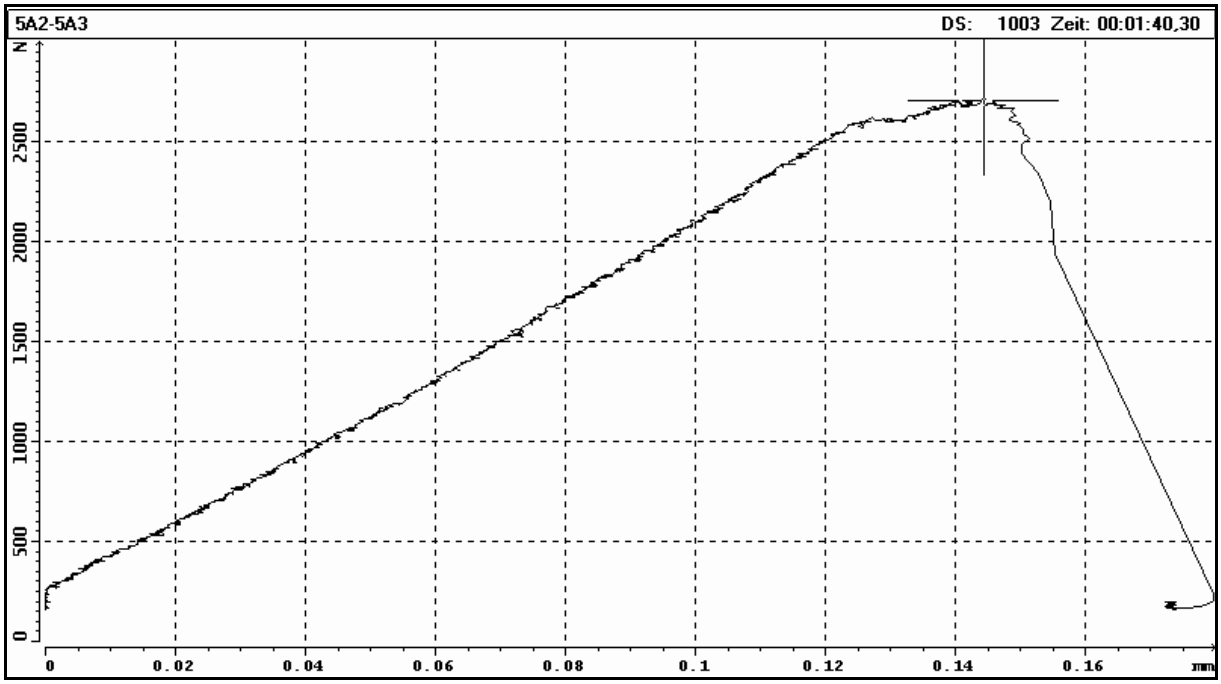

F_{max}, N	2698
K_{IC}, MN·m$^{1/2}$	2.30

FRACTURE TOUGHNESS TEST ISRM standard 1988

borehole:	KOV01
sample - no.:	6A1-6A2
mean depth, m:	559.90
diameter, mm:	47.2
initial crack length, mm:	7.0
date of unpacking / sampling:	08.11.01
sample ready for testing:	09.11.01
date of testing:	09.11.01
operated by	U. Weber
checked by	U. Weber

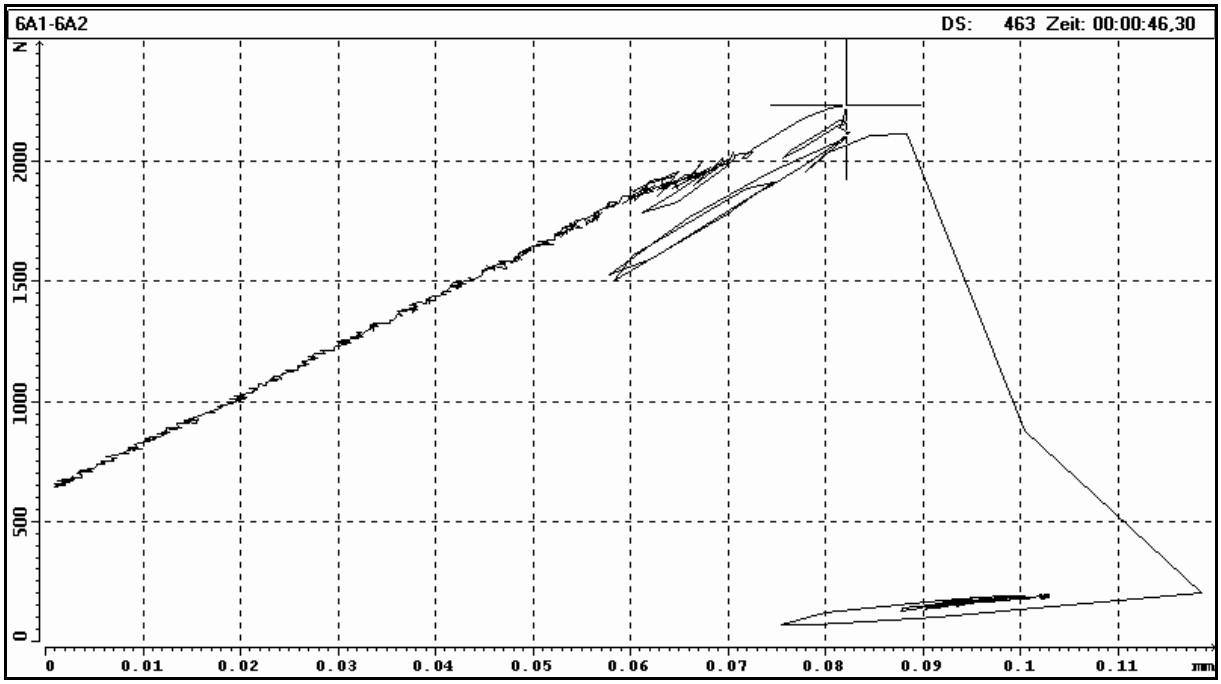

F_{max}, N	2228
K_{IC}, MN·m$^{1/2}$	2.25

FRACTURE TOUGHNESS TEST ISRM standard 1988

borehole:	KOV01
sample - no.:	6A2-6A3
mean depth, m:	559.90
diameter, mm:	47.2
initial crack length, mm:	7.0
date of unpacking / sampling:	08.11.01
sample ready for testing:	09.11.01
date of testing:	09.11.01
operated by	U. Weber
checked by	U. Weber

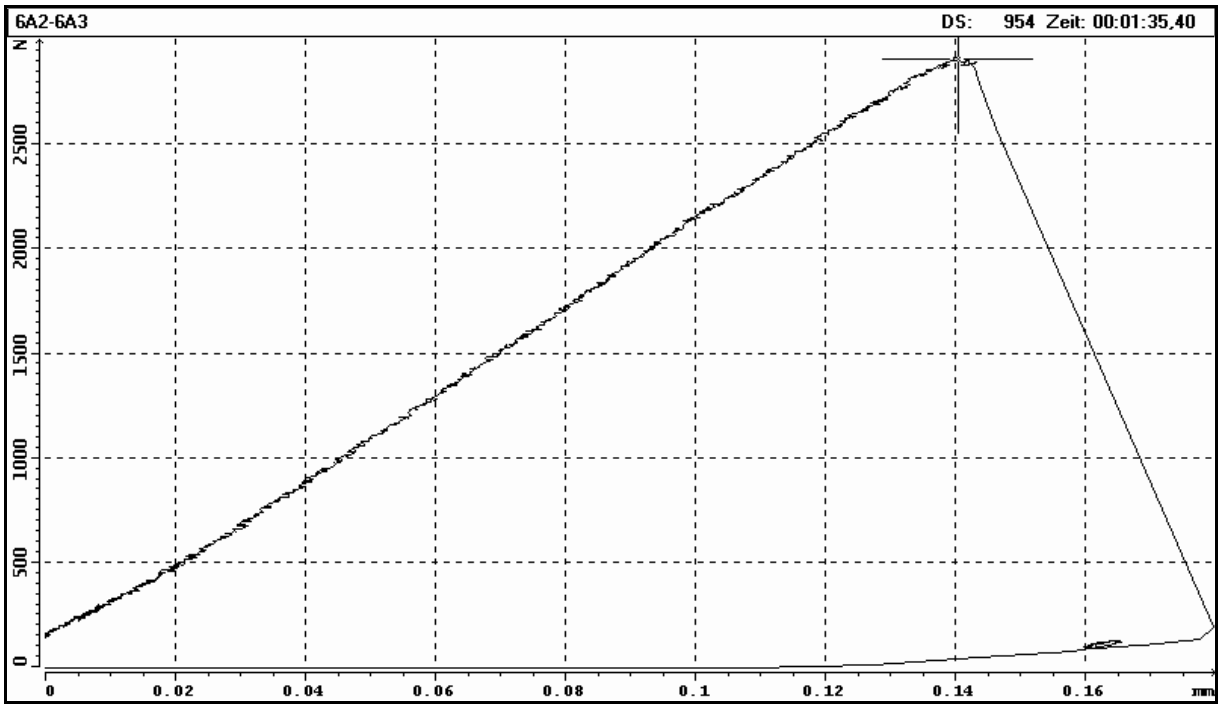

F_{max}, N	2900
K_{IC}, MN·m$^{1/2}$	2.93

FRACTURE TOUGHNESS TEST ISRM standard 1988

borehole:	KOV01
sample - no.:	7A1-7A2
mean depth, m:	596.65
diameter, mm:	47.2
initial crack length, mm:	7.1
date of unpacking / sampling:	08.11.01
sample ready for testing:	09.11.01
date of testing:	09.11.01
operated by	U. Weber
checked by	U. Weber

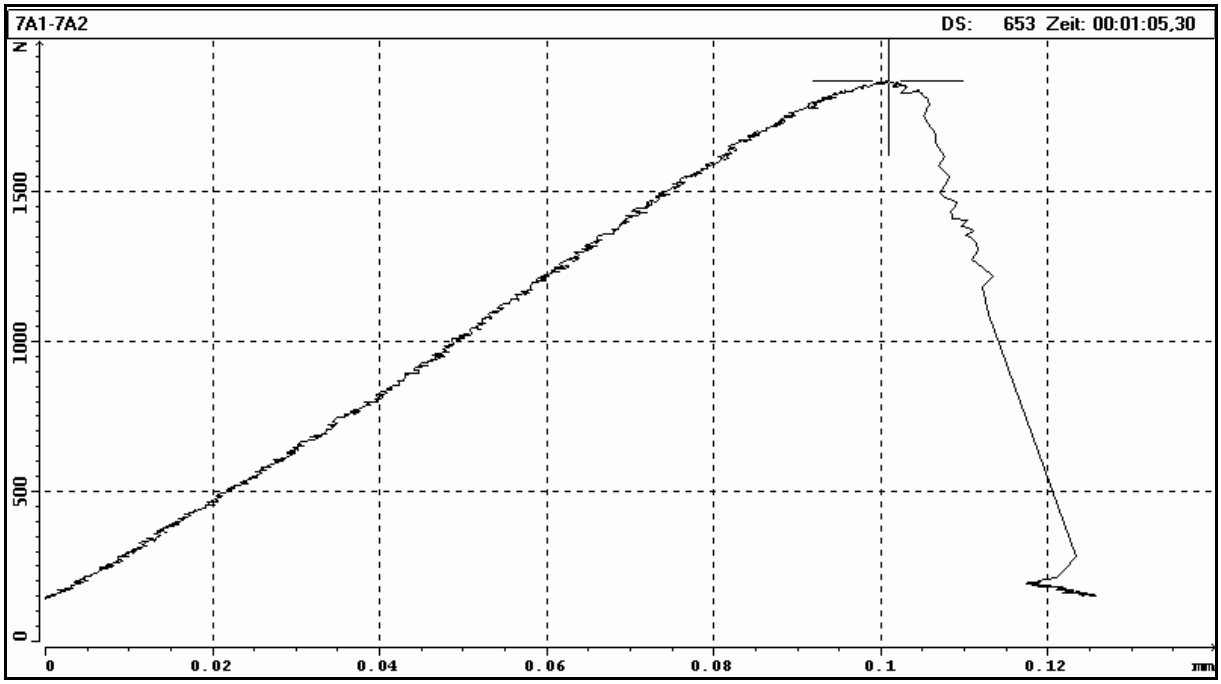

F_{max}, N	1866
K_{IC}, MN·m$^{1/2}$	1.90

FRACTURE TOUGHNESS TEST ISRM standard 1988

borehole:	KOV01
sample - no.:	7A2-7A3
mean depth, m:	596.65
diameter, mm:	47.2
initial crack length, mm:	7.3
date of unpacking / sampling:	08.11.01
sample ready for testing:	09.11.01
date of testing:	09.11.01
operated by	U. Weber
checked by	U. Weber

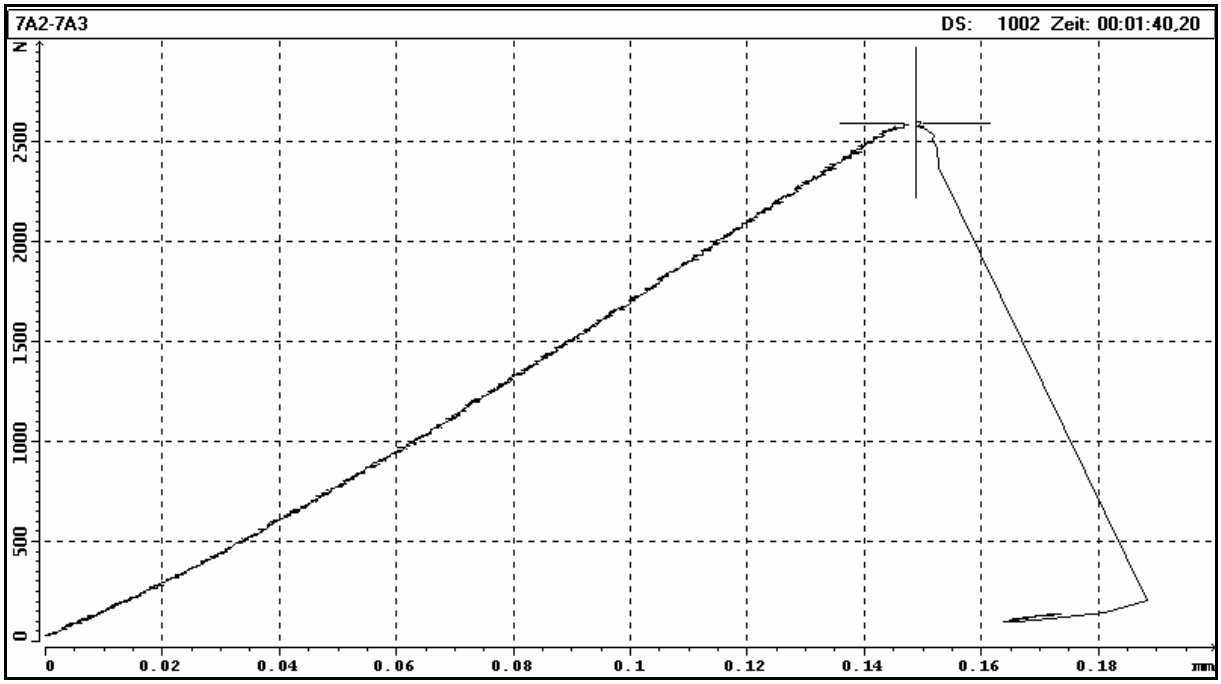

F_{max}, N	2585
K_{IC}, MN·m$^{1/2}$	2.67

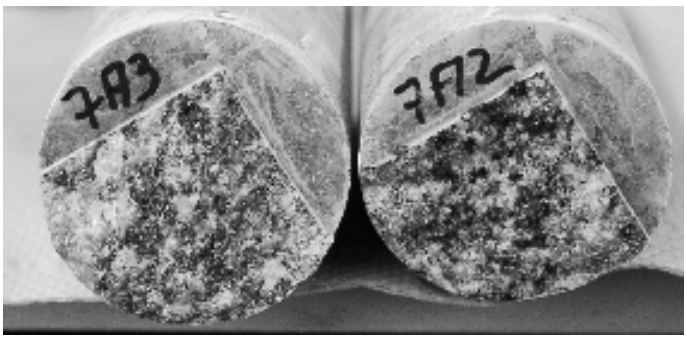

FRACTURE TOUGHNESS TEST ISRM standard 1988

borehole:	KOV01
sample - no.:	8B1-8B2
mean depth, m:	648.89
diameter, mm:	47.3
initial crack length, mm:	7.2
date of unpacking / sampling:	08.11.01
sample ready for testing:	09.11.01
date of testing:	09.11.01
operated by	U. Weber
checked by	U. Weber

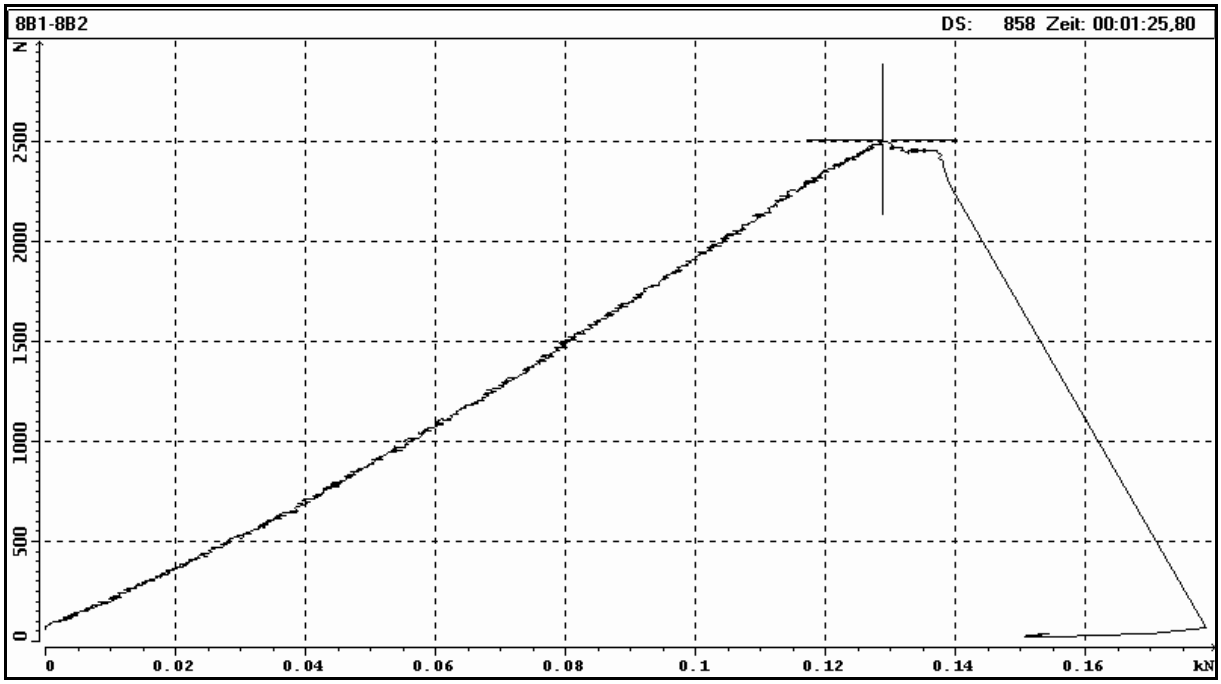

F_{max}, N	2500
K_{IC}, MN·m$^{1/2}$	2.55

FRACTURE TOUGHNESS TEST ISRM standard 1988

borehole:	KOV01
sample - no.:	8B2-8B3
mean depth, m:	648.89
diameter, mm:	47.3
initial crack length, mm:	6.6
date of unpacking / sampling:	08.11.01
sample ready for testing:	09.11.01
date of testing:	09.11.01
operated by	U. Weber
checked by	U. Weber

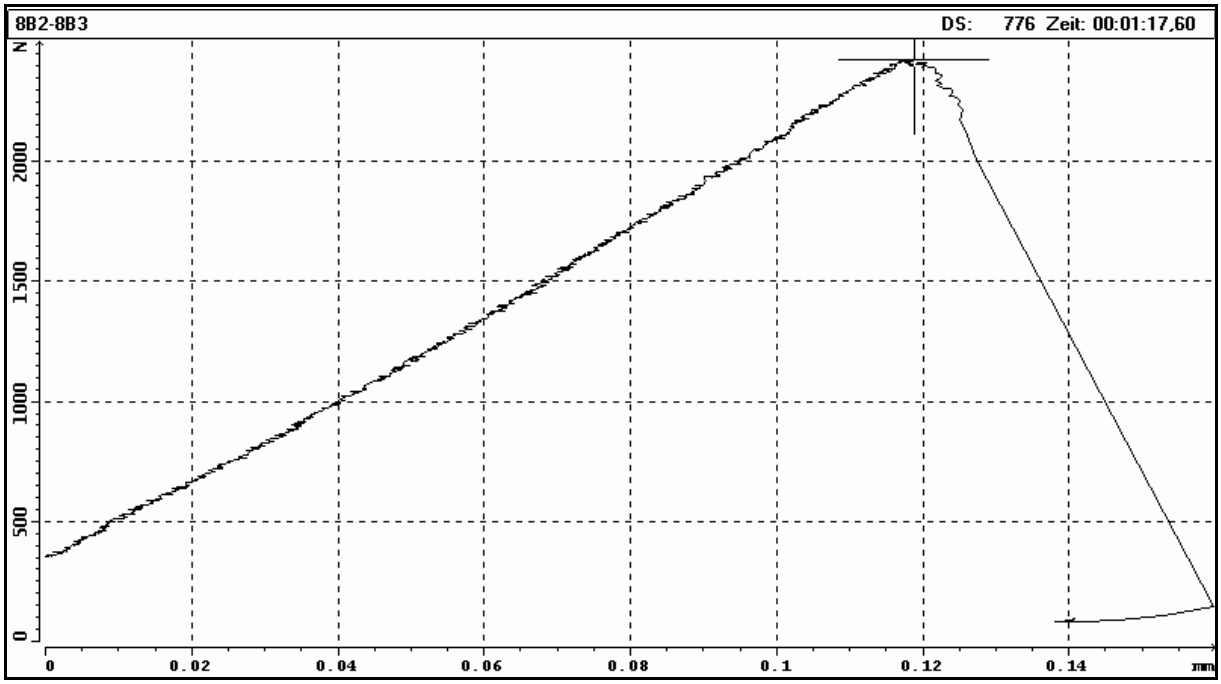

F_{max}, N	2416
K_{IC}, MN·m$^{1/2}$	2.37

FRACTURE TOUGHNESS TEST ISRM standard 1988

borehole:	KOV01
sample - no.:	9A1-9A2
mean depth, m:	692.78
diameter, mm:	51.9
initial crack length, mm:	7.0
date of unpacking / sampling:	08.11.01
sample ready for testing:	09.11.01
date of testing:	09.11.01
operated by	U. Weber
checked by	U. Weber

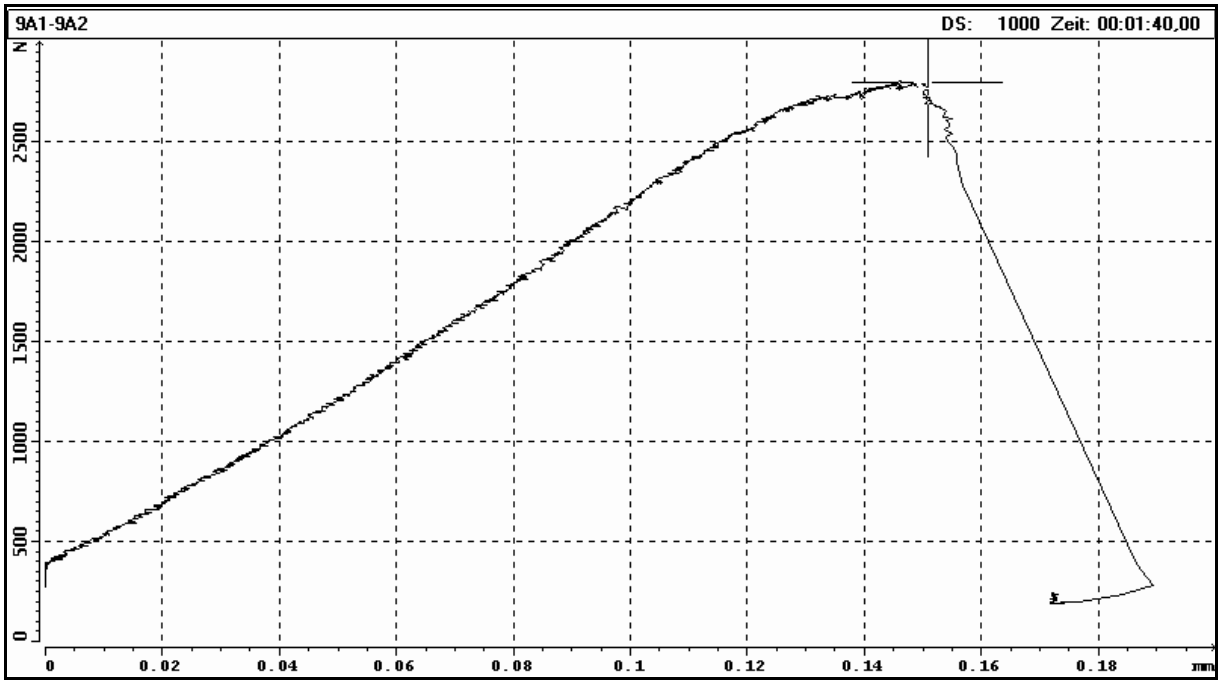

F_{max}, N	2789
K_{IC}, MN·m$^{1/2}$	2.34

FRACTURE TOUGHNESS TEST ISRM standard 1988

borehole:	KOV01
sample - no.:	10A1-10A2
mean depth, m:	709.55
diameter, mm:	51.9
initial crack length, mm:	5.2
date of unpacking / sampling:	08.11.01
sample ready for testing:	09.11.01
date of testing:	09.11.01
operated by	U. Weber
checked by	U. Weber

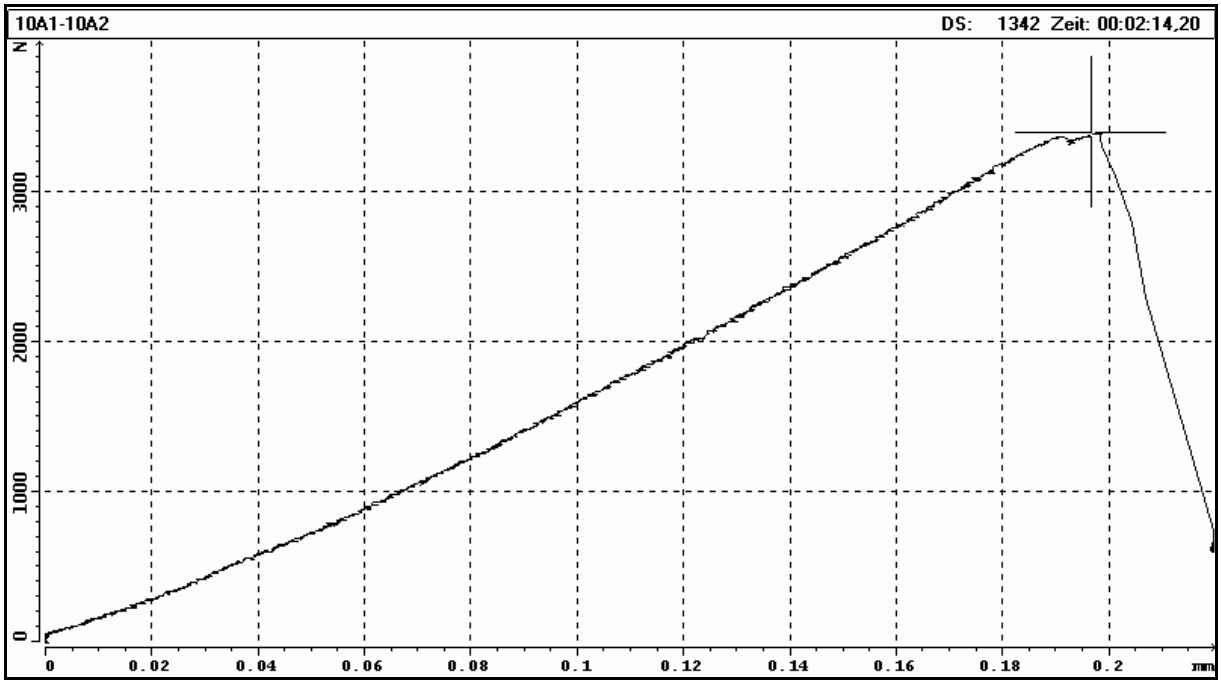

F_{max}, N	3385
K_{IC}, MN·m$^{1/2}$	2.53

APPENDIX H

Laboratory hydrofrac data sheets

MINI-FRAC TEST DATA SHEET

borehole:	KOV01
sample - no.:	1A2a
mean depth, m:	333.79
diameter, mm:	29.9
length, mm:	44.5
date of unpacking / sampling:	12.11.01
mini - sample ready for testing:	14.11.01
date of testing:	16.11.01
operated by	J. Orzol
checked by	U. Weber

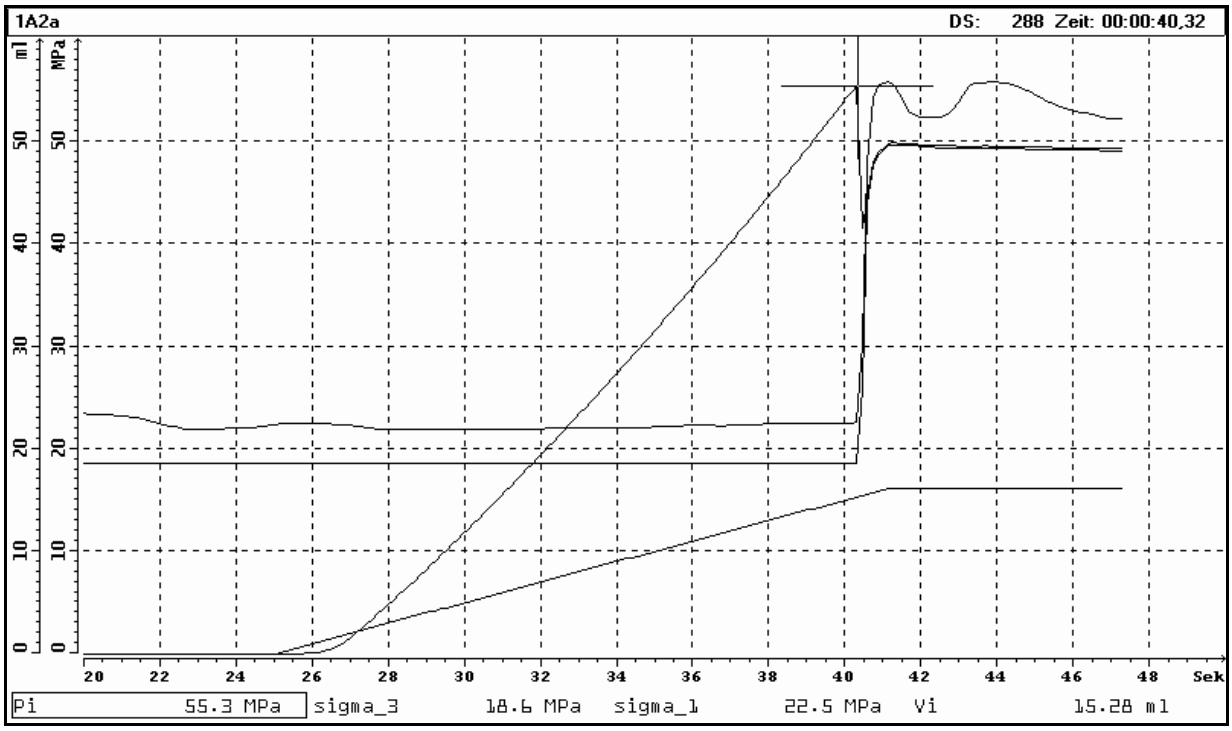

Initial conditions	
σ_1, MPa	22.5
σ_3, MPa	18.6
Injection Characteristics at failure	
P_i, MPa	55.3
V_i, ml	15.28

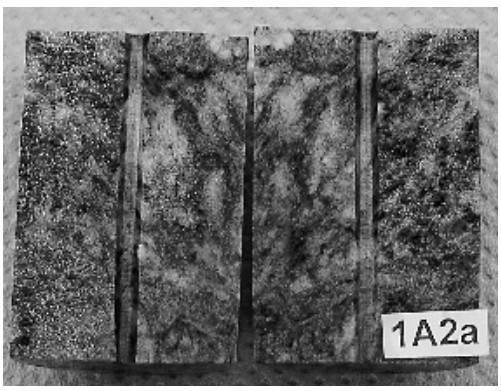

MINI-FRAC TEST DATA SHEET

borehole:	KOV01
sample - no.:	1A2b
mean depth, m:	333.79
diameter, mm:	29.9
length, mm:	44.5
date of unpacking / sampling:	12.11.01
mini - sample ready for testing:	14.11.01
date of testing:	16.11.01
operated by	J. Orzol
checked by	U. Weber

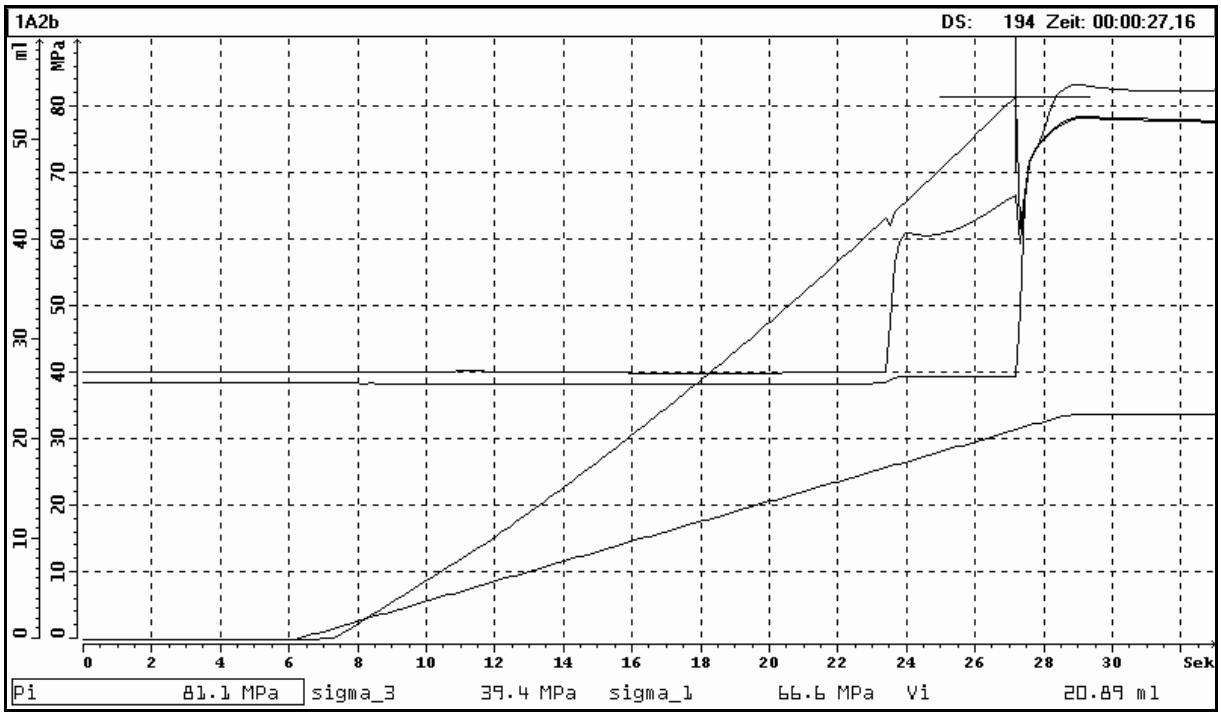

Initial conditions	
σ_1, MPa	66.6
σ_3, MPa	39.4
Injection Characteristics at failure	
P_i, MPa	81.1
V_i, ml	20.89

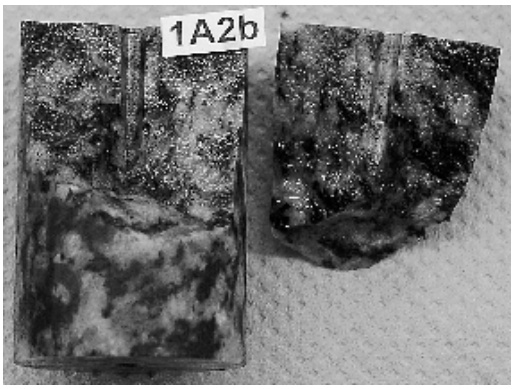

MINI-FRAC TEST DATA SHEET

borehole:	KOV01
sample - no.:	2A3a
mean depth, m:	383.16
diameter, mm:	29.9
length, mm:	44.2
date of unpacking / sampling:	12.11.01
mini - sample ready for testing:	14.11.01
date of testing:	16.11.01
operated by	J. Orzol
checked by	U. Weber

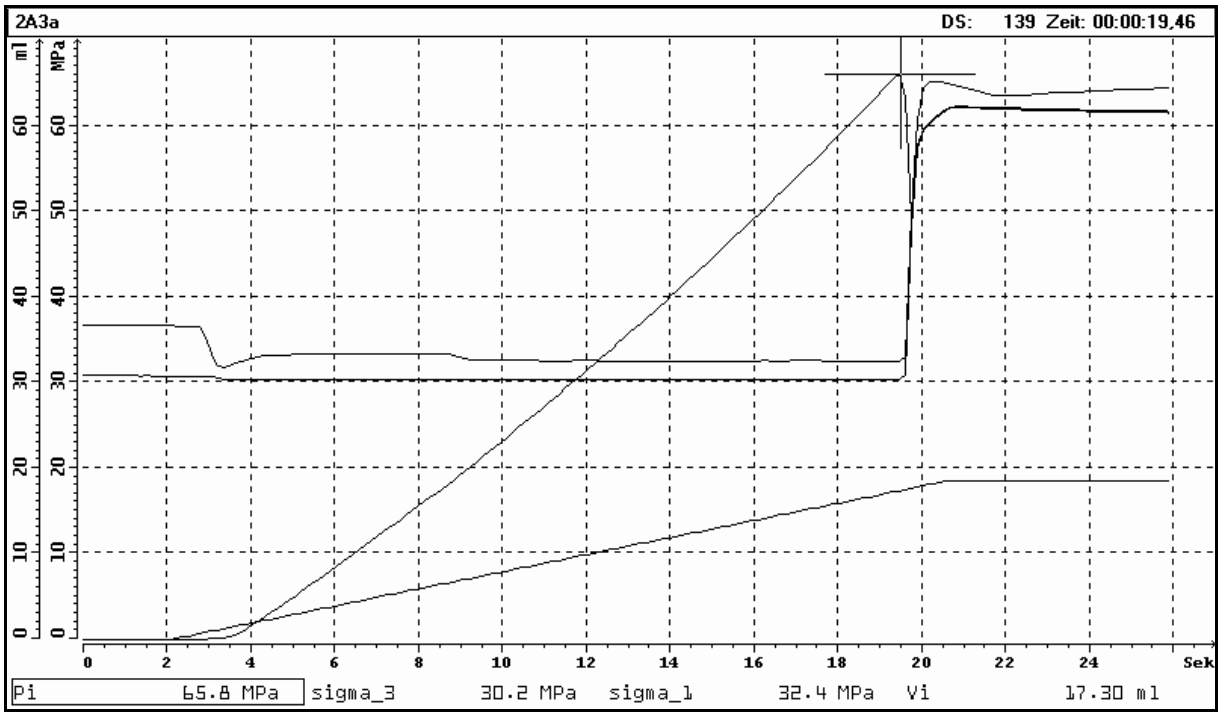

Initial conditions	
σ_1, MPa	32.4
σ_3, MPa	30.2
Injection Characteristics at failure	
P_i, MPa	65.8
V_i, ml	17.30

MINI-FRAC TEST DATA SHEET

borehole:	KOV01
sample - no.:	2A3b
mean depth, m:	383.16
diameter, mm:	29.9
length, mm:	45.0
date of unpacking / sampling:	12.11.01
mini - sample ready for testing:	14.11.01
date of testing:	16.11.01
operated by	J. Orzol
checked by	U. Weber

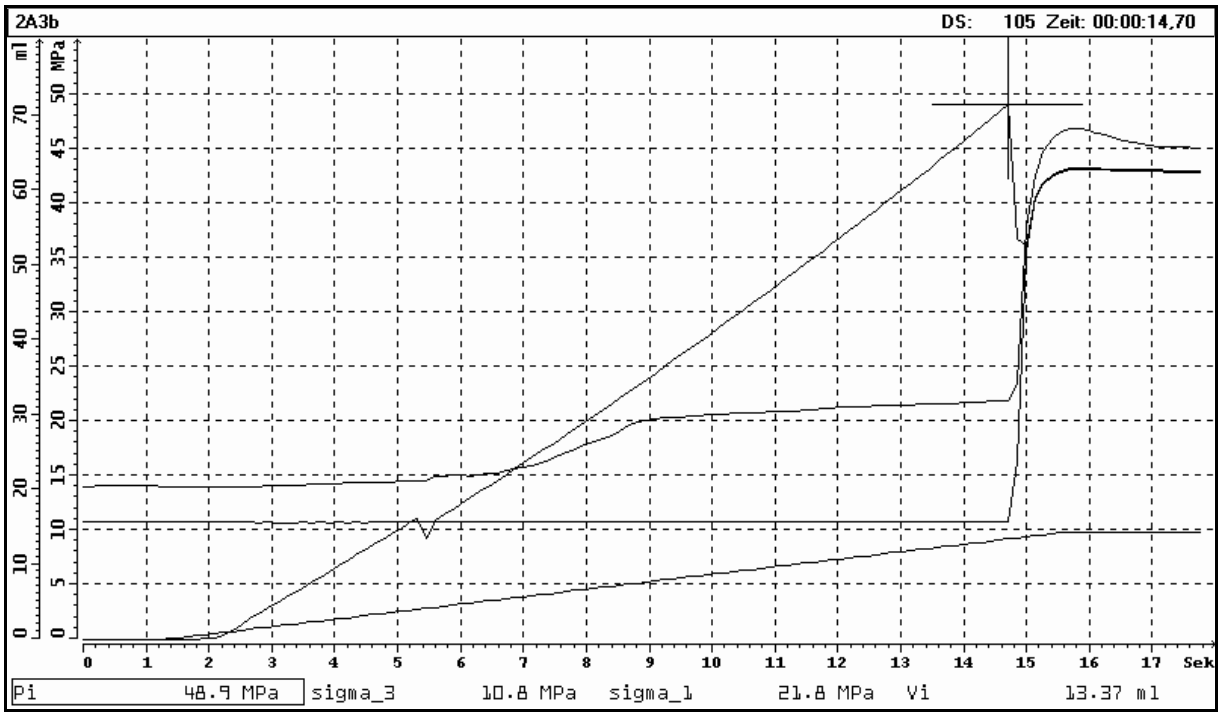

Initial conditions	
σ_1, MPa	21.8
σ_3, MPa	10.8
Injection Characteristics at failure	
P_i, MPa	48.9
V_i, ml	13.37

MINI-FRAC TEST DATA SHEET

borehole:	KOV01
sample - no.:	3Ca
mean depth, m:	438.33
diameter, mm:	29.9
length, mm:	43.8
date of unpacking / sampling:	12.11.01
mini - sample ready for testing:	14.11.01
date of testing:	16.11.01
operated by	J. Orzol
checked by	U. Weber

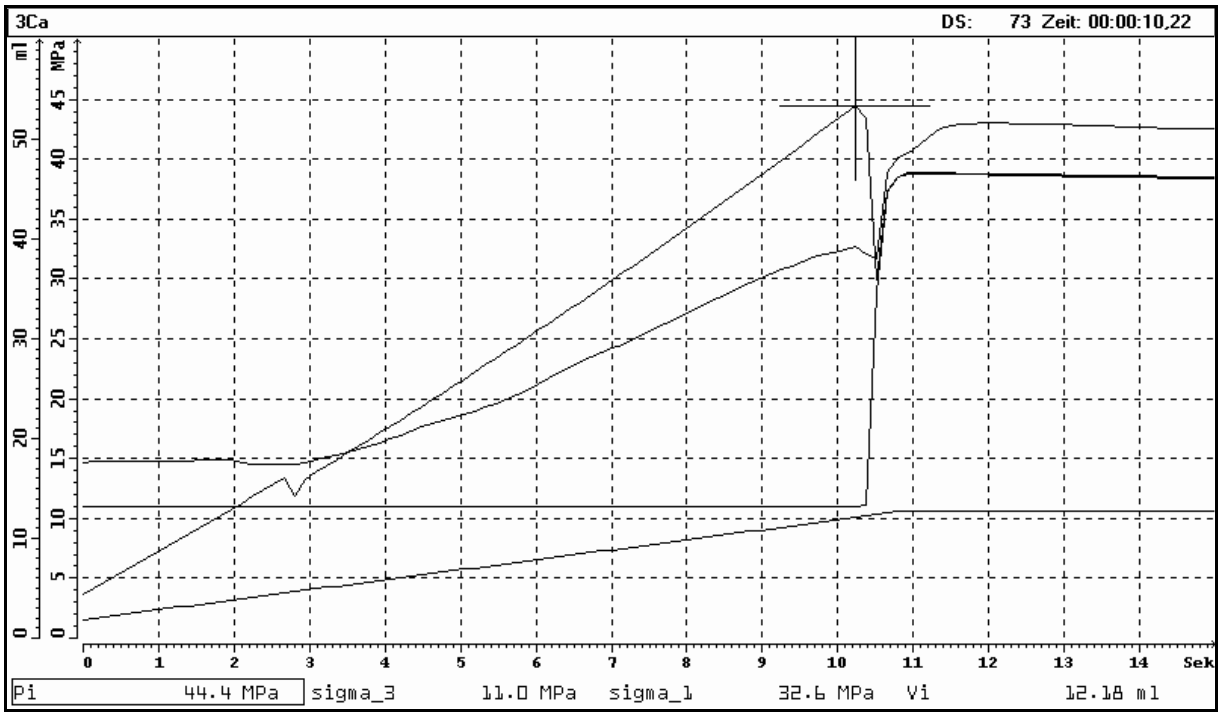

Initial conditions	
σ_1, MPa	32.6
σ_3, MPa	11.0
Injection Characteristics at failure	
P_i, MPa	44.4
V_i, ml	12.18

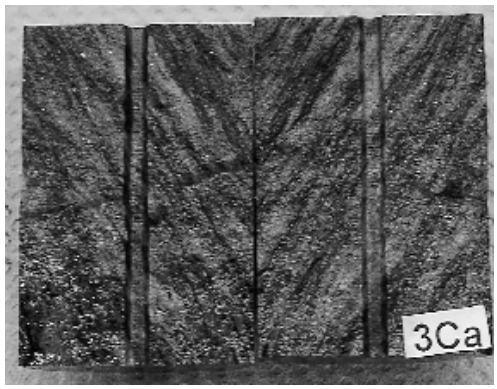

MINI-FRAC TEST DATA SHEET

borehole:	KOV01
sample - no.:	3Cb
mean depth, m:	438.33
diameter, mm:	29.9
length, mm:	40.8
date of unpacking / sampling:	12.11.01
mini - sample ready for testing:	14.11.01
date of testing:	16.11.01
operated by	J. Orzol
checked by	U. Weber

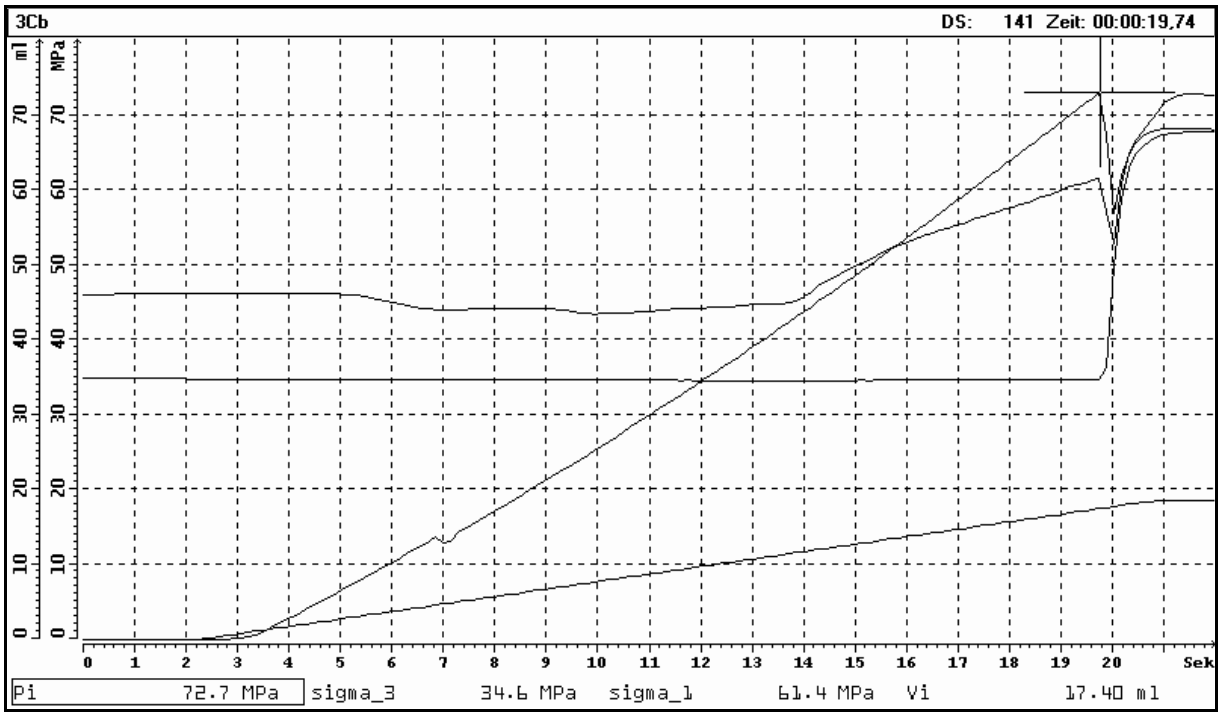

Initial conditions	
σ_1, MPa	61.4
σ_3, MPa	34.6
Injection Characteristics at failure	
P_i, MPa	72.7
V_i, ml	17.40

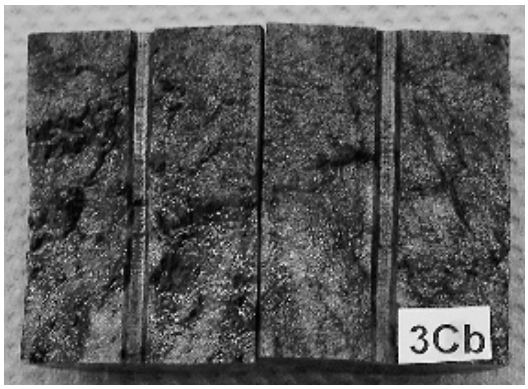

MINI-FRAC TEST DATA SHEET

borehole:	KOV01
sample - no.:	4B1a
mean depth, m:	463.85
diameter, mm:	29.9
length, mm:	40.8
date of unpacking / sampling:	12.11.01
mini - sample ready for testing:	14.11.01
date of testing:	16.11.01
operated by	J. Orzol
checked by	U. Weber

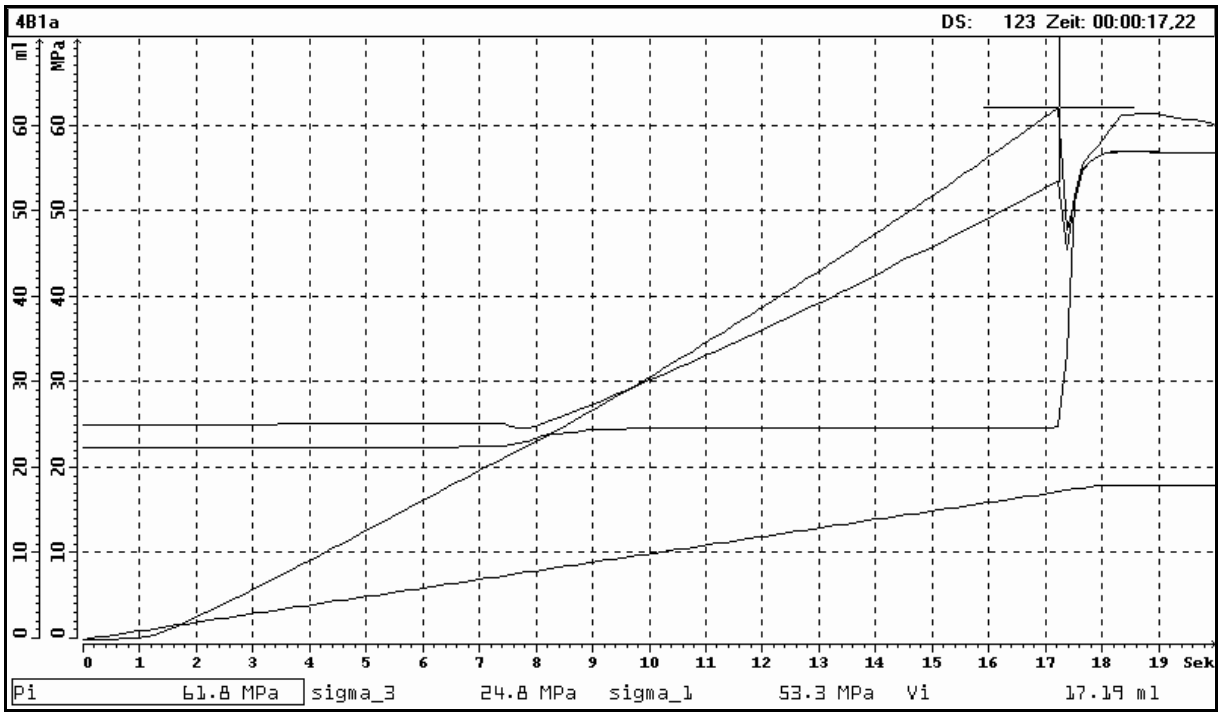

Initial conditions	
σ_1, MPa	53.3
σ_3, MPa	24.8
Injection Characteristics at failure	
P_i, MPa	61.8
V_i, ml	17.19

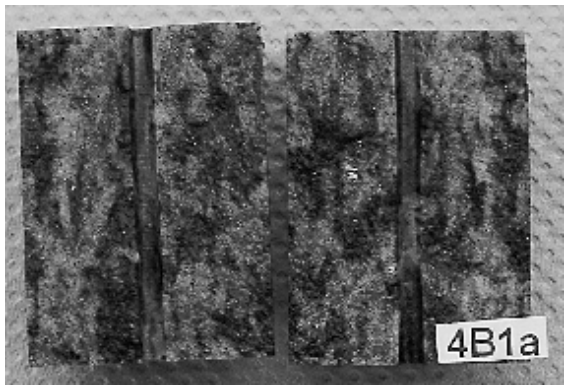

MINI-FRAC TEST DATA SHEET

borehole:	KOV01
sample - no.:	4B1b
mean depth, m:	463.85
diameter, mm:	29.9
length, mm:	45.6
date of unpacking / sampling:	12.11.01
mini - sample ready for testing:	14.11.01
date of testing:	16.11.01
operated by	J. Orzol
checked by	U. Weber

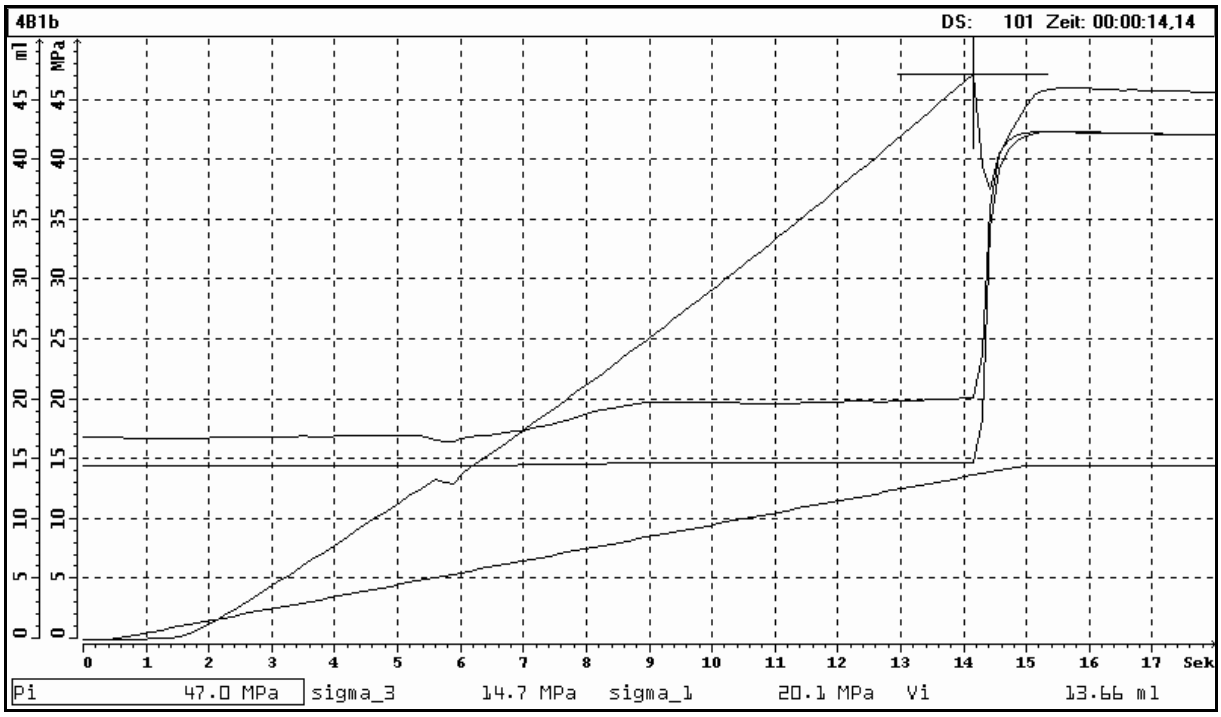

Initial conditions	
σ_1, MPa	20.1
σ_3, MPa	14.7
Injection Characteristics at failure	
P_i, MPa	47.0
V_i, ml	13.66

MINI-FRAC TEST DATA SHEET

borehole:	KOV01
sample - no.:	5A1a
mean depth, m:	500.40
diameter, mm:	29.9
length, mm:	44.5
date of unpacking / sampling:	12.11.01
mini - sample ready for testing:	14.11.01
date of testing:	16.11.01
operated by	J. Orzol
checked by	U. Weber

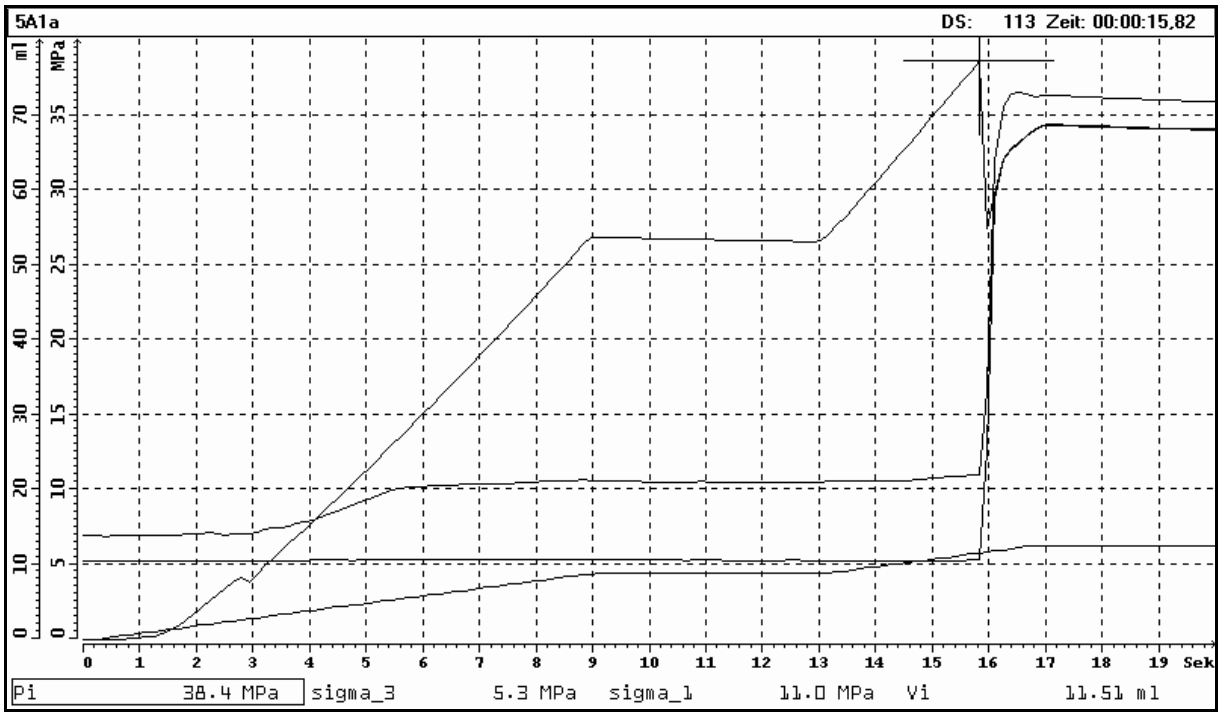

Initial conditions	
σ_1, MPa	11.0
σ_3, MPa	5.3
Injection Characteristics at failure	
P_i, MPa	38.4
V_i, ml	11.51

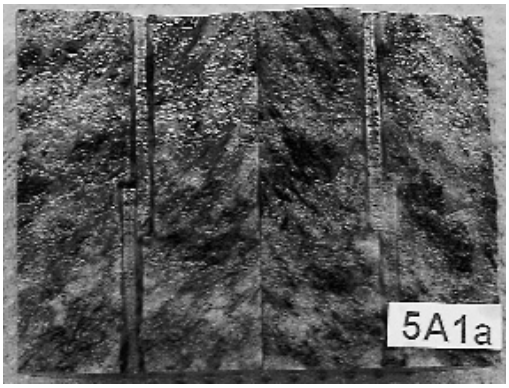

MINI-FRAC TEST DATA SHEET

borehole:	KOV01
sample - no.:	5A1b
mean depth, m:	500.40
diameter, mm:	29.9
length, mm:	44.1
date of unpacking / sampling:	12.11.01
mini - sample ready for testing:	14.11.01
date of testing:	16.11.01
operated by	J. Orzol
checked by	U. Weber

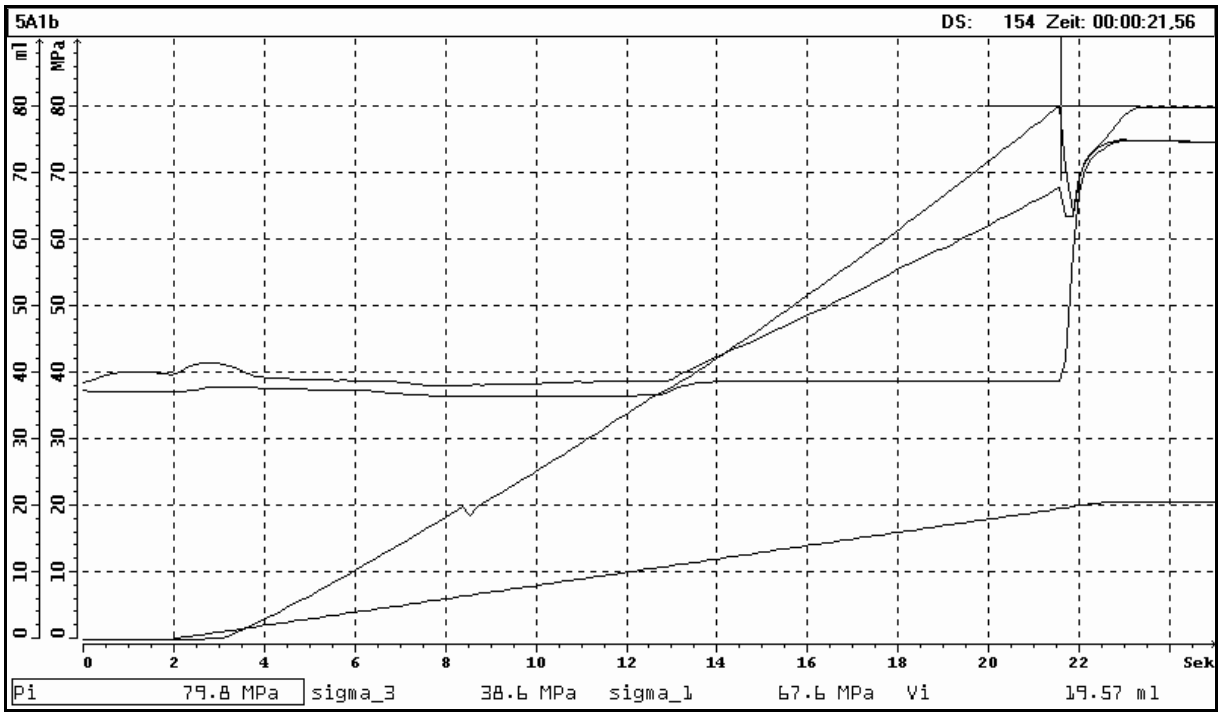

Initial conditions	
σ_1, MPa	67.6
σ_3, MPa	38.6
Injection Characteristics at failure	
P_i, MPa	79.8
V_i, ml	19.57

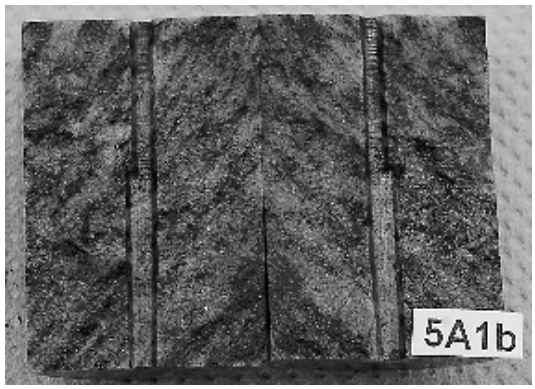

MINI-FRAC TEST DATA SHEET

borehole:	KOV01
sample - no.:	6A1a
mean depth, m:	559.90
diameter, mm:	29.9
length, mm:	43.9
date of unpacking / sampling:	12.11.01
mini - sample ready for testing:	14.11.01
date of testing:	16.11.01
operated by	J. Orzol
checked by	U. Weber

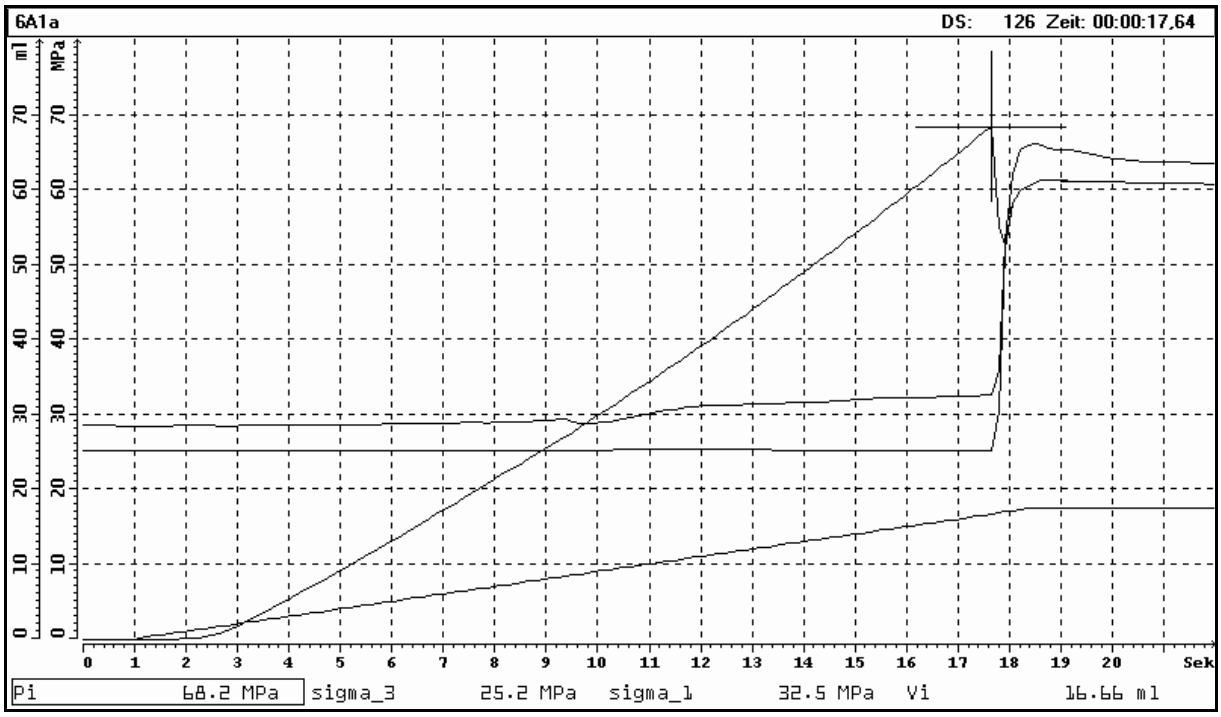

Initial conditions	
σ_1, MPa	32.5
σ_3, MPa	25.2
Injection Characteristics at failure	
P_i, MPa	68.2
V_i, ml	16.66

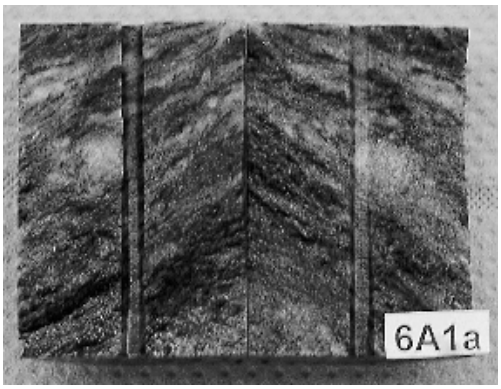

MINI-FRAC TEST DATA SHEET

borehole:	KOV01
sample - no.:	6A1b
mean depth, m:	559.9
diameter, mm:	29.9
length, mm:	45.0
date of unpacking / sampling:	12.11.01
mini - sample ready for testing:	14.11.01
date of testing:	16.11.01
operated by	J. Orzol
checked by	U. Weber

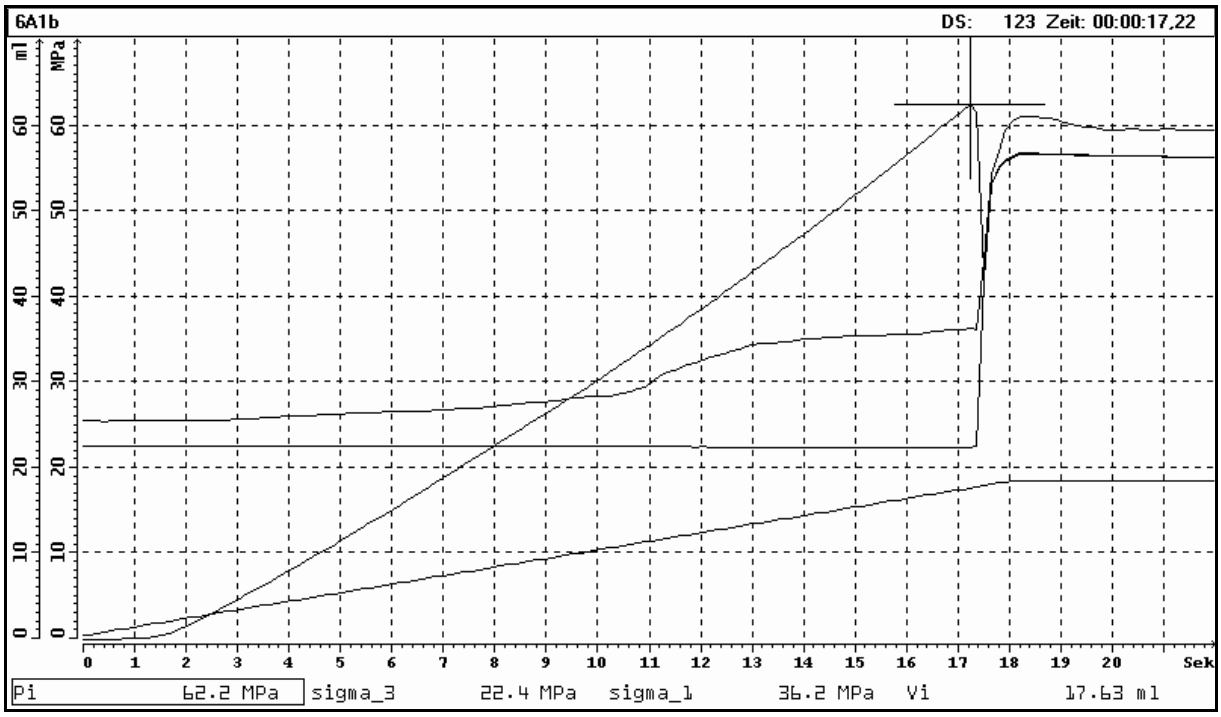

Initial conditions	
σ_1, MPa	36.2
σ_3, MPa	22.4
Injection Characteristics at failure	
P_i, MPa	62.2
V_i, ml	17.63

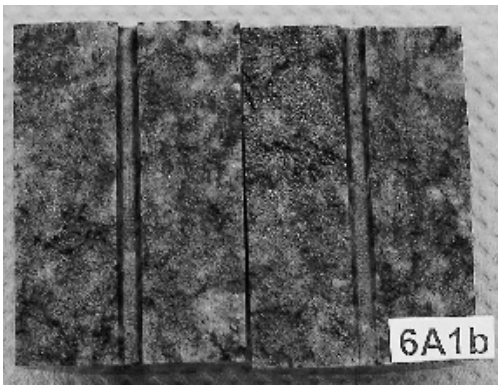

MINI-FRAC TEST DATA SHEET

borehole:	KOV01
sample - no.:	7A1a
mean depth, m:	596.65
diameter, mm:	29.9
length, mm:	42.4
date of unpacking / sampling:	12.11.01
mini - sample ready for testing:	14.11.01
date of testing:	16.11.01
operated by	J. Orzol
checked by	U. Weber

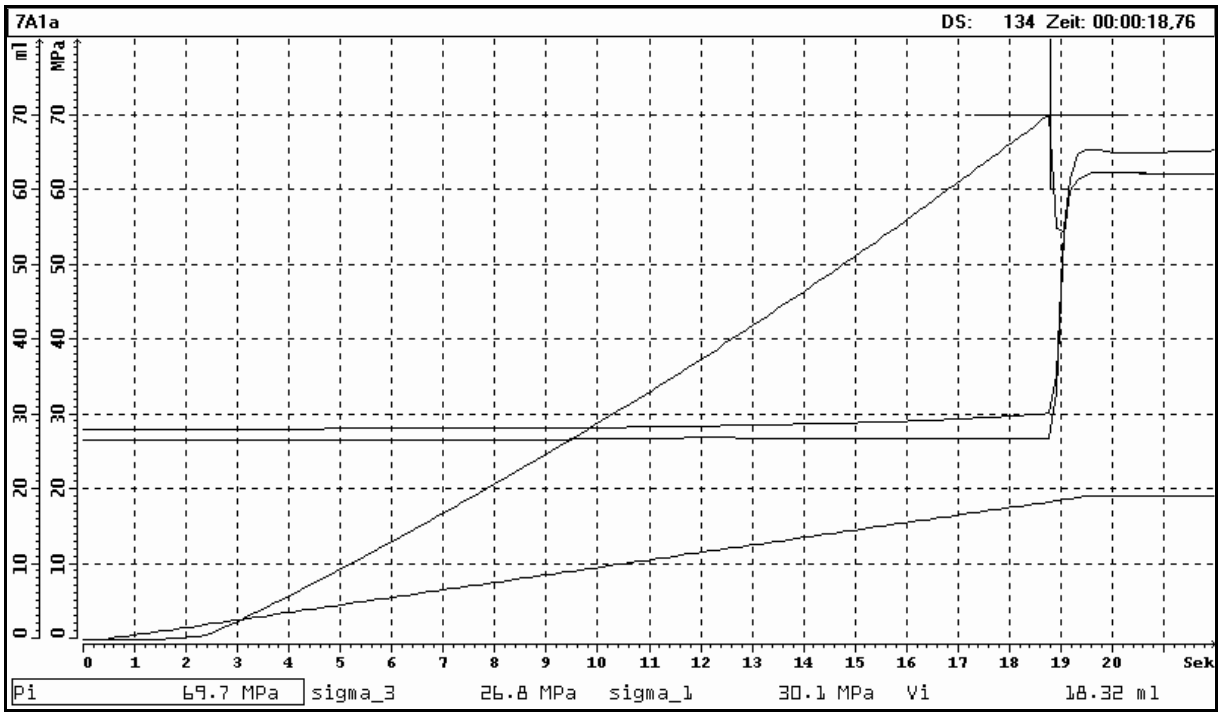

Initial conditions	
σ_1, MPa	30.1
σ_3, MPa	26.8
Injection Characteristics at failure	
P_i, MPa	69.7
V_i, ml	18.32

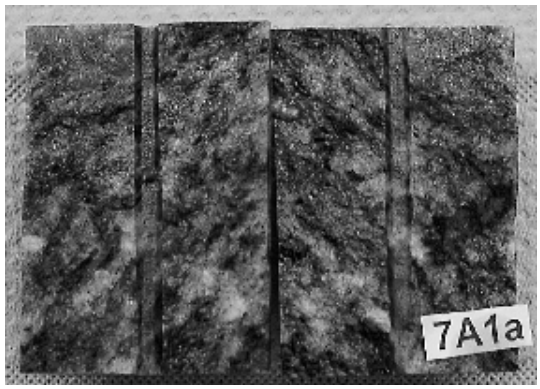

MINI-FRAC TEST DATA SHEET

borehole:	KOV01
sample - no.:	7A1b
mean depth, m:	596.65
diameter, mm:	29.9
length, mm:	45.3
date of unpacking / sampling:	12.11.01
mini - sample ready for testing:	14.11.01
date of testing:	16.11.01
operated by	J. Orzol
checked by	U. Weber

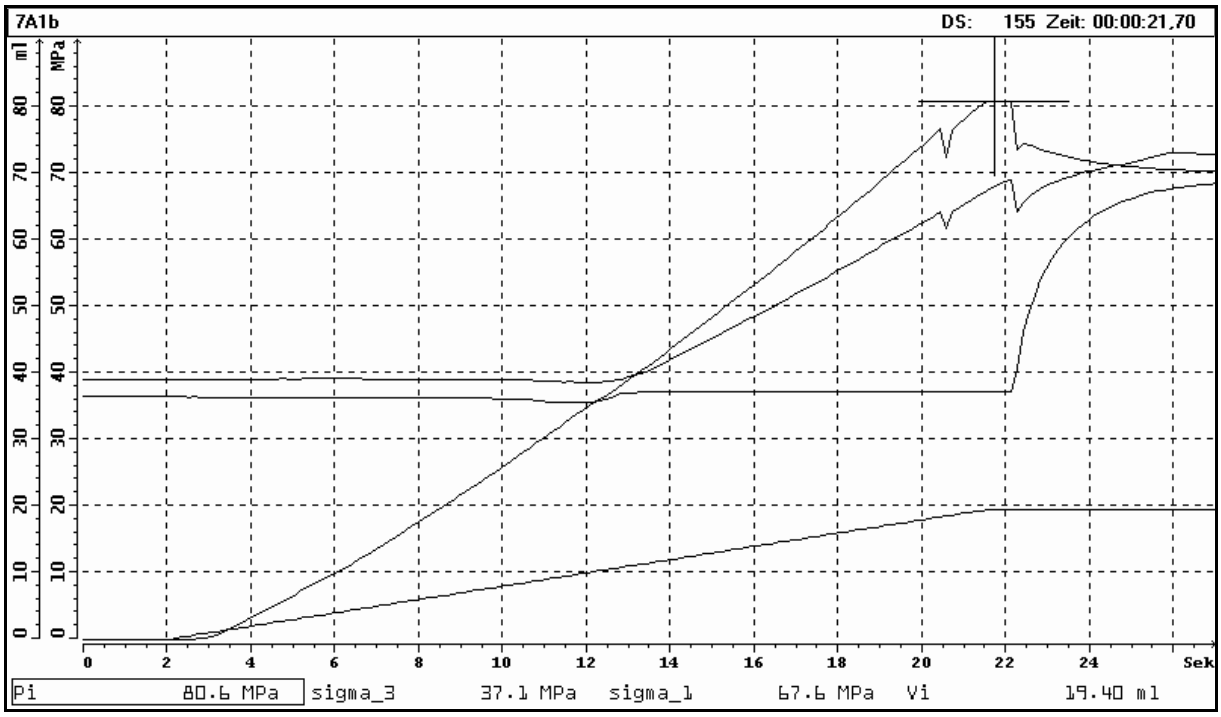

Initial conditions	
σ_1, MPa	67.6
σ_3, MPa	37.1
Injection Characteristics at failure	
P_i, MPa	80.6
V_i, ml	19.40

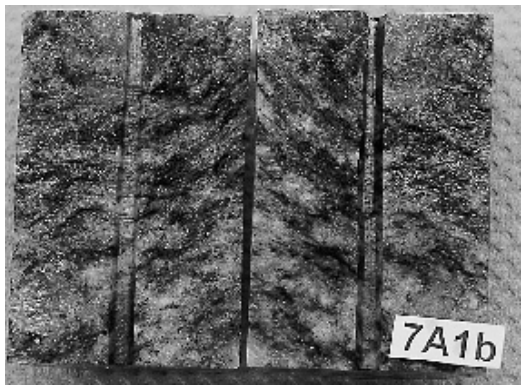

MINI-FRAC TEST DATA SHEET

borehole:	KOV01
sample - no.:	8B2a
mean depth, m:	648.89
diameter, mm:	29.9
length, mm:	44.1
date of unpacking / sampling:	12.11.01
mini - sample ready for testing:	14.11.01
date of testing:	16.11.01
operated by	J. Orzol
checked by	U. Weber

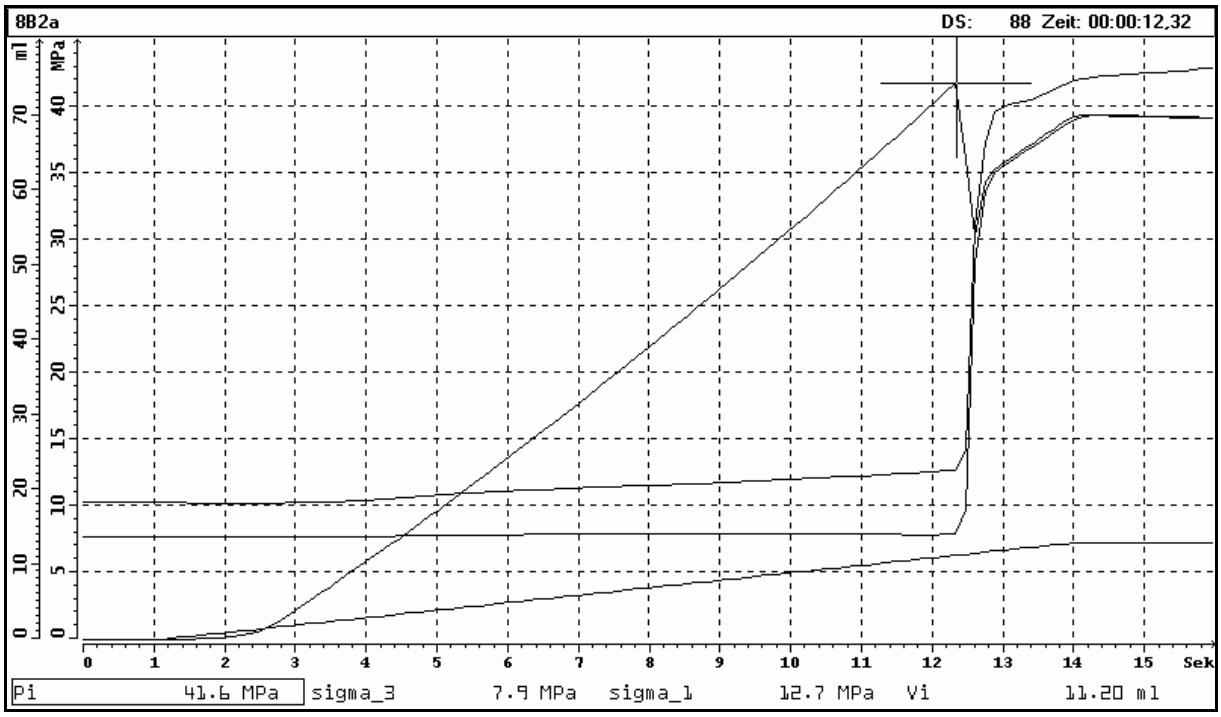

Initial conditions	
σ_1, MPa	12.7
σ_3, MPa	7.9
Injection Characteristics at failure	
P_i, MPa	41.6
V_i, ml	11.20

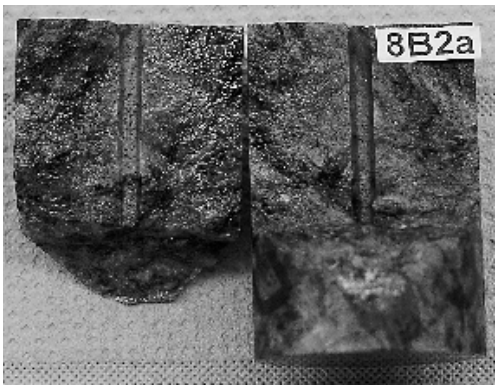

MINI-FRAC TEST DATA SHEET

borehole:	KOV01
sample - no.:	9A1a
mean depth, m:	692.78
diameter, mm:	29.9
length, mm:	44.0
date of unpacking / sampling:	12.11.01
mini - sample ready for testing:	14.11.01
date of testing:	16.11.01
operated by	J. Orzol
checked by	U. Weber

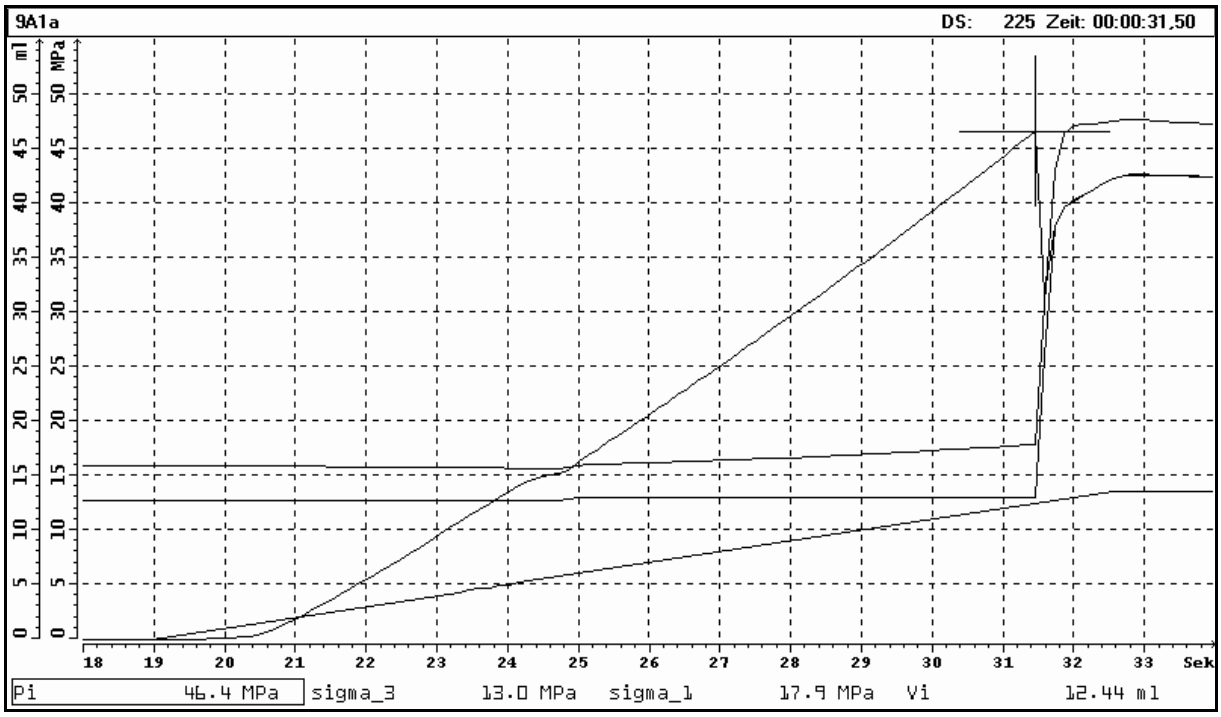

Initial conditions	
σ_1, MPa	17.9
σ_3, MPa	13.0
Injection Characteristics at failure	
P_i, MPa	46.4
V_i, ml	12.44

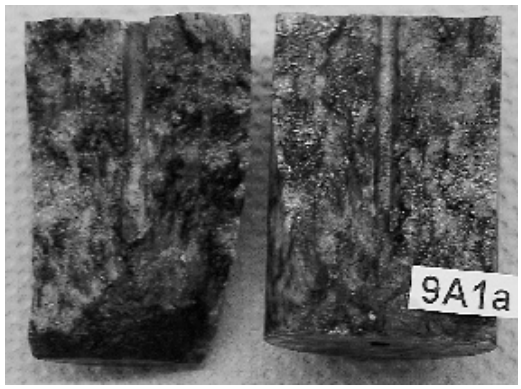

MINI-FRAC TEST DATA SHEET

borehole:	KOV01
sample - no.:	9A1b
mean depth, m:	692.78
diameter, mm:	29.9
length, mm:	43.9
date of unpacking / sampling:	12.11.01
mini - sample ready for testing:	14.11.01
date of testing:	16.11.01
operated by	J. Orzol
checked by	U. Weber

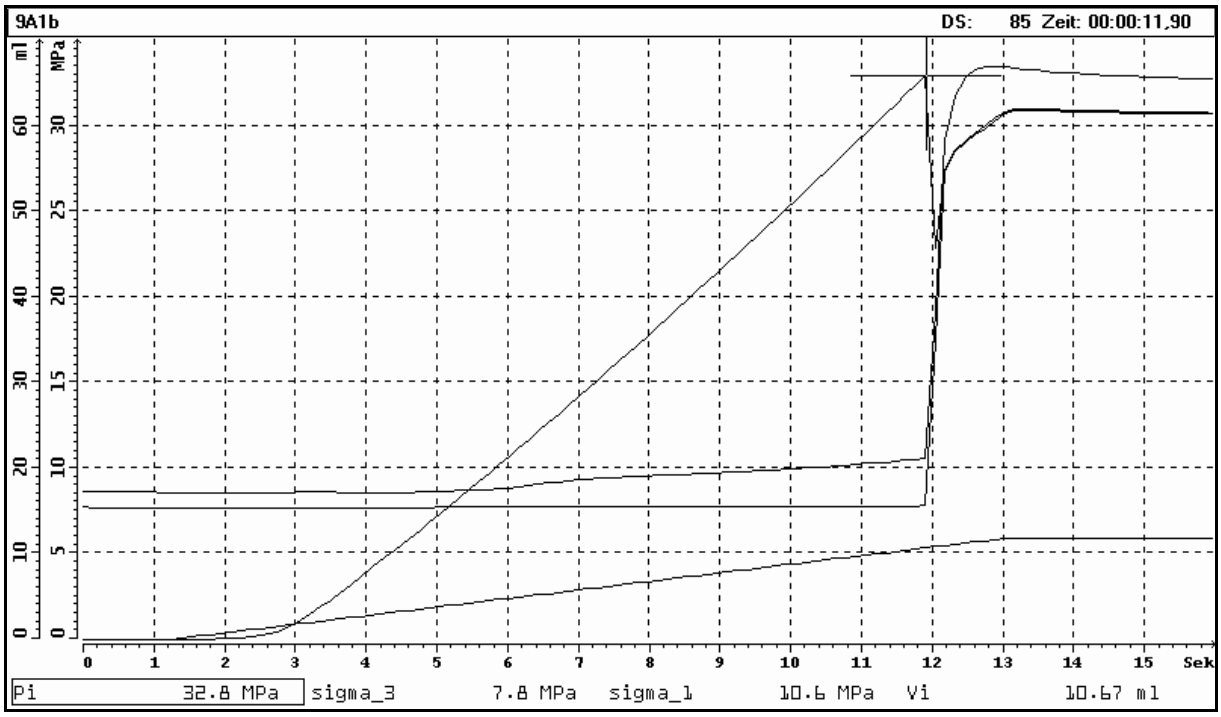

Initial conditions	
σ_1, MPa	10.6
σ_3, MPa	7.8
Injection Characteristics at failure	
P_i, MPa	32.8
V_i, ml	10.67

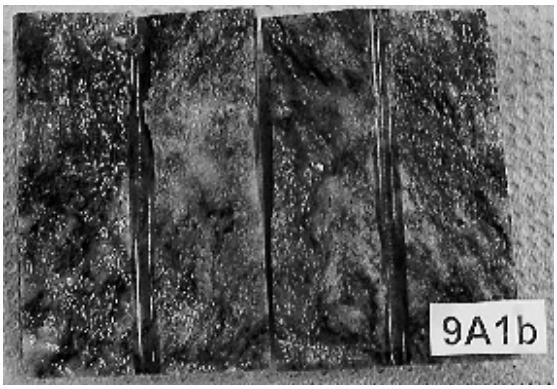

MINI-FRAC TEST DATA SHEET

borehole:	KOV01
sample - no.:	10A1a
mean depth, m:	709.55
diameter, mm:	29.9
length, mm:	45.0
date of unpacking / sampling:	12.11.01
mini - sample ready for testing:	14.11.01
date of testing:	16.11.01
operated by	J. Orzol
checked by	U. Weber

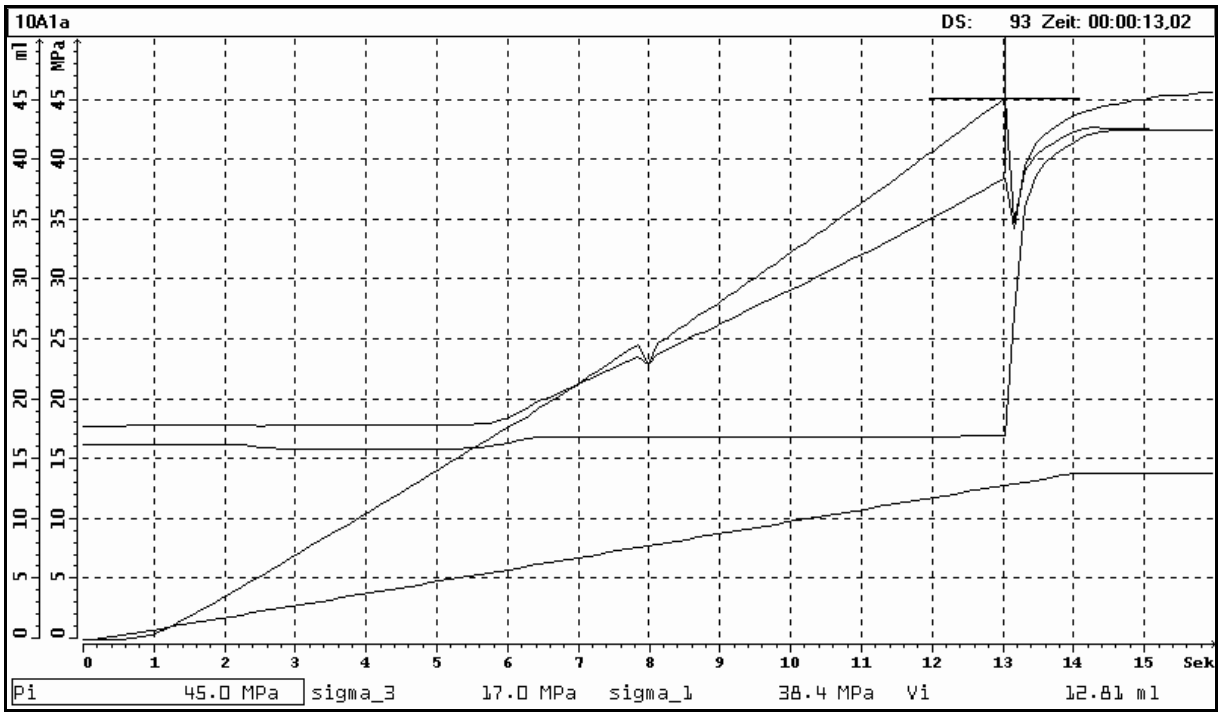

Initial conditions	
σ_1, MPa	38.4
σ_3, MPa	17.0
Injection Characteristics at failure	
P_i, MPa	45.0
V_i, ml	12.81

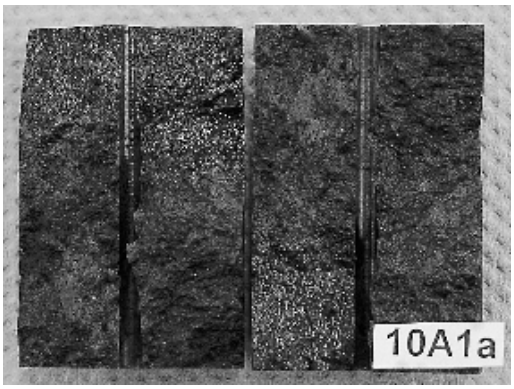

APPENDIX I

Pressure Pulse Test Records and Permeability Analysis

TEST AT 296.0 m MD / 280.9 m TVD

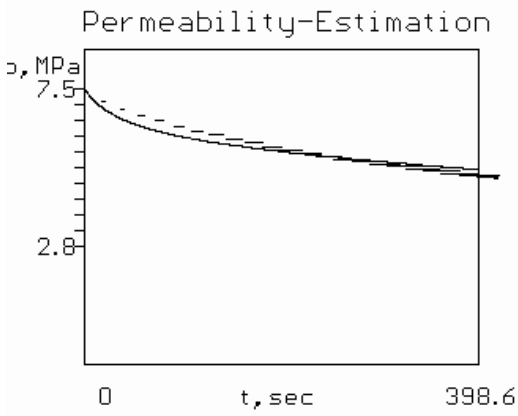

INPUTPARAMETERS

filename:	296.txt
samplingrate, sec:	0.20
inv. Stiffness m².m/Pa:	2.2E-11
interval length, m:	0.70
hole diameter, mm:	76.00
Phyd, MPa:	2.76
Tm (min, max), sec:	1 1000
number of models:	20000
error:	2.7E-02

result (mean value of all fitting models):

Permeability	: (	26.4 ±	0.8) µdarcy
Kf	: (	2.6 ±	0.1) e-10 m/s
Alpha	: (	0.01000)	

Number of fitting models: 144

TEST AT 303.5 m MD / 288.0 m TVD

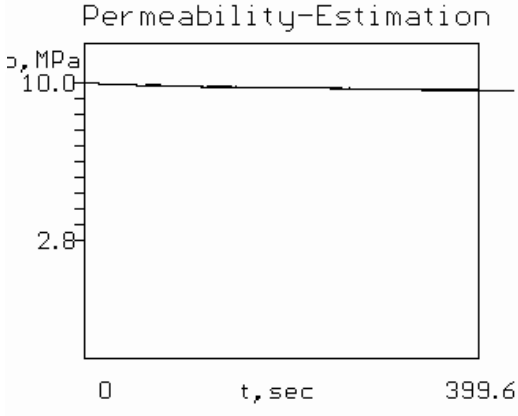

INPUTPARAMETERS

filename:	303.txt
samplingrate, sec:	0.20
inv. Stiffness m².m/Pa:	2.2E-11
interval length, m:	0.70
hole diameter, mm:	76.00
Phyd, MPa:	2.79
Tm (min, max), sec:	5001 15002
number of models:	20000
error:	2.5E-03

result (mean value of all fitting models):

Permeability	: (	1.5 ±	0.1) µdarcy
Kf	: (	1.5 ±	0.1) e-11 m/s
Alpha	: (	0.00100)	

Number of fitting models: 462

TEST AT 319.3 m MD / 302.8 m TVD

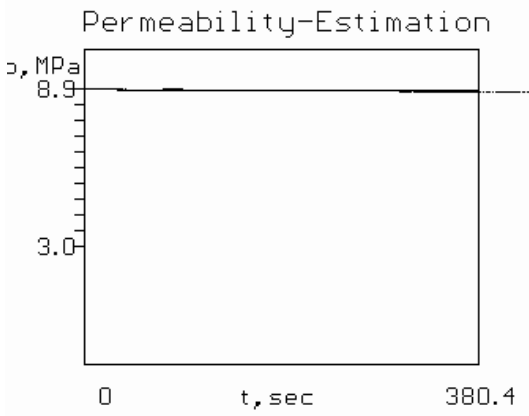

INPUTPARAMETERS

filename:	319.txt
samplingrate, sec:	0.20
inv. Stiffness m³.m/Pa:	2.2E-11
interval length, m:	0.70
hole diameter, mm:	76.00
Phyd, MPa:	2.95
Tm (min, max), sec:	100100000
number of models:	20000
error:	2.0E-03

result (mean value of all fitting models):

Permeability	: (	0.6 ±	0.0) µdarcy
Kf	: (	5.9 ±	0.4) e-12 m/s
Alpha	: (	0.00010)	

Number of fitting models: 150

TEST AT 325.4 m MD / 308.5 m TVD

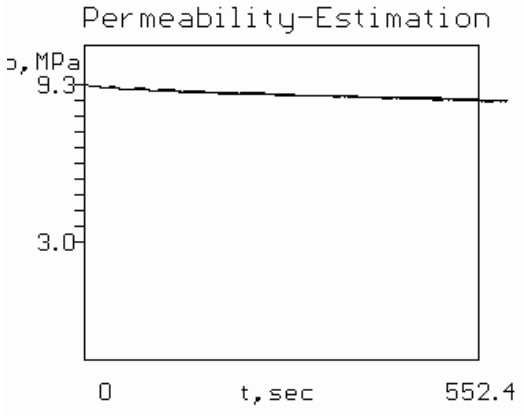

INPUTPARAMETERS

filename:	325.txt
samplingrate, sec:	0.40
inv. Stiffness m³.m/Pa:	2.2E-11
interval length, m:	0.70
hole diameter, mm:	76.00
Phyd, MPa:	3.01
Tm (min, max), sec:	5401 16202
number of models:	20000
error:	5.0E-03

result (mean value of all fitting models):

Permeability	: (	1.3 ±	0.1) µdarcy
Kf	: (	1.3 ±	0.1) e-11 m/s
Alpha	: (	0.01000)	

Number of fitting models: 377

TEST AT 331.5 m MD / 314.2 m TVD

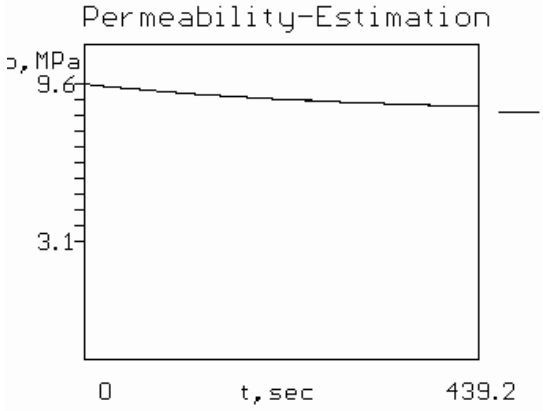

INPUTPARAMETERS

filename:	331.txt
samplingrate, sec:	0.40
inv. Stiffness m³.m/Pa:	2.2E-11
interval length, m:	0.70
hole diameter, mm:	76.00
Phyd, MPa:	3.06
Tm (min, max), sec:	1701 5102
number of models:	20000
error:	1.0E-03

result (mean value of all fitting models):

Permeability	: (2.1 ±	0.0) µdarcy
Kf	: (2.1 ±	0.1) e-11 m/s
Alpha	: (0.10000)	

Number of fitting models: 524

TEST AT 383.5 m MD / 363.0 m TVD

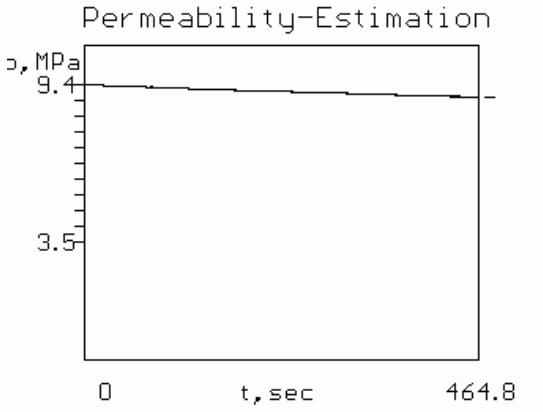

INPUTPARAMETERS

filename:	383.txt
samplingrate, sec:	0.40
inv. Stiffness m³.m/Pa:	2.2E-11
interval length, m:	0.70
hole diameter, mm:	76.00
Phyd, MPa:	3.54
Tm (min, max), sec:	5001 15002
number of models:	20000
error:	8.0E-04

result (mean value of all fitting models):

Permeability	: (1.3 ±	0.0) µdarcy
Kf	: (1.3 ±	0.0) e-11 m/s
Alpha	: (1.00000)	

Number of fitting models: 46

TEST AT 416.0 m MD / 393.8 m TVD

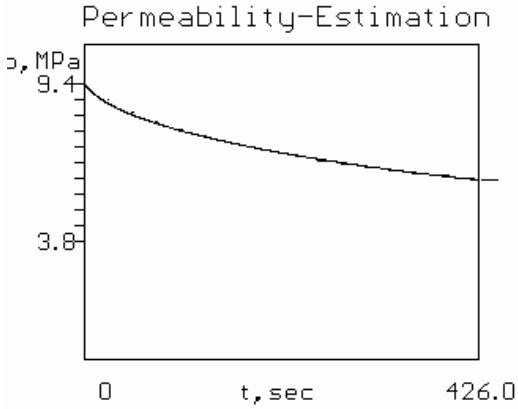

INPUTPARAMETERS

filename:	416.txt
samplingrate, sec:	0.40
inv. Stiffness m³.m/Pa:	2.2E-11
interval length, m:	0.70
hole diameter, mm:	76.00
Phyd, MPa:	3.81
Tm (min, max), sec:	258 773
number of models:	20000
error:	5.0E-03

result (mean value of all fitting models):

Permeability	: (19.5 ±	0.2) µdarcy
Kf	: (1.9 ±	0.0) e-10 m/s
Alpha	: (0.10000)	

Number of fitting models: 151

TEST AT 417.7 m MD / 395.5 m TVD

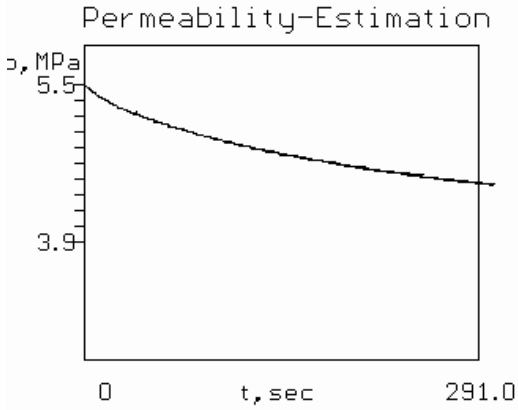

INPUTPARAMETERS

filename:	417.txt
samplingrate, sec:	0.20
inv. Stiffness m³.m/Pa:	2.2E-11
interval length, m:	0.70
hole diameter, mm:	76.00
Phyd, MPa:	3.87
Tm (min, max), sec:	126 377
number of models:	20000
error:	2.0E-03

result (mean value of all fitting models):

Permeability	: (47.3 ±	0.7) µdarcy
Kf	: (4.7 ±	0.1) e-10 m/s
Alpha	: (0.01000)	

Number of fitting models: 163

TEST AT 471.0 m MD / 446.9 m TVD

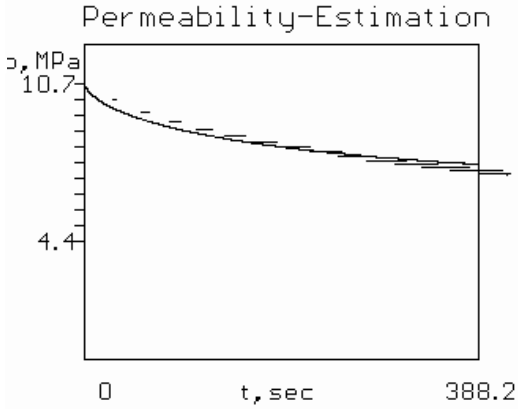

INPUTPARAMETERS

filename:	471.txt
samplingrate, sec:	0.20
inv. Stiffness m³.m/Pa:	2.2E-11
interval length, m:	0.70
hole diameter, mm:	76.00
Phyd, MPa:	4.36
Tm (min, max), sec:	301 902
number of models:	20000
error:	2.0E-02

result (mean value of all fitting models):

Permeability	: (17.0 ±	0.6) µdarcy
Kf	: (1.7 ±	0.1) e-10 m/s
Alpha	: (0.10000)	

Number of fitting models: 513

TEST AT 490.5 m MD / 465.8 m TVD

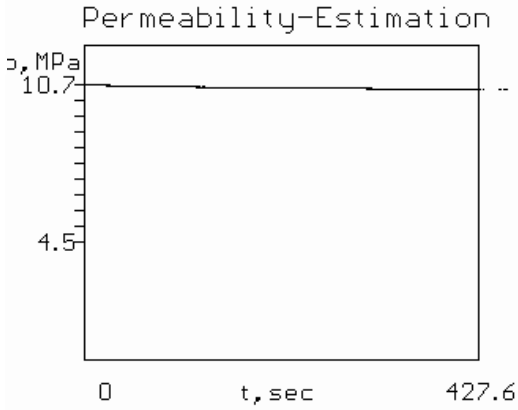

INPUTPARAMETERS

filename:	490.txt
samplingrate, sec:	0.40
inv. Stiffness m³.m/Pa:	2.2E-11
interval length, m:	0.70
hole diameter, mm:	76.00
Phyd, MPa:	4.53
Tm (min, max), sec:	10001 30002
number of models:	20000
error:	9.0E-04

result (mean value of all fitting models):

Permeability	: (0.8 ±	0.0) µdarcy
Kf	: (7.8 ±	0.1) e-12 m/s
Alpha	: (0.00100)	

Number of fitting models: 33

TEST AT 499.8 m MD / 474.8 m TVD

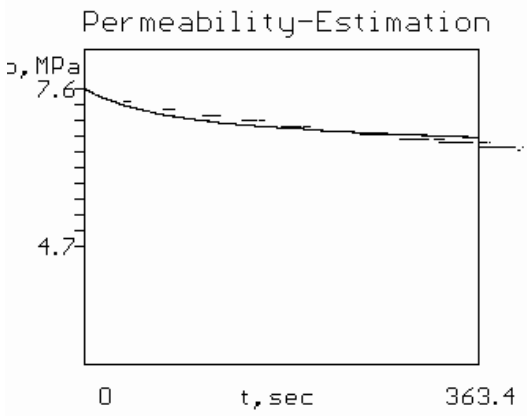

INPUTPARAMETERS

filename:	499.txt
samplingrate, sec:	0.20
inv. Stiffness m³.m/Pa:	2.2E-11
interval length, m:	0.70
hole diameter, mm:	76.00
Phyd, MPa:	4.72
Tm (min, max), sec:	376 1127
number of models:	20000
error:	1.0E-02

result (mean value of all fitting models):

Permeability	: (13.1 ±	0.5) µdarcy
Kf	: (1.3 ±	0.0) e-10 m/s
Alpha	: (0.01000)	

Number of fitting models: 415

TEST AT 510.8 m MD / 485.6 m TVD

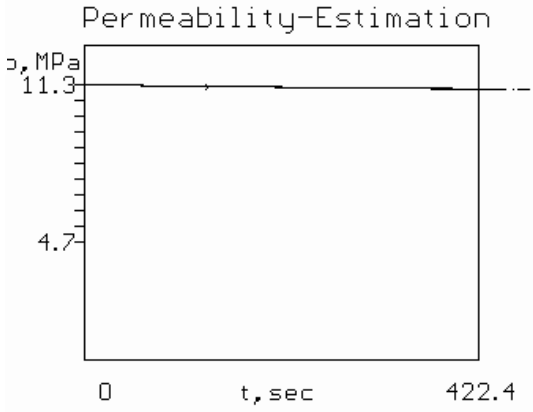

INPUTPARAMETERS

filename:	510.txt
samplingrate, sec:	0.40
inv. Stiffness m³.m/Pa:	2.2E-11
interval length, m:	0.70
hole diameter, mm:	76.00
Phyd, MPa:	4.72
Tm (min, max), sec:	10001 30002
number of models:	20000
error:	3.0E-04

result (mean value of all fitting models):

Permeability	: (0.9 ±	0.0) µdarcy
Kf	: (9.3 ±	0.2) e-12 m/s
Alpha	: (0.00010)	

Number of fitting models: 201

TEST AT 517.0 m MD / 491.6 m TVD

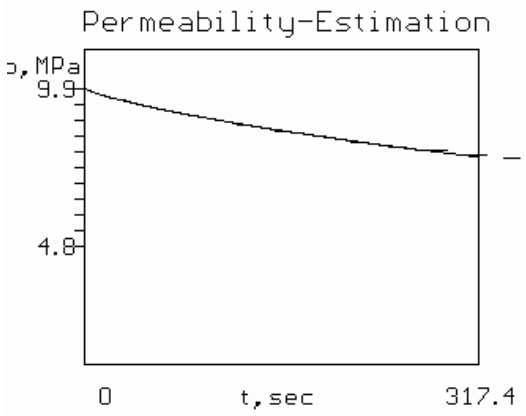

INPUTPARAMETERS

filename:	517.txt
samplingrate, sec:	0.20
inv. Stiffness m³.m/Pa:	2.2E-11
interval length, m:	0.70
hole diameter, mm:	76.00
Phyd, MPa:	4.80
Tm (min, max), sec:	326 977
number of models:	20000
error:	3.0E-03

result (mean value of all fitting models):

Permeability	: (15.9 ±	0.2) µdarcy
Kf	: (1.6 ±	0.0) e-10 m/s
Alpha	: (1.00000)	

Number of fitting models: 216

TEST AT 579.0 m MD / 552.2 m TVD

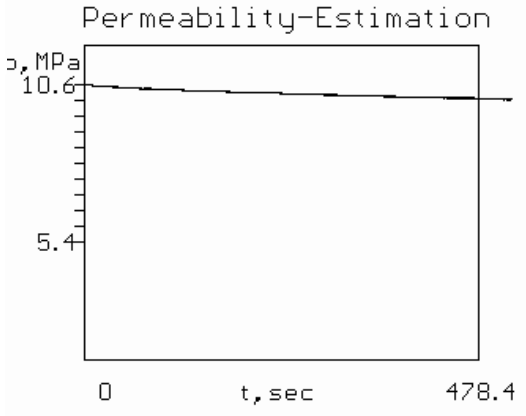

INPUTPARAMETERS

filename:	579.txt
samplingrate, sec:	0.40
inv. Stiffness m³.m/Pa:	2.2E-11
interval length, m:	0.70
hole diameter, mm:	76.00
Phyd, MPa:	5.39
Tm (min, max), sec:	5001 15002
number of models:	20000
error:	1.5E-03

result (mean value of all fitting models):

Permeability	: (1.3 ±	0.0) µdarcy
Kf	: (1.3 ±	0.0) e-11 m/s
Alpha	: (0.01000)	

Number of fitting models: 265

TEST AT 604.2 m MD / 577.0 m TVD

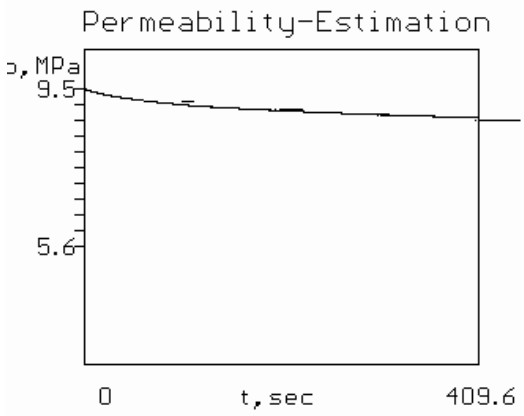

INPUTPARAMETERS

filename:	604.txt
samplingrate, sec:	0.40
inv. Stiffness m³.m/Pa:	2.2E-11
interval length, m:	0.70
hole diameter, mm:	76.00
Phyd, MPa:	5.64
Tm (min, max), sec:	1501 4502
number of models:	20000
error:	5.0E-03

result (mean value of all fitting models):

Permeability	: (4.7 ±	0.1) µdarcy
Kf	: (4.7 ±	0.1) e-11 m/s
Alpha	: (0.01000)	

Number of fitting models: 292

TEST AT 681.0 m MD / 652.9 m TVD

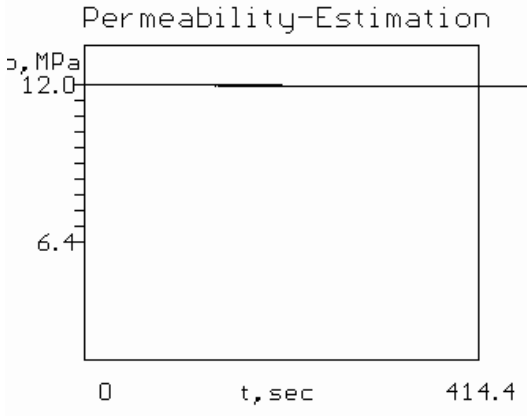

INPUTPARAMETERS

filename:	681.txt
samplingrate, sec:	0.40
inv. Stiffness m³.m/Pa:	2.2E-11
interval length, m:	0.70
hole diameter, mm:	76.00
Phyd, MPa:	6.37
Tm (min, max), sec:	15001 45002
number of models:	20000
error:	5.0E-04

result (mean value of all fitting models):

Permeability	: (0.3 ±	0.0) µdarcy
Kf	: (3.0 ±	0.3) e-12 m/s
Alpha	: (0.00010)	

Number of fitting models: 1818

TEST AT 689.5 m MD / 661.3 m TVD

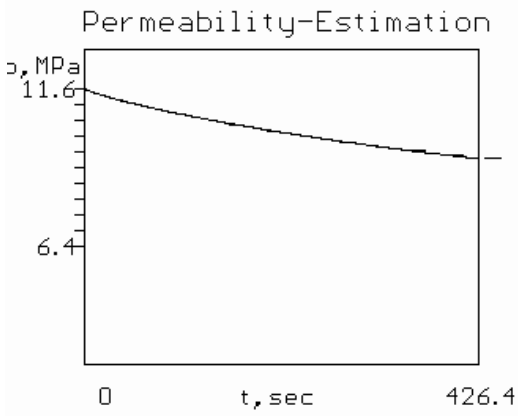

INPUTPARAMETERS

filename:	689.txt
samplingrate, sec:	0.40
inv. Stiffness m³.m/Pa:	2.2E-11
interval length, m:	0.70
hole diameter, mm:	76.00
Phyd, MPa:	6.45
Tm (min, max), sec:	401 1202
number of models:	20000
error:	2.0E-03

result (mean value of all fitting models):

Permeability	: (12.5 ±	0.1) µdarcy
Kf	: (1.3 ±	0.0) e-10 m/s
Alpha	: (1.00000)	

Number of fitting models: 141

TEST AT 702.5 m MD / 674.2 m TVD

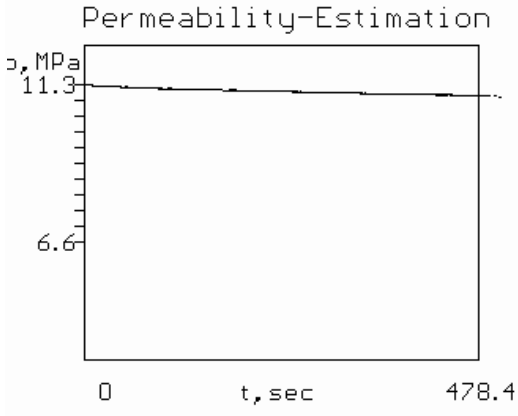

INPUTPARAMETERS

filename:	702.txt
samplingrate, sec:	0.40
inv. Stiffness m³.m/Pa:	2.2E-11
interval length, m:	0.70
hole diameter, mm:	76.00
Phyd, MPa:	6.59
Tm (min, max), sec:	5001 15002
number of models:	20000
error:	1.1E-03

result (mean value of all fitting models):

Permeability	: (2.0 ±	0.0) µdarcy
Kf	: (2.0 ±	0.0) e-11 m/s
Alpha	: (0.00100)	

Number of fitting models: 51

TEST AT 708.0 m MD / 679.6 m TVD

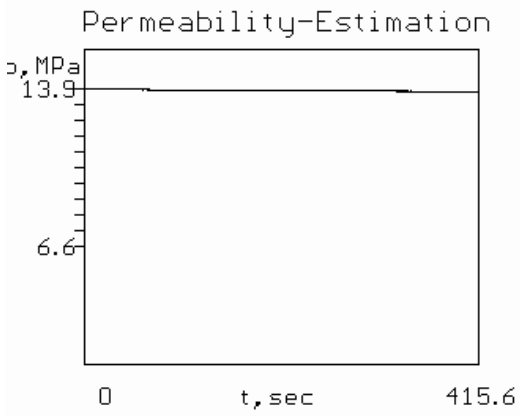

INPUTPARAMETERS

filename:	708.txt
samplingrate, sec:	0.40
inv. Stiffness m³.m/Pa:	2.2E-11
interval length, m:	0.70
hole diameter, mm:	76.00
Phyd, MPa:	6.61
Tm (min, max), sec:	15001 45002
number of models:	20000
error:	2.0E-04

result (mean value of all fitting models):

Permeability	: (0.4 ±	0.0) µdarcy
Kf	: (4.0 ±	0.0) e-12 m/s
Alpha	: (0.00100)	

Number of fitting models: 10

TEST AT 712.8 m MD / 684.8 m TVD

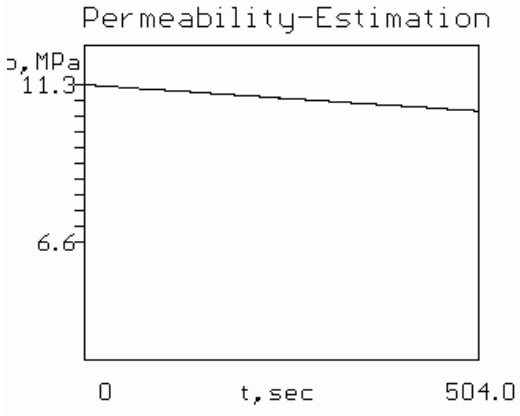

INPUTPARAMETERS

filename:	712.txt
samplingrate, sec:	0.40
inv. Stiffness m³.m/Pa:	2.2E-11
interval length, m:	0.70
hole diameter, mm:	76.00
Phyd, MPa:	6.61
Tm (min, max), sec:	1951 5852
number of models:	20000
error:	1.0E-03

result (mean value of all fitting models):

Permeability	: (2.5 ±	0.0) µdarcy
Kf	: (2.5 ±	0.0) e-11 m/s
Alpha	: (1.00000)	

Number of fitting models: 209